Statistical Analysis of Central Aortic Blood Pressure Parameters Derived From the Peripheral Pulse

By
Fernando Camacho

A Thesis Presented for the Degree of
DOCTOR OF PHILOSOPHY
AT
THE UNIVERSITY OF NEW SOUTH WALES
NOVEMBER, 2005 SYDNEY

ORIGINALITY STATEMENT

'I hereby declare that this submission is my own work and to the best of my knowledge it contains no material previously published or written by another person, nor material which to a substantial extent has been accepted for the award of any other degree or diploma at UNSW or any other educational institution, except where due acknowledgement is made in the thesis. Any contribution made to the research by others, with whom I have worked at UNSW or elsewhere, is explicitly acknowledged in the thesis. I also declare that the intellectual content of this thesis is the product of my own work, except to the extent that assistance from others in the project's design and conception or in style, presentation and linguistic expression is acknowledged.'

Fernando Camacho

Felicidad, Salud, Energía y Honestidad!

Acknowledgment

Many thanks to Albert Avolio and Nigel Lovell for their support, advice, patience and friendship. To Andy for his time during many hours of valuable discussions, and to all the other friends at the Graduate School of Biomedical Engineering with whom I shared this special time of my life.

This study was supported by the Australian Research Council Linkage Grant LP0235210 with AtCor Medical as the industrial partner.

Abstract

With the rise in prevalence of cardiovascular (CV) disease, risk stratification is becoming increasingly important. Accurate characterization of the CV system is required, for which central aortic blood pressure (BP) parameters form an integral part. However, invasive measurement of central aortic BP parameters (${}_a\mathcal{P}$) is difficult. Therefore, non-invasive methods to estimate ${}_a\mathcal{P}$ from the radial pressure pulse (${}_rPulse$) have been proposed.

To analyze accuracy of estimated ${}_a\mathcal{P}$ (${}_a\widehat{\mathcal{P}}$) and applicability in risk stratification and diagnosis, this study presents: (1) a novel representation of the ${}_rPulse$ with minimal loss of information, (2) a framework for strict definition and statistical analysis of ${}_a\widehat{\mathcal{P}}$, and (3) a dynamic analysis of effects of mean BP (MP) and heart rate (HR) in the ${}_rPulse$ shape.

Methods: (1) 2671 ${}_rPulse$s measured by applanation tonometry were represented using the first eight principal components (PC) scores after standard PC transformation. ${}_rPulse$ shapes were compared in three subpopulations. (2) The concept of "estimation option" (EO) for ${}_a\mathcal{P}$ estimation was presented. A framework for strict definition of ${}_a\widehat{\mathcal{P}}$ and the comparison of EOs was proposed, and 7 different EOs compared. (3) A sequence of ${}_rPulse$s was analyzed during soft exhalation maneuver (SEM) in eight healthy subjects. Radial BP and respiration pressure were continuously measured. The effects of MP and HR in the ${}_rPulse$ parameters were analyzed by standard linear regression for each subject.

Results: (1) PC representation of the ${}_rPulse$ improves accuracy of the estimation of ${}_a\widehat{\mathcal{P}}$ compared with the simple use of ${}_rPulse$ parameters. Subpopulations have distinctive ${}_rPulse$ shapes. (2) No single EO was better for the estimation of all ${}_a\widehat{\mathcal{P}}$. Inclusion of MP improves estimation accuracy. Despite further improvement when ${}_rPulse$ is included, the general transfer function EO is a biased estimator. (3) The dynamic analysis of the ${}_rPulse$ provides information of the effects of MP and

HR in the ${}_rPulse$ not available in static analysis. The effects were specific for each individual and different from the results obtained from a general population.

Conclusions: For accurate CV risk stratification, future studies should include a dynamic measurement of calibrated radial pressure pulse during SEM maneuver. Risk analysis and diagnosis should be based on representations of the ${}_rPulse$ with minimum loss of information. ${}_a\widehat{\mathcal{P}}$ should be used for better understanding of the underlying physiological principles.

Contents

List of Figures

List of Tables

1

Introduction

Sphygmomanometric blood pressure (BP) readings are common in clinical practice and are widely used for diagnosis and risk stratification [Kannel et al., 1968, Dawber, 1980]. Despite its importance, BP is measured in the arm and the difference between central aortic and peripheral pressures is overlooked [Pauca et al., 1992, Dahlof et al., 1997, 2002].

Prevalence of cardiovascular disease is increasing substantially. Accurate characterization of the cardiovascular system is becoming more important, for which the measurement of central aortic pressure is an integral part. Central parameters are difficult to measure invasively. Therefore, non-invasive methods have been proposed. The technique based on the transformation of the radial pulse [Karamanoglu et al., 1993, Takazawa et al., 1996, Chen et al., 1997, Hope et al., 2003b], has been extensively used, although other methods are also available. As with most estimation techniques, there are problems that have let to substantial controversy in terms of the validity of the technique [Soderstrom et al., 2002, Hope et al., 2003a, Cloud et al., 2003a,b, Millasseau et al., 2003a,b, Hoeks et al., 2003, Williams, 2004]. To clarify the problems of this or any other technique, it is essential to know the accuracy of estimated parameters. This information has only been reported for central augmentation index, systolic and diastolic pressures, and only for estimations using a fixed general transfer function. In addition, these studies do not analyze the effects of model variability in the estimated parameters.

This present study investigates the accuracy of the most commonly used central aortic BP parameters ($\mathcal{P}$), and provides a consistent framework for parameter definition and error analysis. This investigation is based on a new metric to quantify and compare the radial blood pressures pulse, and a comparative analysis of different estimation options (EO). The dynamic analysis of the radial pressure pulse is presented as an addition to the study of static parameters. The importance and applicability of estimated central parameters for risk stratification and the retrospective analysis of existing studies is presented last.

1.1 Conceptual Framework of this Thesis

The conceptual framework of this thesis is based on seven major concepts: (i) Measurements ($\mathcal{M}$), (ii) Derivation methods ($\mathcal{D}$), (iii) Parameters ($\mathcal{P}$), (iv) Estimation options (EO), (v) Outcome ($\mathcal{Y}$), (vi) Blood pressure wave ($Wave$), (vii) Blood pressure pulse ($Pulse$).

Figure 1.1 represents the concepts in a schematic way, and their definitions are provided as follows:

Measurements ($\mathcal{M}$) refer to the 'raw' data before any further analysis or transformation (e.g., sphygmomanometric readings, invasive radial blood pressure waves). $\mathcal{M}$ are explained in detail in section 4.1.

Derivation Methods ($\mathcal{D}$) refer to the processes of mathematically adjusting and/or transforming measured data into more meaningful and 'useful' data. As an example, a well known $\mathcal{D}$ is the one used to estimate mean BP by adding 1/3 of the pulse pressure to diastolic pressure. It is simple, but it is a way of estimating mean BP from measured data. Other $\mathcal{D}$ are much more complex. $\mathcal{D}$ are explained in detail in section 4.2.

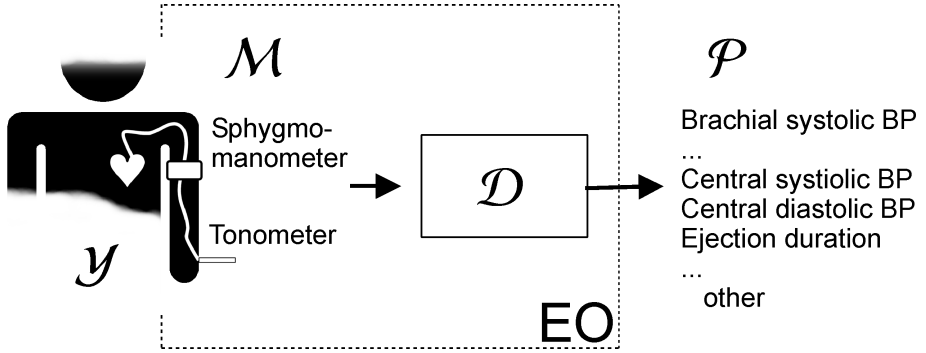

Figure 1.1: Definition of terms in the estimation of arterial BP parameters ($\mathcal{P}$). Measurements ($\mathcal{M}$) taken from a subject are transformed using a Derivation Method ($\mathcal{D}$) into the $\mathcal{P}$ of interest. An EO is a specific combination of $\mathcal{M}$ and $\mathcal{D}$. Subject's outcome ($\mathcal{Y}$) can be modeled from $\mathcal{P}$.

Parameters ($\mathcal{P}$) are values extracted either directly from the measurements (when $\mathcal{D}$ is the identity function, e.g., brachial systolic pressure measure with the sphygmomanometer) or after transformation using a specific $\mathcal{D}$ (e.g., aortic systolic pressure estimated from the brachial BP wave). $\mathcal{P}$ are explained in detail in section 4.3.

Estimation Option (EO) refers to a specific combination of $\mathcal{M}$ and $\mathcal{P}$. This concept is important because the same $\mathcal{P}$ estimated using two different EO will be different.

Outcome ($\mathcal{Y}$) refers to possible future subject's events such as myocardial infarction, stroke or death. The analysis of the prevalence and incidence of $\mathcal{Y}$ can be correlated with subject's current cardiovascular condition described by arterial BP parameters.

With the previous definitions in place it is possible to summarize the concepts covered in this study as:

$$\mathcal{P} = \mathcal{D}(\mathcal{M}) + \epsilon_{\mathcal{D}} \tag{1.1}$$

$$\mathcal{Y} = f(\mathcal{P}) + \epsilon_{\mathcal{Y}} \tag{1.2}$$

that will read:

- (Equation 1.1) Arterial parameters ($\mathcal{P}$) are estimated by transformation, using

derivation methods ($\mathcal{D}$), of subjects' measurements ($\mathcal{M}$). A derivation error ($\epsilon_{\mathcal{D}}$) describes the difference between the real and estimated $\mathcal{P}$.

- (Equation 1.2) Outcome ($\mathcal{Y}$) can be modeled by a function (f) of the subject parameters ($\mathcal{P}$). The difference between the real and modeled $\mathcal{Y}$ is represented by the outcome error ($\epsilon_{\mathcal{Y}}$).

The concepts of $Wave$ and $Pulse$ are specifically defined within the context of this document to prevent confusion, as these terms are widely used in many different contexts with many different meanings.

Blood Pressure Wave ($Wave$) refers to the blood pressure values in time (see Figure 1.2). It is usually represented in a discrete form as a list of numbers (i.e., the BP values for discrete points in time).

Blood Pressure Pulse ($Pulse$) refers to the values of blood pressure during one cardiac cycle (see Figure 1.2). A $Wave$ can contain many $Pulse$s.[1]

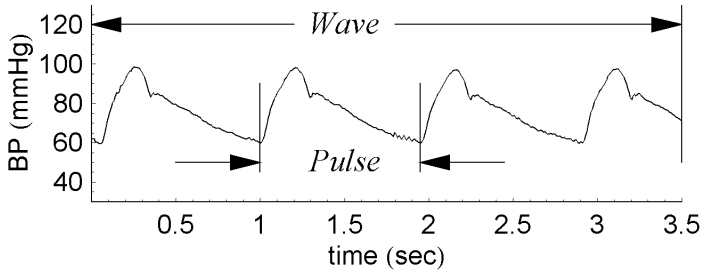

Figure 1.2: Definition of $Pulse$ and $Wave$.

The previous definitions provide the concepts required to follow this document; the following conventions provide the keys to read it.

1.2 Document Structure and Conventions

This document is divided in nine chapters. Chapter 2 describes the current practice and instrumentation for BP measurement. The databases of BP measurements used

[1] $Pulse$ does NOT refer, in this document, to the generic term used to denominate arterial BP.

in this current study are also presented in Chapter 2. Chapter 3 presents the radial pulse pressure space ($\mathbb{PP}$). The $\mathbb{PP}$ provides a metric for radial *Pulse* representation, comparison and analysis. A framework for the statistical analysis of BP parameters is defined in Chapter 4. Chapter 5 describes the statistical analysis of measurement (estimation) of central aortic BP parameters. Chapter 6 expands the concepts presented in chapter 5, but includes a new data set of non-invasive measurements in the analysis. Chapter 7 presents a dynamic analysis of the effects of mean BP and heart rate in BP parameters. Chapter 8 analyzes the value and applicability of central aortic BP parameters for risk assessment and for the retrospective analysis of previous studies in which BP *Wave*s were not measured. The final chapter presents the conclusions obtained in this study. Details of the results and methods are presented in the Appendices.

Typographic Conventions

The abbreviations for the most commonly used terms in this document are presented in Table 1.1. Note that special symbols are used to represent specific concepts.

In addition to the abbreviations and special symbols, a specific nomenclature conventions is used, as shown in Table 1.2. The subscript on the left indicates parameter's location (i.e., the anatomically position where the parameter refers to). The possible locations, and the letters use for their representation, are: aortic (a), brachial (b) and radial (r). The dimensionality of a parameter is represented with normal font for scalars and **bold** font for vectors or matrices. For example $\boldsymbol{x} = (x_1, x_1, \ldots, x_n)$. The 'hat' is used for estimated parameters (e.g., $\hat{\beta}$)). It is common to generate an average *Pulse* from a *Wave* by averaging the *Pulse*s contained in the *Wave*. When this fact is to be emphasized an overline symbol $\overline{x}$ is used.

The concepts explained above, the nomenclature and typographic conventions will be used throughout the document. Before presenting the details of the statistical analysis of BP parameters, a general background on the measurement of blood

pressure is presented in the following chapter.

Table 1.1: Special symbols and abbreviations

Symbol	*Definition*	*Symbol*	*Definition*
$\mathcal{M}$	measurement	LR	linear
$\mathcal{D}$	derivation method	LRM	linear mean
$\mathcal{P}$	parameter	MP	mean pressure
$\mathcal{Y}$	outcome	PC	principal components
$\mathbb{P}$	pressure space	PP	pulse pressure
$\mathcal{T}$	transfer function	PPA	pulse pressure amplification
μ	population mean	PPA^{-1}	1/PPA
		Pr	period
AIx	augmentation index	SBI	subject's basic information
Avg	average	SP	systolic pressure
bpm	beats per minute	*Pulse*	blood pressure pulse
BP	blood pressure	RMS	root mean square
DP	diastolic pressure	sec	second
ED	ejection duration	SD	standard deviation
EO	estimation option	SE	standard error
GTF	generalized transfer function	Var	variance
HR	heart rate	*Wave*	blood pressure wave

Table 1.2: Notation

Symbol	*Meaning*
$\widehat{\mathcal{P}}$	Estimated parameter
$\overline{\mathcal{P}}$	Average over a series of *Pulses*.
${}_a\mathcal{P}$	Aortic parameter
${}_b\mathcal{P}$	Brachial parameter
${}_r\mathcal{P}$	Radial parameter
$\boldsymbol{\mathcal{P}}$	vector or matrix
${}_{\mathsf{L}}\widehat{\mathcal{P}}\{\mathsf{S}\text{:sc}, \mathcal{M}\text{:ms } \mathcal{D}\text{:dr}\}$	Parameter's strict definition (see section 4.3.2).

2

Measurement of Blood Pressure

The evolution of clinical diagnosis has been paralleled by the measurement of blood pressure , which has become an important clinical and cardiovascular index as has been reported in imporant studies such as the *LIFE Study* [Dawber, 1980]. With an increasing and changing prevalence of different categories of cardiovascular disease, the need for a better characterization of the cardiovascular system and improved risk stratification is becoming more important. For this reason more comprehensive techniques that provide additional information to the well established measurement of ${}_bSP$ and ${}_bDP$ are needed.

This chapter introduces the measurement of BP with a short description of the BP itself. A brief history of BP measurement is presented, followed by the description of the current BP measurement practice. The importance of a more comprehensive measurement of BP, where BP wave contour in included, is discussed. The chapter concludes describing the data (i.e., the BP measurements) used in this study.

2.1 The Arterial Blood Pressure

Nutrients and oxygen need to be provided and waste removed from the tissue for cells to survive. Blood is the transport medium; hence it needs to flow through the network of arteries and veins to reach all body organs. The heart pumps blood

from the venous system to the arterial system. Blood flow is proportional to pressure gradient and inversely proportional to resistance. Since the arterioles and capillaries (the small passages from the arterial to the venous system, where mass transfer takes place by diffusion) are highly resistive to blood flow (due to their small diameter) pressure in the arterial system increases until a dynamic equilibrium is reached. Because the heart is a pulsatile pump and the mechanical characteristics of the arteries are not homogenous throughout the arterial system, the arterial BP can not be described in a simple way. Many models for this complex system have been proposed. The Windkessel model [Manning et al., 2002] or the asymmetric T-tube [O'Rourke, 1967, Burattini, 1989] are examples of models to approximate and analyze the arterial tree. In the computer model proposed by Avolio [1980] it is possible to model BP in many locations of the arterial tree. The arterial system is different from person to person, and even varies in the same person with aging and disease. However, for any particular individual, the BP wave contour is the result of the superposition of BP waves traveling within the arterial tree, and therefore characteristics of the arterial system should be reflected in the BP shape. In particular, the relationship between the ${}_{r}Pulse$ and the ${}_{a}Pulse$ and the pulse pressure amplification, are of special interest for the non-invasive estimation of central pressures. Therefore, it has been suggested, that the BP $Pulse$ shape can be used for cardiovascular (CV) diagnosis and risk analysis. To validate this approach, it is important to have a clear understanding of the system, the elements that affect it and the type of models (and their restrictions) that could be used to synthesize its complexity. These are the topics of following chapters. The history of BP, presented next, provides the foundation that has lead to the current practise in BP measurement and to the reasoning of using other measurements in addition to ${}_{b}SP$ and ${}_{b}DP$ alone.

2.2 Brief History of Blood Pressure Measurement

Blood pressure has been used since the beginning of medical practice [O'Rourke et al., 1992, Amber and Babey-Brooke, 1966]. Since ancient times BP was palpated by hand until the time of Frederick Akbar Mahomed when the development of the sphygmograph, in the late nineteenth century, started to be used in the medical practice. His work was diverted to the measurement of absolute values of systolic and diastolic BP when Riva-Rocci invented the mercury sphygmomanometer in 1896. Mahomed's work was almost forgotten behind the acceptance and great clinical value of Riva-Rocci's instrument. With the introduction of new pressure sensing technologies the study of BP dynamics was facilitated and is again gaining momentum. BP waveform analysis combined with measurement of absolute BP values is the natural merge between the ancient palpation technique and current occidental practice into the 'new' way of measuring BP. A more detailed history of BP measurement is presented by O'Rourke et al. [1992], Naqvi and Blaufox [1998], and Amber and Babey-Brooke [1966] in a very comprehensive, illustrative and informative way. A list of important historical events, from the arterial BP analysis perspective, are presented in Table 2.1.

2.3 Current Methods of Measurement of Blood Pressure

This section presents the current state on BP measurement without quantitative details of the 'quality' of the measurement. Chapter 4, section 4.1, presents the instrumentation accuracy and measurements quality necessary for the analysis of arterial parameters derived from BP measurements. The use of the measured cardiovascular parameters is presented next followed by a short description of BP measurements instruments.

Table 2.1: Important historical facts. (1):Amber and Babey-Brooke [1966], (2):O'Rourke et al. [1992], (3):Ruskin [1956], (4):Kannel et al. [1968], Dawber [1980], (5):Karamanoglu et al. [1993].

Author	*Facts*	*Year*	*ref*
Chinese, Indian	Palpation		(1)
Hippocrates	Recognized and named pulses	4^{th} c. B.C.	(1)
Galen	Wrote on the pulse	A.D. 131	(2)
William Harvey	'An Anatomical Essay on the Movement of the Heart and Blood in Animals'	1626	(2)
Rev. S. Hales	'Windkessel' model.	1769	(2)
Poiseuille	Measured arterial pressure.	1828	(2,3)
Mahomed	Clinical use of the sphygmograph.	1894	(2,3)
Riva-Rocci	Invention of the Sphygmomanometer.	1896	(3)
Korotkov	Auscultation sounds.	1905	(3)
Framingham	Most influential epidemiological study.	1948	(4)
Karamanoglu	General transfer function.	1993	(5)

2.3.1 Current Use of Blood Pressure Parameters

What determines the value of any BP parameter is its known relationship with outcome or subject's diagnosis. Results of epidemiological studies, like the Framingham Heart Study, have demonstrated the importance of BP in cardiovascular risk assessment. Therefore, the measurement of absolute values of BP ($_bSP$ and $_bDP$) is performed regularly in the clinical practice as part of an effective control of hypertension.

In additions to absolute BP values, other arterial parameters derived from the radial $Wave$ have been investigated and their relationship with patient's condition and outcome have been determined [Yasmin and Brown, 1999, Avolio et al., 2001, Wilkinson et al., 2001, Lemogoum et al., 2004]. These are not, as yet, a regular diagnostic test.

In addition to non-invasive measurement of BP, its invasive measurement is common in the intensive care unit and operating theater to monitor the patient's condition. But, although a continues invasive measurement, in which all features of the $Wave$ are available, only SP, DP and MP are considered for diagnosis.

From current medical practice it seems that an accurate measurement of BP is important. But in reality what is important is a good diagnosis and risk assessment, either by measuring ${}_bSP$ and ${}_bDP$ or any other parameter. With the increasing acceptance of the use of BP $Wave$ in the set of CV measurements, there is an increasing number of central parameters available. The estimation of such parameters is still controversial and for a correct diagnosis or risk analysis their accuracy must be considered. This study provides the tools and methodology for assessing their accuracy based on BP measurements, derivation methods (see Chapter 4), the radial pulse pressure space (see Chapter 3) and statistical analysis.

2.3.2 Blood Pressure Measurement Instruments

Blood pressure measurement can be either *invasive* or *non-invasive*. Invasive measurements are performed using catheters, either fluid filled catheters in which the pressure transducer is extracorporeal, or catheters in which the transducer is at the measurement location. Fluid filled catheters have, generally, a low narrow frequency response band. Modern pressure transducers have become small and with a wide frequency response band, such as the Millar transducer (Millar Instruments, Inc., Houston, TX, USA.) The frequency response, linearity, precision and resolution of modern invasive BP sensors is better then the one obtained with non-invasive measurements. Because non-invasive measurements are subject to operator's movement, skin thickness, holding down pressure and absolute calibration this problem is unsolved. However, Kelly et al. [1989b] demonstrated that for the frequency range of the $Wave$, the invasive and non-invasive measurements are comparable. In this study, the invasive measurements will be considered, unless otherwise stated, to be the same as the real BP values.

In non-invasive BP measurements errors should not be neglected. In addition, there are many different types of BP measuring devices with different error sources. BP measurement devices are presented in Table 2.2 where a clear distinction is

Table 2.2: BP measurement instrumentation. Some methods provide a BP waveform and some only provide a maximum and minimum (or mean) of the waveform with a subsequent loss of information in the latter.

	Instrument reading		
Instrument	SP and DP	BP wave contour	Calibrated BP wave
Sphygmomanometer (Hg)	✓		
Sphygmomanometer (Auscultatory)	✓		
Sphygmomanometer (Oscillometric)	✓		
Tonometer		✓	
Finapress			✓
VasoTrac™			✓
Ultrasound (analysis of wall motion)		✓	
Catheter (invasive)			✓

made between instruments to read absolute pressure values, BP wave contour, or a combined calibrated measurement. The instruments are described in the following sections.

The Mercury Sphygmomanometer

The mercury sphygmomanometer is the most widely used medical instrument for measurement of BP in clinical practice. The sphygmomanometer consists of a cuff placed around the subject's arm to occlude blood flow in a controlled manner. The cuff can be inflated with an air pump, and the indication of pressure is made by a column of mercury. ${}_bSP$ and ${}_bDP$ are measured by relating the pressure in the cuff with the appearance and vanishing of the Korotkov sounds. This simple technique has been used for over 100 years with minimal changes. Although this technique is still the gold standard for BP measurements it is not error free and only provides measurements of ${}_bSP$ and ${}_bDP$. Chapter 4 in section 4.1 discusses in detail the error of the sphygmomanometer and its implications in the estimation of cardiovascular parameters.

Automated Blood Pressure Cuff Sphygmomanometer (Auscultatory and Oscillometric)

The advances in electronics and transducer technologies have also percolated in the measurement of BP. There are two major branches on these developments. One is the automatic application of the same technique used with the mercury sphygmomanometer. A pressure transducer replaces the mercury column and a microphone 'listens' to the Korotkov sounds. A computer algorithm analyzes the information and calculates the measured ${}_bSP$ and ${}_bDP$. This is known as the auscultatory technique. A second branch, known as the oscillometric technique, is based in the measurement of the mean BP. This is achieved by finding the cuff pressure that maximizes the intra-cuff pressure oscillations. Algorithms that analyze the pressure variation during the complete deflation of the cuff, estimate ${}_bSP$ and ${}_bDP$. This instrument, although technologically advanced, has not proved better than the mercury sphygmomanometer. However, it is worth mentioning that the gold standard for validation of BP measurement instruments is still the mercury sphygmomanometer [O'Brien and Atkins, 1994, O'Brien, 1998, O'Brien et al., 2002]. In this document all absolute values of BP will be assumed to comply with international BP standards, without making any distinction between automated BP cuff sphygmomanometers or mercury sphygmomanometer, unless stated otherwise.

The Tonometer

The tonometer is a directional pressure sensor, measuring pressure perpendicular to a flat surface, as shown in Figure 2.1 . The flat surface is located against the wall of a vessel (e.g., the radial artery) flattening it - hence the name 'applanation' tonometry. Because, in theory, there are no forces in the direction of measurement exerted by the vessel wall the pressure measured by the tonometer is identical to the pressure inside the vessel. That may not be strictly correct because, in practice, the vessel wall and other tissues such as muscle and skin, exert force in the direction of measurement.

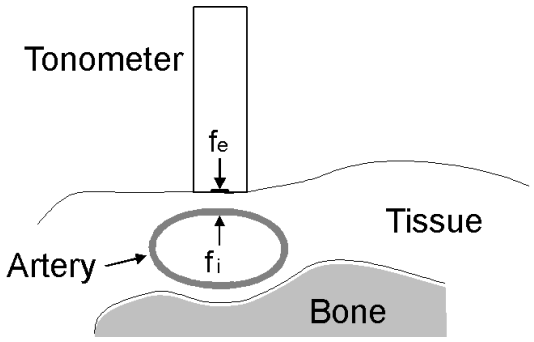

Figure 2.1: Applanation tonometry. f_e and f_i are equal if the tissue and artery walls don't exert collinear force.

However, although the absolute pressures measured by the tonometer may not be similar to intra-vascular pressure, the waveform contour is maintained and dynamic characteristics are preserved [Kelly et al., 1989b, Sato et al., 1993]. The dynamic characteristics of the tonometer itself determine the response of the measurement. The review by Matthys and Verdonck [2002] of the applanation tonometry technique explains the theory in much greater detail. However, without the need for theoretical details, it is important to mention that modern tonometers have a frequency response beyond the required frequency range for BP waveform analysis [Gardner, 1981] and transcutaneous response.

The tonometric measurements are not restricted to single pressure sensors. As described by Sato et al. [1993] multiple sensor arrays could be used in BP waveform measurements. The advantage of the multiple sensor array is to facilitate the location of the best BP signal. Still, the absolute pressure values have to be calibrated.

Details on the accuracy of tonometric measurements are presented in section 4.1.3

Finapres™

The *Finapres*™ (FMS Finapres Medical Systems BV, Amsterdam ZO The Netherlands) measures BP by a counter-pulsating pressure in a finger cuff using the technique described by Penaz [1973] and Wesseling et al. [1985]. This pressure is controlled to maintain the diameter of the cuff constant. BP will tend to expand the finger's diameter while the counter pressure will tend to reduce it. The diameters is

kept constant if the counter pressure is the same as the BP. The cuff is initially calibrated to mean BP. The *Finapres*™ is an accurate instrument, but problems exist [Birch and Morris, 2003]. The system is susceptible to vasoconstriction in the hand as the measurement takes place in the finger. In addition, the BP wave contour, although similar, is different from the radial wave contour, which is more widely referred to in the literature for the derivation of central aortic BP.

Vasotrac

The Vasotrac (MEDWAVE, INC., St. Paul, MN, USA) instrument also provides measurements of absolute BP ($_rSP$ and $_rDP$) and a BP $Wave$ contour. The instrument is based on a wrist cuff that occludes the radial artery. The technology used by this instrument is similar to the oscillometric automatic sphygmomanometer. However, because the measurement is made at the radial artery at the wrist, the calibrated $Pulse$ contour is available. The quality of the contour was validated by Cua et al. [2005] and Belani et al. [1999].

Ultrasound

The ability of ultrasound to obtain dimensional changes of internal structures has been used to measure BP wave contours. By analyzing the distention of the arteries, the BP waveform can be estimated, as distention is essentially proportional to BP. This is a valid approach for small variations in BP, as the relationship between BP and arterial distension is not linear [Wada et al., 1997, Freund and Wranne, 1986, Aaslid and Brubakk, 1981]. The main advantage of this technique, is the ability to make non-invasive measurements in central structures such as the aorta or carotid arteries.

2.4 Blood Pressure Data

Three separate sets of data were used in this study: (i) Invasive DB, (ii) Integrated DB, and (iii) Soft exhalation maneuver (SEM) data. The SEM data is only used in Chapter 7 and will be explained there. Table 2.3 summarizes the characteristics of the sample populations for the Invasive and the Integrated datasets. The details of each these two datasets are presented next.

Table 2.3: Invasive and Integrated datasets' characteristics. Value (SD).

	Invasive DB	*Integrated DB*
N	59	2671
Male/Female	43/16	1346/1300
Age (yrs)	60.5(11.4)	57.7(18.3)
Height (cm)	172.(8.68)	170.(11.1)
Weight (Kg)	83.2(15.6)	77.9(20.1)
${}_rSP$ (mmHg)	121.(12.7)	136.(20.5)
${}_rDP$ (mmHg)	59.1(10.9)	77.0(11.4)

2.4.1 Invasive Database

These data was collected for a previous study [Pauca et al., 2001]. The invasive measurements were completed in 62 subjects undergoing cardiac surgery. The equipment and methodology used were initially described by Pauca et al. [1992]. Fluid-filled manometer systems were used. Blood pressure was measured from the radial artery and ascending aorta using a 20-gauge, 91.4 cm long, Teflon catheter. Recordings were obtained simultaneously during a period of 2 to 5 minutes. Anthropometric data was recorded. Table 2.4 summarizes the characteristic of the Invasive DB.

[The provision of the data by Dr. Alfredo Pauca (Wake Forest University School of Medicine, North Carolina, United States) during his sabbatical visit to the Graduate School of Biomedical Engineering, University of New South Wales, in 1997 is greatly acknowledged.]

Table 2.4: Invasive DB population characteristics ($N : 59$). Outlier due to incorrect measurement.

	Min	*Max*	*Avg.*	*Std*	*Outliers*
Gender (M:1, F:0)	0	1	0.729	0.448	0
Age (yrs)	34	84	60.5	11.4	0
Height (cm)	150	189	172.	8.68	0
Weight (Kg)	54	112	83.2	15.6	0
${}_rSP$ (mmHg)	89	149	121.	12.7	0
${}_rDP$ (mmHg)	34	91	59.1	10.9	0
${}_aSP$ (mmHg)	84	149	105.	14.1	0
${}_aDP$ (mmHg)	36	93	59.7	11.2	0
${}_aAIx$	0.64	2.27	1.40	0.360	1

2.4.2 Integrated Database

A centralized and integrated database was created with data collected from seven different studies of central pressure conducted in different sites in Australia. The data was collected with the *SphygmoCor*® instrument, which consists of four distinctive parts as shown in Figure 2.2: (1) Tonometer for waveform measurement, (2) Blood pressure cuff for calibration, (3) Data acquisition box for analogue to digital conversion of waveform signal, and (4) Personal computer with *SphygmoCor*® software for data collection, storage and presentation. The databases were analyzed outside the *SphygmoCor*® software environment. Data was integrated in a single database. The database platform used was *MySQL*® *4.1*. Due to the nature of the original studies, the number of readings of BP per subject was not constant. Therefore, for each subject only the measurement corresponding to median HR was selected. The selection was done using SQL commands in *MySQL*® *4.1*. Data was exported to *Mathematica*™ *5.0* for analysis using a Java™ link. The available fields in the Integrated DB and the SQL commands used to select for median HR are presented in Appendix C. Subjects younger then 18 years of age were not included because the brachial to central general transfer (GTF) function, used in the derivation of the central aortic parameters, was determined for adults only [Karamanoglu et al., 1993, Chen et al., 1997].

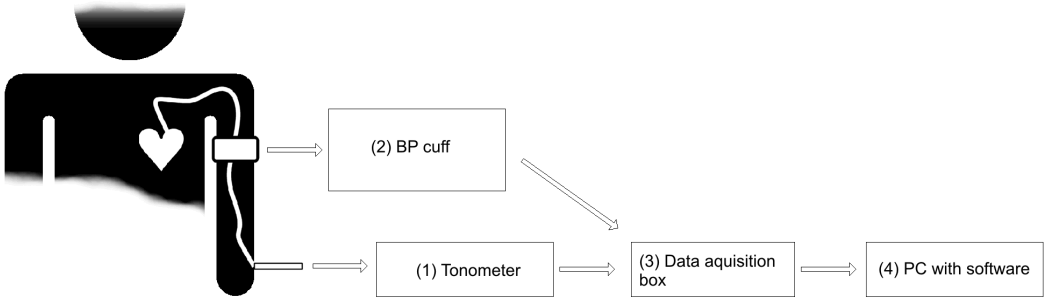

Figure 2.2: The *SphygmoCor*® Instrument consists of four distinctive parts: (1) Tonometer, (2) Blood pressure cuff, (3) Data acquisition box, and (4) Personal computer with *SphygmoCor*® software.

Table 2.5: Integrated (non-invasive) DB population characteristics ($N : 2671$). Outlier due to missing values or incorrect non-physiological measurements.

	Min	*Max*	*Avg.*	*Std*	*Outliers*
Gender (M:1, F:0)	0	1	0.509	0.500	25
Age (yrs)	19	101	57.7	18.3	3
Height (cm)	112.	204.	170.	11.1	897
Weight (Kg)	39.	180.	77.9	20.1	847
${}_rSP$ (mmHg)	70.	227.	136.	20.5	0
${}_rDP$ (mmHg)	32.	130.	77.0	11.4	0

The population includes both healthy and diseased subjects. The complete range of conditions for the diseased subjects is not known. These data included subjects' gender, height, weight, HR, age, ${}_rSP$, ${}_rDP$, ${}_rMP$, ${}_a\widehat{SP}$, ${}_a\widehat{DP}$, ${}_a\widehat{AIx}$, ED, ${}_rWave$ and ${}_a\widehat{Wave}$, along with other parameters not used in this study. A total of 2671 records were available with BP $Wave$s. Only 1727 measurements were available in which age, gender, height, weight, and ${}_aAIx$ were known. Table 2.5 presents the characteristics of the population of the Integrated DB.

The radial BP $Wave$ was obtained by applanation tonometry and central BP was estimated using the GTF estimation option (EO) using the *SphygmoCor*® device. The details of the GTF EO are presented in Chapter 4 section 4.2.

The measurement of BP was presented as the supporting background for the topics presented in the subsequent chapters. Next chapter will present a new metric

to describe the radial BP pulse, which will provide a way to describe and manipulate the $Pulse$ shape in a consistent way.

3

Representation of the Radial Pressure Pulse: The Radial Pressure Pulse Space

BP *Pulse*s, although basically similar, can have different morphology from person to person. Their shapes are related to subject characteristics, and one who is familiar with the *Pulse* shape will be able to differentiate a *Pulse* from a young or an old person. However, this qualitative analysis is not sufficient to give a quantitative answer to questions like: What is the minimum set of information to describe a *Pulse*? What are 'similar' *Pulse*s? What are possible human *Pulse*s? Are *Pulse*s distributed in a certain way? To provide answers to these questions, a metric has to be defined that makes it possible to compare the pulses.

There are two main difficulties in the representation of the *Pulse*: (i) *Pulse* length, and (ii) information redundancy. *Pulse* length varies with HR, and so does its representation as an array of points (when sampling rate is constant). This difference in length makes the comparison of *Pulse*s difficult. The second difficulty, information redundancy, refers to the fact that most of the values representing the *Pulse* are highly correlated. This high correlation is due to physiological restrictions in the human *Pulse*.

The *Pulse* has been represented in different ways, but these problems have not been properly addressed. A common representation of the *Pulse* is by its features (maximum (SP), minimum (DP), augmentation (AIx), etc...) instead of using a list of BP values. Although, a common approach, this is not strictly a representation of

the $Pulse$ but the description of a set of preestablished features.

A method based on the Fourier decomposition of the $Pulse$ [Camacho et al., 2004] has also been used. Although this method makes use of all information of the pulse, and the waves are represented by an n dimensional vector (not a variable list of numbers), there are three main difficulties in using this method: (i) the elements of the vector are highly correlated, (ii) the vector elements do not provide a meaningful physiological representation, and (iii) the method is based on signal periodicity and stationarity, which is not necessarily true for the ${}_rPulse$.

In order to overcome the difficulties associated with the representation of the $Pulse$, an n-dimensional orthogonal pulse pressure space ($\mathbb{P}$) is defined based on principal components (PC) transformation. PC transformation is an efficient way of identifying patterns in data, expressing the data in such a way as to highlight their similarities and differences [Smith, 2002b]. Mathematically, it is a multidimensional rotation in which a maximum representation of variance is obtained for a defined number of variables making it a good tool for dimensionality reduction. Therefore, if each point in $\mathbb{P}$ represents a $Pulse$ shape, this will be the best linear representation of such pulse with n different variables. Based on the defined $\mathbb{P}$, the distribution of subpopulations within the $\mathbb{P}$ were analyzed. As each point in $\mathbb{P}$ represents a specific $Pulse$ shape, different distributions within $\mathbb{P}$ are associated with differences in the $Pulse$ shape.

3.1 Methods

The process of defining $\mathbb{P}$ using PC transformation consists of two parts: (i) limitation of the length of the ${}_rPulse$ to 0.43 seconds and (ii) the PC analysis of the ${}_rPulse$, based on a sample population described next.

3.1.1 Data

Data collected from seven different studies in Australia, in which radial arterial pulse was measured, was integrated in a single database. A total of 2671 subjects (age 19-101 yrs, 1300 female), with subject's basic information (SBI) — age, gender, height, weight, radial systolic and diastolic BP — were available. Radial artery pulses were obtained by applanation tonometry and calibrated with sphygmomanometer reading of ${}_rSP$ and ${}_rDP$, using the *SphygmoCor*® instrument. The data used is described in detail in Chapter 2 in section 2.4 as the Integrated DB.

3.1.2 Limitation of Radial Pulses to the Initial 0.43 Seconds

Because for the PCA the data vectors have to be of constant length, the $Pulse$s were limited to a constant length of 55 sample points (sampled at 128 samples / sec) that correspond to 0.43 seconds. The selection was made to include all the available measurements (except one that was considered an outlier due to its high heart rate at rest $\approx 180BPM$). Although this restricts the analysis to $Pulse$s with a maximum HR of 140 BPM, over 95% of the population (at rest) will be included. The initial 55 data points of the $Pulse$ are called the 'head' and the rest the 'tail'. Because the PC vectors are of a defined length (55 pts) and the $Pulse$s are of variable length, the tails are not modeled by the PC. To assess the amount of information lost during this process, the BP values from sample 56 onwards (i.e., the tails) were reconstructed by linear regression from the corresponding PC scores and errors were analyzed. For example, the first point of the tail, i.e., sample point 56 of the ${}_rPulse$ was reconstructed using equation 3.1. The coefficients k_1 to k_{55} of equation 3.1 were calculated by linear regression using the complete dataset.

$$tail_{56} = k_{56,0} + k_{56,1}s1 + \ldots + k_{56,55}s55 \tag{3.1}$$

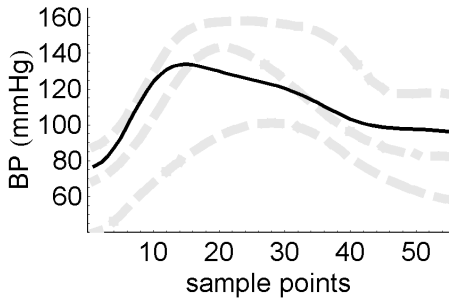

Figure 3.1: Dark solid line: ${}_rPulse$ average ($\overline{{}_rPulse}$). Thick dashing lines: three sample ${}_rPulse$s. The $\overline{{}_rPulse}$ is an order 0 approximation to the sample ${}_rPulse$s.

3.1.3 Principal Components Analysis

Principal component analysis (PCA) is a method to identify patterns in data. Therefore, it can be used to identify patterns in the ${}_rPulse$, in particular in the ${}_rPulse$ heads.

The data, as previously explained, consists of the first 55 sample points (i.e., the head) of 2671 observations of the ${}_rPulse$.[1] An average ${}_rPulse$ ($\overline{{}_rPulse}$) is the first common pattern to all ${}_rPulse$s, and it can be used as a first approximation for their description, as shown in Figure 3.1. This is an order 0 approximation because 0 values (i.e., no values) are associated to each ${}_rPulse$ for their description.

If one value (v) is associated with each ${}_rPulse$ (i.e., an order one approximation) a more accurate representation is possible. For example if the value represents the difference in the mean values between the $\overline{{}_rPulse}$ and each ${}_rPulse$ the estimates will have a correct mean value, as shown in Figure 3.2. The addition (or substraction if v is negative) of a constant value to the $\overline{{}_rPulse}$ can be expressed as:

$$\begin{aligned} \widehat{{}_rPulse_i} &= \overline{{}_rPulse} + v_i \\ &= \overline{{}_rPulse} + \text{vector of 1s} \times v_i \end{aligned} \tag{3.2}$$

However, the use of a 'vector of 1s' is not the best selection in terms of maximizing the description of the variance of the ${}_rPulse$s. What is the best vector to use? The answer is the first PC vector (**PC1**), shown in Figure 3.4a. The v used to describe

[1] In this section ${}_rPulse$ will refer to the ${}_rPulse$ head.

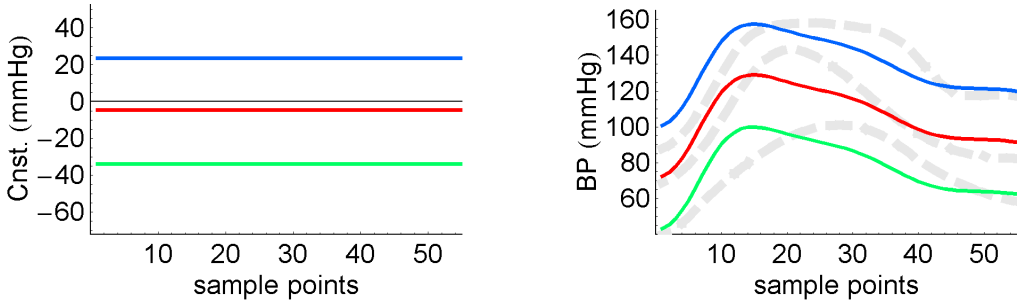

(a) 'vector of 1s' × Δmean **(b)** $\overline{{}_rPulse}$ + 'vector of 1s' × Δmean

Figure 3.2: Estimation of ${}_rPulse$s. Plot (a) shows the 'vector of 1s' × Δmean′ to adjust for mean values. Plot (b) shows the three estimated $\widehat{{}_rPulse}$, by adding the vectors in plot (a) and the $\overline{{}_rPulse}$. Three original sample ${}_rPulse$ plotted with thick dashing lines.

the ${}_rPulse$s is called the PC score (s1). Note that there is one s1_i for each ${}_rPulse_i$ that indicates how much of the **PC1** vector (i.e., the common pattern) is present in ${}_rPulse_i$ after removing the $\overline{{}_rPulse}$. The representation of ${}_rPulse$s using $\overline{{}_rPulse}$ and **PC1** is shown in Figure 3.3, first row. In a formal representation $\widehat{{}_rPulse}$ can be expressed as:

$$\widehat{{}_rPulse_i} = \overline{{}_rPulse} + \mathbf{PC1} \times \text{s1}_i \tag{3.3}$$

The representation of ${}_rPulse$ can be further improved if an additional value (s2) is used. In a formal representation

$$\widehat{{}_rPulse_i} = \overline{{}_rPulse} + \mathbf{PC1} \times \text{s1}_i + \mathbf{PC2} \times \text{s2}_i \tag{3.4}$$

The vector **PC2**, Figure 3.4b, that maximizes the representation of ${}_rPulse$ variance is the second PC vector, and the values s2 are the second PC scores. The estimation of ${}_rPulse$ with the first two PC is shown in Figure 3.3, second row.

Approximations of higher orders $(3, 4, \ldots, 54)$ are also possible. Order 55 is not an approximation but an exact representation of the ${}_rPulse$s, and higher order will have redundant information. Equation 3.4 can be extended up to order 55 and be

expressed in matrix form as

$$\begin{aligned}\begin{bmatrix} \widehat{{}_rPulse_1} \\ \vdots \\ \widehat{{}_rPulse_N} \end{bmatrix} &= \overline{{}_rPulse} + \begin{bmatrix} \mathrm{s1}_1 & \cdots & \mathrm{s55}_1 \\ \vdots & & \vdots \\ \mathrm{s1}_N & \cdots & \mathrm{s55}_N \end{bmatrix} \begin{bmatrix} \mathbf{PC1} \\ \vdots \\ \mathbf{PC55} \end{bmatrix} \\ &= \overline{{}_rPulse} + \quad \mathbf{scores} \quad \cdot \quad \mathbf{Mtx}\end{aligned} \tag{3.5}$$

An important characteristic of the PC vectors ($\mathbf{PC1}, \mathbf{PC2}, \ldots$) is their mutual orthogonality. That is, their shapes are independent from each other, and no one PC vector ($\mathbf{PC}_i$) can be represented as a linear combination of the others. This is expected because if this were not the case, it would be possible to vary $\mathbf{PC}_i$ and still obtain the same representation of the ${}_rPulse$s. This would contradict the maximum variance representation property of the PC vectors.

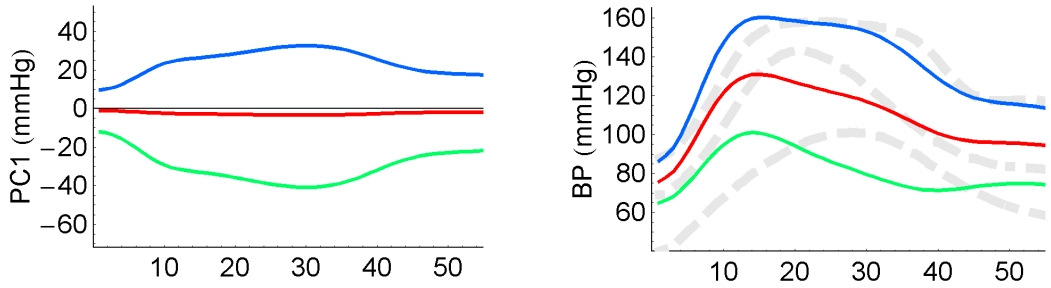

(a) **PC1** × s1

(b) $\overline{{}_rPulse}$ + **PC1** × s1

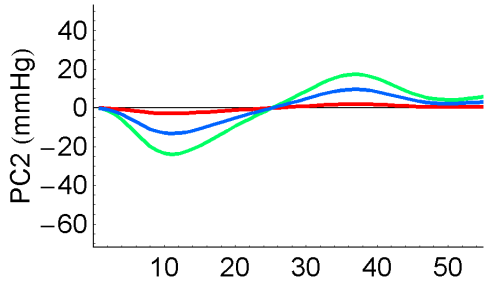

(c) **PC2** × s2

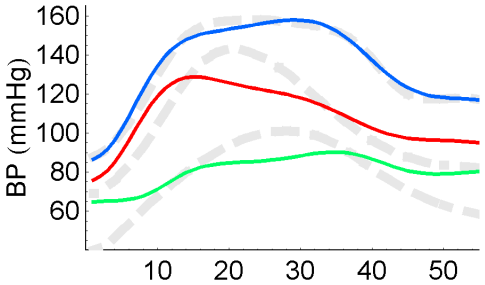

(d) $\overline{{}_rPulse}$ + **PC1** × s1 + **PC2** × s2

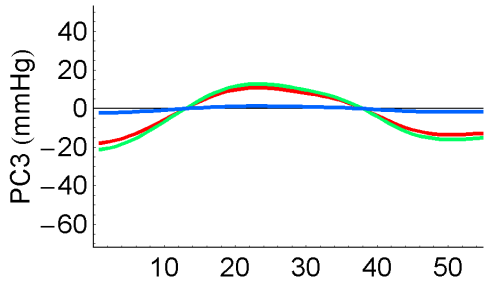

(e) **PC3** × s3

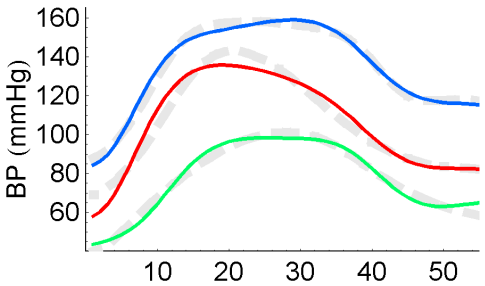

(f) $\overline{{}_rPulse}$ + **PC1** × s1 + **PC2** × s2 + **PC3** × s3

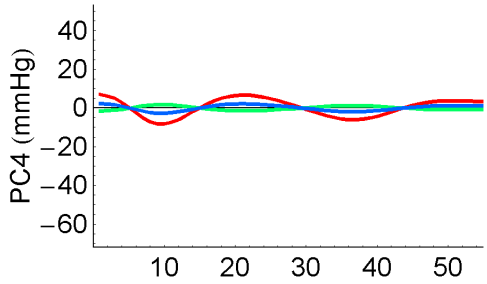

(g) **PC4** × s4

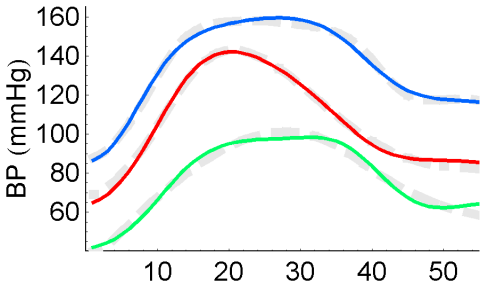

(h) $\overline{{}_rPulse}$+**PC1**×s1+...+**PC4**×s4

Figure 3.3: Estimation of ${}_rPulse$s. Left plots: PC vectors times the corresponding PC scores. Right plots: Reconstruction of $\widehat{{}_rPulse}$ (thin lines) using 1 (first row) to 4 (last row) PC for three sample ${}_rPulse$s (thick dashing lines). x axes in sample points.

Mathematical derivation of PC

The description of the derivation of the PC vectors and scores will be based on equation 3.5. The elements of equation 3.5 are: (i) measured ${}_rPulse$s (known), (ii) $\overline{{}_rPulse}$(known), (iii) PC scores: **scores** (unknown), and (iv) PC vectors: **Mtx** (unknown).

Without loss of generality the ${}_rPulse$s can be replaced by the ${}_rPulse$s - $\overline{{}_rPulse}$ to obtain

$$\begin{bmatrix} \widehat{{}_rPulse_1}' \\ \vdots \\ \widehat{{}_rPulse_N}' \end{bmatrix} = \begin{bmatrix} \mathrm{s1}_1 & \cdots & \mathrm{s55}_1 \\ \vdots & & \vdots \\ \mathrm{s1}_N & \cdots & \mathrm{s55}_N \end{bmatrix} \begin{bmatrix} \mathbf{PC1} \\ \vdots \\ \mathbf{PC55} \end{bmatrix} \tag{3.6}$$

$$= \quad \mathbf{scores} \quad \cdot \quad \mathbf{Mtx}$$

where $\widehat{{}_rPulse_i}' = \widehat{{}_rPulse_i}' - \overline{{}_rPulse}$.

Mtx (i.e., the PC vectors) is calculated first. Conceptually, the PC vectors point in the directions of maximum data variance. **PC1** points in the direction of maximum variance for all data. **PC2** points in the direction of maximum variance orthogonal to **PC1**. **PC3** points in the direction of maximum variance orthogonal to **PC1** and **PC2**, and the same for all the remaining $\mathbf{PC}_i$. Therefore, with all 55 PC vectors, a new set of orthogonal coordinates is created with which the original data can be described exactly. The PC transformation performs a multidimensional rotation of the data (in a 55 dimensional space for the case discused in this study) to eliminate cross-correlation.

To calculate the PC vectors, the covariance matrix (*cov*) of the data is calculated. The eigenvectors of *cov* correspond to the PC vectors. The eigenvalues of *cov* indicate the value of variation in the direction of the corresponding eigenvector. The PC vectors (i.e., the eigenvectors) are sorted by magnitude of their corresponding eigenvalues [Smith, 2002a].

Once **Mtx** (i.e., the PC vectors) is calculated, it is straightforward to calculate

the **scores** from equation 3.6. **Mtx** is an invertible matrix as all PC vectors are orthogonal (therefore independent from each other). Therefore the **scores** can be calculated from

$$\mathbf{scores} = \begin{bmatrix} \widehat{{}_rPulse_1}' \\ \vdots \\ \widehat{{}_rPulse_N}' \end{bmatrix} \cdot \mathbf{Mtx}^{-1} \tag{3.7}$$

It is possible to reconstruct $\widehat{{}_rPulse}$ using a limited number of PC vectors, as explained earlier. This could be done by simply replacing the corresponding PC vector with a vector of 0s in **Mtx** or by removing the corresponding columns in **scores** and vectors in **Mtx**.

The variance of the estimated PC was analyzed using the bootstrap technique (explained in detail in Chapter 5 section 5.1.1) using 196 bootstrap samples.

Most mathematic and data analysis software packages provide tools for PC analysis. For this study, the algorithms were custom made in *Mathematica*™ *5.0*. The resulting **Mtx** and $\overline{{}_rPulse}$ derived in this study are available in Appendix B.

3.1.4 Information Content of Principal Components

*Pulse*s were reconstructed using reduced number of PC (1 to 20). The differences between original and estimated *Pulse*s were analyzed and the differences measured by root mean square (RMS) errors.

3.1.5 Distribution of Specific Subpopulations in ℙ

The dependency of the ${}_rPulse$ shape with specific subpopulations' characteristics can be analyzed by comparing their PC scores distributions with that of the total population. Three specific subpopulations where analyzed: (i) Younger ($\leq$ 40 yrs), (ii) Female, and (iii) Low HR ($\leq$ 55 BPM).

3.2 Results

From the PC decomposition of the 2671 ${}_rPulse$, a set of 55 (Figure 3.4) PC orthogonal vectors of length 55, and a set of PC scores (2671 × 55) associating each original ${}_rPulse$ with a PC vector, were obtained. The PC vectors are, by definition, organized in such a way that the first PC represents a maximum possible amount of variance. The resulting PC shapes are presented in Figure 3.4 and the distributions of the PC scores for the total population are presented in Figure 3.5. The results of a bootstrap variance analysis of the estimated PC vectors is presented in Figure 3.4.

The ${}_rPulse$ can be reconstructed from its associated scores. If all PCs are used, the reconstructed ${}_rPulse$ head is identical to the original. The tail cannot be reconstructed identical to the original because information is lost when the length were reduced to 55 pts. Figure 3.6 shows the result of such reconstructions for six randomly selected waves. The heads and tails were reconstructed from the first 12 PC. The errors of the tails are presented in Figure 28.

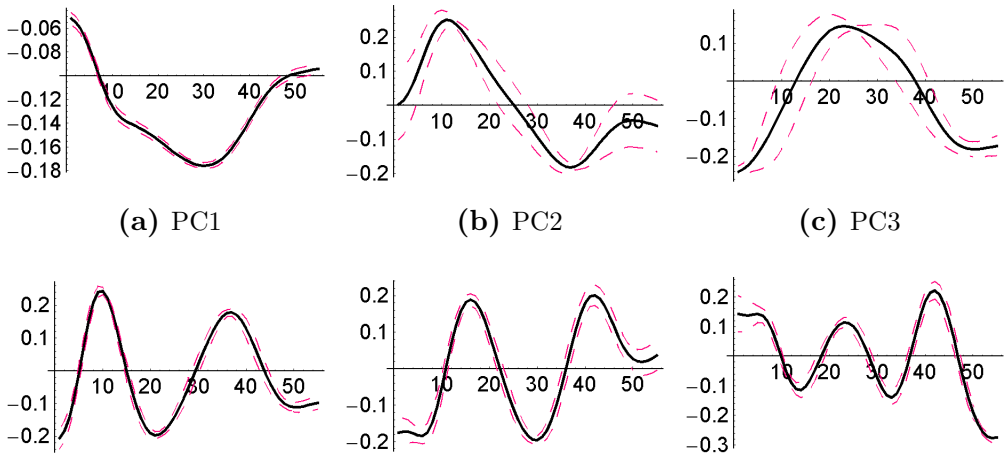

(a) PC1 **(b)** PC2 **(c)** PC3

(d) PC4 **(e)** PC5 **(f)** PC6

Figure 3.4: Estimated first six PC vectors (Mean and 95% CI). x axis in samples (128 samples/sec). y axis is dimensionless.

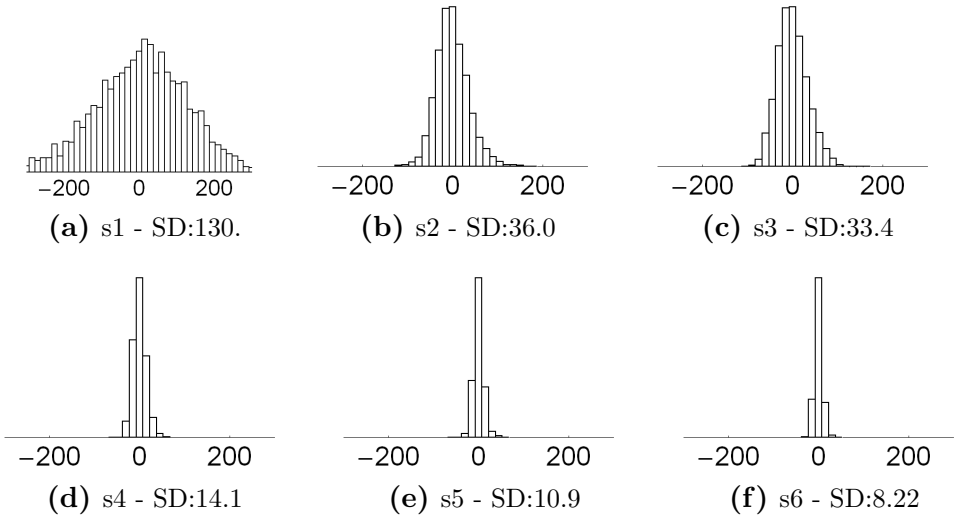

(a) s1 - SD:130. **(b)** s2 - SD:36.0 **(c)** s3 - SD:33.4

(d) s4 - SD:14.1 **(e)** s5 - SD:10.9 **(f)** s6 - SD:8.22

Figure 3.5: Distribution of the first six PC scores. Standard deviation (SD) in mmHg.

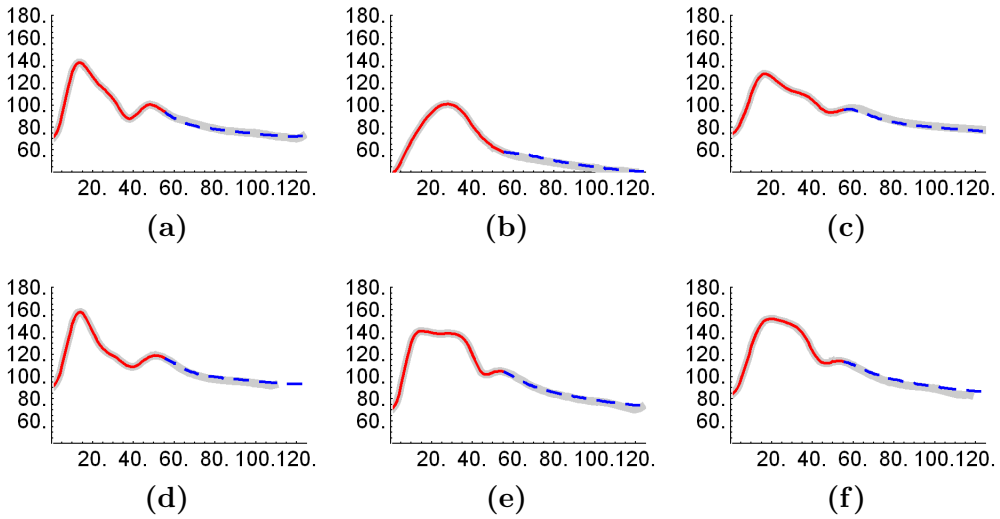

(a) **(b)** **(c)**

(d) **(e)** **(f)**

Figure 3.6: Estimated ${}_rPulse$ heads and tails. Original ${}_rPulse$ represented with thick line. Estimated head with dark thin line. Estimated tail with thin dashed line. x axis in samples (at 128 samples per second). y axis in mmHg.

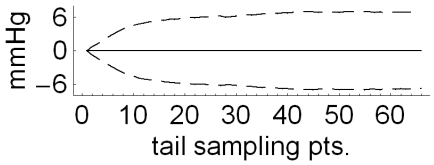

Figure 3.7: Error of tails estimation (Mean and 99% CI). Tail sampling point 0 corresponds to ${}_rPulse$ sampling point 55. Therefore, the error for the reconstruction of tail sampling 0 (i.e., sampling point 55 of PC vector) is 0.

Subpopulations

The distribution of the PC scores of three different subpopulations were compared with that of the total population for the first 4 PC.

Subpopulation of subjects less then 40 yrs

From the total population (2671 observations) 661 subjects were 40 years old or younger. The distribution histograms of the PC scores are presented in Figure 3.8. The distribution of PC 1 is shifted to the right, while the distribution of PC 3 is shifted to the left.

Table 3.1: Statistical comparison of PC for subpopulation of age 40 yrs or younger. CI_T: Confidence interval for total population. $Means_S$: Mean value for subpopulation. CI_S: Confidence interval for subpopulation.

	PC1	PC2	PC3	PC4
CI_T	(-5.0,5.0)	(-1.4,1.4)	(-1.3,1.3)	(-0.55,0.55)
$Means_S$	79.	3.6	-23.	3.5
CI_S	(71.,87.)	(1.5,5.8)	(-25.,-21.)	(2.5,4.5)

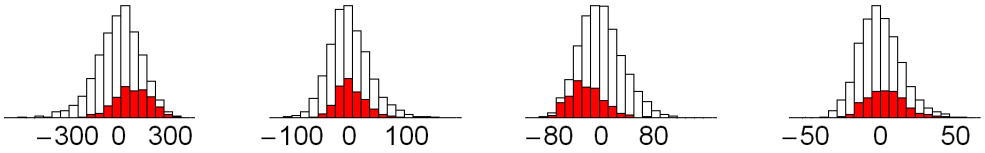

(a) PC1 **(b)** PC2 **(c)** PC3 **(d)** PC4

Figure 3.8: Distribution of PC scores for subpopulation of age 40 yrs or younger (N:661). Unshaded bars refer to whole population. Filled bars to subpopulation.

Subpopulation of female

From the total population (2671 observations) 1300 subjects were females. The distribution histograms of the PC scores are presented in Figure 3.9. The distribution of the PCs for the subpopulation are similar to the total population. There is no statistical difference between the *Pulse* shape (i.e., statistical difference in the

mean values for the PC1, PC2, PC3, and PC4 distributions with 95% confidence) for females and the total population, as is the case with Age and HR.

Table 3.2: Statistical comparison of PC for subpopulation of females. CI_T: Confidence interval for total population. $Means_S$: Mean value for subpopulation. CI_S: Confidence interval for subpopulation.

	PC1	PC2	PC3	PC4
CI_T	(-5.1,5.1)	(-1.4,1.4)	(-1.3,1.3)	(-0.55,0.55)
$Means_S$	8.4	-2.7	-0.76	2.1
CI_S	(0.81,16.)	(-4.7,-0.73)	(-2.7,1.1)	(1.3,2.8)

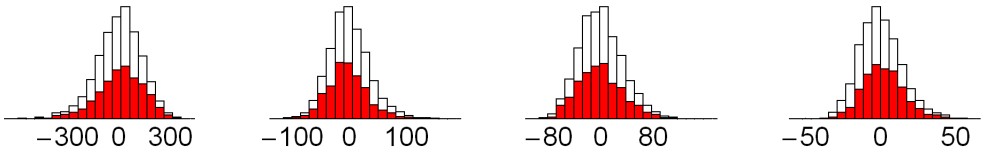

(a) PC1 **(b)** PC2 **(c)** PC3 **(d)** PC4

Figure 3.9: Distribution of PC scores for subpopulation of females (N:1300). Unshaded bars refer to whole population. Filled bars to subpopulation.

Subpopulation of subjects with HR less then 60 BPM

From the total population (2671 observations) 701 subjects have a HR $\leq$ 60 BPM. The distribution histograms of the PC scores are presented in Figure 3.10. The distribution of the PCs 1 and 2 are shifted to the left. A small shift to the right is apparent in PC 3.

Table 3.3: Statistical comparison of PC for subpopulation with HR $\leq$ 60 BPM. CI_T: Confidence interval for total population. $Means_S$: Mean value for subpopulation. CI_S: Confidence interval for subpopulation.

	PC1	PC2	PC3	PC4
CI_T	(-5.0,5.0)	(-1.4,1.4)	(-1.3,1.3)	(-0.55,0.55)
$Means_S$	-41.	-26.	6.6	4.2
CI_S	(-51.,-31.)	(-28.,-24.)	(4.3,9.0)	(3.1,5.3)

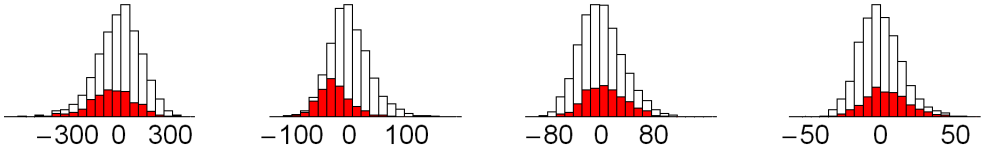

(a) PC1 **(b)** PC2 **(c)** PC3 **(d)** PC4

Figure 3.10: Distribution of PC scores for subpopulation with HR $\leq$ 60 BPM (N:701). Unshaded bars refer to whole population. Filled bars to subpopulation.

3.3 Discussion

It is impossible to measure the ${}_rPulse$ in all subjects of a population. However, the use of a metric defined by the $\mathbb{IP}$ allows for an assessment of the variability of the possible human ${}_rPulse$s. The definition of the $\mathbb{IP}$ based on PC decomposition is consistent (i.e., it does not vary from different population samples). The distribution of the ${}_rPulse$ shapes (i.e., the points in the orthogonal $\mathbb{IP}$) are close to normal distributions. This fact allows for analysis of distribution of subpopulations within the $\mathbb{IP}$.

Another use of the $\mathbb{IP}$ is the evaluation of how representative a subpopulation is according to ${}_rPulse$ shape, not to subject characteristics. In general, population samples are selected to match a certain age, gender or subject condition criteria. However, if the ${}_rPulse$ is to be analyzed, the criteria should be to include a representative set of ${}_rPulse$ shapes.

One of the major difficulties in the comparison of ${}_rPulse$s is the initial pulse synchronization. This could be one of the reasons for the greater variability of the PC 2 and 3, as well as the initial variability of PC 5 and 6.

Some possible expansion of the $\mathbb{IP}$ presented in this chapter is the addition of PC of diastolic wave shape (i.e., synchronize the pulses at beginning of diastole and make the PC decomposition of the diastolic wave only). This, or the combination of both methods, could 'differentiate' the information of cardiac ejection and wave reflection, contained in the ${}_rPulse$.

An important consideration can be raised with the question: 'Is low power infor-

mation contained in higher PC relevant?' The PC technique reduces the dimensionality of a system by discarding the less important (in terms of variance) components of a wave. These PCs can contain important information, even when variance is small. However, which and how many PC have valuable information with regard to diagnosis and/or CVR stratification is still unknown. In addition, for very high PC the variance of the PC is smaller than that of the signal to noise ratio and therefore higher PC are simply representing noise information.

Pulse shape were dependent on the subpopulation. This type of analysis can be extended to other subpopulations such as diabetics or pre-eclampsia patients. An analysis of maximum likelihood can be used within a subpopulation distributions to estimate the probability of a new subject to belong to that specific subpopulation. This could be used for either diagnosis or cardiovascular risk assessment.

3.4 Conclusions

The arterial *Pulse* can be characterized by PC. In contrast to conventional Fourier decomposition, PC analysis does not depend on signal periodicity. It is possible to relate subpopulations to ${}_rPulse$ shape. The head of the ${}_rPulse$ contains sufficient information to estimate the tails with minimum error. It is sufficient to use 8 PC to maintain 95% of the wave power. The information is contained in low frequency components of the waveshape, and therefore high fidelity instrumentation is not required for such measurement. This allows to apply PC analysis to large populations where risk stratification may be improved by mapping the PC distributions to normal and pathological conditions.

4

Framework for Parameter Definition and Error Analysis

Arterial blood pressure parameters ($\mathcal{P}$) are the final descriptors of blood pressure (BP). They provide the units for a quantifiable use of BP in any further analysis, such as medical diagnosis or risk assessment. Equation 1.1 states the important relationship between $\mathcal{P}$, $\mathcal{D}$, and $\mathcal{M}$ and therefore it is presented again as equation 4.1 in this chapter.

$$\mathcal{P} = \mathcal{D}(\mathcal{M}) + \epsilon_{\mathcal{D}} \tag{4.1}$$

A clear understanding of $\mathcal{P}$ and its associated derivation error ($\epsilon_{\mathcal{D}}$) is only possible with a complete description of $\mathcal{M}$ and $\mathcal{D}$, presented in the following sections.

4.1 Measurements ($\mathcal{M}$)

Chapter 1 gave the following definition: "Measurements refer to the 'raw' data before any further analysis or transformation". This section will expand that definition and present the different types of measurements considered in this study. The data used in this study is contained in two databases which are explained in Chapter 2 in section 2.4.

Before discussing the accuracy of measurements of BP, its dynamic characteristics and its physiological range will be presented.

4.1.1 Blood Pressure From an Instrumentation Perspective

The first step in any measurement is to know what is being measured so that the correct instrumentation can be selected.

Blood Pressure Absolute Values

The most common measurements of BP are ${}_bSP$ and ${}_bDP$. In over 99% of men, ${}_bSP$ is between 80 and 240 mmHg, and ${}_bDP$ is between 30 and 150 mmHg. Pulse pressure is not lower then 20 and not higher than 150 mmHg for the same percentage of the population [Joffres et al., 2001, Kesteloot and Joossens, 1980, Birkenhager and Reid, 1985]. Although brachial pressure (mostly ${}_bSP$) differs from central pressure, values are within the same order of magnitude and no special considerations are needed from an instrumentation point of view for its measurement. In addition to the absolute maximum (${}_bSP$) and minimum (${}_bDP$) values of BP, the transient from one to the other (i.e., BP waveshape) requires additional considerations which are explained in the following section.

Blood Pressure Wave Dynamic Characteristics

This section presents the dynamic characteristics of BP waves from a measurement perspective. It does not present the BP parameters that characterize $Pulse$s and $Wave$s, which are discussed in section 4.3. For BP measurements the power spectrum has been used as the criterion for instrument selection [Gardner, 1981]. Nichols et al. [1998] suggest that frequency components over 25 Hz can be ignored with minimal loss of information. The adoption of a maximum frequency of 25 Hz is sensible, and will be assumed correct in this document, for two reasons: (i) the main area of interest of this study is the non-invasive radial arterial BP analysis (including it's relationship with the central arterial BP) where high frequencies (over 25 Hz) will be considerably damped during pulse transmission, and (ii) the signal to noise ratio on the acquired data is such that high frequency components are swamped by noise

— power decays rapidly with frequency in the BP *Pulse*. The previous argument does not mean that BP frequency components over 25 Hz do not contain valuable information.

The characteristics of the BP from an instrumentation point of view, are summarized in Table 4.1. In addition to the instrument, the established protocols for their use during BP measurement play an important role in the quality and consistency of the measurements.

Table 4.1: Summary of BP characteristics from an instrumental point of view.

Characteristics	*Limits*
SP	80 to 240 mmHg
DP	30 to 150 mmHg
PP	20 to 150 mmHg
Frequency ranges	< 25 Hz

4.1.2 Measurement Protocols

A consistent use of the BP measurement instrumentation as well as a controlled, or at least known, state of the subject (relaxed/active, standing/sitting) are as important as the instrumentation itself.

Sphygmomanometric Blood Pressure Measurement

Due to the importance of sphygmomanometric BP measurements, the protocols have been established — and are being reviewed — by international organizations like the British Hypertension Society (BHS) [Beevers et al., 2001a,b], the National Heart, Lung, and Blood Institute (NLBI), the American Heart Association (AHA), and the Pan American Health Organization [PAH, 2003]. In this study it will be assumed that the protocol was followed for all sphygmomanometric measurements, unless stated otherwise.

Sphygmomanometer and Tonometer

No guidelines are available on how to take measurements with a combined sphygmomanometer and tonometer system. For the sphygmomanometric measurements its protocol should be followed, as explained before. For the tonometric measurements, considerations on subject condition (relaxed, active), measurement location, type of tonometer, tonometer support, operators training, and others, should be considered, as they influence the measured data. In addition, the algorithms used to analyze the data, could impose additional conditions on the measurement technique. For example, when multiple $Pulse$s from a measured $Wave$ are averaged, the subject should be in a stable condition during all the $Wave$ measurement as to minimize the variability between $Pulse$s.

4.1.3 Accuracy of Blood Pressure Measurement

The data analyzed in this study was taken either with the *SphygmoCor*® (AtCor Medical Pty Ltd, West Ryde, NSW, Australia) or with invasive high fidelity catheters and monometer systems. The invasive measurements are not analyzed in this study. They are considered correct as they were taken with high fidelity instruments. The *SphygmoCor*® device consists of two independent units: (i) sphygmomanometer for calibration, and (ii) tonometer for wave contour measurement. Their accuracy is discussed next, and the discussion of calibration with non-invasive $\mathcal{M}$, and data sampling are presented in the following sections.

The Mercury Sphygmomanometer

Even when the use of the mercury sphygmomanometer is considered the gold standard in BP measurements, several types of errors are associated with it. This errors could be correlated and are presented in the model of variance presented by Batista-Foguet et al. [2001]. Studies addressing the specific causes of error are listed in Table 4.2. Studies comparing invasive and non-invasive measurements are inconsistent,

and the International Protocol for validation of blood pressure measuring devices in adults, produced by the European Society of Hypertension, uses the mercury sphygmomanometer as the comparing unit [O'Brien et al., 2002].[1] Therefore, there are no guidelines to asses the quality of the mercury sphygmomanometer itself. It can be argued that there is no error in the pressure exerted by a column of mercury of a known hight, but the error is not in the intra-cuff pressure but in the measured intra-arterial BP.

Table 4.2: Mercury sphygmomanometer — main causes of error

Causes of Error	*Reference*
Departure from protocol	Bennett [1994]
Identical duplicate measurements	Bennett [1994]
Operator variability	Bennett [1994]
Rounding error, last digit preference to zero	Bennett [1994]
— attempt to eliminate rounding error —	Conroy et al. [1993]
Cuff size, arm circumference	Higham [1959]
Age variation	Ochiai et al. [1997]
Atherosclerosis variation	Messerli et al. [1985]
Korotkov sound vs. muffling	Breit and O'Rourke [1974]
Measurement error	Hope et al. [2004]
	Sagiv et al. [1999]
	Ochiai et al. [1997]
	O'Brien and O'Malley [1979]
	Raftery and Ward [1968]

The studies from Hope et al. [2004], Ochiai et al. [1997], Raftery [1991], O'Brien and O'Malley [1979], and Raftery and Ward [1968] agree in an underestimation of SP and an overestimation of DP. PP is only included in the study by Hope et al. [2004], showing an overestimation of the measurement. Table 4.3 summarizes their results. The study by Sagiv et al. [1999], in which BP is compared invasively and non-invasively during exercise also demonstrate a discrepancy in BP values. This study includes only 14 subjects ages 23 (SD:2) yrs.

[1]The mercury sphygmomanometer has been banned in several European countries based on environmental grounds. However, the mercury sphygmomanometer errors should be considered, even if the sphygmomanometer is completely phased out, because they will apply to any brachial cuff sphygmomanometer in which the column of mercury is replaced by any other means of cuff pressure indication.

Table 4.3: Errors between direct (invasive) and indirect (non-invasive) BP Measurements. 1:Hope et al. [2004], 2:Ochiai et al. [1997], 3:O'Brien and O'Malley [1979], 4:Raftery and Ward [1968]. Types: Mercury (Hg), auscultation (mic) and oscillometric (oscil). Some data is not available (N/A). Measurements in mmHg (SD).

	1	2			3	4
N:	42	34			N/A	20
Age:	64 (SD:12)	18-73 yrs			N/A	18-44 yrs
Type:	Hg	Hg	mic	oscil	Hg	Hg
SP	-10.(10.)	-10.6(8.1)	-8.1(9.7)	-12.2(10.5)	-10.0	-5.4(11.6)
DP	5.(7.)	+3.7(6.5)	+1.2(8.9)	+4.6(7.6)	+8.0	+11.1(8.8)
PP	15.(11.)	—	—	—	—	—

In order to reduce observer bias, Garrow [1963] proposed the 'zero-muddler for unprejudiced sphygmomanometrey'. This instrument, that after development was called the Hawksley random zero sphygmomanometer, shows an underestimation of both SP and DP against the mercury sphygmomanometer [Conroy et al., 1993]. The following questions arises: Do BP measurement instruments mimic mercury sphygmomanometer errors?

Tochikubo et al. [2001] have proposed a double-cuff sphygmotonometer to improve BP measurement readings. The instrument has proven better then conventional oscillometric and auscultatory methods. However, until his instrument is widely accepted, future studies have to account for these known errors.

In addition, when $\mathcal{P}$s are derived from $\mathcal{M}$ (that have error) and using $\mathcal{D}$ that also introduce errors, the total error (i.e., the combined error of BP measurements and $\mathcal{D}$) of $\mathcal{P}$ can not be calculated. This is an important concept that will explained in detail in the following section (4.1.4). In summary, the error of ${}_a\mathcal{P}$ estimated from the ${}_rWave$ calibrated with sphygmomanometer, is not the added error from the sphygmomanometer and the error due to the derivation method. The error is the combination of both errors that can add or cancel each other, depending on their correlation.

The Tonometer

The tonometer used for collection of the data used in this study is the pencil-type Millar Tonometer. As described by Kelly et al. [1989b] the frequency response for this instrument is over 2 kHz and the harmonics (0 to 8) for invasive and non-invasive measurements are closely correlated. Three sources of artifacts are highlighted: (i) positioning of the tonometer over the artery, (ii) hold-down force , and (iii) angulation between the probe and the vessel. Matthys and Verdonck [2002] developed a model for the analysis of the dynamic characterization of the mechanical elements affecting tonometric measurements, and the effects of applied recording force is explained in more detail by Driscoll et al. [1995].

In the analysis of the non-invasive blood pressure-monitoring instrument (JENTOW, Colin Electronics, Komaki, Japan) [Sato et al., 1993] the tissue-instrument system is considered and its filter characteristics are described. The system behaves like a low pass filter with cut off frequency at about 8 Hz. Some questions arise from the large difference in frequency response between the two instruments. Should the tissue-instrument system be considered in the Millar tonometer? Are the low frequencies of the JENTOW instrument due to post-transducer filtering? In commercially available instruments based on the Millar tonometer (*SphygmoCor*®), is there any post-tonometer filtering?

For this study, in which the ${}_rWave$ contour was measured using the pencil-type tonometer, the distortion in waveshape are not considered and ${}_rWave$ contour are assumed correct. The tonometer does not provide an absolute BP measurement; therefore, it should be calibrated. This calibration is usually done using brachial pressures measured by an oscillometric or mercury sphygmomanometer. In a recent study by Verbeke et al. [2005] the accuracy of this calibration is questioned because radial and brachial SP and DP are different.

4.1.4 Calibration with Non-Invasive Blood Pressure Measurements

Intuition suggests that a $\mathcal{P}$ derived from a waveform calibrated with invasive measurements will have less error then a $\mathcal{P}$ derived from a waveform calibrated with non-invasive measurements. This is not necessarily the case [Verbeke et al., 2005], and this section will explain why. It is not possible to know which of the two parameters have less error, unless the errors from invasive and non-invasive measurements are compared. This is important because the analysis of error of aortic parameters is based on invasive radial measurements. The error due to brachial, instead of radial, BP calibration was presented in the previous section.

Formalization of the problem

The aim is to analyze the effects on an estimated aortic parameter (${}_a\widehat{\mathcal{P}}$) when the calibration is done with non-invasive systolic (${}_{\text{non-}r}SP$) and diastolic (${}_{\text{non-}r}DP$) BP measurements instead of invasive measurements. To analyze this effect, ${}_a\widehat{\mathcal{P}}$ is estimated with the model

$$ {}_a\widehat{\mathcal{P}} = g({}_rPulse, {}_{\text{inv-}r}SP, {}_{\text{inv-}r}DP) \tag{4.2} $$

where ${}_rPulse$ is the non calibrated radial BP shape and ${}_{\text{inv-}r}SP$ and ${}_{\text{inv-}r}DP$ are the invasive measured radial systolic and radial diastolic BP respectively. The model is any function $g : \mathbb{R}^P \rightarrow \mathbb{R}$ where P is the number of independent variables. The relationship between invasive and non-invasive systolic and diastolic pressures is assumed to be

$$ \begin{aligned} {}_{inv-r}\text{SP} &= {}_{non-r}\text{SP} + {}_{\text{SP}}\epsilon \\ {}_{inv-r}\text{DP} &= {}_{non-r}\text{DP} + {}_{\text{DP}}\epsilon \end{aligned} \tag{4.3} $$

where ${}_{\text{SP}}\epsilon$ and ${}_{\text{DP}}\epsilon$ are the differences between an invasive and a non-invasive measurement. ${}_{\text{SP}}\epsilon$ and ${}_{\text{DP}}\epsilon$ are unknown but they are not necessarily random noise. The differences could be due to other factors (e.g., arterial stiffness) that in turn can even have specific effects in the subject's radial pulse (${}_{r}Pulse$).

The ${}_{r}Pulse$ can be represented as a list of P parameters x_i, $1 \leq i \leq P$.

$$ {}_{r}Pulse = (x_1, \cdots, x_P) $$

The representation itself is not relevant for this analysis, but it could be, for example, with PC as explained in Chapter 3.

Solution

The approach to demonstrate that it is not possible to know the effect of the error of non-invasive measurements in the estimation of a parameter ${}_{a}\widehat{\mathcal{P}}$ is to first solve this problem for a linear model. A linear model is a specific case of the more general non-linear model. If it is not possible to know the effects of the error in a linear model, therefore it is not possible to know the effects in the more general case.

Linear model In this model, the function g is assumed linear and therefore ${}_{a}\mathcal{P}$ can be expressed as

$$ \begin{aligned} {}_{a}\mathcal{P} &= g_{\text{linear}}({}_{r}\text{Pulse}, {}_{inv-r}\text{SP}, {}_{inv-r}\text{DP}) + {}_{\text{inv}}\epsilon \\ &= c_0 + \sum_{i=1}^{P} c_i x_i + c_{\text{SP}}({}_{inv-r}\text{SP}) + c_{\text{DP}}({}_{inv-r}\text{DP}) + {}_{\text{inv}}\epsilon \end{aligned} \tag{4.4} $$

If ${}_{r}Pulse$ is a function of ζ

$$ {}_{r}Pulse = {}_{r}Pulse(\zeta) $$

where ζ is a characteristic (not noise) not modeled by g (e.g., arterial stiffness), the model parameters will also be functions of ζ: $c_i = c_i(\zeta)$. By replacing 4.3 in 4.4 the

${}_a\mathcal{P}$ can be represented as

$$
\begin{aligned}
{}_a\mathcal{P} &= c_0 + \sum_{i=1}^{P} c_i x_i + c_{\mathrm{SP}}({}_{non-r}\mathrm{SP} + {}_{\mathrm{SP}}\epsilon) + c_{\mathrm{DP}}({}_{non-r}\mathrm{DP} + {}_{\mathrm{DP}}\epsilon) + {}_{\mathrm{inv}}\epsilon \\
&= c_0 + \sum_{i=1}^{P} c_i x_i + c_{\mathrm{SP}\,non-r}\mathrm{SP} + c_{\mathrm{SPSP}}\epsilon + c_{\mathrm{SP}\,non-r}\mathrm{DP} + c_{\mathrm{DPDP}}\epsilon + {}_{\mathrm{inv}}\epsilon
\end{aligned}
$$

But if the errors ${}_{\mathrm{SP}}\epsilon$ and ${}_{\mathrm{DP}}\epsilon$ are also functions of ζ

$$
{}_{\mathrm{SP}}\epsilon = {}_{\mathrm{SP}}\epsilon(\zeta)
$$

$$
{}_{\mathrm{DP}}\epsilon = {}_{\mathrm{DP}}\epsilon(\zeta)
$$

the covariance between the model parameters c_i and model errors will not be 0: $covar(c_i, {}_{\mathrm{SP}}\epsilon) \neq 0$ and $covar(c_i, {}_{\mathrm{DP}}\epsilon) \neq 0$. This will affect the estimated value $E({}_a\mathcal{P})$ and the variance $Var({}_a\mathcal{P})$. Also, when

$$
{}_{\mathrm{inv}}\epsilon = {}_{\mathrm{inv}}\epsilon(\zeta)
$$

the $covar({}_{\mathrm{inv}}\epsilon, {}_{\mathrm{SP}}\epsilon) \neq 0$ and $covar({}_{\mathrm{inv}}\epsilon, {}_{\mathrm{DP}}\epsilon) \neq 0$ which will also affect $E({}_a\mathcal{P})$and $Var({}_a\mathcal{P})$.

Conclusion

From this analysis it can be concluded that a correct estimation of ${}_a\mathcal{P}$ from non-invasive calibrated pulse can not be derived from the estimation of ${}_a\mathcal{P}$ from invasive calibrated pulse (4.2) and the relationships between invasive and non-invasive systolic and diastolic pressures (4.3). The previous conclusion is supported by the work by Hope et al. [2004] in which the errors between ${}_aSP$ and ${}_rSP$ measured non-invasively where smaller then the errors between ${}_aSP$ and derived ${}_a\widehat{SP}$.

Smulyan et al. [2003] specifies the cuff as the primary source of error in SphygmoCor estimates of central blood pressures and Davies et al. [2003], Cloud et al. [2003a], Hope et al. [2004] and others present the analysis of estimated ${}_a\widehat{\mathcal{P}}$ based

on non-invasive measurements. However, most of the documentation on estimation of central parameters from radial measurements is validated from invasive measurements. It is important to keep in mind, that the total error of a central parameters is not the 'addition' of errors. It is the combined effect of errors, that could even cancel out. Therefore, the only way to create a model to estimate ${}_a\widehat{\mathcal{P}}$ from non-invasive measurements is by experimentation, as presented by Smulyan et al. [2003], Davies et al. [2003], Cloud et al. [2003a]. Going a step further, if the final interest of the measurements of BP is to estimate, for example, cardiovascular risk (CR) the best model would be to estimate CR directly from the $\mathcal{M}$ without going through the extra step of estimating ${}_a\widehat{\mathcal{P}}$, as presented in Chapter 8.

4.1.5 Blood Pressure Wave Data Sampling

BP *Wave*s were recorded in a digital form. Based on the maximum frequency of the BP wave assumed to be 25Hz (see section 4.1.1) and according to the Nyquist theorem, a sampling rate of 50 samples per second will be sufficient. In practice, though, a higher sampling rate is desired to facilitate the analysis and to account for measurement errors. For most of this study, a sampling rate of 128 samples/sec was used. It is important to notice that the period (7.8 ms) is long enough to have to be considered in certain time measurements. The analog to digital conversion of the signal was not considered as a source of error in this study, because the BP resolution was of the order of 0.1 mmHg.

4.1.6 Additional Measurements to Blood Pressure

BP needs to be related to other subject characteristics or outcome for the study of cardiovascular risk or clinical diagnosis. Therefore, additional measurements were taken. Common measurements are subject's age, weight, height, gender and glucose, cholesterol, and electrolyte levels. These data, in conjunction with outcome information can be used to model their relationships and make them useful for diagnosis

or risk assessment. The errors of these data are not considered in this study and are assumed to be correct.

4.2 Derivation Methods ($\mathcal{D}$)

Cardiovascular parameters ($\mathcal{P}$) are derived from BP measurements ($\mathcal{M}$) by different methods, which in this document are referred to as derivation methods ($\mathcal{D}$). A $\mathcal{D}$ represents a series of steps to derive a $\mathcal{P}$ from a known $\mathcal{M}$. If there is no difference between the $\mathcal{P}$ and the $\mathcal{M}$, then the $\mathcal{D}$ is simply the identity function (e.g., ${}_bSP$ measured with the sphygmomanometer). On the other hand, a $\mathcal{D}$ can involve many steps, as shown in Figure 4.4. Independent of the complexity of $\mathcal{D}$, no new information is added, but errors could be introduced. Many of the steps used for a $\mathcal{D}$, involve $Pulse$ and/or $Wave$ manipulations (including wave transformation by transfer function) and specific algorithms to calculate $\mathcal{P}$ from a $Pulse$ or $Wave$. The next section presents the BP $Pulse$ and $Wave$ manipulation methods used in this study, as the background to introduce the specific types of $\mathcal{D}$. The $\mathcal{P}$ conceptual definitions are presented in section 4.3.1. The specific algorithms to calculate a $\mathcal{P}$ from a $Pulse$ or $Wave$ are presented in Chapters 5 and 6, as they are specific for each individual $\mathcal{P}$ and are strongly associated with their own definition and estimation option.

4.2.1 Blood Pressure Pulse and Wave Manipulation Methods

The methods presented in this section are conceptually simple but in their formal specification (as an algorithm) many specific considerations and assumptions have to be made. The final definition of the algorithms affect the definition of $\mathcal{D}$; hence, of the estimated $\mathcal{P}$. This section presents common $Pulse$ and $Wave$ manipulation methods that are used in the definition of the $\mathcal{D}$s used in this study.

Pulses from Waves

Continuous BP measurement instruments acquire data that represents a $Wave$. In many applications it is important to separate each individual $Pulse$ from the $Wave$. This is a conceptually simple task, that consists in finding the $Pulse$'s foot (or starting point) and the $Pulse$'s ending point (i.e., the following $Pulse$'s foot). The $Pulse$'s foot could be defined as the minimum value before the highest BP rise. The main drawback of this approach is that $Pulse$'s time related features are not synchronized because the initial rise in BP is slow and variable from $Pulse$ to $Pulse$.

Another approach, which is the one adopted in this study, is the '2nd derivative' method. The method consists in finding the minimum value of the 2nd derivative of the BP. This method provides good features synchronization. Its main drawback is that the initial BP value of the $Pulse$ does not coincide with the minimum BP of the end of diastole of the previous $Pulse$.

Average Pulse

The main advantage of averaging several $Pulse$s is that if the original $Pulse$s are all identical in shape plus added random noise, the average signal will tend to the original $Pulse$ shape and noise will cancel out due to its random nature. But in practice, many factors have to be considered. If all $Pulse$s are not identical and contain features that differ from one another, these features will tend to fade away. If $Pulse$s are not well synchronized then features of the different $Pulse$s will become 'blurred' with other features. In addition, if the heart rate is not constant or ectopic $Pulse$s exist (which is physiologically common), it does not make sense to average the $Pulse$s.

Parameters from Pulses and Waves

The details of the algorithms to estimate $\mathcal{P}$s from a $Pulse$ or $Wave$ are explained in detail in section 4.3, where the conceptual definitions of the $\mathcal{P}$ are presented.

Transfer Functions ($\mathcal{T}$)

A transfer function can be considered as a $Wave$ manipulation method, with which the ${}_{r}Wave$ can be transformed to a ${}_{a}Wave$. However, it is not only a $Wave$ manipulation method. It is a model that represents the changes in BP from the radial artery to the aorta. Therefore, the transfer function concept is explained in detail in the next section in which the concept of a model is discussed.

4.2.2 Models

A model is a representation of a system, that facilitates its analysis and understanding. Models can be mechanistic or empirical. A mechanistic model is based on a mathematical description of physical phenomena in contrast to an empirical model in which relationships are represented by mathematical functions without a physical meaning. A model is based on experimental data, and the process of adjusting the model parameters to best represent the data is referred to as 'training' or 'fitting'. Some of the $\mathcal{D}$ used to estimate $\mathcal{P}$ from $\mathcal{M}$ are based on models. That is the case of the generalized transfer function ($\mathcal{D}_{\mathcal{T}_G}$), in which the $\mathcal{D}$ is based on a model of the transfer function of the brachial arterial vasculature. The specific details on the 'training' of the $\mathcal{D}$ (i.e., the training of the models) with specific data is presented in section 4.2.3 for the generalized transfer function ($\mathcal{T}_G$). For linear models, as they are specific for each $\mathcal{P}$, the 'training' is presented in Chapters 5 and 6 along with the analysis of the quality of all models. The two models used in the $\mathcal{D}$s used in this study are presented next. The reasons why non-linear models were not use in this study, despite the non-linear nature of wave propagation in the arterial system [Langewouters et al., 1984, Pythoud et al., 1996], are presented in page 63 in section 'Non-Linear Derivation Method'.

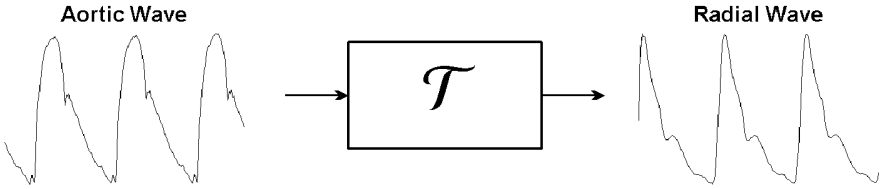

Figure 4.1: Transfer function. The aortic BP waveform is different from the radial BP waveform. The network of vessels that modulate (changes) the waveform can be modeled by a transfer function ($\mathcal{T}$)

Linear Model

A linear model is of the form:

$$\hat{y} = c_0 + c_1 x_1 + c_2 x_2 + \ldots + c_i x_i \tag{4.5}$$

for i independent variables (x) and dependent variable y. The parameters c_i are estimated to minimize certain loss function (L) which is usually given by

$$L = \sum (y - \hat{y})^2$$

which correspond to the minimization of residuals.

Transfer Functions ($\mathcal{T}$)

A system's transfer function ($\mathcal{T}$) is a model that characterizes the transformation of a signal that passes through it. In this analysis the system is the network of vessels from the aortic root to the radial artery at wrist level and the signal is the BP waveform, as represented in Figure 4.1.

Table 4.4 shows the different $\mathcal{T}$ used in this study. Note that the symbol $\mathcal{T}$ refers to transfer function in general and the subindexes G, B, and W refer to General, Brachial, and Wave Model respectively.

Because of physiological differences, each individual subject has a theoretically different $\mathcal{T}_B$. In general it is important that the anatomical factors dominate over physiological conditions in determining the $\mathcal{T}_G$ [Chan, 1997], but not for all subjects.

Table 4.4: Transfer functions ($\mathcal{T}$)

Symbol	*Description*
$\mathcal{T}_B$	Brachial transfer function
$\mathcal{T}_G$	General transfer function
$\mathcal{T}_W$	Wave model transfer function
$\mathcal{T}_{ShygmoCor}$	Unknown *SphygmoCor*® $\mathcal{T}$.
$\mathcal{T}_{SCor}$	$\mathcal{T}$ for the *SphygmoCor*® derived in this study.

Note: $\mathcal{T}_G$ and $\mathcal{T}_W$ are both types of $\mathcal{T}_B$.

An accurate mathematical definition of the $\mathcal{T}_B$ could be very complex, but a simplified representation of the $\mathcal{T}_B$ was first proposed by Karamanoglu et al. [1993] as a general transfer function ($\mathcal{T}_G$). The $\mathcal{T}_G$ approach has also been supported by others [Chen et al., 1997, Takazawa et al., 1996] as well as criticized [Soderstrom et al., 2002, Hope et al., 2003a, Cloud et al., 2003a,b, Millasseau et al., 2003a,b, Hoeks et al., 2003, Williams, 2004]. To resolve the controversy on the validity of the use of the $\mathcal{T}_G$ for estimating central aortic parameters, the derivation and accuracy of the parameters themselves has to be studied within a consistent framework, as presented in Chapters 5 and 6. It is important to notice that the analysis of variance of the parameters has to include the variance of the $\mathcal{T}_G$ itself, which was not done in previous studies. If the interest of the $\mathcal{T}_G$ is to have a model for the general population (and not to derive central aortic parameters) no consideration on the parameters is required. Due to its importance such derivation from invasive BP measurements is described in the following section. It is worth mentioning that the derivation of $\mathcal{T}_G$ is performed for each iteration in the analysis of accuracy, based on the Bootstrapping method, of derived central parameters as explained in section 5.1.1.

The non-invasive data used in this study (i.e., the Integrated DB) was collected using the *SphygmoCor*® instrument. Its specific $\mathcal{T}_G$ (i.e., $\mathcal{T}_{ShygmoCor}$) was also derived as shown in section 4.2.4.

4.2.3 Derivation of a Generalized Transfer Functions ($\mathcal{T}_G$)

A generalized transfer function ($\mathcal{T}_G$) refers to a brachial transfer function ($\mathcal{T}_B$) defined for a population instead of an individual. Of course this is an approximation to the individual $\mathcal{T}_B$.

Two models of representing $\mathcal{T}_G$, the infinite impulse response (IIR) and finite impulse response (FIR) filters, will be presented. The method to model a $\mathcal{T}_G$ from invasive data with an IIR filter will follow, concluding with an analysis of the validity of the IIR representation.

$\mathcal{T}_G$ Representation

The $\mathcal{T}_G$ can be represented with different types of models. The models used in this study are the IIR and FIR filter models, because they have already been used and presented in the literature [Avolio et al., 2001, Chen et al., 1997], commonly referred to as ARX models because of the derivation method used.

Infinite Impulse Response (IIR) Representation of $\mathcal{T}_G$. The model is of the form

$$Y = \frac{B}{A}U$$

or in a more complete form

$$Y(k) = \frac{b_0 + b_1 z + \ldots + b_q z^q}{1 + a_1 z + \ldots + a_s z^s} U(k)$$

were Y is the output of the system, U is the input, A and B are the polynomials $A = 1 + a_1 z + \ldots + a_s z^s$ and $B = b_0 + b_1 z + \ldots + b_q z^q$ and z is the lag operator: $f(k)z = f(k-1)$.

As an example of an IIR model, the polynomials used in the $\mathcal{T}_{SCor}$ are presented here. The derivation of these coefficients was not based on the analysis of invasive data but by reverse engineering the *SphygmoCor*® instrument. The details of the

derivation are presented in section 4.2.4. The coefficients are:

$$\begin{aligned} A =& 1 - 1.03713z - 0.0553583z^2 + 0.0641736z^3 + 0.0509342z^4 + 0.00730289z^5 \\ &+ 0.0178558z^6 + 0.00776283z^7 + 0.0100139z^8 - 0.000197302z^9 \\ B =& -0.0238607 - 0.11752z - 0.0255802z^2 + 0.039044z^3 + 0.0679325z^4 \\ &+ 0.0262791z^5 + 0.0449525z^6 + 0.0110277z^7 + 0.00891183z^8 - 0.0964854z^9 \end{aligned}$$

Finite Impulse Response (FIR) Representation of $\mathcal{T}_G$. The FIR model is of the form

$$Y = CU$$

or in a more complete form

$$Y(k) = (c_0 + c_1 z + \ldots + c_v z^v + \ldots)U(k)$$

were Y is the output of the system, U is the input, C is the polynomials $C = c_0 + c_1 z + \ldots + c_v z^v + \ldots$. It is always possible to create a FIR representation from a IIR. In a general form C is of order ∞ to make the FIR representation identical to the IIR. This is not realistic, because it means that an infinite number of past values of the input are required to estimate an output at $k + 1$. This is the theory, but in practice, C can be approximated with a finite model, as long as the time constant of the system are short compared with v, the degree of the polynomial C; i.e., the order of C to make it a good approximation depends on the dynamic characteristics of the system.

Modeling $\mathcal{T}_G$ as an Infinite Impulse Response (IIR) Filter from Invasive Data

Data Input and output data are required for the modeling process. For the derivation of a $\mathcal{T}_G$ invasive aortic and radial waves ($_aWave_i$, $_rWave_i$) are required. There is no need to pre-filter $_rWave_i$ or $_aWave_i$ as any filter will be reflected in the derived

$\mathcal{T}_G$ coefficients. In the analysis presented in this study, 59 sets of ${}_aWave_i$, ${}_rWave_i$ were used.

Problem: Find A and B that minimizes the total error (ϵ_T) for the set of pairs of invasive radial and aortic waves $({}_rWave_i, {}_aWave_i), 1 \leq i \leq n$ where n is the number of measurements (only one measurement per subject).

$$
\begin{aligned}
{}_aWave_1 &= \frac{B}{A}{}_rWave_1 + \epsilon_1 \\
{}_aWave_2 &= \frac{B}{A}{}_rWave_2 + \epsilon_2 \\
&\vdots \\
{}_aWave_i &= \frac{B}{A}{}_rWave_i + \epsilon_i \\
&\vdots \\
{}_aWave_n &= \frac{B}{A}{}_rWave_n + \epsilon_n
\end{aligned}
$$

and

$$\epsilon_T = \sum_{i=1}^{n} \epsilon_i^2$$

In a more complete form

$${}_aWave_i(k) = \frac{b_0 + b_1 z + \ldots + b_q z^q}{1 + a_1 z + \ldots + a_s z^s}{}_rWave_i(k) + \epsilon_i(k) \tag{4.6}$$

with $A = 1 + a_1 z + \ldots + a_s z^s$ and $B = b_0 + b_1 z + \ldots + b_q z^q$, z is the lag operator $f(k)z = f(k-1)$, and $\epsilon_i = (\epsilon_i(1), \epsilon_i(2), \cdots, \epsilon_i(p_i))$ where p_i is the length (number of samples) of ${}_aWave_i$. All waves, ${}_aWave_i$ and ${}_rWave_i$, are the same length, and all are of length $p = p_1 = p_2 = \cdots = p_n$. Therefore, the total error (ϵ_T) can be defined as:

$$\epsilon_T = \sum_{i=1}^{n} \sum_{j=1}^{p} \epsilon_i^2(j)$$

Solution: ϵ_T can be represented as

$$\epsilon_T = \epsilon_T(\boldsymbol{x})$$

where $\boldsymbol{x} = (x_1, x_2, \ldots, x_{q+s}) = (a_1, a_2, \ldots, a_s, b_0, b_1, \ldots, b_r)$ is a vector of independent variables. This makes vectors A and B the independent variables for minimization.

ϵ_T can minimized using the Levenberg-Marquardt algorithm because ϵ_T is of the special form

$$L(\boldsymbol{x}) = \epsilon_T(\boldsymbol{x}) = \frac{1}{2}\sum_{j=1}^{m} r_j^2(\boldsymbol{x})$$

where $\boldsymbol{r} = (r_1, r_2, \ldots, r_m) = (\epsilon_1(1), \epsilon_1(2), \ldots, \epsilon_2(1), \epsilon_2(2), \ldots, \epsilon_n(p))$. For details see Appendix A.

The initial conditions were set to $A_0 = A_{Scor}$ and $B_0 = B_{Scor}$ were A_{Scor} and B_{Scor} are the IIR coefficients used in the *SphygmoCor*® instrument.

Because the prediction of a value ${}_aWave_i(k)$ depend on previous value of ${}_rWave_i(k-v), 0 \leq v \leq \max_{q,s}$, the first 100 sampling points where not used as part of ϵ_i.

Note of caution: Equation 4.6 can be written as

$${}_a\widehat{Wave_i}(k) = \frac{b_0 + b_1 z + \ldots + b_q z^q}{1 + a_1 z + \ldots + a_s z^s} {}_rWave_i(k)$$

or as

$$\begin{aligned} {}_a\widehat{Wave_i}(k) = b_{0r}Wave_i(k) + b_{1r}Wave_i(k-1) + \ldots + b_{qr}Wave_i(k-q) \\ -a_{1a}Wave_i(k-1) - \ldots - a_{sa}Wave_i(k-s) \end{aligned} \tag{4.7}$$

If the 'hat' in ${}_a\widehat{Wave_i}(k)$ is forgotten, and because ${}_aWave_i(k)$ and ${}_rWave_i(k)$ are known for all k, this will become a linear system that could be easily solved by matrix inversion. This solution will be incorrect.

Validity of $\mathcal{T}_G$

As previously mentioned, $\mathcal{T}_G$ is an approximation to individual $\mathcal{T}_B$. Using the bootstrap technique with 59 observations, the accuracy of the $\mathcal{T}_G$ was tested. In Figure 4.2 the frequency response for the $\mathcal{T}_G$ is presented. From the estimated confidence intervals (95%) it is shown that the $\mathcal{T}_G$ has converged (i.e., the model won't change by adding more observations). On the other hand, the standard deviation lines show that individual models are an approximation to $\mathcal{T}_B$ and are significantly different, mostly in the frequency range above 5 Hz. Therefore, the accuracy of the $\mathcal{P}$ derived using this model will decrease if it depends on high frequencies components.

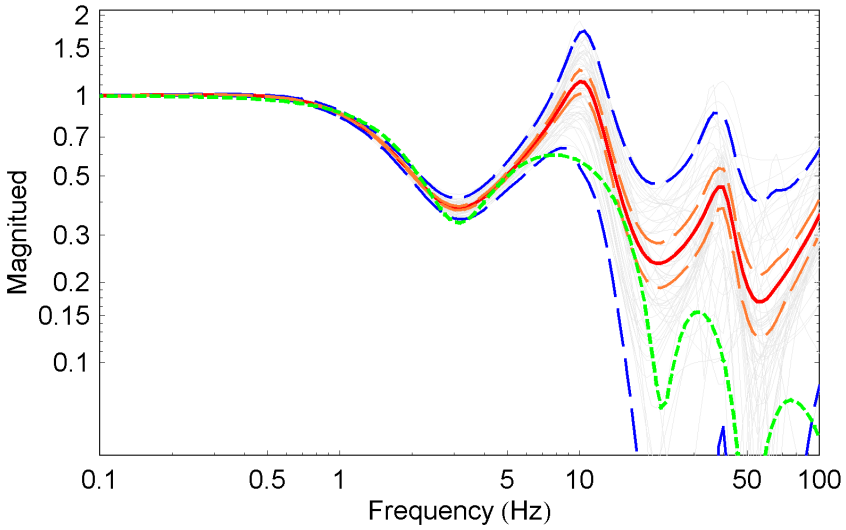

Figure 4.2: Frequency response of $\mathcal{T}_G$. Solid line: Average frequency response. Dashing lines next to solid: 3 standard errors (95% confidence interval). Envelope dashing lines: 2 standard deviations. Dotted line: *SphygmoCor*® response. Background lines: individual response for each of the 59 bootstrap samples.

4.2.4 Derivation of the *SphygmoCor*® Generalized Transfer Function

The $\mathcal{T}_G$ derived by Karamanoglu et al. [1993] has been implemented in a commercial instrument, the *SphygmoCor*® device (AtCor Medical Pty Ltd, West Ryde, NSW, Australia). The *SphygmoCor*® instrument is designed to measure peripheral blood pressure (BP) wave shapes from peripheral arteries and by means of a

generalized mathematical transfer function ($\mathcal{T}_{ShygmoCor}$) estimate the central aortic BP. The $\mathcal{T}_{ShygmoCor}$ was estimated from invasive measurements of radial and aortic invasive BP measurements from a cohort of 14 subject (13 male) undergoing cardiac catheterization. The average age was 53.7 (range 36-70) years [Karamanoglu et al., 1993].

In this document $\mathcal{T}_{ShygmoCor}$ refers to the $\mathcal{T}_G$ used by the *SphygmoCor*®. The $\mathcal{T}_{ShygmoCor}$ is not available from the manufacturer and therefore an almost identical transfer function was derived to use in this study. It will be referred to as the $\mathcal{T}_{SCor}$. The derivation process is presented in detail in this section. For practical purposes the $\mathcal{T}_{ShygmoCor}$ and the $\mathcal{T}_{SCor}$ are interchangeable (see error analysis). $\mathcal{T}_{SCor}$ will be used to refer to both unless stated otherwise.

In the *SphygmoCor*®, the signal obtained by the tonometer and saved in the *SphygmoCor*® database is not calibrated against physiological values of blood pressure. Instead it is a unitless numerical list of integer values. These values are then transformed by the use of the transfer function ($\mathcal{T}_{SCor}$) to obtain a non-calibrated central blood pressure signal. The instrument then analyzes and calibrates the signal to present the final report to the user.

The $\mathcal{T}_{ShygmoCor}$ is described in the literature as a linear transfer function. Linear transfer functions are not difficult to derive if the input and output signals are known. This section describes how the $\mathcal{T}_{SCor}$ with similar time response to the *SphygmoCor*® transfer function ($\mathcal{T}_{ShygmoCor}$) was derived. The analysis of coherence of the two transfer functions is also presented.

Raw Data

It is possible to derive an unknown linear transfer function based on the input and output signals of a system. To derive a transfer function with similar response to the *SphygmoCor*® transfer function the raw data of the instrument was used. The data is not directly available from the instrument via standard commands, but it is available as binary data in the SCor.mdb database in the *SphygmoCor*® installation

folders. The data from several *SphygmoCor*® instruments was put together as the Integrated Data Base, which was explained in Chapter 2.

The binary files from 1007 subjects of radial and aortic blood pressure were converted into *Mathematica*™ *5.0* vectors. The data of the position of the foot of each individual blood pressure pulse (calculated by *SphygmoCor*®) within the blood pressure wave were also imported. These data is refer as triggers. Radial triggers and aortic triggers were aligned and the aortic waves were lagged by 2 sample points. This was done because most of the timing differences between radial and aortic triggers were 31 sample points. In addition most of the aortic waves were 33 sample points shorter then the radial waves. By lagging the aortic by 2 points, most of the waves were set to have the same length. The initial points were padded with the value of the first initial aortic value. After alignment, all waves were chopped to have the length of the shortest wave (1149 data points). In summary, the raw data for the transfer function estimation was obtained by:

1. Convert binary files into *Mathematica*™ *5.0*
2. Align aortic waves with radial waves (with a lag of 2 data points)
3. Chop all waves to have the same length (1149 data points)

The final data for analysis consists of two matrices (aortic and radial) in which each row is a blood pressure wave. It is important to notice, that the blood pressure waves are not calibrated (i.e. not in real physiological values). The dimensions of the matrices were 1007 subjects x 1149 data points.

Part of the data were used to derive the transfer function and part to validate it. The IIR Filter Model, used in the derivation is explained next.

Infinite Impulse Response Filter Model

The Infinite Impulse Response Filter (IIR) is defined for the discrete time as

$$Y = \frac{B}{A}U$$

or in a more complete form

$$Y(k) = \frac{b_0 + b_1 z + \ldots + b_q z^q}{1 + a_1 z + \ldots + a_s z^s} U(k)$$

were Y is the output of the system, U is the input, A and B are the polynomials $A = 1 + a_1 z + \ldots + a_s z^s$ and $B = b_0 + b_1 z + \ldots + b_q z^q$ and z is the lag operator: $f(k)z = f(k-1)$.

With the IIR filter model and the raw data explained in the previous section it is possible to estimate the coefficients of the polynomials A and B, that minimize the errors from an estimated outputs $\hat{Y}$ and the measured values Y. An IIR filter is a specific type of transfer function, and will be the one used to 'match' the unknown *SphygmoCor*® transfer function. The derivation process for this transfer function will be explained next.

Transfer Function Derivation

If the model is applied to the estimated aortic waves ($_a\widehat{Wave}$) and the radial waves ($_rWave$), for each pair of waves

$$\begin{aligned}
{}_a\widehat{Wave}_1 &= \frac{B}{A}{}_rWave_1 \\
{}_a\widehat{Wave}_2 &= \frac{B}{A}{}_rWave_2 \\
&\vdots \\
{}_a\widehat{Wave}_i &= \frac{B}{A}{}_rWave_i \\
&\vdots \\
{}_a\widehat{Wave}_n &= \frac{B}{A}{}_rWave_n
\end{aligned}$$

then the polynomials A and B can be solved. Notice that in contrast to the method presented in section 4.2.3 the right sides of the equation 4.9 are estimates ${}_a\widehat{Wave}$

(with a 'hat') and not ${}_aWave$. In complete form

$$ {}_a\widehat{Wave}_i(k) = \frac{b_0 + b_1 z + \ldots + b_q z^q}{1 + a_1 z + \ldots + a_s z^s} {}_rWave_i(k) \tag{4.8} $$

Equation 4.8 can be written as

$$ \begin{aligned} {}_a\widehat{Wave}_i(k) = b_{0r}Wave_i(k) + b_{1r}Wave_i(k-1) + \ldots + b_{qr}Wave_i(k-q) \\ -a_{1a}\widehat{Wave}_i(k-1) - \ldots - a_{sa}\widehat{Wave}_i(k-s) \end{aligned} \tag{4.9} $$

The system represented by equation 4.9 can be solved by expressing it in a matrix form and solving for the coefficients by matrix inversion.

The derived polynomials A and B are:

$$ \begin{aligned} A =& 1 - 1.03713z - 0.0553583z^2 + 0.0641736z^3 + 0.0509342z^4 + 0.00730289z^5 \\ &+ 0.0178558z^6 + 0.00776283z^7 + 0.0100139z^8 - 0.000197302z^9 \\ B =& -0.0238607 - 0.11752z - 0.0255802z^2 + 0.039044z^3 + 0.0679325z^4 \\ &+ 0.0262791z^5 + 0.0449525z^6 + 0.0110277z^7 + 0.00891183z^8 - 0.0964854z^9 \end{aligned} $$

Validation Against *SphygmoCor*® Transfer Function

Figure 4.3 show a comparison of ${}_a\widehat{Wave}$ estimated using the $\mathcal{T}_{ShygmoCor}$ and $\mathcal{T}_{SCor}$ transfer functions. The initial differences are because values of the ${}_rWave$ were not known for the estimation with $\mathcal{T}_{SCor}$. The residuals for a set of 30 estimated waves have a mean value of -0.00244 and SD of 0.924 arbitrary units. The arbitrary units are used internally in the *SphygmoCor*®. The maximum resolution is of 1 unit. Therefore, the estimation error is cause by resolution error in the digitalization process. The order of magnitude of this error, if scaled to BP values, is $10^{-3}(0.25)$ mmHg.

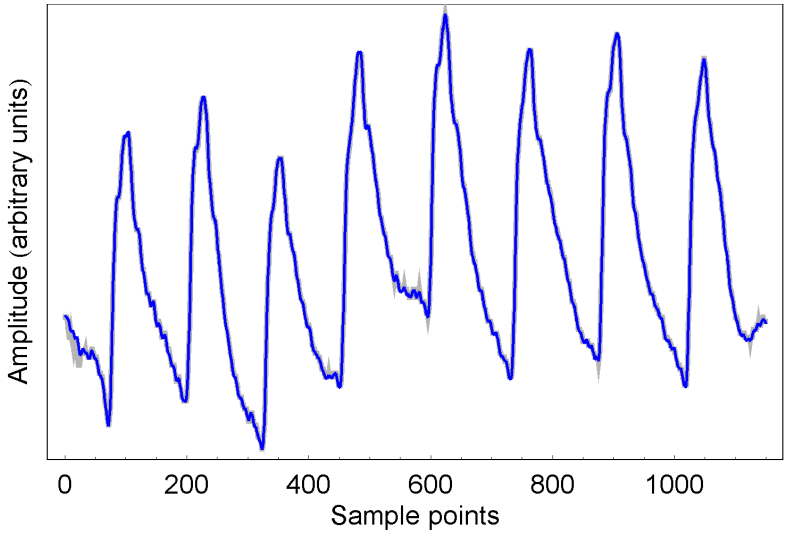

Figure 4.3: Comparison of ${}_a\widehat{Wave}$ estimated by *SphygmoCor*® using $\mathcal{T}_{ShygmoCor}$ (thick line) and by derived $\mathcal{T}_G = \mathcal{T}_{SCor}$ (thin line).

4.2.5 Types of Derivation Methods

There can be infinite possible derivation methods ($\mathcal{D}$), but they all fall into two distinctive categories: (i) based on models, and (ii) direct. This classification is also extended to the $\mathcal{P}$s derived using those $\mathcal{D}$. The $\mathcal{P}$s derived using $\mathcal{D}$ based on models, are referred to as *indirect* $\mathcal{P}$. In contrast, a *direct* $\mathcal{P}$ is the one derived using a $\mathcal{D}$ which is not based on on a model (e.g., ${}_rSP$ derived from the ${}_rPulse$).

Although there is a specific $\mathcal{D}$ for each specific $\mathcal{P}$ and $\mathcal{M}$, some generalization on the type of $\mathcal{D}$ can be made. The types of $\mathcal{D}$ used in this study are shown in Table 4.5 and are by no means the only available.

Table 4.5: Types of derivation methods ($\mathcal{D}$)

Symbol	*Description / Model*
$\mathcal{D}_{direct}$	Direct - no model
$\mathcal{D}_{LR}$	Linear model
$\mathcal{D}_{\mathcal{T}_G}$	Generalized Transfer Function (GTF)
$\mathcal{D}_{NL}$	Non-linear model

Direct Derivation Method

A direct derivation method is one without an underlying model (i.e., it is not based on a sample population). Therefore, its definition is not based on experimental data. The trivial example is the identity function, when a $\mathcal{P}$ is the same as the $\mathcal{M}$ (e.g., ${}_bSP$ measure with the sphygmomanometer). A more complex direct $\mathcal{D}$ is the one used to estimate HR from a $Wave$. No training of the $\mathcal{D}$ (as there is no underlying model) is required.

Linear Derivation Method

Linear $\mathcal{D}$ are based on linear models (i.e., linear combination of independent variables), which are the $\mathcal{M}$ used. A Linear $\mathcal{D}$ can be represented as

$$\begin{aligned}\hat{\mathcal{P}} &= \mathcal{D}(\mathcal{M}) \\ &= c_0 + c_1\mathcal{M}_1 + c_2\mathcal{M}_2 + \ldots + c_i\mathcal{M}_i\end{aligned} \tag{4.10}$$

for i independent measurements (i.e., independent variables). The coefficients c_0, $c_1, \ldots, c_i$ are usually estimated (i.e., the training of the model) by linear regression, which will be one of the methods used in this study.

Generalized Transfer Function Derivation Method

The Generalized Transfer Function Derivation Method ($\mathcal{D}_{\mathcal{T}_G}$), Figure 4.4, is based on a generalized transfer function ($\mathcal{T}_G$) model explained in section 4.2.2. The input (i.e., the $\mathcal{M}$) is a ${}_rWave$ calibrated by sphygmomanometer measurements — the problem with brachial calibration is presented in section 4.1.4. The ${}_rWave$ is 'passed' through the $\mathcal{T}_G$ to obtain an estimated ${}_a\widehat{Wave}$. The $Pulse$s from the ${}_a\widehat{Wave}$ are separated and averaged to obtain an estimated ${}_a\widehat{Pulse}$. The averaging process is done to eliminate measurement error, but it could fade $Pulse$ feature, as explained in section 4.2.1. From the ${}_a\widehat{Pulse}$ the specific $\mathcal{P}$s of interest are calculated.

A major consideration in the $\mathcal{D}_{\mathcal{T}_G}$ is that although an indirect $\mathcal{D}$ (i.e., is based on

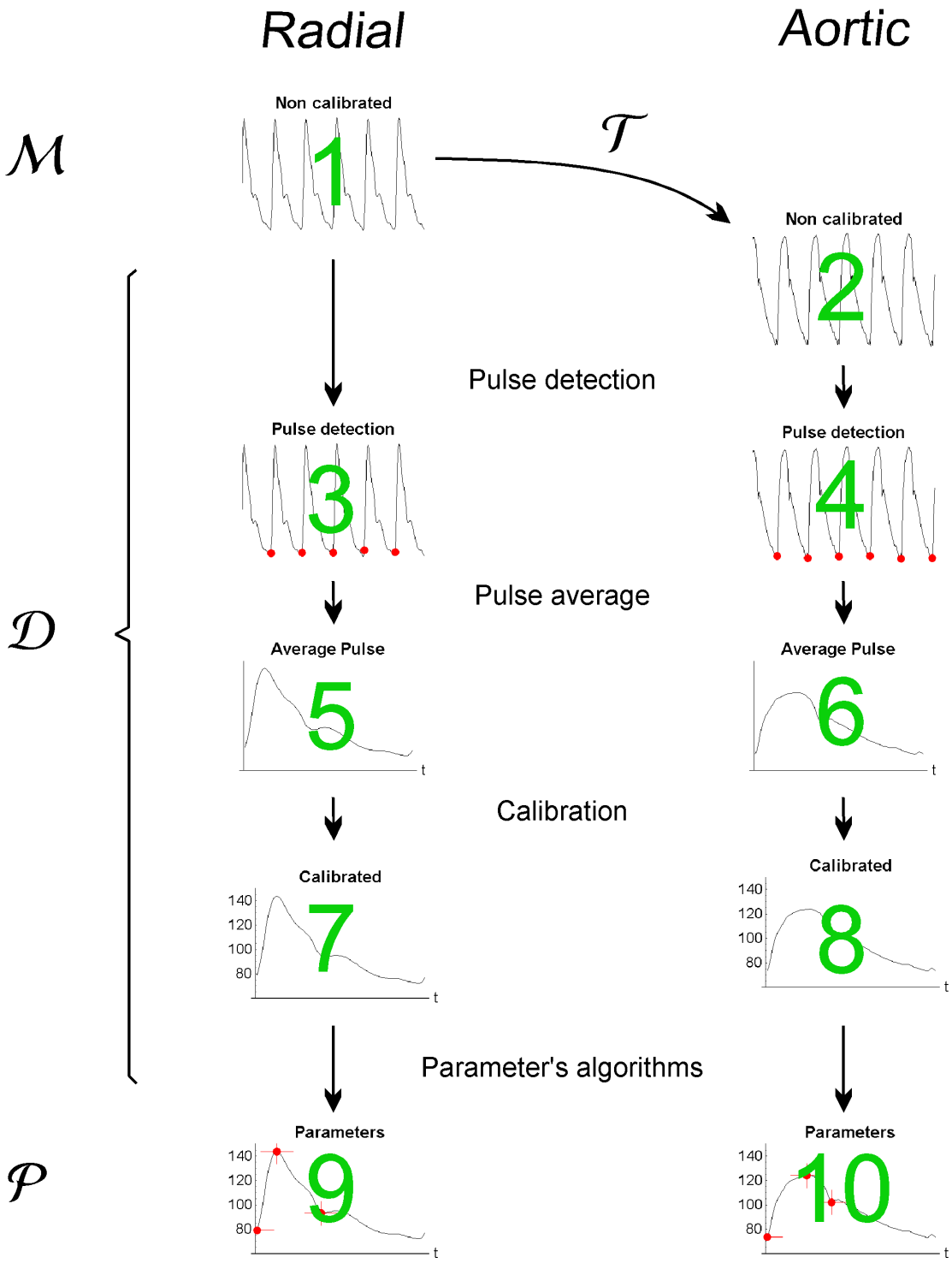

Figure 4.4: Generalized Transfer Function Derivation Method. 1: Non calibrated radial BP wave (tonometric reading). 2: Aortic BP $Wave$ estimated by using transfer function ($\mathcal{T}$). 3,4: Pulse starting points detected. 5,6: Several $Pulse$s from a $Wave$ are averaged to get a single $Pulse$. 7: Radial $Pulse$ is calibrated with noninvasive ${}_rSP$ and ${}_rDP$. 8: Aortic $Pulse$ is calibrated proportional to the calibration of the radial $Pulse$. 9,10: Parameters ($\mathcal{P}$) are measured on the calibrated $Pulse$s. Some other parameters can be measured on the radial and aortic $Wave$s (1,2).

a sample population), the criterion for fitting of the $\mathcal{T}_G$ is to minimize the difference between ${}_aWave$ and ${}_a\widehat{Wave}$. The parameters derived using the $\mathcal{D}_{\mathcal{T}_G}$ (e.g., ${}_aSP$) are not considered in this fitting process, which leads to a more general $\mathcal{D}$, but in general, the estimated $\hat{\mathcal{P}}$ are *biased*. This has note been considered in previous work which concentrate on the estimation of the ${}_aWave$ and not in the estimation of the ${}_a\mathcal{P}$.

Non-Linear Derivation Method

Non-linear derivation methods are based on non-linear models for the estimation of specific parameters or $Wave$s. The advantage of non-linear models is that, as natural systems are generally non-linear, they can be a more accurate model. This is the case for the blood pressure wave propagation in the arterial system [Langewouters et al., 1984, Pythoud et al., 1996]. However, the work done by Langewouters et al. [1984] and Pythoud et al. [1996] showed that the non-linear effects are comparable in magnitude with the accuracy of experimental measurements. The main disadvantage of non-linear models is that the training of the model is more difficult and due to the model's flexibility, they require much larger training sets. This is an important consideration when central arterial parameters are to be estimated, as central invasive measurement are difficult to obtain. With the reduced set of 59 invasive measurements available for this study, and the considerable inter-subject variability, the use of non-linear models was not further explored.

4.3 Parameters ($\mathcal{P}$)

This section will define, in a generic way, the specific arterial BP parameters, i.e., the possible $\mathcal{P}$s. Initially the $\mathcal{P}$s will be conceptually defined, followed by the criteria used for a strict definition. For the detailed derivation and comparative analysis of $\mathcal{P}$s derived using specific $\mathcal{M}$ and $\mathcal{D}$ (i.e., different estimation options (EO)) refer to Chapters 5 and 6.

4.3.1 Conceptual Definitions of $\mathcal{P}$

$\mathcal{P}$ refers, in general, to the parameters that characterize arterial BP. Although not necessary, $\mathcal{P}$s represent a physiological quantity. The conceptual definitions of the $\mathcal{P}$, illustrated in Figure 4.5, are presented next.

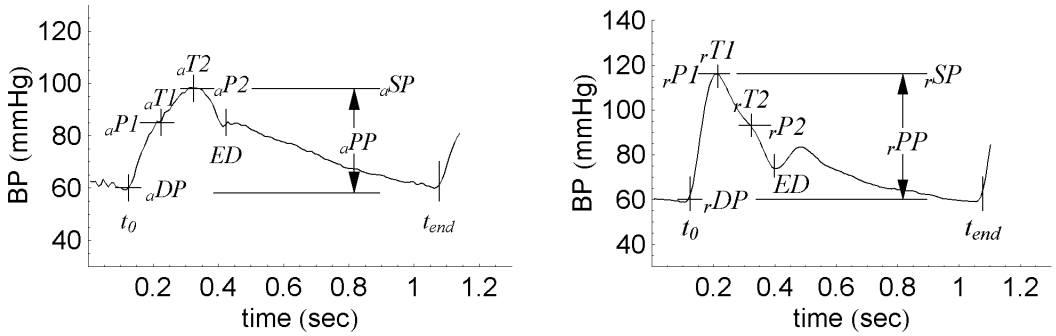

(a) Aortic BP *Wave* **(b)** Radial BP *Wave*

Figure 4.5: Parameters in BP *Pulse*s. Mean pressure (MP), pulse period, heart rate (HR), pulse pressure amplification (PPA) and augmentation index ($_aAIx$) are not shown in the graphs. See text for explanation.

Time Pulse Start (t_0) is by definition the time at which a *Pulse* begins. The implications on the definition of t_0 are discussed in section 4.2.1.

Time Pulse End (t_{end}) is by definition the time at which a *Pulse* ends. It is the same as the t_0 of the following *Pulse*.

Heart Rate (HR) is the number of cardiac cycle per unit time. It is commonly measured in beats per minute (bpm). HR varies with time, i.e., heart beats are of different length. This brings to the concept of heart rate variability, which is not studied in this investigation. Other causes of HR change are physical exercises, change in intrathoracic pressure, and other physiological changes.

Heart Beat Period (Pr) or cardiac cycle period is the time from one cardiac cycle to the next ($t_{end} - t_0$). It can be defined as the inverse of HR ($Pr = 1/HR$). The most common measured unit for Pr is seconds (sec).

Systolic Pressure (SP) is defined as the maximum BP during a specified time interval.

Diastolic Pressure (DP) is defined as the minimum BP during a specified time interval. In a $Pulse$ it is defined as the BP at time t_0. Notice that the DP value will depend on the algorithm used to define t_0.

Pulse Pressure (PP) is defined as the difference between SP minus DP.

Mean Pressure (MP) is defined as the average BP during a specified time interval.

T1 is defined as the time in which the first inflexion point or maximum is found in a $Pulse$. T1 is an indicator of maximum flow during ejection.

P1 is defined as the BP value at time $T1$.

T2 is defined as the time in which the second inflexion point or maximum is found in a $Pulse$.

P2 is defined as the BP value at time $T2$.

Augmentation Index (AIx) is defined as $AIx = \frac{P2-DP}{P1-DP}$.

Ejection Duration (ED) is defined as the time of duration of systole, from t_0 to the time of closure of the aortic valve.

Pulse Pressure Amplification (PPA) is defined as the ratio between radial pulse pressure over central aortic pulse pressure.

Inverse Pulse Pressure Amplification ($\mathbf{PPA}^{-1}$) is defined as the inverse of PPA. This definition is more consistent with the estimation of central aortic BP from peripheral measurements.

There is not a standardized methods to evaluate $T1$ and $T2$. The concept of inflection points is difficult to apply to real measurements that invariable contain noise. If the waves are filtered to remove noise the location of $T1$ and $T2$ will depend on the filter used. Despite the inaccuracy of $T1$ and $T2$ the BP values P1 and P2 are more accurate, as a significant variation in time is reflected in a small variation in BP due to the slope of the BP at $T1$ and $T2$. Physiological concepts (e.g., wave reflection) instead of mathematical concepts like 'inflection point' should be used for conceptual definition of $Pulse$ $\mathcal{P}$s.

The conceptual definitions are important to set a common language when referring to any specific $\mathcal{P}$, but are not sufficient for any quantitative analysis. Therefore a strict definition is required, and will be presented next.

4.3.2 Strict Definition of $\mathcal{P}$

The strict definition of arterial parameters is important. A straight forward example illustrates this point. ${}_aSP$ is defined as the maximum aortic BP value. Is it the maximum pressure for a single $Pulse$? Or, is it the average of maximum pressures of several $Pulse$s in a $Wave$? Or, is it the maximum pressure in a whole $Wave$? From Equation 4.1, the $\mathcal{P}$ depends on the $\mathcal{D}$ and $\mathcal{M}$ from whence it is derived. A complete definition of ${}_aSP$ should specify the $\mathcal{M}$ and $\mathcal{D}$ used, as well as the scope (S) and location (L— explained next). A strict definition could be, for the previous example, the estimated aortic SP averaged over a series of pulses measured in the radial artery and derived using a $\mathcal{T}_G$. This strict definition could be represented as ${}_a\widehat{SP}\{\mathsf{S}$:Pulse, $\mathcal{M}$:tonometer, sphygmo, $\mathcal{D}$:$\mathcal{T}_G\}$. This is obviously different from the aortic SP measured invasively with a catheter, strictly represented as ${}_aSP\{\mathsf{S}$:Pulse, $\mathcal{M}$:catheter, $\mathcal{D}$:direct$\}$. A strict definition of a $\mathcal{P}$ should provide enough information to make a quantitative

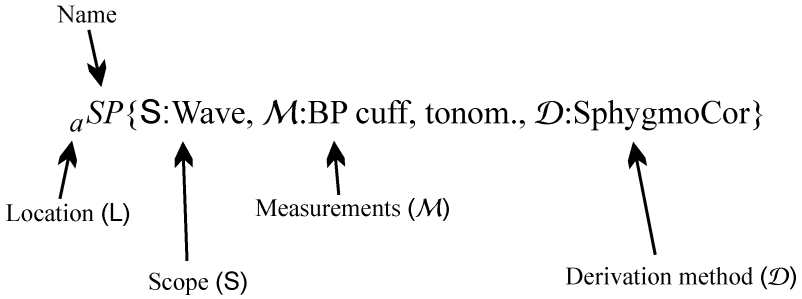

Figure 4.6: Strict $\mathcal{P}$ definition. This figure shows the elements of a $\mathcal{P}$ strict definition. The name of the parameter is SP, abbreviation for systolic pressure. The location is a indicating aortic. The scope is Wave, indicating that it refers to a measurement in a $Wave$ (not a $Pulse$). The $\mathcal{M}$ is done with a BP cuff and a tonometer. The $\mathcal{D}$ is indicated as SphygmoCor, indicating that the derivation method was the one used by the *SphygmoCor*® device. By knowing this information it is possible to describe in detail the errors and valid population for this specific parameter. 1- name: conceptual definition and derive alogrithm. 2-references to the document - pages: def: 4.3.1, location: 4.3.2, scope: 4.3.2, meas: 4.3.2, derive: 4.3.2

statistical analysis possible.

With a strict definition of $\mathcal{P}$, $\mathcal{D}$ and $\mathcal{M}$ are known. Therefore, the information from whence $\mathcal{P}$ is derived and the sources of error are specified. The criteria for a strict definition, presented next, may not be unique, but is the one adopted in this study. The elements considered are listed in Table 4.6 and explained in the following subsections. The nomenclature used to represent strictly defined parameters is illustrated in Figure 4.6.

Table 4.6: BP parameters ($\mathcal{P}$) selection criteria

Criteria	*Question answered*
Location (L)	What is the anatomical location of $\mathcal{P}$?
Scope (S)	What entity does $\mathcal{P}$ refers to ($Pulse$, $Wave$, subject)?
Measurements ($\mathcal{M}$)	What are the measurements required to estimate $\mathcal{P}$?
Derivation method ($\mathcal{D}$)	How was $\mathcal{P}$ calculated from $\mathcal{M}$?

$\mathcal{P}$'s Location (L)

BP changes across the arterial tree [Nichols et al., 1998]. Therefore, the anatomical location of the measurement is important for its definition. The location specifies

where the $\mathcal{P}$ refers to, not where the $\mathcal{M}$ were taken (e.g., the ${}_aSP$ estimated from the ${}_rSP$).

$\mathcal{P}$'s Scope (S)

The scope defines the 'entity' that $\mathcal{P}$ describes. The concept of scope will be better explained with an example. ${}_rSP$ defined per $Pulse$ (i.e., its scope is $Pulse$) refers to the maximum BP value for a specific $Pulse$. In a $Wave$ (i.e., its scope is $Wave$) it could either be the maximum pressure value of the $Wave$, or the average of ${}_rSP$ of each $Pulse$ that is part of that $Wave$ (depending how it is derived). The scopes utilized in this document are: (i) $Pulse$, (ii) $Wave$, (iii) subject, and (iv) population.

$\mathcal{P}$'s Measurements ($\mathcal{M}$)

The way data is obtained makes a difference in the measurement. There are many different instruments and techniques, some more precise then others. Their selection depends on many factor such as cost, availability, time, training, etc. The tonometric measurement of BP waveform, calibrated with brachial absolute pressure values, is used for most of the $\mathcal{P}$ presented in this study. Details on measurement techniques are given in section 4.1.

$\mathcal{P}$'s Derivation Method ($\mathcal{D}$)

$\mathcal{P}$ depends on the way it is derived (i.e., calculated) from $\mathcal{M}$. The most important distinction in the way a $\mathcal{P}$ is derived from $\mathcal{M}$ is if either it is a *direct* $\mathcal{P}$ or an *indirect* $\hat{\mathcal{P}}$, as explained in section 4.2.

A framework for the statistical analysis and strict definitions of BP parameters was presented in this chapter. Specific measurements ($\mathcal{M}$) and derivation methods ($\mathcal{D}$) will be used in the following two chapters for the analysis of accuracy of six selected central aortic BP parameters.

5

Analysis of Estimated Central Arterial Blood Pressure Parameters — Invasive Measurements

Arterial BP parameters ($\mathcal{P}$) are the final descriptors of BP. Due to the practical difficulties for a direct measurement of central BP, these $\mathcal{P}$ are estimated from more accessible measurements ($\mathcal{M}$) using different derivation methods ($\mathcal{D}$), as explained in Chapter 4. The estimation of a $\mathcal{P}$ depends on the selected $\mathcal{D}$ and $\mathcal{M}$, i.e., the selected estimation option (EO). In this chapter ${}_aSP$, ${}_aDP$, ${}_aPP$, ${}_aAIx$, ${}_aED$, and PPA^{-1} are estimated using five different EO: Average (Avg), Linear (LR), Linear Mean (LRM), Principal Components (PC), and Generalized Transfer Function (GTF). The analysis of error for each estimation is presented as well as a comparative analysis of the residuals $({}_a\mathcal{P} - {}_a\widehat{\mathcal{P}})$ between each individual EO.

The required background to make this analysis possible was presented in previous chapters. Specific considerations for the estimation of $\mathcal{P}$, including a general description and specific definitions of $\mathcal{P}$s, were presented in Chapter 4. A method to represent and describe the ${}_rPulse$, the most important element in $\mathcal{M}$, was presented in Chapters 3.

The following sections present the definitions of the EO used in this study, followed by a description of the selected $\mathcal{P}$s. The discussions and conclusions of the analysis are presented last in this chapter. The analysis of the estimation of ${}_a\widehat{\mathcal{P}}$ pre-

sented in this chapter is based in invasive measurements of central aortic $\mathcal{P}$s. The analysis of the estimation of ${}_a\widehat{\mathcal{P}}$ using two different datasets, one (the same used in this chapter) with invasive measurements and a much larger dataset without invasive measurements, is presented in the following chapter.

5.1 Methods

For each of the selected $\mathcal{P}$ five different EO were 'fitted' to best estimate the invasive data, as will be explained later. The residuals (i.e., the differences between the measured and the estimated values) were used to quantify the estimation quality and to compare the different EO. Correlation coefficients (R^2) between real and estimated values were calculated for all $\mathcal{P}$ estimations using all observations. For each individual $\mathcal{P}$ the residuals were characterized with a mean, a standard deviation (SD) and a root mean square (RMS) error value. The analysis of variance for the mean, SD, and RMS of the residuals (not the $\mathcal{P}$) was performed using the bootstrap method.[1] The analysis of variance is based on the testing set of the bootstrap method, i.e., the remaining observations after a bootstrap sample is taken. For each test 196 bootstrap samples were taken. A general description of the method, based on the book by Hastie et al. [2001], is presented in the following section. Mathematical details and discussion about the bootstrap method can be found in the book by Efron and Tibshirani [1993]. Comparisons between any two EO used to estimate a particular ${}_a\widehat{\mathcal{P}}$ was done in a pair basis. The comparison is based on the analysis of residuals, and the method is explained in section 5.1.2.

[1]There is no need to use the bootstrap method to calculate the mean, SD or RMS of the $\mathcal{P}$. They can be calculated directly from the data.

5.1.1 The Bootstrap Methods

Models are used to represent interactions between dependent (y) and independent ($\boldsymbol{x}$) variables[2], and can be represented as:

$$y = g(\boldsymbol{x}) + \epsilon \tag{5.1}$$

Different models can be used to represent the same interactions, and a compromise between complexity and accuracy (how well does the model represent reality) is always present in the selection of the most appropriate model.

A training dataset ($\mathbf{Z} = (z_1, z_2, \ldots, z_N)$ where $z_i = (x_i, y_i)$) — a sample of the population — is required to train (or fit) the model to represent reality as good as possible. The accuracy of the model can be measured by analyzing the residuals (i.e., difference between the real data values and the model estimates). However, $\mathbf{Z}$ is one of many possible training datasets, and if a new training dataset ($\mathbf{Z}_{\text{new}}$) is used, any quantity that describes the model, including the residuals will vary. In other words, any quantity $S(\mathbf{Z})$ computed from $\mathbf{Z}$ will vary if a new $\mathbf{Z}_{\text{new}}$ is used. By how much? This is the question answered with analysis of variance. And bootstrap is a method that provides a measure of the statistical accuracy (i.e., analysis of variance) of non-linear systems with no restrictions in the distribution characteristics of $\mathbf{Z}$.

If g, in Equation 5.1, is linear and ϵ is normal, there is no need for bootstrap analysis because an ANOVA will provide the information of variance.

The bootstrap method will be explained with a comparative example between ANOVA and bootstrap analysis. ANOVA will be used as the gold standard to estimate the statistical accuracy of a linear model. The statistical accuracy will also be calculated using the bootstrap method for the same model and the same sample data.[3] The system and dataset for the comparative example is:

[2]This is a simplistic view of a 'model'. A much deeper definition an discussion about models can be found, for example, in the book by Nelles [2001].

[3]It is important to mention that the only reason for doing a bootstrap analysis of a linear model is for illustration purposes.

The system The 'unknown' system is of the form $y = a + bx + N(0, \sigma)$. The purpose of the analysis is to estimate the parameters $\hat{a}$, $\hat{b}$ and $\hat{\sigma}$ and their statistical accuracy from a sample dataset.

Sample dataset A dataset $\mathbf{Z} = (z_1, z_2, \ldots, z_N)$ where $z_i = (x_i, y_i)$ was generated for $N = 25$. $\mathbf{Z}$ is presented in Table 5.1. The x values were generated randomly from a uniform distribution with range $[0, 1]$. The y values were generated from the x values as $y = a + bx + N(0, \sigma)$ where $a = 5, b = 3, \sigma = 1$ and $N(0, \sigma)$ is the normal distribution with mean zero and standard deviation σ.

Table 5.1: Bootstrap example dataset ($\mathbf{Z}$)

x	y	x	y	x	y
0.669	8.23	0.831	6.52	0.782	7.58
0.125	5.85	0.935	6.30	0.600	5.67
0.758	7.64	0.969	7.98	0.126	5.78
0.576	6.99	0.755	7.60	0.821	6.50
0.605	6.84	0.194	5.77	0.657	8.27
0.560	8.36	0.837	6.10	0.161	5.04
0.854	8.98	0.945	6.47	0.937	9.54
0.261	6.52	0.727	7.11	0.279	5.79
0.268	4.30				

ANOVA

The model was fitted to the sample dataset using standard linear regression. The method is not explained here, as it can be found in any statistics book. Almost any statistics software package includes this functionality. *Mathematica*™ *5.0* was used for the present analysis.

Results for the ANOVA analysis are presented in Table 5.2.

Bootstrap Method

The same analysis presented using ANOVA will be repeated using the bootstrap method. The method consists on randomly drawing, with replacement, B new

sample datasets of size N from $\mathbf{Z}$.[4] For this example $B = 20$. As previously explained, $S(\mathbf{Z})$, any quantity computed from the data $\mathbf{Z}$, is computed again for each of the new $\mathbf{Z}^{*i}$. In our example, for each of the new $\mathbf{Z}^{*i}$ the model $y = \hat{a}_i + \hat{b}_i x$ is fitted again[5] to generate sets of B coefficients $\hat{a}_i$ and $\hat{b}_i$.

It is important to emphasize that, in contrast to linear regression, the model could be linear or non-linear. The process of fitting the model to the data could be any minimization method, such as the Levenberg-Marquardt algorithm, and the variables' distributions do not have to be normal.

The variance of the parameters calculated using ANOVA (Table 5.2) are calculated again from the sets of B coefficients $\hat{a}_i$ and $\hat{b}_i$. The parameters $\hat{a}$, $\hat{b}$ and $\hat{\sigma}$ are the same as they correspond to the best linear fit (calculated with linear regression in this example). The way to calculate the standard errors (SE) is explained next.

The standard error for $\hat{a}$ and $\hat{b}$ are calculated as:

$$\begin{aligned} SE(\hat{a}) &= \sqrt{\frac{1}{N-1}\sum_{i=1}^{N}(\hat{a}_i - \mu_a)^2} \\ &= 0.349 \end{aligned} \tag{5.2}$$

$$\begin{aligned} SE(\hat{b}) &= \sqrt{\frac{1}{N-1}\sum_{i=1}^{N}(\hat{b}_i - \mu_b)^2} \\ &= 0.720 \end{aligned} \tag{5.3}$$

where

$$\mu_a = \frac{1}{B}\sum_{i=1}^{B}\hat{a}_i \quad \mu_b = \frac{1}{B}\sum_{i=1}^{B}\hat{b}_i$$

Comparative results between the ANOVA and bootstrap methods are presented in Table 5.2. The variance of any other quantity (for example the root mean square (RMS) of the residuals could be calculated in the same way).

[4] N, the size of the new datasets $(\mathbf{Z}^{*1}, \mathbf{Z}^{*2}, \ldots, \mathbf{Z}^{*B})$ is the same as the size of the original dataset $\mathbf{Z}$. This is possible because the random drawing of samples is done with replacement.

[5] The fitting of the model is a different problem to the analysis of statistical accuracy. The use of the bootstrap method is to analyze statistical accuracy (variance) of the parameters $\hat{a}$ and $\hat{b}$.

Table 5.2: Variance analysis comparison. SE_{ANOVA} and SE_{BS} are the standard errors calculated using ANOVA and bootstrap, respectively.

Parameter	*Value*	SE_{ANOVA}	SE_{BS}
$\hat{a}$	5.23	(0.489)	(0.349)
$\hat{b}$	2.69	(0.730)	(0.720)

Testing dataset It is convenient to have a separate dataset to test the quality of the model to prevent that model over-fitting looks unrealistically good. In bootstrap, the 'training dataset' ($\mathbf{Z}^{\varnothing i}$) can be formed with the samples not selected for each bootstrap sample ($\mathbf{Z}^{*i}$). This method can be seen as a type of cross validation in which part of the data, $\mathbf{Z}^{*i}$, is used to train the model and part to test it, $\mathbf{Z}^{\varnothing i}$. The main advantage of using this technique is that all data is used for modeling (all $\mathbf{Z}$ is used for the selection of the $\mathbf{Z}^{*i}$), an important benefit when data is scarce.

The bootstrap method will be used in the comparison of the different EOs by pairs. The statistical accuracy of the ratio of variance of residuals will be analyzed, as will be explained in the following section.

5.1.2 Comparing Estimation Options

A parameter ($\mathcal{P}$) can be estimated from measured data ($\mathcal{M}$) using a derivation method ($\mathcal{D}$).

$$\hat{\mathcal{P}} = \mathcal{D}(\mathcal{M}) \tag{5.4}$$

The combined $\mathcal{D}(\mathcal{M})$ is referred to as an Estimation Option (EO). In other words, an EO is a selection of methods and independent variables to estimate $\hat{\mathcal{P}}$. For example, an EO could be a linear regression to estimate ${}_aSP$ using ${}_rSP$ and ${}_rDP$ as independent variables.

The 'quality' of an EO is based on the reduction of the variance of the residuals,

where the variance is given by:

$$Var_{EO} = \frac{\sum_{i=1}^{N} (\mathcal{P} - \hat{\mathcal{P}}_{EO})^2}{N} \tag{5.5}$$

Note that the denominator is N and not $N-$ degrees of freedom. This is because the variance is calculated in a testing dataset, i.e., in data that was not used to estimate the model.

To prove if one EO, say EO1, is better the another, say EO2, the problem can be stated as a set of hypotheses:

$$H_0 : Var_{EO1} \geq Var_{EO2}$$
$$H : Var_{EO1} < Var_{EO2}$$

This set of hypotheses can be written as variance ratios:

$$H_0 : \frac{Var_{EO1}}{Var_{EO2}} \geq 1$$
$$H : \frac{Var_{EO1}}{Var_{EO2}} < 1$$

The distribution of the ratio of variances can be estimated by bootstrap analysis. The method consists in generating B samples of $\frac{Var_{EO1}}{Var_{EO2}}$ $(S(\mathbf{Z}^{*i}))$[6] from B bootstrap samples $(\mathbf{Z}^{*i})$ of the total dataset $(\mathbf{Z})$ from where the models are derived. To calculate each of the $\frac{Var_{EO1}}{Var_{EO2}}$ ratios, the following points were considered:

1. Each model was fully calculated for its corresponding bootstrap sample $(\mathbf{Z}^{*i})$, including to recalculate the $\mathcal{T}_G$.

2. The residuals were calculated from the samples that were not used to estimate the models $(\mathbf{Z}^{\varnothing i})$.

If more then 95% of the samples are < 1, i.e., 95% of the $Var_{EO1} < Var_{EO2}$, then the null hypothesis H_0 can be rejected; therefore, confirming that $Var_{EO1} < Var_{EO2}$

[6]Refer to previous section for notation.

or that EO1 is better then EO2.

5.1.3 Data

The data used for this analysis come from the invasive aortic and radial waves of the invasive dataset. For details in the data refer to section 2.4. The characteristics of the data are summarized in Table 5.3 (copy of Table 2.4).

Table 5.3: Invasive DB population characteristics ($N : 59$).

	Min	*Max*	*Avg.*	*Std*	*Outliers*
Gender (M:1, F:0)	0	1	0.729	0.448	0
Age (yrs)	34	84	60.5	11.4	0
Height (cm)	150	189	172.	8.68	0
Weight (Kg)	54	112	83.2	15.6	0
${}_rSP$ (mmHg)	89	149	121.	12.7	0
${}_rDP$ (mmHg)	34	91	59.1	10.9	0
${}_aSP$ (mmHg)	84	149	105.	14.1	0
${}_aDP$ (mmHg)	36	93	59.7	11.2	0
${}_aAIx$	0.64	2.27	1.40	0.360	1

Extreme values, such as ${}_aAIx = 2.27$, cold be caused by measurement errors or an unusual $Pulse$ shape. They are included in the analysis because if excluded the analysis of error will be unrealistic.

5.1.4 Selected Estimation Options

The $\mathcal{D}$ and the $\mathcal{M}$ (i.e., the EO) are part of the strict definition of $\mathcal{P}$ (see section 4.3).[7] In this study, five specific EOs are compared, and for simplicity they will be referred as: Average (Avg), Linear (LR), Linear Mean (LRM), Principal Components (PC), and Generalized Transfer Function (GTF). Each of these EO and their corresponding $\mathcal{P}$ strict definition are presented in Table 5.4.

The five EOs will be described next. The measurements ($\boldsymbol{\mathcal{M}}$) and derivation option ($\boldsymbol{\mathcal{D}}$), that are part of the formal definition of the EO, will be specifically

[7] S is also part of the strict definition of $\mathcal{P}$ but for all of the EO used in this study S was selected as $Wave$.

Table 5.4: Estimation options (EO) and corresponding $\mathcal{P}$'s strict definitions. The EOs are specified by the specific S, $\mathcal{M}$ and $\mathcal{D}$.

EO Name	*abb.*	$\mathcal{P}$ strict definition
Average	Avg.	$\mathcal{P}\{\mathsf{S}$:$Wave$, $\mathcal{M}$:None, $\mathcal{D}$:Average$\}$
Linear	LR	$\mathcal{P}\{\mathsf{S}$:$Wave$, $\mathcal{M}$:SBI, $\mathcal{D}$:LR$\}$
Linear Mean	LRM	$\mathcal{P}\{\mathsf{S}$:$Wave$, $\mathcal{M}$:SBI, ${}_rMP$, $\mathcal{D}$:LR$\}$
Principal Components	PC	$\mathcal{P}\{\mathsf{S}$:$Wave$, $\mathcal{M}$:Wave invasive, $\mathcal{D}$:PC, LR$\}$
Generalized Transfer Fctn.	GTF	$\mathcal{P}\{\mathsf{S}$:$Wave$, $\mathcal{M}$:Wave invasive, $\mathcal{D}$:$SphygmoCor^{\textcircled{R}}\}$

described for each of them.

Average (Avg): This EO is based on the population average of $\mathcal{P}$. $\mathcal{M}$ and $\mathcal{D}$ for this EO are:

$\boldsymbol{\mathcal{M}}$: None. There is no independent variables in this model. There is no need to take any measurements from a subject to estimate $\hat{\mathcal{P}}$, as it is the population average.

$\boldsymbol{\mathcal{D}}$: $\hat{\mathcal{P}} = \mu_{\mathcal{P}}$

The derivation of $\mu_{\mathcal{P}}$ (i.e., the best fit) is the sample population average. Therefore, $\hat{\mathcal{P}} = \mu_{\mathcal{P}} = \frac{1}{N}\sum_{i=1}^{N}\mathcal{P}_i$.

Linear (LR): This EO is based on a linear model of subject's basic information (SBI) — age, gender, height, weight, heart rate (HR), ${}_rSP$, and ${}_rDP$. $\mathcal{M}$ and $\mathcal{D}$ for this EO are:

$\boldsymbol{\mathcal{M}}$: The independent variables for this model are: Age, gender (S), height (H), weight (W), HR, ${}_rSP$ and ${}_rDP$.

$\boldsymbol{\mathcal{D}}$: $\hat{\mathcal{P}} = C_0 + C_{Age}Age + C_S S + C_H H + C_W W + C_{HR}HR + C_{rSP}{}_rSP + C_{rDP}{}_rSP$

The coefficients C_0, C_S, C_H, C_W, C_{Age}, C_{HR}, C_{rSP}, C_{rDP} are estimated by step wise linear regression (at 95% confidence).

Linear Mean (LRM): This EO is based on a linear model of SBI and MP measured in the radial artery. $\mathcal{M}$ and $\mathcal{D}$ for this EO are:

$\boldsymbol{\mathcal{M}}$: The independent variables for this model are: Age, gender (S), height (H), weight (W), HR, ${}_rSP$, ${}_rDP$ and MP.

$\boldsymbol{\mathcal{D}}$: $\hat{\mathcal{P}} = C_0 + C_{Age}Age + C_S S + C_H H + C_W W + C_{HR}HR + C_{{}_rSP_r}SP + C_{{}_rDP_r}SP + C_{MP}MP$

The parameters C_0, C_H, C_W, C_{Age}, C_S, C_{HR}, $C_{{}_rSP}$, $C_{{}_rDP}$, C_{MP} are estimated by step wise linear regression (at 95% confidence).

Principal Components (PC): This EO is based on a linear model of SBI and the principal components (PC) of the ${}_rPulse$. $\mathcal{M}$ and $\mathcal{D}$ for this EO are:

$\boldsymbol{\mathcal{M}}$: The independent variables for this model are the SBI and the principal component of the ${}_rPulse$ calculated from the ${}_rWave$. The way to calculate the PC is described in detail in Chapter 3.

$\boldsymbol{\mathcal{D}}$: $\hat{\mathcal{P}} = C_0 + C_{Age}Age + C_S S + C_H H + C_W W + C_{HR}HR + C_{{}_rSP_r}SP + C_{{}_rDP_r}SP$
$+C_0 + C_{PC_1}PC_1 + \ldots + C_{PC_6}PC_6 + C_{PC_7}PC_7$

The parameters C_0, C_H, C_W, C_{Age}, C_S, C_{HR}, $C_{{}_rSP}$, $C_{{}_rDP}$, $C_{PC_1}, C_{PC_2}, \ldots, C_{PC_6}$, C_{PC_7} are estimated by step wise linear regression (at 95% confidence).

Generalized Transfer Function (GTF): In this EO, the $\hat{\mathcal{P}}$s are calculated from an estimated ${}_a\widehat{Wave}$ derived from the ${}_rWave$ by the $\mathcal{T}_G$ (see section 4.2). $\mathcal{M}$ and $\mathcal{D}$ for this EO are:

$\boldsymbol{\mathcal{M}}$: The independent variables for this model are the measured values of the ${}_rWave$.

$\boldsymbol{\mathcal{D}}$: $\hat{\mathcal{P}} = f_{\mathcal{P}}({}_a\widehat{Pulse})$ where ${}_a\widehat{Pulse}$ is derived from the ${}_rWave$ in the following steps

$$
\begin{aligned}
{}_a\widehat{Wave} &= \mathcal{T}_G({}_rWave) \\
{}_a\widehat{Pulse} &= \text{Pulse from Wave}({}_a\widehat{Wave}) \\
\hat{\mathcal{P}} &= f_{\mathcal{P}}({}_a\widehat{Pulse})
\end{aligned}
$$

where $\mathcal{T}_G$ is similar to the $\mathcal{T}_{SCor}$ used in the *SphygmoCor*®device. The details on the generalized transfer function derivation method are presented in section 4.2. The function $f_{\mathcal{P}}$ represents the algorithm used to estimate $\mathcal{P}$ from a ${}_aPulse$.

The ${}_a\widehat{Wave}$ is estimated from a measured ${}_rWave$ transformed with the $\mathcal{T}_G$. The estimation process consists in finding the $\mathcal{T}_G$ that minimizes the difference between the measured ${}_aWave$ and the ${}_a\widehat{Wave}$, as explained in detail in section 4.2.3.

5.1.5 Selected Arterial BP Parameters

A selected set of $\mathcal{P}$s was chosen as a comprehensive set to illustrate the methodology necessary to derive any other parameter. The selected $\mathcal{P}$s , that will be explained next, can be grouped in aortic and aortic-radial pressure $\mathcal{P}$.

Aortic Pressure Parameters (${}_a\boldsymbol{\mathcal{P}}$)

Due to their central location and proximity to the heart, aortic pressure parameters are intuitively better indicators of central events such as baro-reflex activity or risk of myocardial infarction [Avolio et al., 2001, Wilkinson et al., 2001]. Their invasive measurement is difficult and not practical for the general clinical practice. For these reasons, the non-invasive measurement of central parameters has been proposed, mostly by the use of a generalized transfer function.

Aortic systolic pressure (${}_a\boldsymbol{SP}$) Because of the arterial transmission characteristics ${}_aSP$ is lower than ${}_rSP$ [Pauca et al., 2001]. This appears to be counterintuitive as pressure would seem to increase with distance from the heart. However, this only applies to pulse pressure, as mean pressure decreases with distance. The estimation method of ${}_aSP$ (and ${}_aDP$ presented in the next section) based on estimation of the ${}_aWave$ from the ${}_rWave$ are well documented [Chen et al., 1997, Takazawa et al., 1996, Karamanoglu et al., 1993] but are not the only possible means of estimation. This and other EO, are presented and compared here.

Aortic diastolic pressure ($_aDP$) In contrast to SP, $_aDP$ and $_rDP$ are similar because of the slow dynamic characteristics of late diastole. The measurement of both $_aDP$ and $_rDP$ is not standardized and inconsistencies could occur if different methods of defining the starting point of a $_rPulse$ (t_0) are used. For this study, the second derivative methods was used and $_rDP$ was defined as the BP value at t_0.

Aortic pulse pressure ($_aPP$) $_aPP$ is the difference between $_aSP$ and $_aDP$ (i.e., $_aPP = {}_aSP - {}_aDP$). As previously mentioned, $_aSP$ is lower the $_rSP$, therefore $_aPP$ is also lower then $_rPP$.

Aortic augmentation index ($_aAIx$) The BP pulse reflected from peripheral sites generates a returning BP wave, which produces an augmentation in central BP. This augmentation is dependent on the amount and time of reflection. It is difficult to define the exact time of reflection, but the 2nd inflexion point of the $_aPulse$ (t_2) have been used as the point of maximum reflection. The time of the peak of the outgoing wave (not the reflected one) is measured as the first inflexion point (t_1). From t_1 and t_2 the $_aAIx$ can be calculated as:

$$_aAIx = \frac{BP(t_2) - BP(t_0)}{BP(t_1) - BP(t_0)}$$

Ejection duration (ED) Ejection duration is the time from t_0 to aortic valve closure. When measured invasively the incisura is clear and the time is measured accurately. When measured non-invasively the ED can be estimated from the first inflexion point before the dicrotic notch in the $_rPulse$.

Aortic-radial Parameters ($_{a-r}\mathcal{P}$)

The only parameters analyzed in this group is the PPA^{-1}.

Inverse pulse pressure amplification (PPA^{-1}) As previously explained, $_aPP$ is lower then $_rPP$. The ratio between $_rPP$ over $_aPP$ is referred to as pulse pressure

amplification (PPA) and is defined as

$$\begin{aligned} \text{PPA} &= \frac{{}_{r}PP}{{}_{a}PP} \\ &= \frac{{}_{r}SP - {}_{r}DP}{{}_{a}SP - {}_{a}DP} \end{aligned}$$

The inverse of PPA is simply defined as PPA^{-1}.

5.2 Results

The results of this chapter are summarized in Table 5.5, where the different EOs are ranked for each individual $\mathcal{P}$, according to the estimation accuracy (maximum reduction of variance). That is, the EO that best estimates a certain $\mathcal{P}$ is placed first and others are placed in order of increasing variance. The comparative analysis of EOs by pairs (e.g., GTF and LMR) is presented in Table 5.6.

Table 5.5: Best EO for each specific $\mathcal{P}$. Best: maximum reduction of variance. Worst: less reduction of variance. pag.: page where models and analysis of residuals is presented.

	${}_{a}SP$	${}_{a}DP$	${}_{a}PP$	${}_{a}AIx$	${}_{a}ED$	PPA^{-1}
pag.	83	85	87	89	91	93
Best: 1	GTF	PC	PC	PC	GTF	PC
2	PC	LRM	GTF	GTF	PC	GTF
3	LRM	LR	LRM	LRM	LR	LRM
4	LR	GTF	LR	LR	LRM	LR
Worst: 5	Avg	Avg	Avg	Avg	Avg	Avg

The results for all selected $\mathcal{P}$ are presented next. For each EO the best fit model's will be presented along with a Figure of $\mathcal{P}$ vs. $\hat{\mathcal{P}}$. For all models the Parson Correlation Coefficient (R^2) is provided. A comparative whisker plot of the mean and RSM of the residuals is also presented. No model is presented for the GTF EO because its training is independent of the $\mathcal{P}$ of interest. The estimated model ($\mathcal{T}_G$), as explained in section 4.2.3, was 'trained' with the invasive aortic and radial $Waves$.

Table 5.6: Comparison of different EO by pairs (column, row). When '??' appears on a cell, there is no significant difference (95% confidence) between the two EOs. The EO on a cell is the best (less variance of residuals) of the two. This table is based on the histograms of variance ratios. For histograms refer to Appendix D, Figures D.2, D.4, D.6, D.8, D.10 and D.12.

	Avg	LR	LRM	PC	GTF
Avg	-				
LR	LR	-			
LRM	LRM	LRM	-		
PC	PC	PC	??	-	
GTF	GTF	GTF	??	??	-

(a) ${}_aSP$

	Avg	LR	LRM	PC	GTF
Avg	-				
LR	LR	-			
LRM	LRM	??	-		
PC	PC	??	??	-	
GTF	GTF	??	??	??	-

(b) ${}_aDP$

	Avg	LR	LRM	PC	GTF
Avg	-				
LR	LR	-			
LRM	LRM	LRM	-		
PC	PC	PC	??	-	
GTF	GTF	GTF	??	??	-

(c) ${}_aPP$

	Avg	LR	LRM	PC	GTF
Avg	-				
LR	LR	-			
LRM	LRM	??	-		
PC	PC	PC	??	-	
GTF	GTF	??	??	??	-

(d) ${}_aAIx$

	Avg	LR	LRM	PC	GTF
Avg	-				
LR	LR	-			
LRM	LRM	LRM	-		
PC	PC	PC	PC	-	
GTF	GTF	GTF	GTF	GTF	-

(e) ${}_aED$

	Avg	LR	LRM	PC	GTF
Avg	-				
LR	LR	-			
LRM	LRM	LRM	-		
PC	PC	PC	??	-	
GTF	GTF	GTF	??	??	-

(f) PPA^{-1}

5.2.1 Aortic Systolic Pressure

The models to estimate ${}_a\widehat{SP}$ using the Average, Linear, Linear Mean and Principal Components EO are presented in equations 5.6, 5.7, 5.8, 5.9 respectively. The details of the coefficients for the models are given in Appendix D. The individual distributions of the mean and RMS values of the residual are presented for all EOs in Figure 5.1.

Average (Avg): $R^2 = 0$

$$ {}_a\widehat{SP}_{\text{Avg}} = 107. \tag{5.6}$$

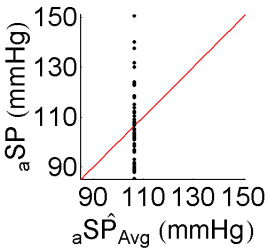

Linear (LR): $R^2 = 0.64$

$$ {}_a\widehat{SP}_{\text{LR}} = -4.20 + 0.904_r SP \tag{5.7}$$

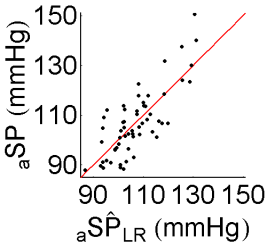

Linear Mean (LRM): $R^2 = 0.86$

$$ {}_a\widehat{SP}_{\text{LRM}} = -33.9 + 0.161Age + 1.77MP \\ -1.16_r DP + 0.511_r SP \tag{5.8}$$

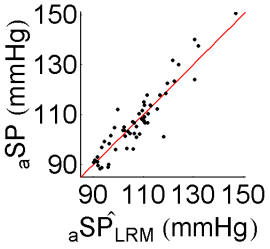

Principal Components (PC): $R^2 = 0.92$

$$ {}_a\widehat{SP}_{\text{PC}} = 118. + 0.406HR + 2.89PC_1 + 0.932PC_2 \\ +0.972PC_3 - 0.635_r DP \tag{5.9}$$

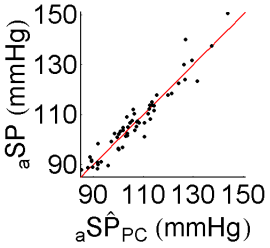

General Transfer Function (GTF): $R^2 = 0.90$

Model explained in section 4.2.3

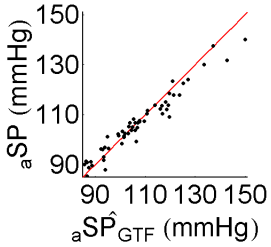

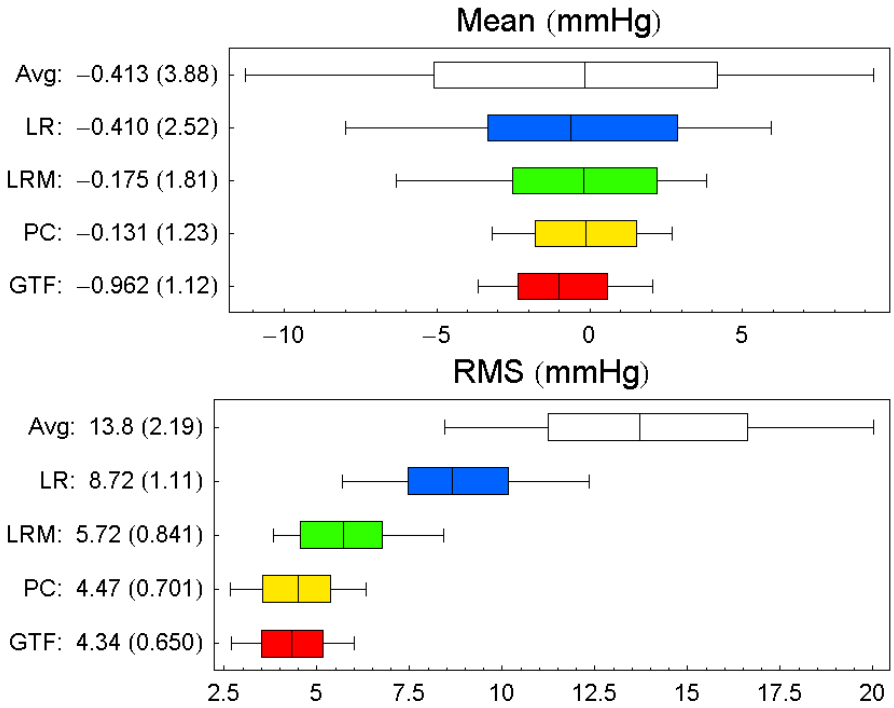

Figure 5.1: Residuals for different EO. Top graph represents distribution of mean values of residuals. Bottom graph represents distributions of RMS values of residuals. The RMS values can be interpreted as 'energy' of the errors. Histograms of distributions of means and RMS are presented in Appendix D. Box contains 80% of the data points. Wiskers indicate full range of values. Centre line indicates mean value.

The comparative analysis of the different EOs is presented in Table 5.6.

5.2.2 Aortic Diastolic Pressure

The models to estimate ${}_a\widehat{DP}$ using the Average, Linear, Linear Mean and Principal Components EO are presented in equations 5.10, 5.11, 5.12, 5.13 respectively. The details of the coefficients for the models are given in Appendix D. The individual distributions of the mean and RMS values of the residual are presented for all EOs in Figure 5.2.

Average (Avg): $R^2 = 0$

$$ {}_a\widehat{DP}_{\text{Avg}} = 62.0 \tag{5.10}$$

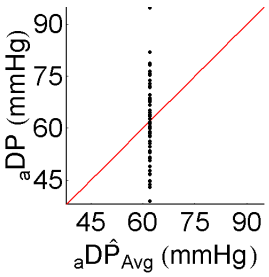

Linear (LR): $R^2 = 0.94$

$$ \begin{aligned} {}_a\widehat{DP}_{\text{LR}} = &-9.65 - 0.0757Age + 0.0894H \\ &+0.0890HR + 0.843{}_rDP \end{aligned} \tag{5.11}$$

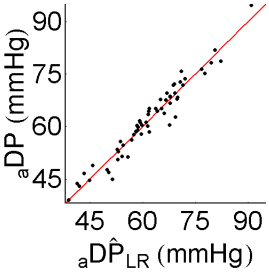

Linear Mean (LRM): $R^2 = 0.96$

$$ \begin{aligned} {}_a\widehat{DP}_{\text{LRM}} = &1.51 - 0.0710Age + 0.0973HR + 0.402MP \\ &+0.568{}_rDP - 0.102{}_rSP + 1.53S \end{aligned} \tag{5.12}$$

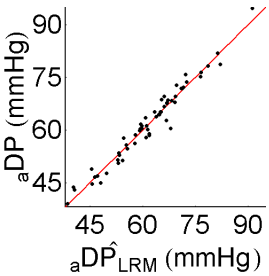

Principal Components (PC): $R^2 = 0.96$

$$ \begin{aligned} {}_a\widehat{DP}_{\text{PC}} = &8.29 + 0.682MP - 0.764PC_2 - 0.731PC_4 \\ &+0.302{}_rDP - 0.170{}_rSP \end{aligned} \tag{5.13}$$

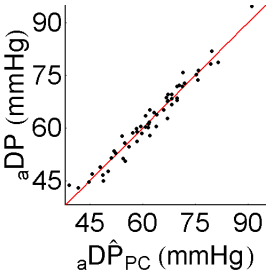

General Transfer Function (GTF): $R^2 = 0.91$

Model explained in section 4.2.3

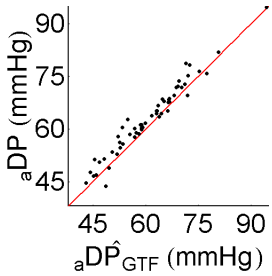

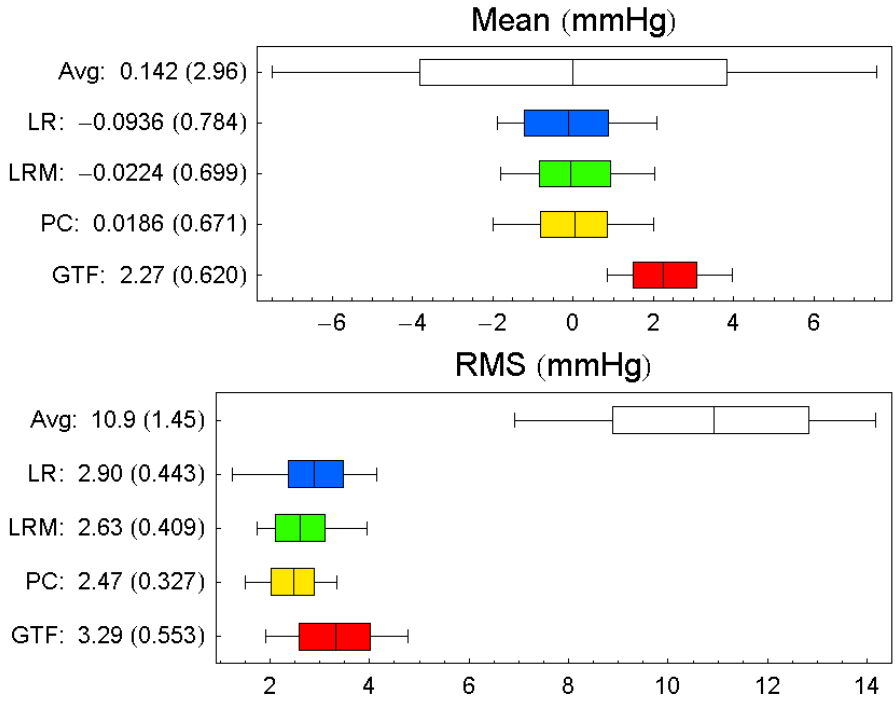

Figure 5.2: Residuals for different EO. Top graph represents distribution of mean values of residuals. Bottom graph represents distributions of RMS values of residuals. The RMS values can be interpreted as 'energy' of the errors. Histograms of distributions of means and RMS are presented in Appendix D. Box contains 80% of the data points. Wiskers indicate full range of values. Centre line indicates mean value.

The comparative analysis of the different EOs is presented in Table 5.6.

5.2.3 Aortic Pulse Pressure

The models to estimate ${}_a\widehat{PP}$ using the Average, Linear, Linear Mean and Principal Components EO are presented in equations 5.14, 5.15, 5.16, 5.17 respectively. The details of the coefficients for the models are given in Appendix D. The individual distributions of the mean and RMS values of the residual are presented for all EOs in Figure 5.3.

Average (Avg): $R^2 = 0$

$$ {}_a\widehat{PP}_{\text{Avg}} = 44.5 \tag{5.14}$$

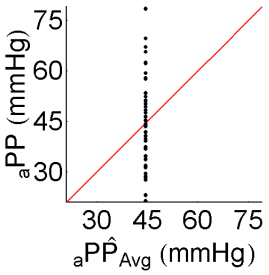

Linear (LR): $R^2 = 0.70$

$$ {}_a\widehat{PP}_{\text{LR}} = -11.4 + 0.238Age - 0.227HR \\ -0.597{}_rDP + 0.787{}_rSP \tag{5.15}$$

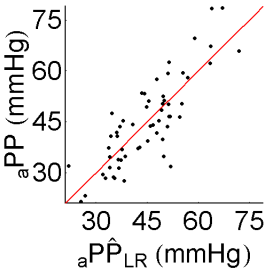

Linear Mean (LRM): $R^2 = 0.82$

$$ {}_a\widehat{PP}_{\text{LRM}} = -31.3 + 0.218Age - 0.164HR + 1.33MP \\ -1.64{}_rDP + 0.597{}_rSP \tag{5.16}$$

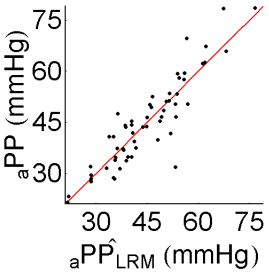

Principal Components (PC): $R^2 = 0.89$

$$ {}_a\widehat{PP}_{\text{PC}} = -36.9 + 0.137Age + 2.05PC_2 + 3.40PC_4 \\ -0.206{}_rDP + 0.705{}_rSP \tag{5.17}$$

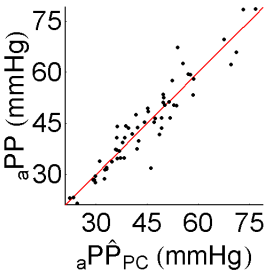

General Transfer Function (GTF): $R^2 = 0.83$

Model explained in section 4.2.3

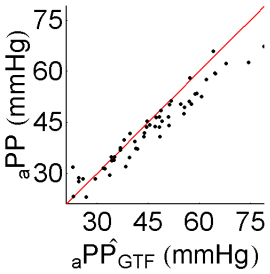

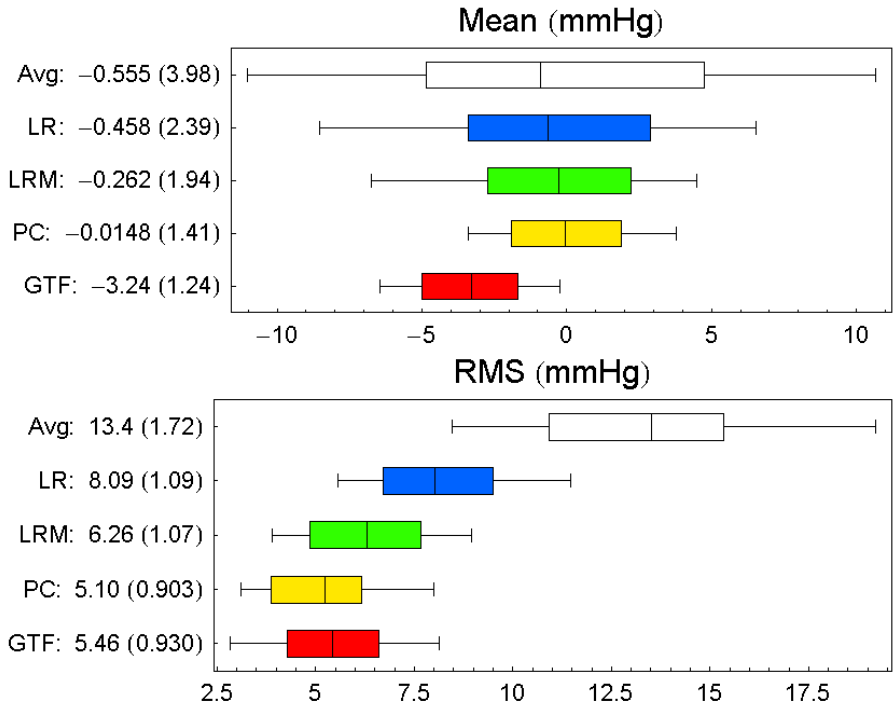

Figure 5.3: Residuals for different EO. Top graph represents distribution of mean values of residuals. Bottom graph represents distributions of RMS values of residuals. The RMS values can be interpreted as 'energy' of the errors. Histograms of distributions of means and RMS are presented in Appendix D. Box contains 80% of the data points. Wiskers indicate full range of values. Centre line indicates mean value.

The comparative analysis of the different EOs is presented in Table 5.6.

5.2.4 Aortic Augmentation Index

The models to estimate ${}_a\widehat{AIx}$ using the Average, Linear, Linear Mean and Principal Components EO are presented in equations 5.18, 5.19, 5.20, 5.21 respectively. The details of the coefficients for the models are given in Appendix D. The individual distributions of the mean and RMS values of the residual are presented for all EOs in Figure 5.4.

Average (Avg): $R^2 = 0$

$$ {}_a\widehat{AIx}_{\text{Avg}} = 127. \tag{5.18}$$

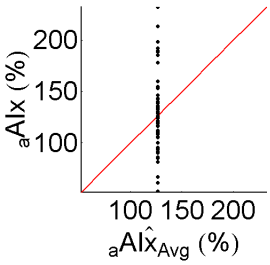

Linear (LR): $R^2 = 0.40$

$$ {}_a\widehat{AIx}_{\text{LR}} = 231. - 1.44HR \tag{5.19}$$

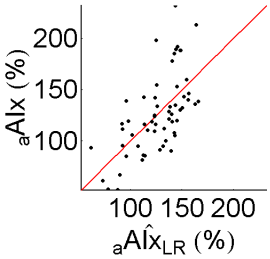

Linear Mean (LRM): $R^2 = 0.50$

$$ {}_a\widehat{AIx}_{\text{LRM}} = 229. - 1.81HR + 1.92MP - 1.02_rSP \tag{5.20}$$

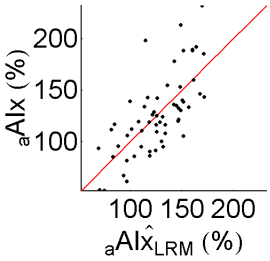

Principal Components (PC): $R^2 = 0.75$

$$ {}_a\widehat{AIx}_{\text{PC}} = 157. - 1.54HR + 12.0PC_4 + 15.1PC_6 + 23.7PC_8 + 1.26_rDP \tag{5.21}$$

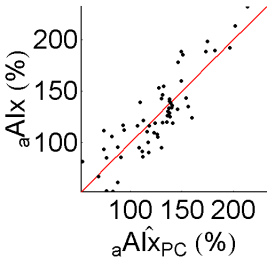

General Transfer Function (GTF): $R^2 = 0.55$

Model explained in section 4.2.3

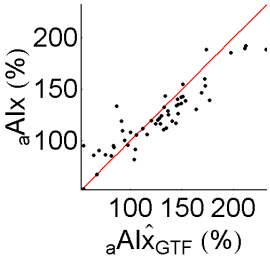

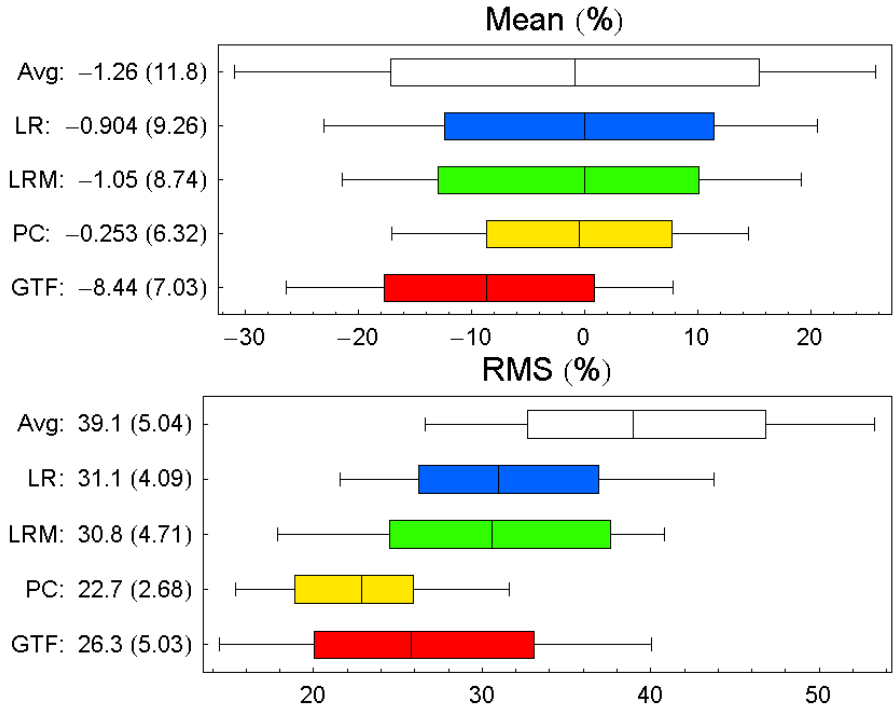

Figure 5.4: Residuals for different EO. Top graph represents distribution of mean values of residuals. Bottom graph represents distributions of RMS values of residuals. The RMS values can be interpreted as 'energy' of the errors. Histograms of distributions of means and RMS are presented in Appendix D. Box contains 80% of the data points. Wiskers indicate full range of values. Centre line indicates mean value.

The comparative analysis of the different EOs is presented in Table 5.6.

5.2.5 Ejection Duration

The models to estimate $\hat{ED}$ using the Average, Linear, Linear Mean and Principal Components EO are presented in equations 5.22, 5.23, 5.24, 5.25 respectively. The details of the coefficients for the models are given in Appendix D. The individual distributions of the mean and RMS values of the residual are presented for all EOs in Figure 5.5.

Average (Avg): $R^2 = 0$

$$\hat{ED}_{\text{Avg}} = 314. \tag{5.22}$$

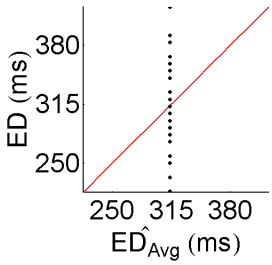

Linear (LR): $R^2 = 0.71$

$$\hat{ED}_{\text{LR}} = 659. - 1.03H - 2.30HR \tag{5.23}$$

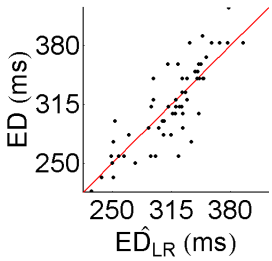

Linear Mean (LRM): $R^2 = 0.71$

$$\hat{ED}_{\text{LRM}} = 659. - 1.03H - 2.30HR \tag{5.24}$$

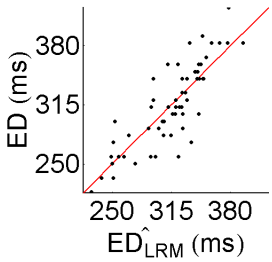

Principal Components (PC): $R^2 = 0.86$

$$\hat{ED}_{\text{PC}} = 556. - 0.663H - 1.76HR + 3.24PC_2 + 8.50PC_4 - 17.0PC_7 \tag{5.25}$$

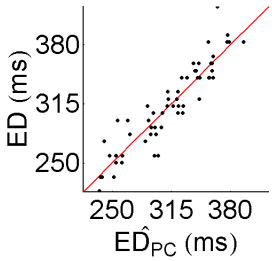

General Transfer Function (GTF): $R^2 = 0.90$

Model explained in section 4.2.3

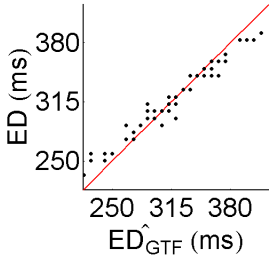

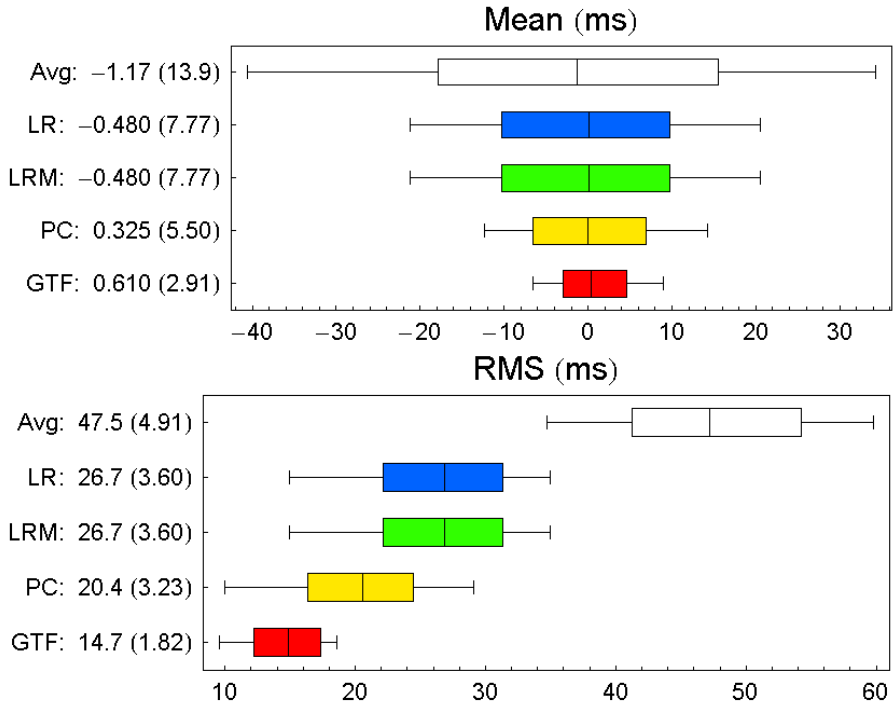

Figure 5.5: Residuals for different EO. Top graph represents distribution of mean values of residuals. Bottom graph represents distributions of RMS values of residuals. The RMS values can be interpreted as 'energy' of the errors. Histograms of distributions of means and RMS are presented in Appendix D. Box contains 80% of the data points. Wiskers indicate full range of values. Centre line indicates mean value.

The comparative analysis of the different EOs is presented in Table 5.6.

5.2.6 Inverse Pulse Pressure Amplification

The models to estimate $\widehat{\text{PPA}^{-1}}$ using the Average, Linear, Linear Mean and Principal Components EO are presented in equations 5.26, 5.27, 5.28, 5.29 respectively. The details of the coefficients for the models are given in Appendix D. The individual distributions of the mean and RMS values of the residual are presented for all EOs in Figure 5.6.

Average (Avg): $R^2 = 0$

$$\widehat{\text{PPA}^{-1}}_{\text{Avg}} = 76.2 \tag{5.26}$$

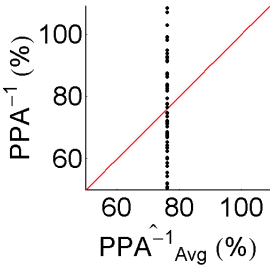

Linear (LR): $R^2 = 0.29$

$$\widehat{\text{PPA}^{-1}}_{\text{LR}} = 81.4 + 0.330Age - 0.348HR \tag{5.27}$$

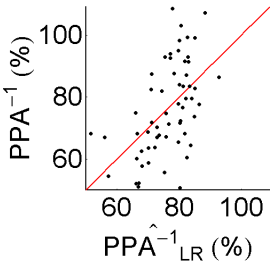

Linear Mean (LRM): $R^2 = 0.59$

$$\widehat{\text{PPA}^{-1}}_{\text{LRM}} = 37.6 + 0.348Age - 0.335HR + 2.27MP - 1.44_rDP - 0.394_rSP \tag{5.28}$$

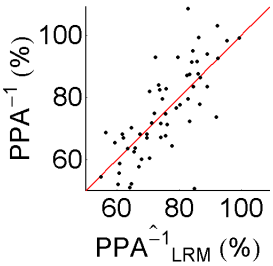

Principal Components (PC): $R^2 = 0.80$

$$\widehat{\text{PPA}^{-1}}_{\text{PC}} = 154. + 0.215Age + 0.271HR + 2.53PC_1 + 2.78PC_2 + 1.58PC_3 + 2.88PC_4 - 0.900_rSP \tag{5.29}$$

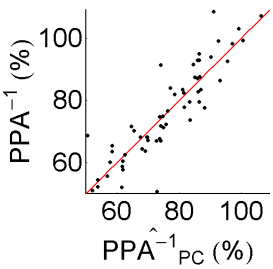

General Transfer Function (GTF): $R^2 = 0.65$

Model explained in section 4.2.3

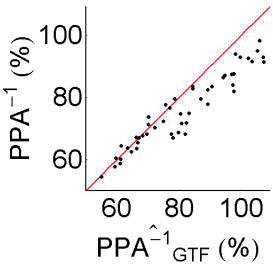

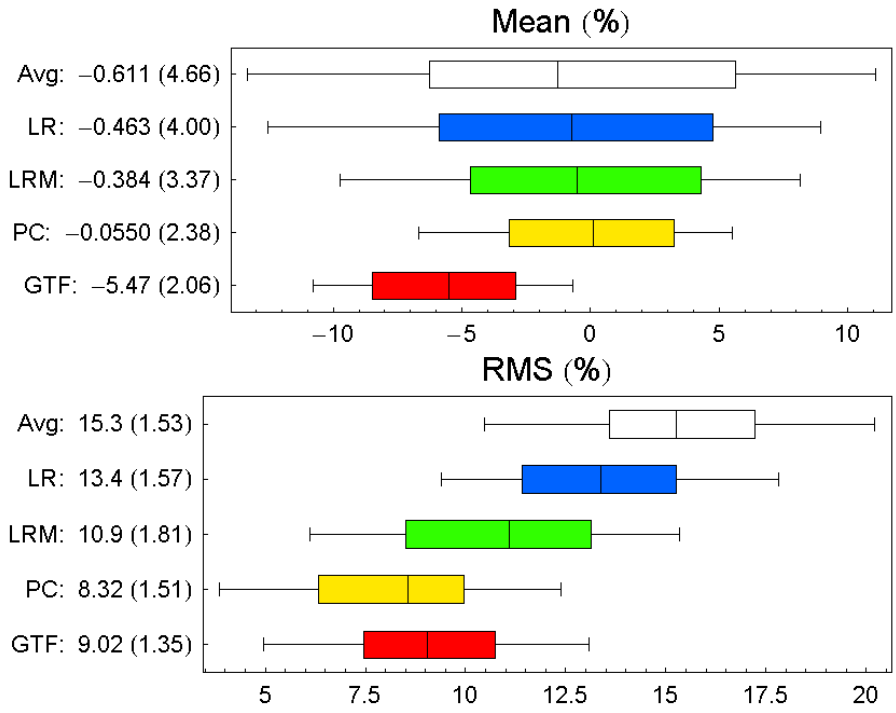

Figure 5.6: Residuals for different EO. Top graph represents distribution of mean values of residuals. Bottom graph represents distributions of RMS values of residuals. The RMS values can be interpreted as 'energy' of the errors. Histograms of distributions of means and RMS are presented in Appendix D. Box contains 80% of the data points. Wiskers indicate full range of values. Centre line indicates mean value.

The comparative analysis of the different EOs is presented in Table 5.6.

5.3 Discussion

A big number of EOs and predictor variables are available for the estimation of ${}_a\widehat{\mathcal{P}}$. No one EO is better then another and their use should be based on data availability, estimated ${}_a\widehat{\mathcal{P}}$, required accuracy and EO complexity. Chapter 8 presents the value of estimated ${}_a\widehat{\mathcal{P}}$. In this study two types of EO were used. First, the GTF was chosen because it is widely referenced in the literature. This EO is based on a $\mathcal{T}_G$. Second, EOs based on linear models (Avg, LR, LRM, PC) were chosen because of their simplicity which prevent data over-fitting for a reduced number of observations ($N = 59$ in this study). However, more sophisticated EO are possible, for example the once based in non-linear models. These more complex EO could better predict ${}_a\widehat{\mathcal{P}}$ but in general require much larger number of observations.

From the EOs used in this study, the inclusion of MP as a predictor significantly improved the estimation (reduction of error). A further improvement was obtained for the EO based on ${}_rPulse$ (PC and GTF). This suggests that ${}_rPulse$ contains additional information to SBI. MP can be seen as an initial approach to the description of the ${}_rPulse$. This is consistent with the fact that for the same ${}_rSP$ and ${}_rDP$, the MP varies with ${}_rPulse$ shape.

Despite the improved estimates when ${}_rPulse$ was used, the GTF EO was biased in the estimation of ${}_a\widehat{\mathcal{P}}$. This is because the intrinsic model ($\mathcal{T}_G$) is obtained by minimization of errors between pulses (${}_aPulse$ and ${}_a\widehat{Pulse}$) and note of the ${}_a\mathcal{P}$s themselves. This is convenient because no additional models are needed for the estimation of a new ${}_a\widehat{\mathcal{P}}$, but the problem of bias still exists. Other advantage is that $\mathcal{T}_G$ can be obtained with a small number of observations, as these models have not much flexibility. In general, there is a tradeoff between model flexibility and required number of observations.

As previously mentioned no one single EO is consistently better in estimating all ${}_a\widehat{\mathcal{P}}$. In addition, the estimation accuracy is different for each ${}_a\widehat{\mathcal{P}}$, even when the best EO for that specific ${}_a\widehat{\mathcal{P}}$ is used. This implies that either the information

about each ${}_a\widehat{\mathcal{P}}$ is not contained in the predictors (${}_rPulse$, SBI, MP) or the models do not represent the relationship between predictors and ${}_a\widehat{\mathcal{P}}$ correctly. ${}_aAIx$ was the parameter with lowest correlation between real and estimated values. This is probably because rapid changes in BP in early systole are dumped and lost in BP pulse transmission in the brachial vasculature. In addition, the times of inflection (t_1 and t_2) are not well defined and incorrect inflexion points could have been used.

As for the analysis of accuracy, the non-parametric bootstrap method provided the required information of variance required for the comparison of EOs and ${}_a\widehat{\mathcal{P}}$ accuracy analysis. In addition, this same technique could be used for future assessment of more complex EO including those based on non-linear models. The use of a testing dataset was also important to evaluate for model over-fitting. In this study, the RMS of the residuals of the best fit model are consistent with the RMS from the bootstrap analysis. This would not be the case if the model did over-fit the data, which is not expected in a simple model like the once used in this study. However, for reduced N verification is recommended.

In general terms, the comparison of different EOs and analysis of accuracy of ${}_a\widehat{\mathcal{P}}$ was only possible for strictly defined ${}_a\mathcal{P}$ and known EO.

5.4 Conclusions

None of the EO evaluated in this study was significantly better (in terms of reduction of variance of residuals) for all the estimated ${}_a\widehat{\mathcal{P}}$. The EOs based on linear models (Avg, LR, LRM and PC) provide good ${}_a\mathcal{P}$ estimates and are simple to use and analyze. The GTF, because its $\mathcal{T}_G$ is based on minimization of errors of waves and not ${}_a\mathcal{P}$, is biased in the estimation of ${}_a\widehat{\mathcal{P}}$. Because of it's more complex derivation method the analysis of error is not as simple as for linear methods.

${}_a\widehat{\mathcal{P}}$ estimated with EOs based on ${}_rPulse$ have smaller error and therefore ${}_rPulse$, should be included when possible. If ${}_rPulse$ is not available MP was an important predictor. As MP is intrinsically available in oscillometric BP measurement devices,

this value could be included without using additional measurement equipment.

Estimated errors are always present independent of which EO or predictor variables are used for the estimation of any ${}_a\mathcal{P}$. Depending on the application of the ${}_a\widehat{\mathcal{P}}$ these errors could be significant and should always be considered. This implies that for the analysis of accuracy of any EO the strict definition of the ${}_a\mathcal{P}$s and the EOs should be known. This implies that many previous studies, in which ${}_a\widehat{\mathcal{P}}$ where considered correct and error analysis was ignored, should be reevaluated.

The reduce number of observations of invasive peripheral and central aortic BP wave prevented the use of more complex EO or more accurate estimation of the ${}_a\widehat{\mathcal{P}}$. Therefore, further studies in which the number of observations is increased are required.

6

Analysis of Estimated Central Arterial BP Parameters from Subject's Basic Information — Invasive and Non-Invasive Measurements

Invasive data of simultaneous recordings of peripheral and central aortic blood pressure (BP) is limited. Therefore, the relationships between subject's basic information (SBI) — age, gender, height, weight, heart rate (HR), ${}_rSP$, and ${}_rDP$ — and arterial BP parameters ($\mathcal{P}$) are difficult to establish. For example, in the previous chapter, it was shown that ${}_aSP$ did not have a significant relationship (with 95% confidence) with age or gender after accounting for ${}_rSP$, when a data set with 59 observations was used. On the other hand, large number of observations of non-invasive BP measurements and ${}_rPulse$, are available. Several methods are available to estimate $\hat{\mathcal{P}}$ from the ${}_rPulse$. If the relationships between SBI and $\mathcal{P}$ are of interest an initial approach is to regress these $\hat{\mathcal{P}}$ (estimated from the ${}_rPulse$) against SBI. However, this method does not provide the relationships between the real $\mathcal{P}$ (not the $\hat{\mathcal{P}}$ estimated from the ${}_rPulse$) and SBI. Other alternative is to regress the $\mathcal{P}$ against SBI directly, but as mentioned earlier, the amount of information is limited. For these reasons, a novel method to find the relationships between $\mathcal{P}$ and SBI is presented in this chapter. The relationships, because of the linear regression

modeling, are given by the coefficients of:

$$\hat{\mathcal{P}} = C_0 + C_{Age}Age + C_S S + C_H H + C_W W + C_{HR}HR + C_{_rSPr}SP + C_{_rDPr}DP \quad (6.1)$$

where Age is age in years, S represents gender (0:female, 1:male), H is height in cm, and W is weight in Kg. In contrast to the standard linear regression method, presented in Chapter 5 (LR EOs), this approach uses two distinct data sets, one with invasive ($N_{inv} = 59$) and a much larger with non-invasive ($N_{int} = 1727$) measurements of SBI and $_rPulse$s wave shape. The use of these two datasets is what allows for the reduction in variance, as will be explained next.

6.1 Methods

The method presented in this chapter consists in improving a simple linear regression to estimate $\mathcal{P}$ from SBI, by using additional information about the relationship between SBI and non-invasive measured $_rPulse$ waveshape parameters. Note that the goal is not to estimate $\mathcal{P}$ from wave shape, but from SBI only; neither is to re-estimate $\hat{\mathcal{P}}$s already estimated using other EO as PC or GTF.[1] The additional information comes from a database of non-invasive measurements of BP and SBI with over 1700 observations. The data used for this study are explained in the next section, followed by the description of the algorithm used to estimate the model's coefficients.

6.1.1 Data

The data for this analysis comes from two distinct databases: (i) Invasive DB and (ii) Integrated DB (see Chapter 2, section 2.4). In both databases the SBI, which are the independent variables in the model, are included. In addition, both databases

[1] Commercially available instruments 'measure' $\hat{\mathcal{P}}$s (such as $_aSP$, $_aDP$ or $_aAIx$) non-invasively, based on the radial $Pulse$ contour. If a regression is used to estimate these $\hat{\mathcal{P}}$s from SBI, this will be a re-estimation. This is because the $\hat{\mathcal{P}}$s are not direct measurements but estimates, as explained in Chapter 5.

contain fields describing the ${}_rPulse$.[2] These data are referred to as 'additional information', because it's not being used as independent variables or target variable in the modeling process. The target variables (${}_aSP$, ${}_aDP$, ${}_aPP$, ${}_aAIx$, ED, PPA^{-1}) are only contained in the Invasive DB. Both datasets can be seen as one single dataset ($N = N_{inv} + N_{int} = 59 + 1727 = 1786$) with missing values (the target variables), as shown in Table 6.1. Note that the proportion of missing values for target parameters is large ($96.7\% = N_{int}/N = 1727/1786$) because of the large discrepancy on the size of the two datasets. Although the number of missing values is large, the method presented in this chapter allows for better inference about relationships in the data, than if standard linear regression was used. This is possible because this method utilizes the ${}_rPulse$ contour (i.e., the additional information) available for all observations ($N = 1786$).

6.1.2 Regression with Additional Information

This section presents the regression method with additional information in a general form, without applying it directly to the estimation of BP $\mathcal{P}$s. However, references to the estimation of $\mathcal{P}$, will be made to facilitate to place the abstract concept in context. In the following sections of this chapter this method will be used to estimate the BP $\mathcal{P}$s (${}_aSP$, ${}_aDP$, ${}_aPP$, ${}_aAIx$, ED, PPA^{-1}) form SBI.

As in linear regression this method aims to determine the parameters $\boldsymbol{\beta_x}$, in

$$\hat{y} = \boldsymbol{x}\boldsymbol{\beta_x} \tag{6.2}$$

where $\hat{y}$ is the dependent variable, $\boldsymbol{x} = \{x_1, x_2, \ldots, x_n\}$ is a vector of independent variables and $\boldsymbol{\beta_x} = \{\beta_1, \beta_2, \ldots, \beta_n\}$ is a vector or parameters. The selection of the $\boldsymbol{\beta_x}$ satisfies a certain criterion. In contrast to linear regression, the criterion used is not to minimize $\sum (y - \hat{y})^2$, but to minimize the variance of the estimated $\hat{\boldsymbol{\beta}}_{\boldsymbol{x}}$.[3]

[2]The possible source of error caused by the difference between invasive and non-invasive calibration of the ${}_rPulse$, as described in Chapter 4, section 4.1.4, is not considered because simultaneous invasive and non-invasive data are not available.

[3]This criterion is also met in standard linear regression. However, the inclusion of the additional

Table 6.1: Parameters available for each of the two datasets (*Inv. DB* and *Int. DB*). The data is divided in three categories: (i) SBI, (ii) Additional information, and (iii) Target $\mathcal{P}$s. SBI and additional information are available in both datasets. $\mathcal{P}$s are only available in the *Inv. DB*. ✓: data available. ◯: missing values.

Group	*Field*	*Description*	*Inv. DB*	*Int. DB*
SBI	Age	Subject's age	✓	✓
	S	Subject's sex	✓	✓
	H	Subject's height	✓	✓
	W	Subject's weight	✓	✓
	HR	Heart rate	✓	✓
	${}_rSP$	Radial systolic pressure	✓	✓
	${}_rDP$	Radial diastolic pressure	✓	✓
Additional info	${}_rPulse$	Radial pulse	✓	✓
	${}_rPC1$	Radial PC 1	✓	✓
	${}_rPC2$	Radial PC 2	✓	✓
	${}_rPC3$	Radial PC 3	✓	✓
	${}_rPC4$	Radial PC 4	✓	✓
Target $\mathcal{P}$	${}_aSP$	Aortic systolic pressure	✓	◯
	${}_aDP$	Aortic diastolic pressure	✓	◯
	${}_aPP$	Aortic pulse pressure	✓	◯
	${}_aAIx$	Aortic augmentation index	✓	◯
	ED	Ejection duration	✓	◯
	PPA	Pulse pressure amplification	✓	◯
Observations			N_{inv} : 59	N_{int} : 1727

Characteristics of the Data

The data, also in contrast to linear regression, comes from two distinct datasets: (i) A dataset (A) containing N_A observations of independent variables ($\boldsymbol{x}$), additional variables ($\boldsymbol{z}$) and target variables (y) (see Table 6.3a) and (ii) A dataset (B) containing N_B observations of independent variables ($\boldsymbol{x}$), additional variables ($\boldsymbol{z} = \{z_1, z_2, \ldots, z_n\}$) but NOT target variables (see Table 6.3b).

The two datasets can be combined in a single dataset of size $N_A + N_B = N$ with N_B missing target variables, as shown in Table 6.3.

information will restrict the variability of $\boldsymbol{\beta_x}$. Therefore, the $\boldsymbol{\beta_x}$ with minimum variance is different from the $\boldsymbol{\beta_x}$ obtained by standard linear regression.

Table 6.2: The required data.

Field	*Description*
$\boldsymbol{x}$	Independent variables
$\boldsymbol{z}$	Independent variables
y	Target variable

(a) Data set A (N_A). Target variables available. In the estimation of BP $\mathcal{P}$ this dataset corresponds to the invasive DB.

Field	*Description*
$\boldsymbol{x}$	Independent variables
$\boldsymbol{z}$	Independent variables
y	N/A

(b) Data set B (N_B). Target variables not available. In the estimation of $\hat{\mathcal{P}}$ this dataset corresponds to the non-invasive DB.

Table 6.3: Data as a single dataset. For the estimation of $\hat{\mathcal{P}}$ this dataset corresponds to the total DB presented in Table 6.1, where $\boldsymbol{x}$ is the SBI, $\boldsymbol{z}$ the additional information of ${}_rPulse$ waveshape and y the target $\mathcal{P}$. ✓: data available. ◯: data not available.

	$\boldsymbol{x}$	$\boldsymbol{z}$	y
1	✓	✓	✓
⋮	⋮	⋮	⋮
N_A	✓	✓	✓
$N_A + 1$	✓	✓	◯
⋮	⋮	⋮	⋮
$N_A + N_B = N$	✓	✓	◯

Orthogonalization of Additional Information

The linear dependency between each z_i and $\boldsymbol{x}$ can be written as

$$z_i = \mathbf{d}_i \cdot \boldsymbol{x} + z^{\perp} \tag{6.3}$$

where $\mathbf{d}$ is a vector of best fit coefficients and $z^{\perp}$ are the residuals. In other words, each of the z_i can be estimated by a linear regression of $\boldsymbol{x}$. The residuals for all regressions, by definition are orthogonal to $\boldsymbol{x}$. All z_i can be represented as $\boldsymbol{z}^{\perp} = \{z_1, z_2, \ldots\}$. Therefore, without loosing information the parameters $\boldsymbol{z}$ can be replaced with $\boldsymbol{z}^{\perp}$, as shown in Table 6.4.

Regression

If $N_B = 0$ (i.e., there are no missing values) and because $\boldsymbol{x}$ is orthogonal to $\boldsymbol{z}^{\perp}$, the estimated $\hat{\boldsymbol{\beta}}_{\boldsymbol{x}}$ by minimizing $\sum (y - \hat{y})^2$ in equation 6.4 or equation 6.5 are the

Table 6.4: Data as a single dataset with orthogonal parameters ($\boldsymbol{z}^{\perp}$).

	$\boldsymbol{x}$	$\boldsymbol{z}^{\perp}$	y
1	✓	✓	✓
⋮	⋮	⋮	⋮
N_A	✓	✓	✓
$N_A + 1$	✓	✓	◯
⋮	⋮	⋮	⋮
$N_A + N_B = N$	✓	✓	◯

same.

$$\hat{y} = \boldsymbol{x}\hat{\boldsymbol{\beta}}_{\boldsymbol{x}} + \boldsymbol{z}^{\perp}\hat{\boldsymbol{\beta}_{\boldsymbol{z}^{\perp}}} \tag{6.4}$$

$$\hat{y} = \boldsymbol{x}\hat{\boldsymbol{\beta}}_{\boldsymbol{x}} \tag{6.5}$$

Equations 6.4 and 6.5 can be written as

$$y = \boldsymbol{x}\hat{\boldsymbol{\beta}}_{\boldsymbol{x}} + \boldsymbol{z}^{\perp}\hat{\boldsymbol{\beta}_{\boldsymbol{z}^{\perp}}} + \epsilon \tag{6.6}$$

$$y = \boldsymbol{x}\hat{\boldsymbol{\beta}}_{\boldsymbol{x}} + \epsilon_{\boldsymbol{x}} \tag{6.7}$$

and the minimization of $\sum (y - \hat{y})^2$ is equivalent to the minimization of $\sum \epsilon^2$ in equation 6.6 and of $\sum \epsilon_{\boldsymbol{x}}^2$ in equation 6.7.

When $N_B > 0$ (i.e., there are missing values) the estimated $\hat{\boldsymbol{\beta}}_{\boldsymbol{x}}$ have to be calculated from dataset A only (as dataset B does note contain target variables for the regression). $\hat{\boldsymbol{\beta}}_{\boldsymbol{x}}$ can be calculated either by using: (i) equation 6.6 or (ii) equation 6.7. In contrast to the case in which $N_B = 0$, the $\hat{\boldsymbol{\beta}}_{\boldsymbol{x}}$ estimated from (i) or (ii) are different. The following mathematical demonstration will prove that equation 6.6 should be used to estimate $\hat{\boldsymbol{\beta}}_{\boldsymbol{x}}$ because its variance is lower than if estimated with equation 6.7.

In both cases, because the linear regression model is not biased, the expected value are the same: $E[\hat{\boldsymbol{\beta}}_{\boldsymbol{x}}] = \boldsymbol{\beta}_{\boldsymbol{x}}$. In contrast, the variance-covariance matrix $Var[\hat{\boldsymbol{\beta}}_{\boldsymbol{x}}]$ differ from (i) and (ii).

For case (i) the variance of $\boldsymbol{\beta}_{\boldsymbol{x}}$ and $\boldsymbol{\beta}_{\boldsymbol{z}}$ can be calculated as (this is the standard

derivation of variance but expressed in matrix form by blocks to separate $\boldsymbol{\beta_x}$ and $\boldsymbol{\beta_z}$):

$$Var\begin{bmatrix}\boldsymbol{\beta_x}\\ \boldsymbol{\beta_z}\end{bmatrix} = \left(\begin{bmatrix}\boldsymbol{x}\\ \boldsymbol{z}\end{bmatrix}^T\begin{bmatrix}\boldsymbol{x}\\ \boldsymbol{z}\end{bmatrix}\right)^{-1}\sigma^2 \tag{6.8}$$

$$= \begin{pmatrix}\boldsymbol{x}^T\boldsymbol{x} & \boldsymbol{x}^T\boldsymbol{z}^\perp\\ \boldsymbol{z}^{\perp T}\boldsymbol{x} & \boldsymbol{z}^{\perp T}\boldsymbol{z}^\perp\end{pmatrix}^{-1}\sigma^2 \tag{6.9}$$

therefore

$$Var[\hat{\boldsymbol{\beta}}_{\boldsymbol{x}}]_i = (\boldsymbol{x}^T\boldsymbol{x})^{-1}\sigma^2 \tag{6.10}$$

where

$$\sigma = \frac{1}{N_A - p - 1}\sum_{i=1}^{N_A}\epsilon^2 \tag{6.11}$$

For case (ii)

$$Var[\hat{\boldsymbol{\beta}}_{\boldsymbol{x}}]_{ii} = (\boldsymbol{x}^T\boldsymbol{x})^{-1}\sigma_{\boldsymbol{x}}^2 \tag{6.12}$$

where

$$\sigma_{\boldsymbol{x}} = \frac{1}{N_A - p_{\boldsymbol{x}} - 1}\sum_{i=1}^{N_A}\epsilon_{\boldsymbol{x}}^2 \tag{6.13}$$

From equations 6.6 and 6.7

$$\begin{aligned}\sum\epsilon_{\boldsymbol{x}}^2 &= \sum(\boldsymbol{z}^\perp\hat{\boldsymbol{\beta}_{\boldsymbol{z}^\perp}} + \epsilon)^2\\ &= \sum((\boldsymbol{z}^\perp\hat{\boldsymbol{\beta}_{\boldsymbol{z}^\perp}})^2 + 2(\boldsymbol{z}^\perp\hat{\boldsymbol{\beta}_{\boldsymbol{z}^\perp}})\epsilon + \epsilon^2)\\ &= \sum(\boldsymbol{z}^\perp\hat{\boldsymbol{\beta}_{\boldsymbol{z}^\perp}})^2 + \sum 2(\boldsymbol{z}^\perp\hat{\boldsymbol{\beta}_{\boldsymbol{z}^\perp}})\epsilon + \sum\epsilon^2\\ &= \sum(\boldsymbol{z}^\perp\hat{\boldsymbol{\beta}_{\boldsymbol{z}^\perp}})^2 + \sum\epsilon^2\end{aligned}$$

therefore

$$\sum\epsilon_{\boldsymbol{x}}^2 \geq \sum\epsilon^2 \tag{6.14}$$

If equation 6.14 is applied to equations 6.11 and 6.13, $N_A >> p$ and $\boldsymbol{z}^{\perp}$ is correlated with y, then

$$\sigma_{\boldsymbol{x}} \geq \sigma$$

and

$$Var[\hat{\boldsymbol{\beta}}_{\boldsymbol{x}}]_{ii} \geq Var[\hat{\boldsymbol{\beta}}_{\boldsymbol{x}}]_i$$

therefore $\hat{\boldsymbol{\beta}}_{\boldsymbol{x}}$ should be estimated using equation 6.6.

Validity

The method was tested experimentally. The simulated data for the experiment was of the form

$$y = 0.1x + 0.9z + \Lambda(\mu = 0, \sigma = 0.1) \tag{6.15}$$

where $\Lambda(\mu = 0, \sigma = 0.1)$ is a normally distributed random variable with mean = 0 and standard deviation = 0.1.[4] The correlation between z and x was given by

$$z = 0.2x + \Lambda(0, 1) \tag{6.16}$$

Therefore, the theoretical expected β_x for this model is given by

$$\begin{aligned} y &= 0.1x + 0.9z \\ &= 0.1x + 0.9(0.2x) \\ &= 0.1x + 0.18x \\ &= 0.28x \\ &= \beta_x x \end{aligned}$$

Using the previous definition, 1000 observations were simulated and the $\boldsymbol{\beta}_{\boldsymbol{x}}$ was estimated using the method described in this section. The number of known target

[4]The notation $\Lambda(\mu = 0, \sigma = 0.1)$ was used instead of the most traditional $N(\mu = 0, \sigma = 0.1)$ because the letter 'N' is used to denote the size of the sample dataset.

variables (i.e., N_A) was varied from 1 to 300. The experiment was repeated 150 times to analyze the mean and standard error of the $\hat{\boldsymbol{\beta}}_{\boldsymbol{x}}$. The expected values and standard error of β_x are plotted in Figure 6.1.

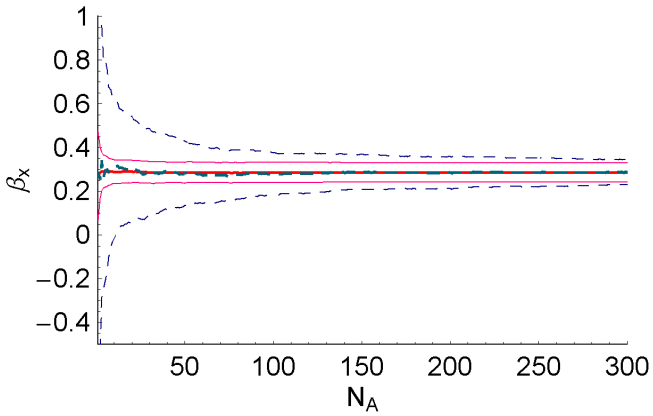

Figure 6.1: Convergence of β_x using standard linear regression (dashed lines) and additional information method (solid lines). The lines are: expected value (center) and $\pm$ 1 standard error for increasing number of N_A. The additional information produces a substantial reduction in variance.

For real data the method can easily be tested by comparing the calculated $Var[\hat{\boldsymbol{\beta}}_{\boldsymbol{x}}]_i$ and $Var[\hat{\boldsymbol{\beta}}_{\boldsymbol{x}}]_{ii}$, or by comparison of RMS error values for a *testing dataset*.

Additional information on linear regression can be found in the book by Seber [1977] and for the use of testing sets in the book by Hastie et al. [2001].

6.1.3 Selected Arterial BP Parameters

Only a set of selected $\mathcal{P}$ is analyzed. The $\mathcal{P}$s were chosen because they are commonly refer in the literature. The different $\mathcal{P}$s are presented in the Table 6.5 and were explained in detail in section 5.1.5.

6.1.4 Selected Additional Information

Two sets of additional information were used for the estimation of BP parameters ${}_a\mathcal{P}$ (${}_aSP$, ${}_aDP$, ${}_aPP$, ${}_aAIx$, ED and PPA^{-1}). Both sets describe the ${}_rPulse$,

and therefore are correlated with ${}_a\mathcal{P}$ (i.e., the target variables). The two sets of additional information are explained next.

Principal Components

The first 8 principal components (PC) scores, obtained by PC decomposition of the ${}_rPulse$, were used as additional information for the analysis of ${}_a\mathcal{P}$. The PC decomposition is described in Chapter 3. The EO using the PC as additional information will be referred to as 'LR-PC'.

Generalized Transfer Function

The ${}_a\widehat{\mathcal{P}}$ estimated using the GTF estimation option (as described in the previous chapter) were used as additional information. Only the corresponding ${}_a\widehat{\mathcal{P}}_{GTF}$ was used to estimate a specific ${}_a\mathcal{P}$ (e.g., only the estimated ${}_a\widehat{SP}_{GTF}$, not ${}_a\widehat{DP}_{GTF}$, ${}_a\widehat{AIx}_{GTF}$, etc..., was used to estimate ${}_aSP$). The EO using the $\hat{\mathcal{P}}_{GTF}$ as additional information will be referred to as 'LR-GTF'.

6.1.5 Analysis of Residuals $({}_a\widehat{SP} - {}_aSP)$

The residuals $({}_a\widehat{SP} - {}_aSP)$ for the 59 subjects of the Invasive DB were analyzed using the bootstrap method, as in the previous chapter. The number of bootstrap samples (B) was again 196. In this study the orthogonalization of the additional information is maintained constant and only the regressions with the invasive data is analyzed for variance. This is done because $N_{inv} << N_{int}$, and the significance of the values in d_i, in equation 6.3, is high ($p << 0.001$). Correlation coefficients (R^2) between real and estimated values were calculated for all $\mathcal{P}$ estimations using all 59 observations.

6.2 Results

No single EO, of the three compared in this chapter, is better (i.e., greater variance reduction) for estimating all ${}_a\widehat{\mathcal{P}}$. Table 6.5 summarizes the results. For all $\mathcal{P}$s, except ED, the LR EO was inferior than LR-PC and LR-GTF.

Table 6.5: Best EO for each specific $\mathcal{P}$. Best: maximum reduction of variance. Worst: less reduction of variance. In this table PC and GTF represent LR-PC and LR-GTF, respectively. pag.: page where models and analysis of residuals is presented.

	${}_aSP$	${}_aDP$	${}_aPP$	${}_aAIx$	${}_aED$	PPA^{-1}
pag.	109	111	113	115	117	119
Best: 1	PC	GTF	PC	GTF	PC	PC
2	GTF	PC	GTF	PC	LR	GTF
Worst: 3	LR	LR	LR	LR	GTF	LR

The results per $\mathcal{P}$ are presented next. For each EO the best fit model will be presented followed by the analysis of residuals. The analysis of each individual $\mathcal{P}$ concludes with the comparison of the use of the three EO: LR, LR-PC, and LR-GTF. Details of the results, including model coefficient statistics and histograms of mean, SD and RMS of residuals are presented in Appendix E.

6.2.1 Aortic Systolic Pressure

The models to estimate ${}_a\widehat{SP}$ using the LR, LR-PC and LR-GTF EO are presented in equations 6.17, 6.18 and 6.19 respectively. The details of the coefficients for the models are given in Appendix E.

Linear (LR): $R^2 = 0.64$

$$ {}_a\widehat{SP}_{\text{LR}} = -4.20 + 0.904_r SP \tag{6.17}$$

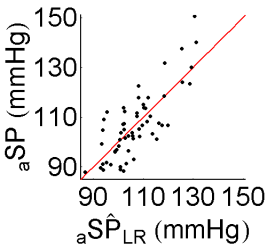

LR-PC: $R^2 = 0.69$

$$ {}_a\widehat{SP}_{\text{LR-PC}} = -23.2 + 0.226Age - 0.213HR + 0.356_r DP + 0.903_r SP \tag{6.18}$$

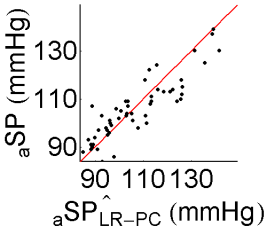

LR-GTF: $R^2 = 0.66$

$$ {}_a\widehat{SP}_{\text{LR-GTF}} = -21.8 + 0.234Age - 0.151HR + 0.186_r DP + 0.955_r SP - 5.37S \tag{6.19}$$

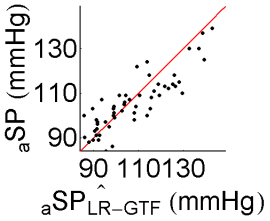

The comparative distribution of the mean and RMS values of the residuals are presented in Figure 6.2. None of the mean values is significantly different from 0 with 95% confidence.

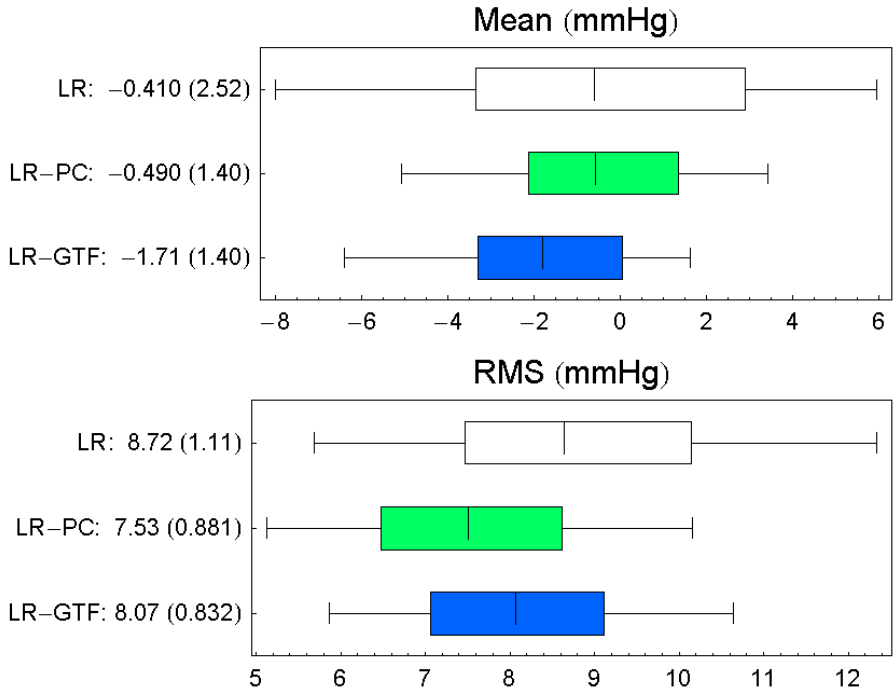

Figure 6.2: Residuals for LR, LR-PC and LR-GTF EO ($_aSP$). Top graph represents distribution of mean values of residuals. Bottom graph represents distributions of RMS values of residuals.

The distributions of the ratios of variance of residuals (see histograms of distributions in Figure E.2) by pairs of EO did not show significant difference at 95% confidence.

6.2.2 Aortic Diastolic Pressure

The models to estimate ${}_a\widehat{DP}$ using the LR, LR-PC and LR-GTF EO are presented in equations 6.20, 6.21 and 6.22 respectively. The details of the coefficients for the models are given in Appendix E.

Linear (LR): $R^2 = 0.94$

$$ {}_a\widehat{DP}_{\text{LR}} = -9.65 - 0.0757Age + 0.0894H + 0.0890HR + 0.843{}_rDP \tag{6.20} $$

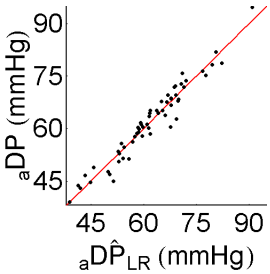

LR-PC: $R^2 = 0.97$

$$ {}_a\widehat{DP}_{\text{LR-PC}} = 3.85 - 0.0516Age + 0.0317HR + 0.965{}_rDP \tag{6.21} $$

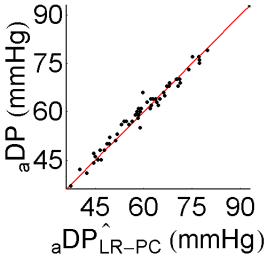

LR-GTF: $R^2 = 0.98$

$$ {}_a\widehat{DP}_{\text{LR-GTF}} = -1.97 + 0.0709HR + 0.956{}_rDP \tag{6.22} $$

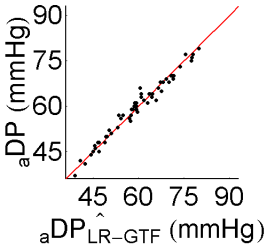

The comparative distribution of the mean and RMS values of the residuals are presented in Figure 6.3. None of the mean values is significantly different from 0 with 95% confidence.

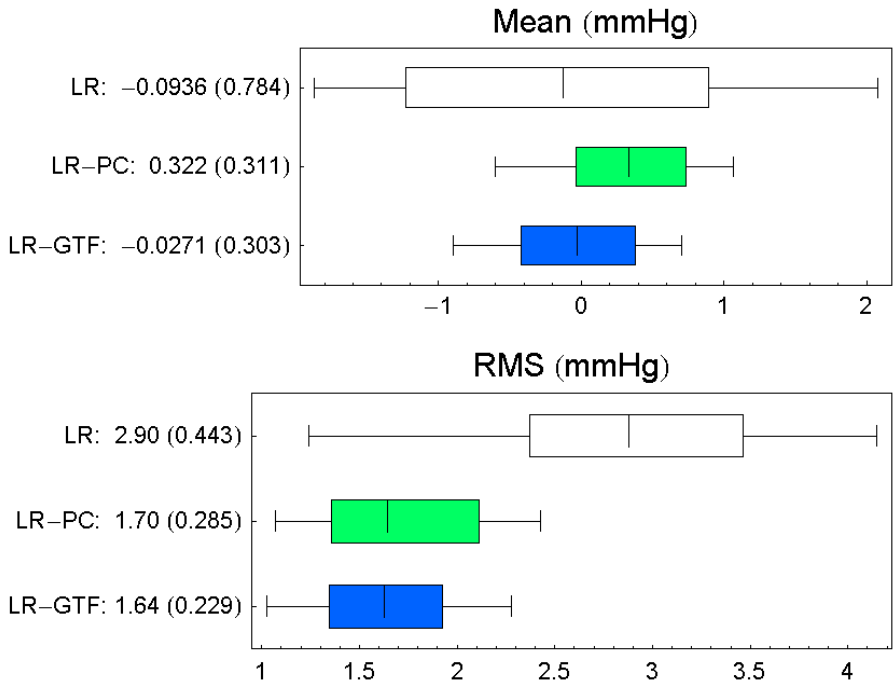

Figure 6.3: Residuals for LR, LR-PC and LR-GTF EO ($_aDP$). Top graph represents distribution of mean values of residuals. Bottom graph represents distributions of RMS values of residuals.

The distributions of the ratios of variance of residuals (see histograms of distributions in Figure E.4) by pairs of EO show significant difference (95% confidence) between the LR EO and LR-PC and LR-GTF. No difference was found between the LR-PC and LR-GTF EOs.

6.2.3 Aortic Pulse Pressure

The models to estimate ${}_a\widehat{PP}$ using the LR, LR-PC and LR-GTF EO are presented in equations 6.23, 6.24 and 6.25 respectively. The details of the coefficients for the models are given in Appendix E.

Linear (LR): $R^2 = 0.70$

$$ {}_a\widehat{PP}_{\text{LR}} = -11.4 + 0.238Age - 0.227HR - 0.597{}_rDP + 0.787{}_rSP \tag{6.23} $$

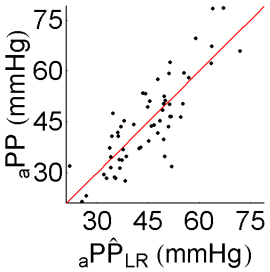

LR-PC: $R^2 = 0.67$

$$ {}_a\widehat{PP}_{\text{LR-PC}} = -28.5 + 0.322Age - 0.238HR - 0.548{}_rDP + 0.846{}_rSP \tag{6.24} $$

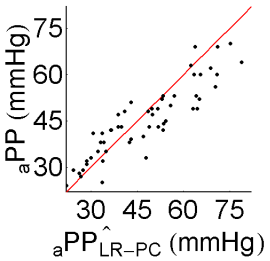

LR-GTF: $R^2 = 0.67$

$$ {}_a\widehat{PP}_{\text{LR-GTF}} = -13.8 + 0.262Age - 0.221HR - 0.772{}_rDP + 0.940{}_rSP - 3.66S - 0.0870W \tag{6.25} $$

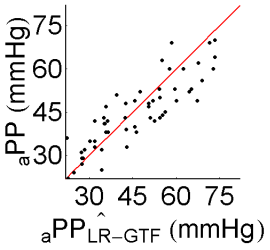

The comparative distribution of the mean and RMS values of the residuals are presented in Figure 6.4. None of the mean values is significantly different from 0 with 95% confidence.

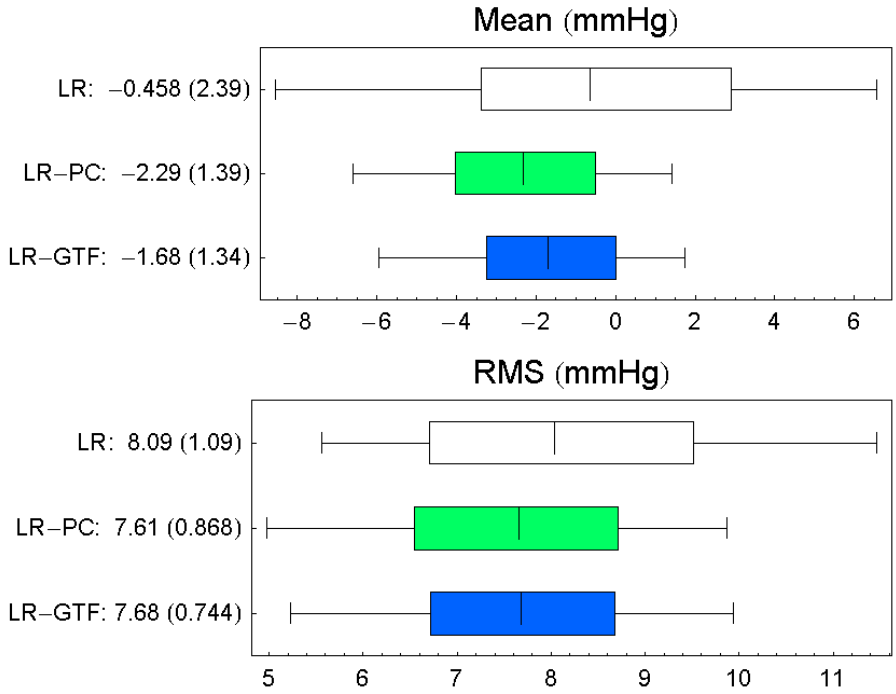

Figure 6.4: Residuals for LR, LR-PC and LR-GTF EO ($_aPP$). Top graph represents distribution of mean values of residuals. Bottom graph represents distributions of RMS values of residuals.

The distributions of the ratios of variance of residuals (see histograms of distributions in Figure E.6) by pairs of EO did not show significant difference at 95% confidence.

6.2.4 Aortic Augmentation Index

The models to estimate ${}_a\widehat{AIx}$ using the LR, LR-PC and LR-GTF EO are presented in equations 6.26, 6.27 and 6.28 respectively. The details of the coefficients for the models are given in Appendix E.

Linear (LR): $R^2 = 0.40$

$$ {}_a\widehat{AIx}_{\text{LR}} = 231. - 1.44HR \tag{6.26}$$

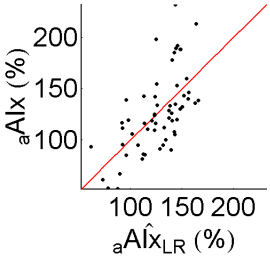

LR-PC: $R^2 = 0.39$

$$ {}_a\widehat{AIx}_{\text{LR-PC}} = 208. - 1.48HR + 0.757_r DP_r DP \tag{6.27}$$

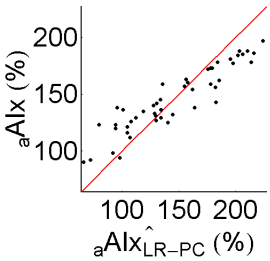

LR-GTF: $R^2 = 0.40$

$$ {}_a\widehat{AIx}_{\text{LR-GTF}} = 200. - 1.49HR + 0.804_r DP_r DP \tag{6.28}$$

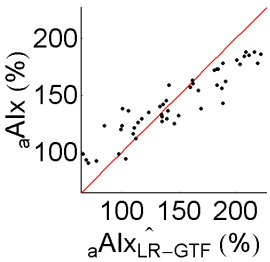

The comparative distribution of the mean and RMS values of the residuals are presented in Figure 6.5. None of the mean values is significantly different from 0 with 95% confidence.

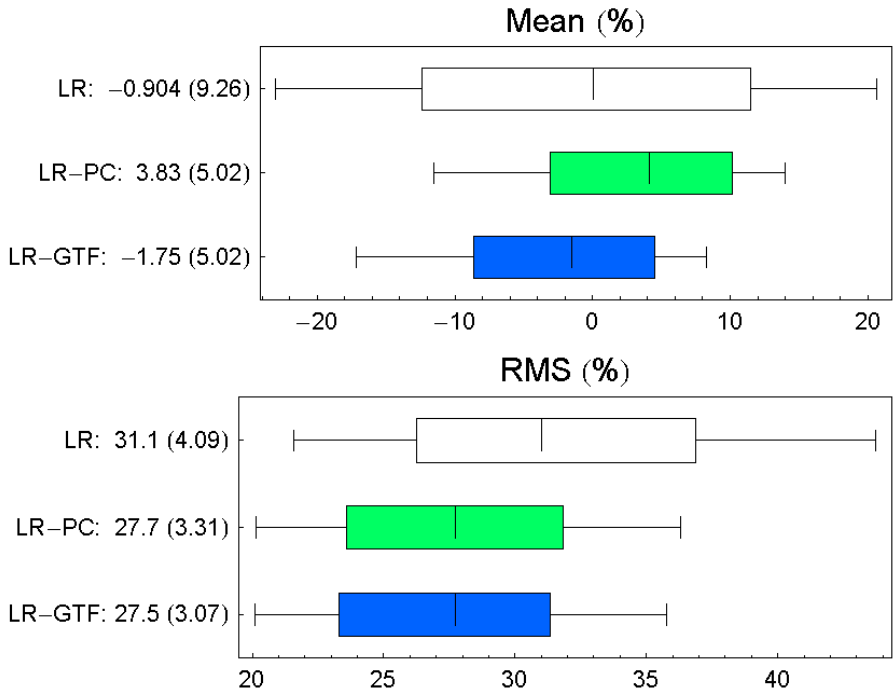

Figure 6.5: Residuals for LR, LR-PC and LR-GTF EO ($_aAIx$). Top graph represents distribution of mean values of residuals. Bottom graph represents distributions of RMS values of residuals.

The distributions of the ratios of variance of residuals (see histograms of distributions in Figure E.8) by pairs of EO did not show significant difference at 95% confidence.

6.2.5 Ejection Duration

The models to estimate $\hat{ED}$ using the LR, LR-PC and LR-GTF EO are presented in equations 6.29, 6.30 and 6.31 respectively. The details of the coefficients for the models are given in Appendix E.

Linear (LR): $R^2 = 0.71$

$$\hat{ED}_{\text{LR}} = 659. - 1.03H - 2.30HR \tag{6.29}$$

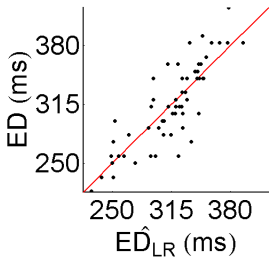

LR-PC: $R^2 = 0.73$

$$\hat{ED}_{\text{LR-PC}} = 683. - 1.10H - 2.45HR \tag{6.30}$$

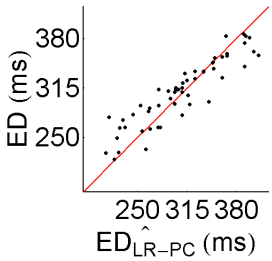

LR-GTF: $R^2 = 0.70$

$$\hat{ED}_{\text{LR-GTF}} = 438. - 1.91HR - 0.912_r DP + 0.568_r SP - 12.5S \tag{6.31}$$

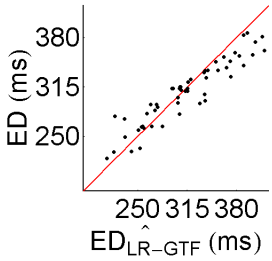

The comparative distribution of the mean and RMS values of the residuals are presented in Figure 6.6. None of the mean values is significantly different from 0 with 95% confidence.

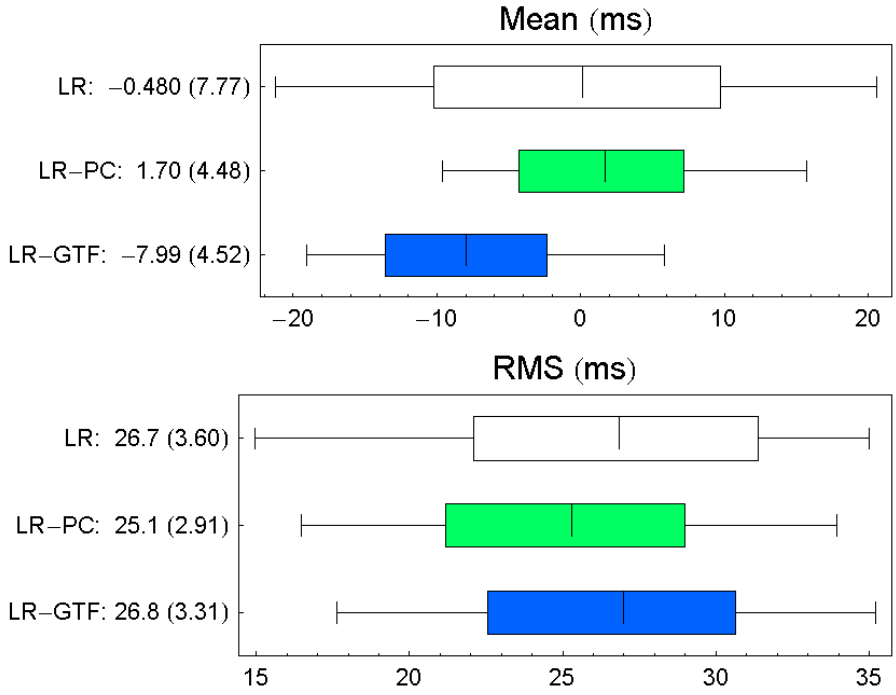

Figure 6.6: Residuals for LR, LR-PC and LR-GTF EO (ED). Top graph represents distribution of mean values of residuals. Bottom graph represents distributions of RMS values of residuals.

The distributions of the ratios of variance of residuals (see histograms of distributions in Figure E.10) by pairs of EO did not show significant difference at 95% confidence.

6.2.6 Inverse Pulse Pressure Amplification

The models to estimate $\widehat{\text{PPA}^{-1}}$ using the LR, LR-PC and LR-GTF EO are presented in equations 6.32, 6.33 and 6.34 respectively. The details of the coefficients for the models are given in Appendix E.

Linear (LR): $R^2 = 0.29$

$$\widehat{\text{PPA}^{-1}}_{\text{LR}} = 81.4 + 0.330Age - 0.348HR \tag{6.32}$$

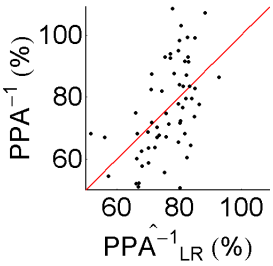

LR-PC: $R^2 = 0.29$

$$\widehat{\text{PPA}^{-1}}_{\text{LR-PC}} = 51. + 0.353Age - 0.410HR + 0.256_rSP \tag{6.33}$$

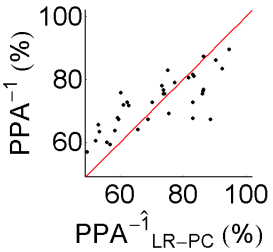

LR-GTF: $R^2 = 0.19$

$$\widehat{\text{PPA}^{-1}}_{\text{LR-GTF}} = 57. + 0.461Age - 0.359HR + 0.219_rSP - 6.51S - 0.121W \tag{6.34}$$

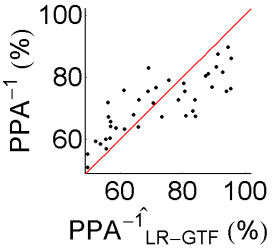

The comparative distribution of the mean and RMS values of the residuals are presented in Figure 6.7. None of the mean values is significantly different from 0 with 95% confidence.

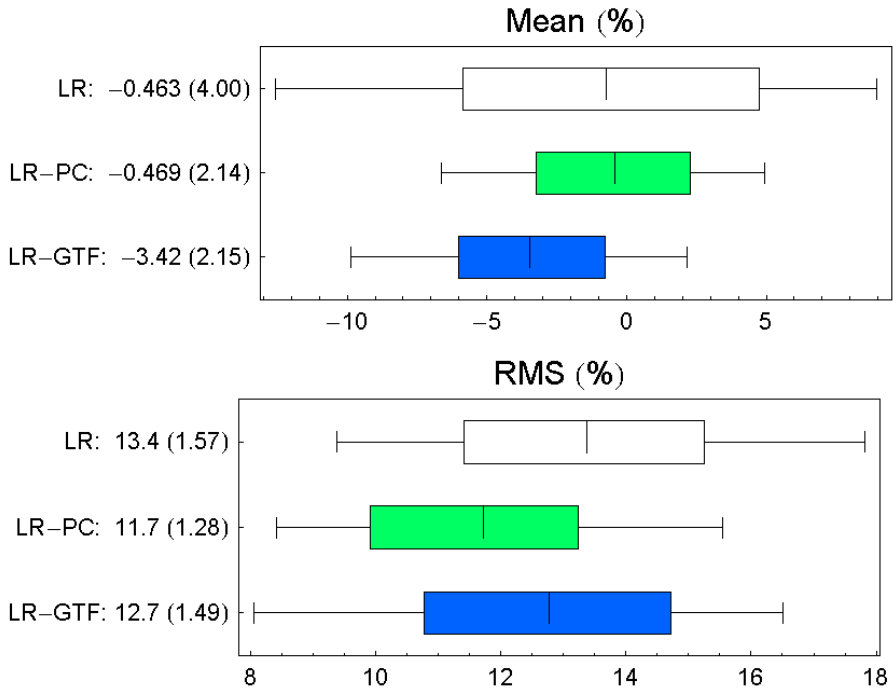

Figure 6.7: Residuals for LR, LR-PC and LR-GTF EO (PPA^{-1}). Top graph represents distribution of mean values of residuals. Bottom graph represents distributions of RMS values of residuals.

The distributions of the ratios of variance of residuals (see histograms of distributions in Figure E.2) by pairs of EO did not show significant difference at 95% confidence.

6.3 Discussion

The estimation of ${}_a\mathcal{P}$ from SBI (Age, Gender, Height, Weight, ${}_rSP$, ${}_rDP$) using standard linear regression (SLR) is possible, as presented in the previous chapter. However, because of the small number of observations ($N = 59$) the standard error of the coefficients of the estimation models is high and many predictor variables can not be considered significant.

The ${}_rPulse$ is related to ${}_a\mathcal{P}$ and also related to SBI. It is possible to model the relationships between SBI and ${}_r\widehat{Pulse}$ based on large datasets because invasive measurements are not required. The method presented in this chapter explores this mutual relationship between ${}_rPulse$, SBI and ${}_a\mathcal{P}$ to improve the estimates of ${}_a\widehat{\mathcal{P}}$ based on SBI.

The method is based on orthogonalization of the predictors describing the ${}_rPulse$, i.e., a linear process. Other more sophisticated techniques using non-linear relationships could be implemented, but were not included in this study.

By using this new estimation methods it is possible to improve the LR EO with reduction in RMS errors. The new models include predictor variables which were not significant when SLR was used. However, some predictor variables, selected as significant with SLR were excluded. The correlation (R^2) between estimated and real values (calculated from all data, not testing datasets) was maintained approximately constant. The cases in which R^2 was reduced or predictor variables excluded was probably because an exaggerated initial R^2 of slightly over-fitted models.

The method presented in this chapter improves the estimation of ${}_a\widehat{\mathcal{P}}$ from SBI only. However, the same technique could be used when SBI and MP are available. The estimation of ${}_a\widehat{\mathcal{P}}$ based on SBI and MP was not analyzed in this study but better estimation are expected.

Non-invasive measurements of ${}_a\widehat{\mathcal{P}}$ using the GTF EO provided the additional information that makes the improvement of the LR EO possible. However, these ${}_a\widehat{\mathcal{P}}$ estimated from the ${}_rPulse$ should not be confused with real ${}_a\mathcal{P}$ measure invasively

to analyze the relationships between real ${}_a\mathcal{P}$ and SBI.

6.4 Conclusions

The method proposed in this chapter improves the accuracy of estimated ${}_a\widehat{\mathcal{P}}$ and should be used when ${}_rPulse$ is not available. The estimation error of estimated ${}_a\mathcal{P}$ based on SBI only, even using this new technique, are greater than the once using SBI and MP. The implementation of a combined SBI and MP using this new technique could further improve the estimation and should be tested.

For previous studies in which ${}_rPulse$ or MP are not available, this technique provides better models that could be used for the retrospective analysis of previous studies in which ${}_rPulse$ or MP are not available. However, better understanding and modeling of the relationships between ${}_rPulse$, MP and SBI are only possible with further studies in which invasive central aortic and peripheral BP are measured.

7

Beat by Beat Analysis of the Radial Pressure Pulse — Effect of Mean Blood Pressure and Heart Rate Changes

The radial pressure pulse (${}_rPulse$) provides additional information to the subject basic information (SBI) for the description of the cardiovascular system. For example, it was shown in Chapters 5 and 6 that the estimation of ${}_a\mathcal{P}$s was improved if the ${}_rPulse$ contour was used (i.e., PC and GTF EO were used).

It is known that MP and HR affect the arterial tree, therefore affecting the BP wave shape and the $\mathcal{P}$s derived from it. However, the analysis presented in previous chapters, as well as other studies conducted by different groups [Kelly et al., 1989a,b, O'Rourke and Pauca, 2004], have been population studies based in the analysis of only one $Pulse$ per subject (static analysis) instead of a continues analysis of a trend of ${}_rPulse$s (dynamic analysis). Even more, in studies in which more then one $Pulse$ per subject was analyzed, the $Pulse$s were not analyzed for each independent subject at a time.

Although these studies present information on the relationships between $\mathcal{P}$s in a population, they don't provide information for individual subjects. This is because in a static analysis of the ${}_rPulse$ (i.e., the analysis of a single ${}_rPulse$) these changes are not present, preventing their analysis and their correlation to cardiovascular risk or diagnosis. Does HR affect wave shape? Does MP affect wave shape in a specific subject? Are the effects of MP or HR changes in the ${}_rPulse$ similar form subject to

subject? These questions cannot be answered based on a static analysis. Therefore, a beat by beat (dynamic) analysis, in which the ${}_rPulse$ variations can be observed, is required.

This chapter proposes a method to analyze the independent effects of HR and MP in $\mathcal{P}$s at an individual level, and compares the results with a population based static analysis. The method is based on the soft exhalation manoeuver (SEM), a new technique to exaggerate spontaneous MP and HR variability.

7.1 Methods

7.1.1 Population

For the beat by beat (dynamic) analysis of the ${}_rPulse$, data were collected from 8 subjects (5 male, 3 female) with an average age of 33.9 years with MP and HR mean values and SD as presented in Table 7.1. For comparison to a static analysis a subgroup of the IntDB (see Chapter 2, section 2.4) was selected. The selection was performed to match the age range of the 8 subjects. The characteristics of this subgroup, that will be referred to as 'general population' (GP), are also presented in Table 7.1.

7.1.2 Data Collection

Non-invasive radial BP and expiration pressure were measured continuously during the soft exhalation maneuver (SEM — explained later). The subjects were in supine position and feedback on expiration was provided graphically. Radial BP data were collected using the JENTOW (Colin Electronics, Komaki, Japan). A pre and post calibrations were made and the auto-calibration option was disabled to prevent auto-calibration during the SEM. Because of no instrument calibration and minimal subject movement, the hold-down pressure of the JENTOW device is assumed constant. The analogue output signal was conditioned using an SCXI condition box

Table 7.1: Dynamic analysis population. Values are mean(SD). N: Total number of ${}_rPulse$ available.

	Gender	*Age* (years)	*N*	*HR* (bpm)	*MP* (mmHg)
GP	315 M, 637 F	38.3(9.)	952	73.7(14.)	95.1(13.)
1	Female	23	460	64.7(5.9)	106.(3.0)
2	Female	22	502	67.7(6.3)	84.7(5.6)
3	Female	26	271	77.2(8.9)	106.(6.2)
4	Male	39	570	73.9(8.1)	86.4(4.8)
5	Male	55	606	77.6(4.7)	98.3(6.9)
6	Male	42	560	76.8(9.6)	89.1(6.5)
7	Male	39	216	64.5(5.8)	86.0(7.1)
8	Male	25	211	63.8(8.8)	78.5(4.4)
Avg:	5M, 3F	33.9	—	70.78	91.88

(SCXI-1000 & SCXI-1321), and was digitized using a PCI-6024E data acquisition (DAQ) board (National Instruments, Austin, TX., U.S.). Expiration pressure data were collected with a SDX01G2 BP sensor (Sensortechnics GmbH, Puchheim, Germany), connected to the same SCXI conditioning box and DAQ board. The system was calibrated against a mercury column. Data were collected at 384 samples per second. The system was custom made and was programmed in *LabVIEW® 7.1* (National Instruments, Austin, TX, U.S.). Data was saved in text format to facilitate compatibility with other software during analysis.

7.1.3 Soft Exhalation Maneuver

The soft exhalation maneuver (SEM) is a technique similar to the Valsalva maneuver, in which the subjects tries to exhale into a close chamber. In the SEM the subject exhales into a close tube in which a pressure sensor is built. In contrast to the Valsalva manoeuver the exhalation pressure is controlled and the times of exhalation are short (5 sec). The sequence of exhalation pressure and the exhalation times are specified. The protocol is presented in Table 83. Subjects 3, 7, and 8 completed only expirations $E1$ to $E5$, therefore the reduced N. The negative pressures mean inhalation. The system gives online expiration pressure feedback to the subject.

Table 7.2: SEM protocol. *E#*: Exhalation (or inhalation if pressure is negative). The exhalation periods were of 5 seconds followed by 25 seconds rest. Before the initial (*E1*) and after the last (*E11*) exhalations the subject went through resting periods of 60 seconds, The total procedure takes $60 + 10(5 + 25) + 5 + 60 = 425$ seconds.

	E1	*E2*	*E3*	*E4*	*E5*	*E6*	*E7*	*E8*	*E9*	*E10*	*E11*
eP (mmHg)	15	-15	15	-15	20	-20	20	-20	30	40	30

7.1.4 Data Analysis

The data were analyzed using *Mathematica*™ *5.0*. The raw BP data was corrected for discontinuities and drift of the JENTOW instrument. These errors were caused because the auto-calibration option of the JENTOW was disabled and continuous measurements were taken for periods over 5 minutes long. The automatic corrections for the drift, by the instrument, produce discontinuities in the data. The errors of the JENTOW instrument were previously analyzed by Sato et al. [1993]. The discontinuities were corrected visually. The drift was corrected by detrending the data and adjusting the final values to recalibrated measurements at the end of the data acquisition process.

For the analysis of aortic parameters (${}_a\mathcal{P}$), an aortic $Wave$ was estimated using the *SphygmoCor*® generalized transfer function ($\mathcal{T}_{SCor}$, see section 4.2.4 for derivation details). It is important to notice that data were not measured invasively and the ${}_a\mathcal{P}$ are all estimates using the GTF EO (see Chapter 5 for details).

The BP $Wave$s (${}_aWave$ and ${}_rWave$) were divided into aortic and radial $Pulse$s (${}_aPulse$ and ${}_rPulse$). The pulse starting points (t_0) were calculated on the ${}_rWave$ using the second derivative method. The pulses were inspected visually to verify correct location of the cutting points. For each pair of ${}_aPulse$ and ${}_rPulse$ the following parameters ($\mathcal{P}$) were calculated: MP, HR, ${}_rSP$, ${}_rDP$, ${}_rPP$, ${}_aSP$, ${}_aDP$, ${}_aPP$, ${}_rAIx$, ${}_aAIx$, ED, PPA^{-1} and expiration pressure (eP). The parameters are explained in detail in Chapter 4, section 4.3.1.[1] eP was defined as the average of

[1]For consistency of MP for different HR, the MP was calculated on the first 0.625 sec (80 sample pints) of the wave.

the expiration pressure for the duration of the pulse.

For each $\mathcal{P}$ a linear regression model of the form

$$\hat{\mathcal{P}} = C_0 + C_{MP}MP + C_{HR}HR + C_{eP}eP \tag{7.1}$$

was estimated. The variances ($Var[\mathcal{P}]$) were also calculated.

For each of the ${}_rPulse$ and ${}_aPulse$ of each subject of the general population (only one ${}_rPulse$ and ${}_aPulse$ per subject) the same model coefficients were estimated (except for C_{eP}) and the variance ($Var[\mathcal{P}_{GP}]$) was also calculated.

The variance of the $\mathcal{P}$s, for all 8 subjects, was normalized against the variance of the $\mathcal{P}$s in the GP. In other words, the ratios of the variance per subject over variance of the GP was calculated. As an example, for ${}_aSP$ and subject 1, the ratio was calculated as:

$$\|{}_aSP\|_1 = \frac{Var[{}_aSP_1]}{Var[{}_aSP_{GP}]} \tag{7.2}$$

Note that $\|{}_aSP\|$ are normalized variances and therefore have no units.

7.2 Results

The use of the SEM increases HR and MP variability, as shown in Figure 7.1.[2] The ranges of MP and HR before starting and during resting periods (i.e., normal respiration) during SEM are presented in Table 7.3.

By initial visual inspection of the ${}_rPulse$s per individual (Figure 7.2), it was possible to notice that HR and MP did not affect the ${}_rPulse$ contour in the same manner as observed in population analysis. Figure 7.2a shows several pulses of different periods (i.e., different HR) with very similar pulse shape. On the other hand, Figure 7.2b shows different ${}_rPulse$ shapes for different MP but almost identical HR.

[2]The HR and MP variability refer to the changes of HR and MP. Not specific frequencies or cyclic patterns are analyzed.

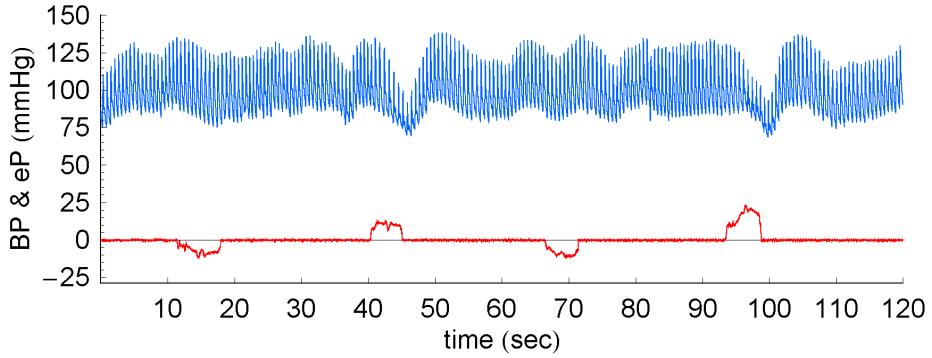

Figure 7.1: Effect of Soft Exhalation Maneuver (SEM). BP: Blood pressure, top trace. eP: exhalation pressure, bottom trace.

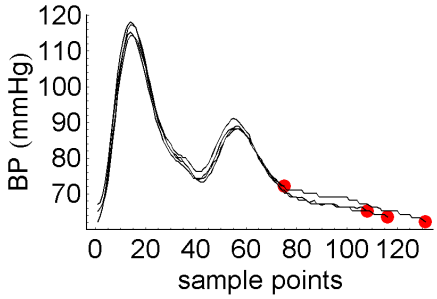

(a) Similar pulse shape and MP but different HR.

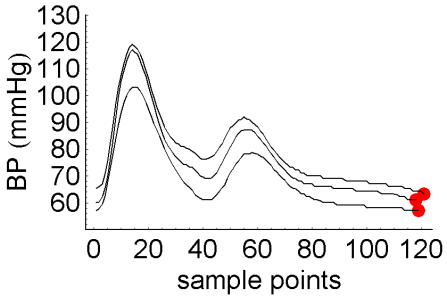

(b) Similar HR but different pulse shape and MP.

Figure 7.2: Comparison of HR, MP and ${}_rPulse$ shape. Points indicate t_{end}. Extracted from subject 1 measurements.

All coefficients (C_0, C_{MP}, C_{HR} and C_{eP}) of the model (equation 7.1) were calculated for all $\mathcal{P}$s. As an example, the model coefficients for ${}_r\widehat{SP}$ are presented for the first subject (Equation 7.3) and the GP (Equation 7.4).

The models and statistics of the coefficients for the first subject and the general population are:

$$ {}_rSP_1 = 63.1 - 0.00730HR + 0.714MP + 0.0387eP \tag{7.3} $$

$$ {}_rSP_{GP} = -2.29 + 0.242HR + 1.12MP \tag{7.4} $$

	Subject 1			*GP*		
	Estimate	SE	TStat	Estimate	SE	TStat
C_0	63.1	2.87	22.0	-2.29	2.50	-0.92
C_{MP}	0.714	0.0209	34.2	1.12	0.0184	61.
C_{HR}	-0.00730	0.0125	-0.59	0.242	0.0191	12.6
C_{eP}	0.0387	0.00845	4.58	—	—	—

Table 7.3: Effect of SEM in MP and HR. * only fist part of SEM was completed (see text section 7.1.3).

MP (mmHg)

	before SEM			during SEM			Δ(%)	
	min	max	mean(SD)	min	max	mean(SD)	mean	(SD)
1	100.	107.	103.(1.61)	98.8	114.	106.(2.52)	2.92	(56.3)
2	79.5	95.8	83.8(3.14)	69.1	97.2	84.0(5.30)	0.265	(69.1)
3*	91.9	109.	102.(3.86)	87.7	121.	105.(5.63)	2.32	(45.8)
4	79.5	97.8	86.3(3.88)	68.0	105.	86.1(4.47)	-0.272	(15.2)
5	89.9	106.	99.5(4.38)	68.6	117.	98.6(6.76)	-0.886	(54.2)
6	76.3	97.9	88.3(4.76)	69.4	103.	88.0(6.08)	-0.422	(27.6)
7*	70.4	80.4	77.7(2.83)	70.4	102.	85.6(6.22)	10.2	(120.)
8*	76.0	85.8	82.9(2.27)	64.0	88.9	78.3(4.51)	-5.46	(98.1)

HR (bpm)

	before SEM			during SEM			Δ(%)	
	min	max	mean(SD)	min	max	mean(SD)	mean	(SD)
1	56.1	77.6	65.6(3.69)	51.9	80.0	65.0(5.79)	-0.824	(57.2)
2	61.0	85.3	67.7(5.86)	56.5	88.3	68.1(6.11)	0.587	(4.37)
3*	66.2	97.2	78.8(7.79)	57.7	98.5	76.7(9.25)	-2.65	(18.8)
4	63.5	89.3	70.8(5.39)	57.3	101.	75.0(8.23)	5.90	(52.8)
5	71.1	81.7	77.1(3.09)	67.4	91.4	78.2(4.49)	1.42	(45.4)
6	53.7	85.3	78.5(6.07)	45.2	107.	76.5(8.69)	-2.56	(43.1)
7*	56.1	76.8	65.3(6.47)	52.6	80.8	65.1(6.01)	-0.336	(-7.08)
8*	53.7	71.1	61.5(5.28)	51.5	120.	65.0(8.74)	5.70	(65.5)

The coefficients C_{MP} and C_{HR} are summarized in Figure 7.6 (see Figure 7.3 for description of 'coefficient figures'). The effect of exhalation (inhalation) pressures (i.e., C_{eP}) are significant, but different from subject to subject as shown in Figure 7.4 for the case of ${}_rSP$. The C_{eP} for other $\mathcal{P}$ are also significant without any apparent pattern (data not presented).

The distributions of the ratio of variances ($\|\mathcal{P}\|$) are presented as whisker plots in Figure 7.5. All $\|\mathcal{P}\|$ have mean value less then unity, except for $\|{}_aAIx\|$.

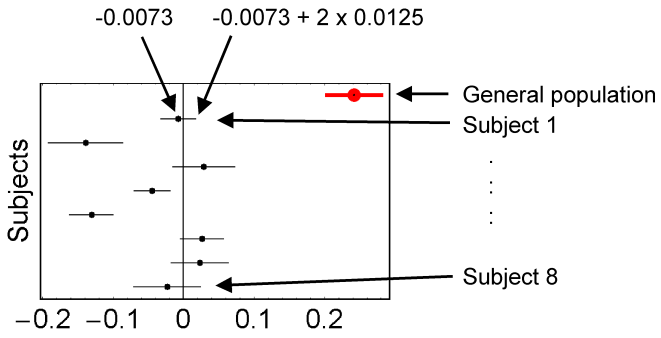

Figure 7.3: Description of 'coefficient figures' (Figures 7.4 and 7.6). Coefficient figures present the regression coefficients for all 8 subjects and general population. The figure presented here is a copy of Figure 7.6d. For subject 1 the coefficient that represent the effect of HR on ${}_r\widehat{SP}$ in equation 7.3 is presented. All points represent mean values. Error lines represent 95% confidence intervals.

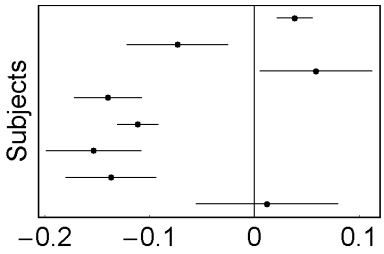

Figure 7.4: Effect of eP on ${}_rSP$. Coefficient for the general population is not shown because respiration was not monitored.

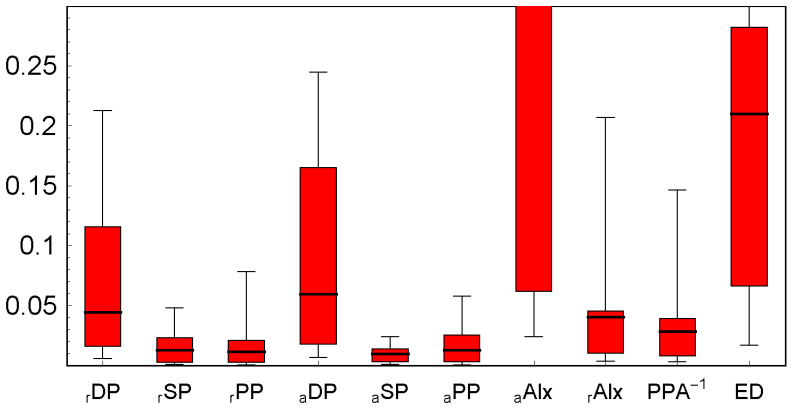

Figure 7.5: The distributions of ratio of variances ($\|\mathcal{P}\|$). Middle line represents mean value. Box represents 25% quantiles. Whiskers represent max and min. For ${}_aAIx$: mean = 1.38, min=0.0239 and max=6.3.

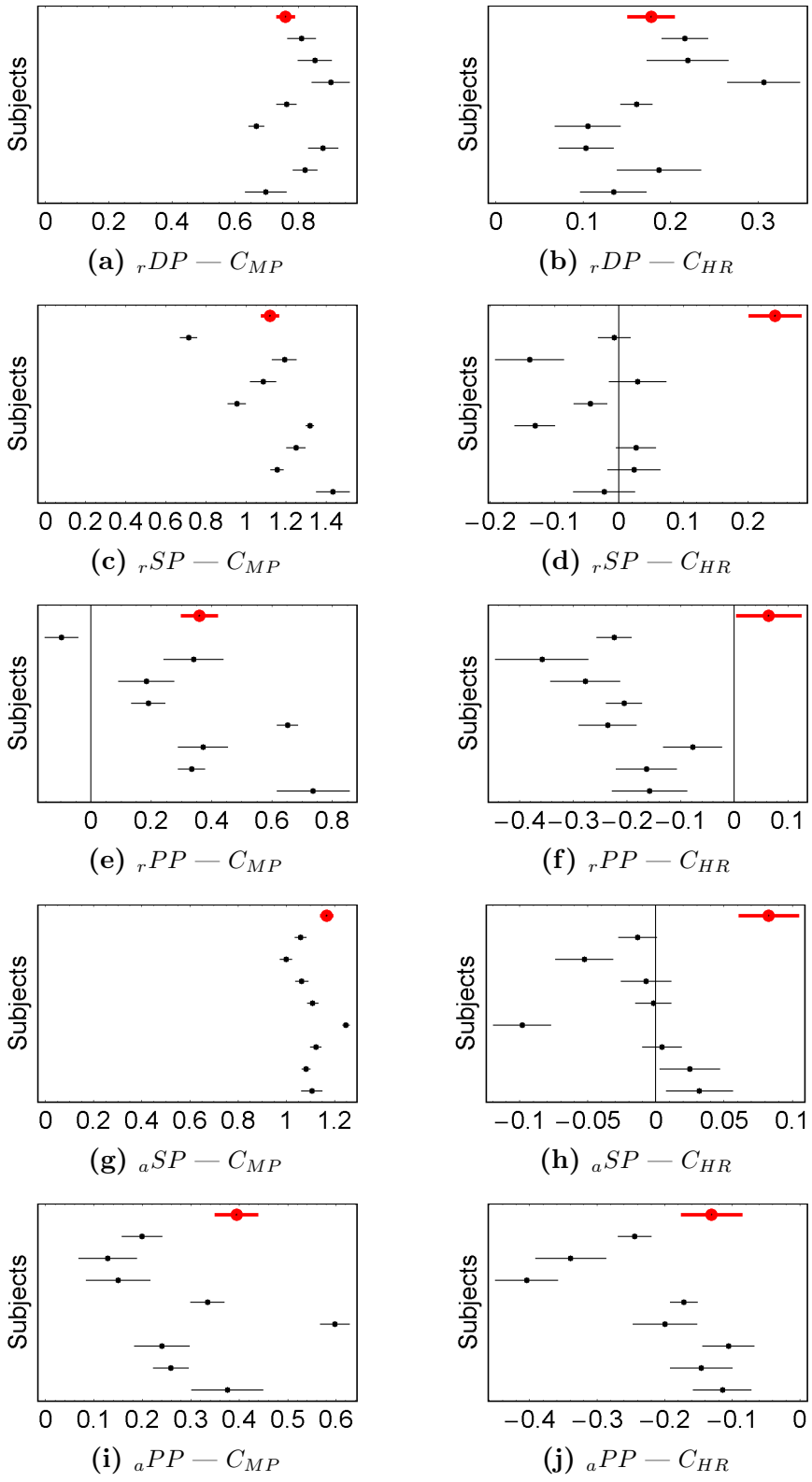

Figure 7.6: Coefficients C_{MP} and C_{HR} estimated in models described in equation 7.1. See Figure 7.3 for description of 'coefficient figures' (*continue in next page*).

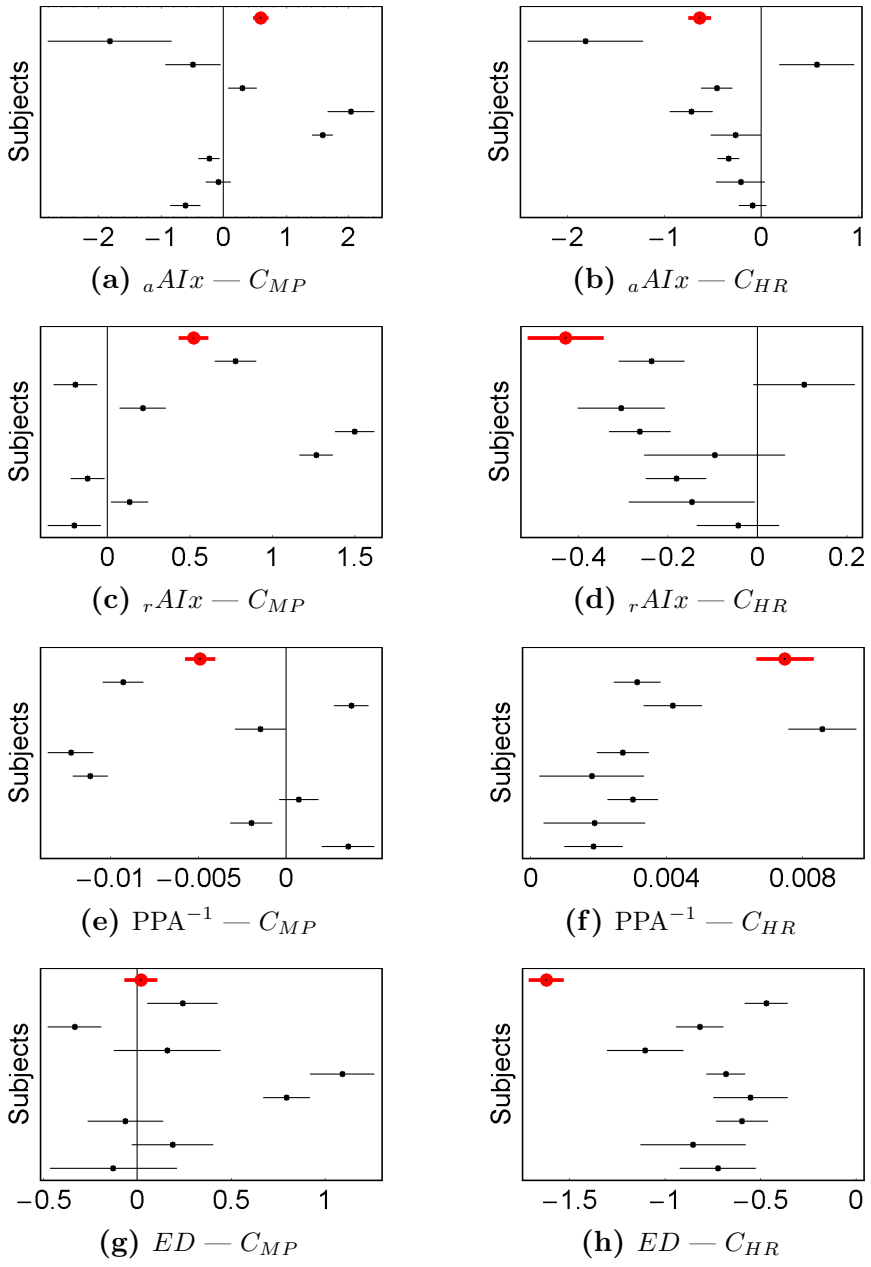

(a) ${}_aAIx$ — C_{MP} **(b)** ${}_aAIx$ — C_{HR}

(c) ${}_rAIx$ — C_{MP} **(d)** ${}_rAIx$ — C_{HR}

(e) PPA^{-1} — C_{MP} **(f)** PPA^{-1} — C_{HR}

(g) ED — C_{MP} **(h)** ED — C_{HR}

Figure 7.6: Coefficients C_{MP} and C_{HR} estimated in models described in equation 7.1. See Figure 7.3 for description of 'coefficient figures' (*from previous page*).

7.3 Discussion

The SEM proved to be an effective way to exaggerate MP and HR variability. Even more, the fact that the subjects 3,7,8 did not complete the test and still improvement in variability was obtained, suggests that only a reduced SEM is necessary. Even though SEM is not as extreme as the Valsalva manoeuver it still has a significant effect in the ${}_rPulse$ and therefore the $\mathcal{P}$s derived from it (including ${}_a\widehat{\mathcal{P}}$). However, because eP is known, the coefficients C_{MP} and C_{HR} can be estimated after compensating for eP. Much more complex (including non-linear) models could be analysed in futures studies to account for the apparent delay between eP and BP changes.

A possible source of error during SEM is the drift of the non-invasive measurement. However, because the instrument was calibrated at the beginning and at the end of the experiment, detreending of the signal was made, and the HR and BP signals are of much higher frequency than the drift itself, this possible source of error was not analysed.

The dynamic analysis expands the static analysis providing new indicators to characterize the cardiovascular system. The coefficients C_{MP} and C_{HR} could be used to stratify subjects as they reflect the response of the ${}_rPulse$ to changes in MP and HR that could be related to, for example, arterial stiffness. Further studies have to be conducted to analyzed their value as cardiovascular risk predictors or for clinical diagnosis.

The coefficients C_{MP} and C_{HR} for individual subjects are significantly different than the estimated for the general population. Specifically for ${}_rSP$ and ${}_rAIx$, C_{HR} estimated per subject differs from the estimated from the GP in a consistent manner. Most of the values are closer to zero, confirming the observations presented in Figure 7.2, that the $Pulse$ shape is more dependent on MP than on HR. The relationship between ED and MP is not significant for the GP but is significant for most individuals. In general, the coefficients C_{MP} and C_{HR} are specific for the individuals and different from the estimated from the GP. Therefore, the coefficients

estimated for the GP cannot be used to adjust or compensate $\mathcal{P}$s in individuals. For example, adjusting ${}_aAIx$ measured in an individual with HR of 60 bpm to an expected ${}_aAIx$ at 75bpm, using the C_{HR} coefficient estimated for the population (instead of the estimated for that specific individual), as is done in the algorithm currently implemented in the *SphygmoCor*® (Atcor Medical) apparatus, will result in incorrect estimates.

7.4 Conclusions

The reduced SEM, is a simple technique that exaggerates spontaneous MP and HR variability. This technique, combined with the dynamic analysis of ${}_rPulse$ provides additional information not available in static analysis. Therefore the analysis of the effects of MP and HR in ${}_rPulse$ shape and estimated $\hat{\mathcal{P}}$s is possible.

The relationship between MP and HR with radial and aortic $\mathcal{P}$ is particular to individual subjects and is different if derived from a population study.

Further studies in large populations and/or subpopulations with specific conditions (e.g., diabetics, pre-eclamptic women) should be conducted to analyze the relevance of these new methodology in cardiovascular risk stratification and clinical diagnosis.

8

The Value of Estimated Central Aortic Parameters

Large clinical studies have provided the scientific support for correct diagnosis and cardiovascular risk assessment. These studies are based on thousands of observation and long follow up periods. In addition to most traditional variables, including SBI, the arterial wave shape is a recent addition to the set of measurements [O'Rourke, 2004]. However, wave shape is measured in the periphery (e.g., ${}_rPulse$) and central aortic invasive measurements are not yet part of large epidemiological studies. However, ${}_a\widehat{\mathcal{P}}$ can be estimated from the ${}_rPulse$, as explained in previous chapters, and have been included in recent studies. So, the question arises: Is there any value in using estimated central aortic parameters (${}_a\widehat{\mathcal{P}}$), as they are estimated and not measured? There are two perspectives to this problem. (1) Can risk stratification be improved by using estimated ${}_a\widehat{\mathcal{P}}$? (2) Does the use of estimated ${}_a\widehat{\mathcal{P}}$ give new insight in the physiological understanding of cardiovascular risk?

This chapter will analyze both perspectives to this problem based on two different case studies. Initially, the use of estimated ${}_a\widehat{\mathcal{P}}$ as risk predictors will be analyzed in the context of the study by Roman et al. [2005], which is based on the COX proportional hazard model. Second, the dependency of ${}_a\widehat{SP}$ with *HR* will be analyzed in the context of the *LIFE*[1] *Study* [Dahlof et al., 1997, 2002] to illustrate the importance of the estimated ${}_a\widehat{\mathcal{P}}$ (even from a simple model based on SBI) to provide

[1]The Losartan Intervention For Endpoint reduction (*LIFE*) in Hypertension study.

an insight in the physiological understanding of cardiovascular risk.

8.1 Analysis of the Use of Estimated Central Aortic Parameters as Predictor Variables in the COX Model: *The Strong Heart Study*

The COX Proportional Hazard model (COX model) is widely used in the analysis of cardiovascular risk. Many different parameters, such as *HR*, BP, smoking, and others, have been analyzed to establish their relationship with CV risk or death. Central parameters are difficult to measure invasively and therefore large studies with ${}_a\mathcal{P}$ are not available. However, not invasive, but estimated ${}_a\widehat{\mathcal{P}}$ have been included in these analyzes and as shown in the study by Roman et al. [2005] ${}_a\widehat{\mathcal{P}}$ have proven to be a significant indicator of CV risk.

Affirmation: 'Noninvasively-determined central aortic pressure better predicts incident cardiovascular disease then does brachial pressure, ...' [Roman et al., 2005]

Question: Can risk stratification be improved by using estimated ${}_a\widehat{\mathcal{P}}$?

Analysis

The COX Proportional Hazard Model

The COX Proportional Hazard Model (COX model) is of the form

$$h(t, \boldsymbol{X}) = h_0(t) \exp \sum_{i=1}^{p} \beta_i X_i \tag{8.1}$$

where $\boldsymbol{X} = (X_1, X_2, \ldots, X_p)$ is the vector of predictor variables, $h_0(t)$ is the baseline hazard, and $\exp \sum_{i=1}^{p} \beta_i X_i$ is the modulator of hazard dependent on the predictor variables.

It is important to notice that in this specific model, the baseline hazard is dependent of time, but not of the predictor variables. In contrast, the modulator is independent of time but dependant on the predictor variables. The modulator is the exponent of a *linear combination* of the predictor variables. There is a more complex model called the extended COX model, in which the predictor variables are time dependent. That model is not considered here, but the result presented can be extended to it.

The solution of the COX model is based on the selection of the values of $\boldsymbol{\beta}$ based on maximum likelihood. A clear explanation of the COX model is given by Kleinbaum [1996] and a more detail mathematical explanation can be found in the book by Shoukri and Pause [1999].

Estimated Central Arterial Parameters

As previously explained, the accuracy of any specific estimated central arterial parameter depends on the estimation option (i.e., measured data ($\mathcal{M}$) and derivation method ($\mathcal{D}$)). The estimation options analyzed in Chapters 5 and 6 can be represented as *linear combinations* of the predictor variables (i.e., $\mathcal{M}$), except for the GTF EO. However, for many of the ${}_a\widehat{\mathcal{P}}$ the GTF EO was not the best EO or was only marginally better. Therefore, the ${}_a\widehat{\mathcal{P}}$ will be treated as linear combinations of $\mathcal{M}$.

Using Estimated Parameters

When the estimated central arterial parameters are used as predictor variables in the COX model, a set of coefficients βs are estimated to 'fit' the data (i.e., maximize likelihood).

Estimated central parameters (${}_a\hat{\mathcal{P}}$) can be included as predictor parameters (e.g., ${}_a\widehat{SP}$). If peripheral parameters ${}_r\mathcal{P}$ are also included as predictors, ${}_a\hat{\mathcal{P}}$ will be redundant if the ${}_r\mathcal{P}$s are the same used to estimate ${}_a\hat{\mathcal{P}}$ (e.g., if ${}_rSP$, ${}_rDP$ and HR where used to estimate ${}_a\widehat{SP}$ and ${}_a\widehat{SP}$ is included as predictor). This is due to the linear

dependency between them (i.e., ${}_a\widehat{\mathcal{P}}$ is estimated with a linear model from the ${}_r\mathcal{P}$s. This argument is also valid for more complex estimation options (e.g., Principal Components) when radial waveshape descriptors, such as the PC1, are used). In this case, the use of the estimated central aortic BP parameters does not add any additional information and can be ignored. Instead, other parameter can be ignored if the relationship of risk with the estimated central parameters is of interest.

If the ${}_r\mathcal{P}$s are not the same used to estimate ${}_a\widehat{\mathcal{P}}$, it can be replaced (in equation 8.1) with its model equation (e.g., ${}_a\widehat{SP} = C_0 + C_{HR}HR + C_{rSPr}SP$). This will increase the number of degrees of freedom if the model uses more then one predictor variable. If the number of samples is large compared with the number of predictor variables (so that over fitting does not occur) the flexibility of the model will increase.

Results

Risk stratification cannot be improved by using ${}_a\widehat{\mathcal{P}}$s. It is better to use the raw data from where the ${}_a\widehat{\mathcal{P}}$s were estimated. Nevertheless, improved representation of the cardiovascular system is possible, as will be explained in the following section.

8.2 Better Representation of the Cardiovascular System with Estimated Central Aortic Parameters: *LIFE Study*

Important studies have not included BP wave shape, neither peripheral or central. A relationship between SBI and ${}_rPulse$ was presented in previous chapters. The analysis of the results of the *LIFE Study* from a central perspective will be presented in this section, as an example of the importance of the use of ${}_a\widehat{\mathcal{P}}$.

Affirmation: 'Losartan prevents more cardiovascular morbidity and death then Atenolol for a similar reduction in blood pressure...' [Dahlof et al., 2002]

Question: Does the use of estimated ${}_a\widehat{\mathcal{P}}$ give new insight in the physiological understanding of cardiovascular risk?

Analysis

Difference in ${}_a\widehat{SP}$ ($\Delta_a\widehat{SP}$) for the same brachial BP will be analyzed. The analysis is based on $\widehat{\text{PPA}^{-1}}$ estimated using the LR-GTF estimation option (EO) (see Chapter 6), with ${}_rSP$ and HR as predictor variables. ${}_rDP$ was not included because it is not a significant predictor of $\widehat{\text{PPA}^{-1}}$.

Regression of PPA^{-1}

PPA and PPA^{-1} were defined in Chapter 4 section 4.3. The relationship between $\widehat{\text{PPA}^{-1}}$ predicted by HR and ${}_rSP$ was calculated using the LR-GTF EO and is presented in equation 8.2.

$$\begin{aligned}\widehat{\text{PPA}^{-1}} &= C_0 + C_{HR}HR + C_{{}_rSP}{}_rSP \\ &= 74.6 - 0.438HR + 0.232{}_rSP\end{aligned} \tag{8.2}$$

with parameters estimated as

	Estimate	SE	TStat	PValue
C_0	74.6	12.3	6.08	< 0.01
C_{HR}	-0.438	0.0644	-6.80	< 0.01
$C_{{}_rSP}$	0.232	0.0915	2.54	0.0139

Note that PPA^{-1} is expressed in % and therefore the coefficients are also in %.

The $R^2 = 0.23$ for this regression is low, however the coefficients C_0, C_{HR} and $C_{{}_rSP}$ are significant.

Derivation of $\boldsymbol{\Delta_a SP}$

A change in ${}_rSP$ does not represent an identical change in ${}_aSP$. Even more, the same change in ${}_rSP$ can be caused by infinite different combinations of changes in ${}_aSP$ and HR. Δ_aSP is the difference between two estimated aortic systolic pressures,

${}_a\widehat{SP}_1$ and ${}_a\widehat{SP}_2$, based on known radial BPs and HR. $\Delta_a SP$ can be derived as follows. Based on the regression of $\widehat{\text{PPA}^{-1}}$, the ${}_a\widehat{SP}$ is expressed in terms of ${}_rSP$, ${}_rDP$ and HR

$$\begin{aligned}
{}_a\widehat{SP} &= {}_aDP + {}_aPP \\
&= {}_rDP + {}_rPP \times \text{PPA}^{-1} \\
&= {}_rDP + ({}_rSP - {}_rDP)(C_0 + C_{HR}HR + C_{{}_rSP{}_r}SP)
\end{aligned}$$

The difference between two ${}_a\widehat{SP}$ is calculated as (note: the 'hat' will be dropped for simplicity):

$$\begin{aligned}
\Delta_a SP &= {}_aSP_2 - {}_aSP_1 \\
&= ({}_rDP_2 + ({}_rSP_2 - {}_rDP_2)(C_0 + C_{HR}HR_2 + C_{{}_rSP{}_r}SP_2)) - \\
&\quad ({}_rDP_1 + ({}_rSP_1 - {}_rDP_1)(C_0 + C_{HR}HR_1 + C_{{}_rSP{}_r}SP_1))
\end{aligned}$$

Reorganizing and grouping by C_0, C_{HR} and $C_{{}_rSP}$, $\Delta_a SP$ can be expressed as:

$$\begin{aligned}
\Delta_a SP &= ({}_rDP_2 - {}_rDP_1) + \\
&\quad C_0({}_rSP_2 - {}_rDP_2 - {}_rSP_1 + {}_rDP_1) + \\
&\quad C_{HR}(HR_2({}_rSP_2 - {}_rDP_2) - HR_1({}_rSP_1 - {}_rDP_1)) + \\
&\quad C_{{}_rSP}({}_rSP_2({}_rSP_2 - {}_rDP_2) - {}_rSP_1({}_rSP_1 - {}_rDP_1)) \\
&= \text{T}_{ind} + C_0\text{T}_0 + C_{HR}\text{T}_{HR} + C_{{}_rSP}\text{T}_{{}_rSP}
\end{aligned} \tag{8.3}$$

where T_{ind} is a known independent term and T_0, T_{HR} and $\text{T}_{{}_rSP}$ are known terms associated with C_0, C_{HR} and $C_{{}_rSP}$, respectively.

Because C_0, C_{HR}, and $C_{{}_rSP}$ are random variables, the $\Delta_a SP$ is also a random

variable, with expected value:

$$\begin{aligned} E(\Delta_a SP) &= E(\mathrm{T}_{ind} + C_0\mathrm{T}_0 + C_{HR}\mathrm{T}_{HR} + C_{rSP}\mathrm{T}_{rSP}) \\ &= \mathrm{T}_{ind} + E(C_0)\mathrm{T}_0 + E(C_{HR})\mathrm{T}_{HR} + E(C_{rSP})\mathrm{T}_{rSP} \\ &= \mathrm{T}_{ind} + 0.746 \times \mathrm{T}_0 - 0.00438 \times \mathrm{T}_{HR} + 0.00232 \times \mathrm{T}_{rSP} \end{aligned} \tag{8.4}$$

and variance:

$$\begin{aligned} Var(\Delta_a SP) &= Var(\mathrm{T}_{ind} + C_0\mathrm{T}_0 + C_{HR}\mathrm{T}_{HR} + C_{rSP}\mathrm{T}_{rSP}) \\ &= Var(C_0)\mathrm{T}_0^2 + Var(C_{HR})\mathrm{T}_{HR}^2 + Var(C_{rSP})\mathrm{T}_{rSP}^2 \\ &\quad + Covar(C_0, C_{HR})\mathrm{T}_0\mathrm{T}_{HR} + Covar(C_0, C_{rSP})\mathrm{T}_0\mathrm{T}_{rSP} \\ &\quad + Covar(C_{HR}, C_{rSP})\mathrm{T}_{HR}\mathrm{T}_{rSP} \\ &= 0.0151\mathrm{T}_0^2 + 4.15 \times 10^{-7}\mathrm{T}_{HR}^2 + 8.37 \times 10^{-7}\mathrm{T}_{rSP}^2 \\ &\quad - 0.0000320\mathrm{T}_0\mathrm{T}_{HR} - -0.000103\mathrm{T}_0\mathrm{T}_{rSP} \\ &\quad + 1.20 \times 10^{-8}\mathrm{T}_{HR}\mathrm{T}_{rSP} \end{aligned} \tag{8.5}$$

From equation 8.4 and if $\Delta_r SP = -10mmHg$ and $\Delta_r DP = -5mmHg$ the following relationship between ${}_a\widehat{SP}$ and HR can be established:

$$\Delta_a SP = -10.1 - 0.197\Delta HR \tag{8.6}$$

which is represented in Figure 8.1. The dependency of ${}_aSP$ on HR should be considered in large clinical trial, because changes in ${}_aSP$ can be significantly different to changes in ${}_rSP$.

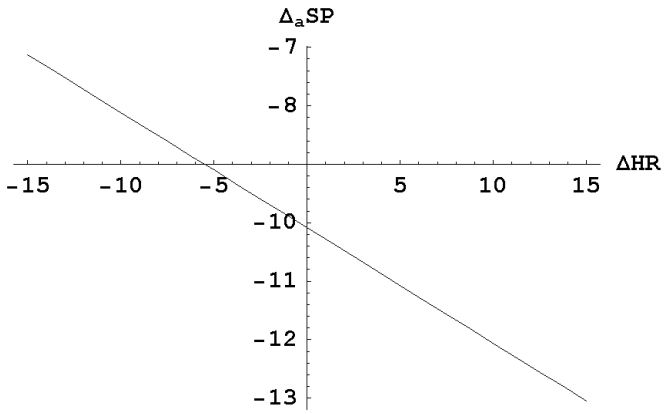

Figure 8.1: $\Delta_a SP$ for a fixed change of $\Delta_r SP/_r DP = -10/-5 mmHg$

Application to the *LIFE Study*

In the *LIFE Study* a cohort of $N = 9193$ aged 55-80 yrs with essential hypertension was followed during $T = 4$ yrs for two different BP interventions: (i) β-blocker (Atenolol) and (ii) angiotensin II receptor blocker (Losartan). The details of the study have been already published [Dahlof et al., 1997, 1998]. BP was reduced but maintained similar between the two groups as shown in Figure 8.2.

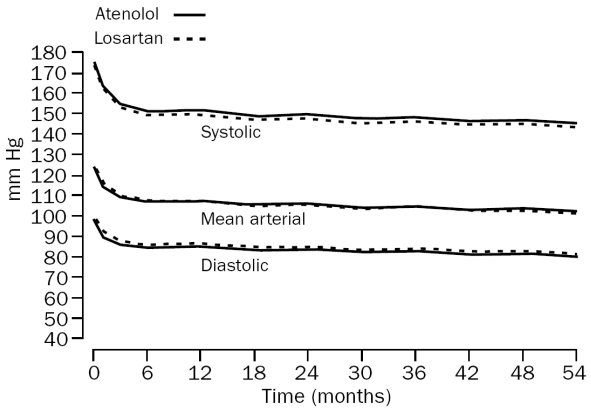

Figure 8.2: BP follow up in the *LIFE Study*. [Dahlof et al., 1997, 2002]

Despite the similar reduction in BP, the outcome of the Losartan group was significantly better. An overall relative risk reduction of 13% and stroke relative risk reduction of 24.9% were obtained with Losartan compared with Atenolol. The better outcome cannot be correlated to brachial BP differences between the two

groups. However, the β-blocker group has a reduction in HR of 7.7 bpm compared with only 1.8 bpm for the Losartan group. This difference leads to a reduction in ${}_aSP$ that in turn could explain the better outcome.

The differences in ${}_a\widehat{SP}$ for two groups in the *LIFE Study* is shown in Table 8.1. For the reported difference in HR of 5.9 bpm the ${}_a\widehat{SP}$ in the Losartan group is 2.8 mmHg lower then in the atenolol group, which support the comments by O'Rourke and Safar [2005], that the better outcome is due to lower central aortic BP.

Table 8.1: Δ_aSP dependency on HR. If $\Delta HR = 0$ the reduction of ${}_aSP$ in the Losartan group would 1.08 mmHg. With the reported HR difference of 5.9 bpm the reduction of ${}_aSP$ in the Losartan group is ≈ 2.78 mmHg. (*LIFE Study*).

ΔHR (bpm)	Δ_aSP	SD (mmHg)
0	1.08	0.277
-2.00	1.65	0.277
-4.00	2.21	0.301
-6.00	2.78	0.343
-8.00	3.34	0.399
-10.0	3.91	0.463
-12.0	4.47	0.532

Risk reduction associated with Δ_aSP

The concept presented in the previous section based on the *LIFE Study* can be extended to a general analysis of CV risk. According to Staessen et al. [1999] there is a reduction of 25% in overall cardiovascular risk for a reduction in systolic/diastolic BP of 10/5 mmHg. Therefore, for any combination of ΔHR and $\Delta_a\widehat{SP}$ that satisfies equation 8.6 a 25% reduction in overall cardiovascular risk is expected. If it were assumed that HR does not contribute to risk and all risk is associated with changes in ${}_aSP$ only, then the real risk reduction for a specific reduction in ${}_aSP$ is unknown, when HR changes are unknown. However, if $\Delta HR = 0$, then the reduction in risk in relation to changes in ${}_aSP$ (Risk $\downarrow_{aSP}$) can be calculated as the ratio of risk reduction over change in ${}_aSP$:

$$\text{Risk} \downarrow_{aSP} = \frac{25\% \text{ risk reduction}}{\Delta_aSP} = \frac{25\% \text{ risk reduction}}{-10.1}$$

If HR changes are note 0 (but are not considered to affect risk), then Risk $\downarrow_{aSP}$ could be expressed as:

$$\text{Risk}\downarrow_{aSP} = \frac{25\%\text{ risk reduction}}{-10.1 - 0.197\Delta HR} \tag{8.7}$$

Figure 8.3 presents the risk reduction dependency on HR if ${}_rSP/{}_rDP$ decrease in 10/5 mmHg. If reduction of cardiovascular risk is associated to reduction of ${}_aSP$ the importance of HR is evident when calculated from peripheral measurements. A reduction of 10 mmHg in ${}_aSP$ can be associated with a Risk $\downarrow_{aSP}$ of 32% (with a reduction in HR of 10 bpm) to only 22% (with an increase in HR of 10 bpm).[2]

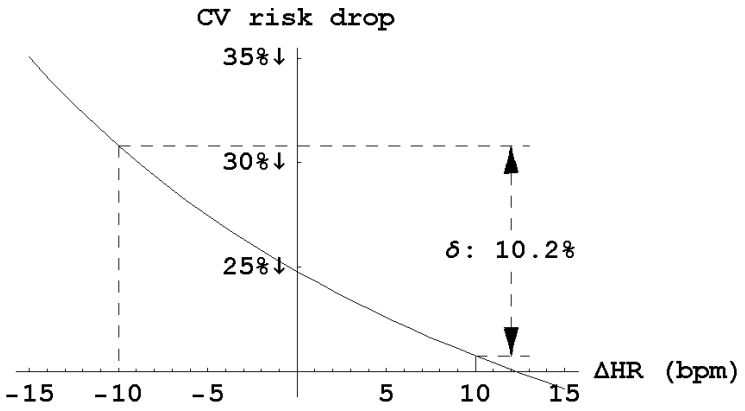

Figure 8.3: Change in relative overall CV risk associated to reduction of 10 mmHg in ${}_aSP$.

Results

${}_a\widehat{\mathcal{P}}$ and HR are significantly correlated and similar brachial BP changes can be caused by a range of central aortic BP changes. If HR is unknown the importance of ${}_a\mathcal{P}$ for CV risk prediction can not be determined. However, the range of variation can be calculated for a known range of HR changes.

[2]It was assumed that the reduction of risk is proportional to the reduction of ${}_aSP$.

8.3 Discussion

BP in humans is pulsatile. For each cardiac cycle, BP waves are propagated, reflected and damped throughout the arterial tree. The propagation velocity, the damping rate and the amount of wave reflection are determined by the specific characteristics of the arterial tree itself, therefore affecting the BP wave shape. In other words, characteristics of the arterial tree are reflected in the BP pulse wave shape.

The radial BP pulse ($_rPulse$) is readily accessible, making it an ideal location for non-invasive BP wave measurements. It contains additional information that can be associated with CV risk as has been demonstrated by the use of estimated $_a\widehat{\mathcal{P}}$ from the $_rPulse$. However, the estimation of $_a\widehat{\mathcal{P}}$s does not add any additional information, suggesting that the analysis should be done directly from the $_rPulse$ data. If non-linear models were to be used to estimate $_a\widehat{\mathcal{P}}$ this 'data transformation' could be valuable for more accurate estimates of risk, but these models are yet to be established based on invasive measurements of simultaneous $_aWave$ and $_rWave$.

$_a\widehat{\mathcal{P}}$ can be estimated either based on the $_rPulse$ or on the SBI only. These estimates provide a better representation of the CV system and can be used for interpretation of data from a central aortic perspective. Any model used to estimate $_a\widehat{\mathcal{P}}$ is good or bad depending on its use and its real value depends on the sensitivity and specificity of the tests associated with it.

8.4 Conclusions

Independent of the complexity of an estimated $_a\widehat{\mathcal{P}}$, it is only an estimate and not a real $_a\mathcal{P}$. Therefore the original measurements (without estimation of $_a\widehat{\mathcal{P}}$) should be used for quantitative analysis of CV risk. However, independent of the simplicity of an estimated $_a\widehat{\mathcal{P}}$, it still can provide new insight of the physiological understanding of the cardiovascular system and should be considered.

9

Conclusions

The conclusions reached in this study are in three areas. (1) ${}_rPulse$ representation, (2) Estimation of ${}_a\widehat{\mathcal{P}}$, and (3) Importance of dynamic analysis of the BP wave.

${}_r\boldsymbol{Pulse}$ representation

The representation of the ${}_rPulse$ is the key for its analysis. A poor representation will impair a proper analysis of its characteristics and information will be lost. The ${}_rPulse$ has been traditionally represented by its features. As presented in Chapter 3 the principal component (PC) decomposition of the ${}_rPulse$ provides a consistent representation with minimal loss of information. This representation also provides the possibility of the definition of a radial pulse pressure space ($\mathbb{PP}$) in which the distribution of the ${}_rPulse$ can be analyzed and subpopulations stratified. Therefore, to maximize the benefits of using the ${}_rPulse$ more comprehensive methods of pulse representation (such as PC) should be used in addition to features description.

Estimation of ${}_a\widehat{\boldsymbol{\mathcal{P}}}$

Techniques for the estimation of central aortic parameters (${}_a\mathcal{P}$) have been proposed based on the analysis of the ${}_rPulse$. This study have presented a framework for the strict definition and analysis of error of ${}_a\widehat{\mathcal{P}}$ (Chapter 4). It was shown that the estimated values and errors of a ${}_a\widehat{\mathcal{P}}$ are dependent on its estimation option (EO). Because the EO makes part of the strict definition of the ${}_a\widehat{\mathcal{P}}$ itself, the error is

dependent on its own definition. If errors are to be analyzed in a consistent manner, standardization of the ${}_a\widehat{\mathcal{P}}$ and EOs is required.

The most known method to estimated ${}_a\widehat{\mathcal{P}}$, the generalized transfer function (GTF-EO), was compared against other EOs (Chapter 5 and 6). It was concluded that there is no single best EO and their estimation accuracy varies between different ${}_a\widehat{\mathcal{P}}$. However, EOs that included the ${}_rPulse$ (PC, GTF) outperform the once that don't. Therefore, further studies should consider the use of different EO, preferable GTF or PC. However, independent of the EO used, the estimation errors should be considered; i.e., the accuracy of the specific EO used should be known. The error due to cuff calibration, which have been overlooked, should be included in the analysis of EO accuracy. Therefore, more studies analyzing the relationship between ${}_a\widehat{\mathcal{P}}$ and non-invasive BP measurements are required.

In addition to the considerations of the EO error the concept that ${}_a\widehat{\mathcal{P}}$ is an estimate and not a measured ${}_a\mathcal{P}$ with additional information to the ${}_rPulse$ measurement, should not be forgotten. That is, the ${}_a\widehat{\mathcal{P}}$ is a descriptor of *radial* pulse (${}_rPulse$), not the *aortic*. This in consequence implies that any analysis of risk stratification should use the original data (${}_rPulse$) and not the ${}_a\widehat{\mathcal{P}}$. However, the ${}_a\widehat{\mathcal{P}}$ is still valuable in the understanding of the physiological principles. This implies that any ${}_a\widehat{\mathcal{P}}$, even if estimated using a simple model based only in SBI, could give an insight of the physiological principles and better representation of CV system.

Importance of dynamic analysis of the BP wave

Most of the studies have focused their attention to the analysis of the ${}_rPulse$ shape, but not to the dynamic of the ${}_rPulse$ change in a single subject. This study proposed the soft exhalation manoeuver (SEM), a method to exaggerate spontaneous variability of mean blood pressure (MP) and heart rate (HR). It was found that the relationship between the changes of ${}_rPulse$ features for changes in MP and HR are different from subject to subject and from the values derived from a general population. This suggests a potential use of this relationships as markers for subject

stratification as they are particular for each subject.

The results obtained in this study suggest that estimated ${}_a\widehat{\mathcal{P}}$, even if derived from simple models that do not include the ${}_rPulse$, can be used for a better understanding of physiological principles such as effects of left ventricular load. In addition, the use of ${}_a\widehat{\mathcal{P}}$ derived without using the ${}_rPulse$ opens the possibility for retrospective analysis of previous studies from a central aortic BP perspective.

The importance of the ${}_rPulse$ for better CV risk stratification and clinical diagnosis will only be known if future studies include measurements of the ${}_rWave$. Measurements of the ${}_rWave$ should be performed under SEM (dynamic analysis) and the analysis of the ${}_rPulse$ should be based on representations with minimal loss of information.

Appendices

A

The Levenberg-Marquardt Algorithm

The Levenberg-Marquardt is an algorithm for non-linear least-squares minimization. The minimization strategy is a combination of the Newton and maximum gradient techniques. This algorithm can be used non-linear regression methods, by minimization of non-linear loss functions (i.e., minimization of error).

Goal: Minimize a loss function $L(\boldsymbol{x}) : \mathbb{R}^m \rightarrow \mathbb{R}$ of the special form

$$L(\boldsymbol{x}) = \frac{1}{2} \sum_{j=1}^{m} r_j^2(\boldsymbol{x})$$

where $\boldsymbol{r}(\boldsymbol{x}) = (r_1(\boldsymbol{x}), r_2(\boldsymbol{x}), \cdots, r_m(\boldsymbol{x}))$ is the vector of residuals, and $\boldsymbol{x} = (x_1, x_2, \cdots, x_n)$ is the vector of independent variables $x_i, 1 \leq i \leq n$, and $m \geq n$. Note that $r_j(\boldsymbol{x})$ could be a non-linear function of $\boldsymbol{x}$.

Solution: The minimization is done iteratively as shown in Figure A.1.

The vector $\boldsymbol{x}$ is set to initial conditions $\boldsymbol{x}_0$, and on each iteration is updated to

$$\boldsymbol{x}_{i+1} = \boldsymbol{x}_i - (H + \lambda \text{diag}\,[H])^{-1} \nabla L(\boldsymbol{x}_i)$$

where the Hessian (H) the gradient of $L(\boldsymbol{x})$ ($\nabla L(\boldsymbol{x})$) and the Jacobian of $\boldsymbol{x}$ ($J(\boldsymbol{x})$)

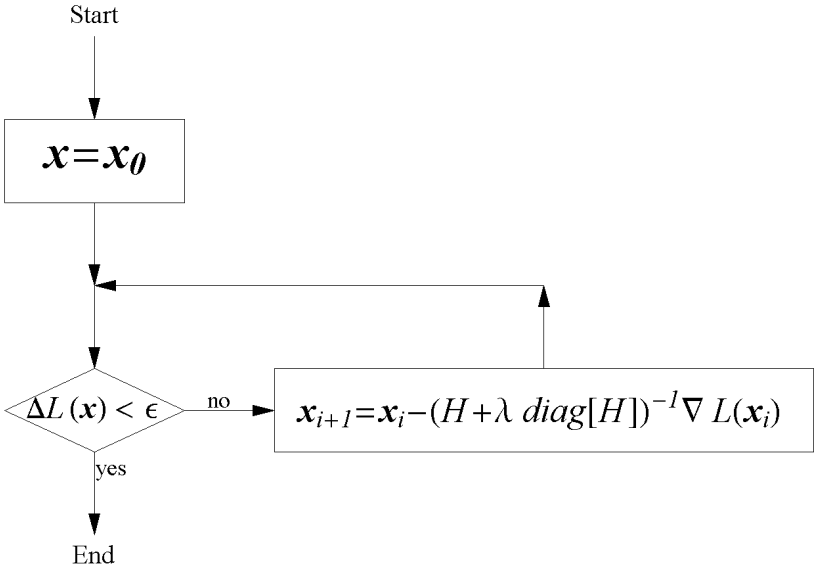

Figure A.1: Levenberg-Marquardt algorithm iteration diagram.

are defined as

$$H = \nabla^2 L(\boldsymbol{x}) = J(\boldsymbol{x})^T J(\boldsymbol{x}) + \sum_{j=1}^{m} r_j(\boldsymbol{x}) \nabla^2 r_j(\boldsymbol{x}) \approx J(\boldsymbol{x})^T J(\boldsymbol{x})$$

$$\text{diag}\,[H] = \text{ matrix of diagonals of } H$$

$$\nabla L(\boldsymbol{x}) = \sum_{j=1}^{m} r_j(\boldsymbol{x}) \nabla r_j(\boldsymbol{x}) = J(\boldsymbol{x})^T \boldsymbol{r}(\boldsymbol{x})$$

$$J(\boldsymbol{x}) = \frac{\partial \boldsymbol{r}}{\partial x_i}, 1 \leq i \leq n$$

$$\approx \begin{bmatrix} \frac{\boldsymbol{r}(x_1+\delta,\ldots,x_i,\ldots,x_n)-\boldsymbol{r}(x_1,\ldots,x_i,\ldots,x_n)}{\delta} \\ \vdots \\ \frac{\boldsymbol{r}(x_1,\ldots,x_i+\delta,\ldots,x_n)-\boldsymbol{r}(x_1,\ldots,x_i,\ldots,x_n)}{\delta} \\ \vdots \\ \frac{\boldsymbol{r}(x_1,\ldots,x_i,\ldots,x_n+\delta)-\boldsymbol{r}(x_1,\ldots,x_i,\ldots,x_n)}{\delta} \end{bmatrix}$$

λ is a scalar to adjust the behavior of the algorithm.

$$\lambda : \text{scalar} \begin{cases} \lambda \to 0, \text{approaches Newton's method.} \\ \lambda \to \infty, \text{approaches maximum gradient method.} \end{cases}$$

λ is adjusted for each iteration. It is reduced if error decreases to reduce the influence of the gradient descent. If error increases λ is increased to follow the gradient more.

The scalar δ is selected small enough so that the numerical representation of $J(\boldsymbol{x})$ approaches the partial derivatives $\frac{\partial \boldsymbol{r}}{\partial x_i}$.

Notes of caution: Due to the non linearity of $\boldsymbol{r}(\boldsymbol{x})$, local minimums could occur. Therefore, the starting point $\boldsymbol{x}_0$ should be located close to the solution region. The criteria for the selection of the $\boldsymbol{x}_0$ should be based on physical or physiological characterization of the system.

A more detail description of the Levenberg-Marquardt is presented by Ranganathan [2004]. A more formal mathematical description and details of implementation can be found in the book by Nocedal and Wright [1999].

B

Principal Components Transformation Tables

The principal components (PC) decomposition of the radial pulses ($_rPulse$, dimension 55×1), presented in Chapter 3 generates a vector with the average $_rPulse$ ($\overline{_rPulse}$) and a matrix for PC transformation (**Mtx**). [1] $\overline{_rPulse}$ and **Mtx** are presented in Tables B.1 and B.2, respectively.

For a new $_rPulse$, the PC scores ($PCscors$), a vector of dimensions 55×1, can be obtained by

$$PCscors = \mathbf{Mtx} \times (_rPulse - \overline{_rPulse})$$

With the inverse process, $_rPulse$ can be reconstructed form the $PCscors$.

Table B.1: Average wave ($\overline{_rPulse}$). Dimension 55×1.

	1	2	3	4	5	6	7	8	9	10
0	77.0	79.0	82.3	87.0	92.8	99.4	106.	113.	119.	124.
10	128.	131.	133.	134.	134.	133.	133.	132.	131.	130.
20	129.	128.	127.	126.	125.	124.	124.	123.	122.	120.
30	119.	118.	116.	114.	112.	110.	108.	107.	105.	103.
40	102.	101.	99.8	99.1	98.6	98.3	98.0	97.9	97.8	97.6
50	97.5	97.3	97.0	96.6	96.2					

Table B.2: Principal component transformation matrix (**Mtx**) — next 7 pages. Dimension 55×55.

[1] As explained in the text, for the PC decomposition only the first 55 sampling points are used, for $_rPulse$ sampled at 128 samples per sec.

Table B.2: **Mtx** columns 1 to 8

	1	2	3	4	5	6	7	8
1	-0.0519	-0.0551	-0.0603	-0.0677	-0.0771	-0.0878	-0.0989	-0.109
2	0.00237	0.0139	0.0338	0.0625	0.0984	0.138	0.176	0.209
3	-0.242	-0.235	-0.225	-0.212	-0.195	-0.175	-0.153	-0.129
4	-0.207	-0.185	-0.145	-0.0853	-0.00934	0.0734	0.150	0.209
5	-0.176	-0.173	-0.173	-0.178	-0.183	-0.185	-0.175	-0.149
6	0.140	0.136	0.136	0.139	0.142	0.138	0.121	0.0889
7	0.304	0.284	0.242	0.178	0.0955	0.00893	-0.0653	-0.112
8	-0.229	-0.205	-0.145	-0.0484	0.0653	0.166	0.222	0.213
9	0.125	0.111	0.0552	-0.0346	-0.131	-0.196	-0.199	-0.132
10	-0.111	-0.0973	-0.0435	0.0395	0.122	0.167	0.151	0.0731
11	-0.116	-0.101	-0.0318	0.0695	0.156	0.183	0.127	0.00443
12	-0.155	-0.118	-0.0149	0.109	0.191	0.182	0.0788	-0.0717
13	0.172	0.112	-0.0239	-0.158	-0.212	-0.152	-0.00333	0.148
14	0.214	0.0960	-0.0795	-0.200	-0.198	-0.0789	0.0861	0.190
15	-0.277	-0.0708	0.155	0.246	0.178	0.00484	-0.167	-0.202
16	0.240	0.0102	-0.166	-0.183	-0.0773	0.0734	0.156	0.0962
17	0.230	-0.0423	-0.172	-0.135	-0.0181	0.0992	0.131	0.0223
18	0.310	-0.106	-0.246	-0.135	0.0548	0.156	0.115	-0.0596
19	-0.177	0.0974	0.135	0.0466	-0.0616	-0.105	-0.0265	0.0974
20	-0.303	0.227	0.214	0.0280	-0.174	-0.173	0.0725	0.240
21	0.147	-0.0869	-0.148	-0.0580	0.187	0.149	-0.175	-0.201
22	0.129	-0.294	0.0340	0.395	-0.153	-0.410	0.246	0.312
23	0.135	-0.0808	-0.349	0.222	0.447	-0.299	-0.425	0.265
24	0.0749	-0.126	0.00820	0.0940	-0.0491	-0.0309	0.0639	-0.0249
25	0.148	-0.220	-0.0448	0.170	0.0368	-0.105	-0.0133	-0.00737
26	-0.0660	0.128	-0.0159	-0.130	0.0755	0.0785	-0.117	0.0473
27	-0.0173	0.00874	0.0236	-0.00772	-0.0229	0.0261	-0.0137	-0.0224
28	0.0438	-0.0662	-0.0332	0.103	-0.0204	-0.0567	0.0329	-0.0150
29	-0.00325	0.0126	0.0118	-0.0498	0.0102	0.0463	-0.0205	-0.0118
30	-0.0404	0.0389	0.0587	-0.0519	-0.0657	0.0605	0.0275	-0.0322
31	0.0206	-0.0769	0.0792	0.0393	-0.121	0.0406	0.0616	-0.0805
32	-0.0661	0.149	-0.0376	-0.148	0.113	0.0316	-0.0813	0.103
33	-0.131	0.275	-0.106	-0.148	0.114	0.0210	-0.0580	0.139
34	0.104	-0.231	0.150	0.0326	-0.103	0.0783	-0.0161	-0.109
35	-0.0464	0.0810	-0.00540	-0.0483	0.00265	0.0123	-0.00781	0.0564
36	-0.0449	0.119	-0.0622	-0.0981	0.130	-0.0480	-0.00891	0.0802
37	0.0812	-0.218	0.194	-0.0190	-0.0845	0.0938	-0.0759	-0.0529
38	0.0132	-0.0460	0.0587	-0.0159	-0.0571	0.117	-0.132	0.0758
39	-0.0622	0.199	-0.245	0.131	-0.0224	0.00261	-0.0196	0.123
40	-0.0480	0.134	-0.126	0.0143	0.0692	-0.104	0.129	-0.0805
41	-0.0176	0.0530	-0.0521	-0.00150	0.0479	-0.0547	0.0382	-0.00563
42	-0.0617	0.208	-0.294	0.237	-0.133	0.0313	0.0686	-0.0648
43	0.0319	-0.124	0.236	-0.313	0.336	-0.288	0.190	-0.115
44	-0.00518	0.0442	-0.103	0.143	-0.177	0.193	-0.164	0.109
45	-0.0219	0.0745	-0.101	0.0674	-0.0268	-0.00343	0.0642	-0.117
46	0.0131	-0.00445	-0.0368	0.0374	-0.0139	0.0314	-0.0490	0.0388
47	-0.0238	0.0581	-0.0229	-0.0477	0.0508	-0.0324	0.0330	0.0248
48	-0.0435	0.145	-0.186	0.0833	0.0740	-0.207	0.318	-0.324
49	0.0232	-0.0365	-0.0371	0.151	-0.214	0.229	-0.191	0.0430
50	-0.0135	0.0624	-0.117	0.121	-0.0693	-0.0191	0.136	-0.223
51	0.00491	-0.00900	-0.00450	0.0310	-0.0530	0.0627	-0.0479	-0.00513
52	0.0281	-0.106	0.188	-0.210	0.162	-0.0642	-0.0817	0.221
53	0.0203	-0.0505	0.0299	0.0436	-0.106	0.134	-0.138	0.0831
54	-0.0176	0.0429	-0.0240	-0.0358	0.0807	-0.0964	0.0884	-0.0304
55	-0.0178	0.0596	-0.0891	0.0731	-0.0173	-0.0582	0.134	-0.171

Table B.2: **Mtx** columns 9 to 16

	9	10	11	12	13	14	15	16
1	-0.119	-0.126	-0.132	-0.136	-0.138	-0.140	-0.142	-0.144
2	0.233	0.248	0.253	0.250	0.240	0.225	0.207	0.186
3	-0.104	-0.0775	-0.0509	-0.0244	0.00161	0.0268	0.0506	0.0726
4	0.241	0.244	0.221	0.178	0.121	0.0585	-0.00342	-0.0602
5	-0.106	-0.0499	0.0113	0.0703	0.121	0.159	0.182	0.189
6	0.0434	-0.00769	-0.0551	-0.0912	-0.112	-0.116	-0.104	-0.0796
7	-0.126	-0.107	-0.0660	-0.0128	0.0415	0.0883	0.122	0.140
8	0.145	0.0416	-0.0655	-0.150	-0.196	-0.201	-0.170	-0.116
9	-0.0177	0.101	0.182	0.205	0.172	0.0975	0.00606	-0.0808
10	-0.0369	-0.131	-0.173	-0.152	-0.0820	0.00859	0.0908	0.144
11	-0.128	-0.202	-0.187	-0.0942	0.0291	0.134	0.188	0.180
12	-0.187	-0.200	-0.108	0.0324	0.149	0.195	0.159	0.0629
13	0.209	0.140	-0.00866	-0.146	-0.194	-0.141	-0.0208	0.107
14	0.158	0.0123	-0.136	-0.185	-0.115	0.0223	0.144	0.183
15	-0.0660	0.121	0.198	0.112	-0.0506	-0.177	-0.184	-0.0798
16	-0.0566	-0.160	-0.115	0.0399	0.157	0.158	0.0480	-0.103
17	-0.121	-0.138	-0.00870	0.135	0.156	0.0446	-0.104	-0.178
18	-0.182	-0.109	0.0981	0.212	0.111	-0.0938	-0.218	-0.139
19	0.107	-0.0139	-0.132	-0.106	0.0439	0.146	0.108	-0.0368
20	0.0726	-0.188	-0.197	0.0326	0.173	0.151	-0.0139	-0.195
21	0.0858	0.215	0.0375	-0.158	-0.132	0.0323	0.153	0.0987
22	-0.247	-0.225	0.220	0.160	-0.145	-0.134	0.0389	0.102
23	0.334	-0.167	-0.233	0.0843	0.138	-0.0371	-0.0576	0.0158
24	-0.0902	0.0691	0.110	-0.0416	-0.168	-0.0120	0.233	0.0657
25	-0.0265	0.140	0.0661	-0.234	-0.0950	0.238	0.108	-0.173
26	0.0869	-0.179	0.00412	0.264	-0.169	-0.171	0.262	-0.00555
27	0.0674	-0.00786	-0.115	0.0376	0.171	-0.0974	-0.160	0.105
28	-0.0259	0.117	-0.0404	-0.163	0.0948	0.152	-0.0916	-0.135
29	0.0226	-0.0841	0.0389	0.192	-0.164	-0.213	0.195	0.227
30	0.0540	-0.0667	-0.108	0.171	0.137	-0.260	-0.103	0.254
31	0.0628	0.0264	-0.154	0.0603	0.211	-0.172	-0.155	0.151
32	-0.0421	-0.169	0.191	0.100	-0.217	-0.00897	0.146	-0.0877
33	-0.117	-0.149	0.245	-0.00574	-0.159	0.134	-0.0604	-0.106
34	0.155	-0.0222	-0.114	0.140	-0.0541	-0.123	0.131	0.0867
35	-0.00295	-0.136	0.0747	0.0547	0.0547	-0.104	-0.0877	0.0216
36	-0.109	-0.0572	0.198	-0.0562	-0.0831	0.000266	-0.0123	0.110
37	0.202	-0.126	-0.0738	0.129	-0.0629	-0.00647	0.112	-0.194
38	0.0102	-0.0148	-0.0826	0.160	-0.151	0.126	-0.111	0.0674
39	-0.281	0.280	-0.132	0.0596	-0.0662	0.0826	-0.200	0.332
40	-0.00423	-0.0269	0.136	-0.190	0.214	-0.234	0.162	-0.0401
41	-0.0104	-0.0323	0.0894	-0.0958	0.0802	-0.0843	0.0845	-0.0720
42	-0.0577	0.131	-0.0725	-0.0560	0.195	-0.273	0.231	-0.105
43	0.0983	-0.115	0.155	-0.180	0.122	-0.0161	-0.0624	0.114
44	-0.0549	-0.00358	0.0177	0.0394	-0.0566	-0.0209	0.0865	-0.124
45	0.111	-0.0983	0.109	-0.0920	0.0917	-0.177	0.214	-0.113
46	-0.0612	0.0749	-0.0211	0.0183	-0.0667	-0.00863	0.0809	0.0210
47	-0.0778	0.00388	0.0602	-0.0175	0.0557	-0.129	-0.0262	0.176
48	0.178	-0.0261	-0.0307	0.0462	-0.0407	0.00245	0.00493	0.0603
49	0.143	-0.241	0.278	-0.280	0.182	-0.0486	0.00809	0.0119
50	0.203	-0.0835	-0.0582	0.165	-0.196	0.120	0.0293	-0.157
51	0.0862	-0.162	0.187	-0.119	-0.0136	0.128	-0.196	0.203
52	-0.278	0.250	-0.155	0.00557	0.135	-0.207	0.229	-0.202
53	0.0242	-0.104	0.134	-0.149	0.139	-0.0902	0.0309	0.0366
54	-0.0605	0.123	-0.146	0.135	-0.0571	-0.0617	0.136	-0.161
55	0.140	-0.0645	-0.0282	0.120	-0.170	0.144	-0.0580	-0.0504

Table B.2: **Mtx** columns 17 to 24

	17	18	19	20	21	22	23	24
1	-0.146	-0.149	-0.151	-0.154	-0.157	-0.160	-0.163	-0.166
2	0.165	0.143	0.121	0.1000	0.0794	0.0595	0.0403	0.0216
3	0.0922	0.109	0.123	0.134	0.141	0.145	0.147	0.146
4	-0.109	-0.147	-0.174	-0.191	-0.197	-0.194	-0.183	-0.165
5	0.182	0.162	0.131	0.0942	0.0528	0.00980	-0.0326	-0.0725
6	-0.0470	-0.0105	0.0261	0.0592	0.0861	0.105	0.114	0.114
7	0.142	0.128	0.103	0.0695	0.0307	-0.0100	-0.0493	-0.0848
8	-0.0484	0.0198	0.0801	0.127	0.156	0.165	0.155	0.127
9	-0.146	-0.181	-0.183	-0.154	-0.102	-0.0344	0.0377	0.104
10	0.157	0.132	0.0771	0.00660	-0.0653	-0.125	-0.162	-0.168
11	0.118	0.0268	-0.0683	-0.144	-0.182	-0.176	-0.127	-0.0480
12	-0.0518	-0.142	-0.184	-0.171	-0.109	-0.0138	0.0848	0.157
13	0.184	0.183	0.106	-0.00790	-0.119	-0.188	-0.188	-0.119
14	0.129	0.0179	-0.100	-0.172	-0.168	-0.0898	0.0255	0.130
15	0.0736	0.175	0.176	0.0928	-0.0314	-0.144	-0.182	-0.125
16	-0.198	-0.153	-0.00415	0.132	0.196	0.162	0.0231	-0.138
17	-0.120	0.0365	0.165	0.175	0.0766	-0.0712	-0.179	-0.171
18	0.0535	0.195	0.168	0.0363	-0.134	-0.212	-0.106	0.0778
19	-0.163	-0.143	0.0324	0.159	0.146	0.0349	-0.105	-0.201
20	-0.176	0.0520	0.188	0.152	-0.0186	-0.162	-0.157	-0.0105
21	-0.0756	-0.160	-0.0222	0.0516	0.102	0.105	-0.0320	-0.205
22	0.0572	-0.0247	-0.101	-0.0417	0.0351	0.0872	0.0285	-0.0351
23	0.00404	-0.0321	0.0515	0.0312	-0.0517	-0.0542	0.0661	0.0147
24	-0.291	-0.110	0.366	0.0611	-0.373	0.0739	0.291	-0.214
25	-0.0445	0.0723	-0.0911	-0.0171	0.234	0.0652	-0.340	-0.0938
26	-0.312	0.259	0.194	-0.348	-0.0459	0.315	-0.147	-0.138
27	0.131	-0.105	-0.0345	0.0365	-0.0478	0.0664	0.0433	-0.108
28	0.0883	0.0770	-0.0595	-0.0302	0.0220	0.0440	-0.0415	-0.0590
29	-0.126	-0.241	-0.00506	0.229	0.158	-0.266	-0.126	0.208
30	0.0597	-0.188	0.0180	0.0268	-0.00872	0.0716	-0.00397	-0.133
31	0.117	-0.0807	-0.0318	-0.0874	0.0308	0.154	-0.0145	-0.123
32	0.0220	0.128	-0.206	-0.0440	0.205	-0.0156	-0.0965	0.0697
33	0.189	-0.00685	-0.128	0.0923	-0.0688	-0.0781	0.250	-0.0732
34	-0.0955	-0.0352	-0.113	0.137	0.186	-0.182	-0.114	0.0800
35	0.217	-0.0255	-0.148	-0.162	0.150	0.241	-0.0428	-0.299
36	0.111	-0.309	-0.00742	0.222	0.0554	-0.115	-0.0465	-0.146
37	0.0687	0.187	-0.223	0.0245	0.0499	0.00121	0.0182	0.0658
38	-0.0518	0.141	-0.269	0.325	-0.260	0.120	-0.0601	0.138
39	-0.264	0.130	-0.123	0.117	-0.0923	0.182	-0.255	0.170
40	0.00714	-0.0384	0.0486	-0.0476	0.0301	0.0379	-0.156	0.254
41	0.0800	-0.100	0.0789	-0.0140	-0.0340	0.0465	-0.0611	0.0734
42	-0.0407	0.121	-0.0548	-0.0574	0.0904	-0.0938	0.0455	0.0955
43	-0.113	0.0422	-0.0257	0.103	-0.141	0.127	-0.143	0.117
44	0.181	-0.139	-0.00155	0.0186	0.0186	0.0721	-0.0773	-0.0614
45	0.0468	-0.0259	-0.120	0.220	-0.112	0.0605	-0.102	0.0194
46	-0.00653	-0.173	0.0788	0.114	0.0723	-0.211	0.00362	-0.0503
47	-0.0494	0.0414	-0.211	0.0544	0.104	0.165	-0.166	-0.183
48	-0.164	0.258	-0.266	0.149	0.0104	-0.132	0.211	-0.208
49	-0.0526	0.00951	0.000209	0.153	-0.230	0.138	-0.114	0.0979
50	0.195	-0.134	-0.00932	0.182	-0.269	0.227	-0.114	-0.0367
51	-0.0855	-0.0751	0.117	-0.0859	0.0477	0.0662	-0.182	0.144
52	0.108	-0.00908	-0.0554	0.123	-0.156	0.106	-0.0628	0.0591
53	-0.117	0.164	-0.168	0.165	-0.110	-0.0223	0.128	-0.169
54	0.167	-0.102	-0.0449	0.161	-0.198	0.197	-0.128	-0.0176
55	0.146	-0.195	0.186	-0.122	0.0129	0.106	-0.190	0.215

Table B.2: **Mtx** columns 25 to 32

	25	26	27	28	29	30	31	32
1	-0.169	-0.171	-0.173	-0.174	-0.175	-0.176	-0.176	-0.175
2	0.00314	-0.0153	-0.0339	-0.0530	-0.0726	-0.0925	-0.112	-0.131
3	0.143	0.138	0.133	0.126	0.118	0.110	0.102	0.0924
4	-0.142	-0.114	-0.0830	-0.0497	-0.0149	0.0207	0.0559	0.0896
5	-0.109	-0.140	-0.165	-0.183	-0.194	-0.196	-0.188	-0.170
6	0.102	0.0810	0.0501	0.0119	-0.0304	-0.0722	-0.108	-0.132
7	-0.114	-0.134	-0.144	-0.141	-0.124	-0.0923	-0.0477	0.00653
8	0.0853	0.0334	-0.0228	-0.0774	-0.124	-0.155	-0.166	-0.154
9	0.156	0.187	0.190	0.164	0.113	0.0416	-0.0382	-0.112
10	-0.141	-0.0832	-0.00372	0.0827	0.158	0.203	0.204	0.156
11	0.0438	0.126	0.179	0.187	0.146	0.0641	-0.0379	-0.130
12	0.188	0.164	0.0884	-0.0157	-0.116	-0.177	-0.176	-0.113
13	-0.00951	0.104	0.182	0.193	0.131	0.0173	-0.103	-0.179
14	0.182	0.157	0.0596	-0.0643	-0.160	-0.185	-0.122	0.000735
15	-0.0161	0.101	0.166	0.145	0.0499	-0.0689	-0.151	-0.147
16	-0.209	-0.157	-0.0204	0.131	0.193	0.139	0.00334	-0.132
17	-0.0566	0.0979	0.183	0.150	0.0211	-0.120	-0.182	-0.112
18	0.173	0.155	0.0221	-0.134	-0.175	-0.0742	0.0654	0.152
19	-0.0995	0.0858	0.190	0.139	-0.0297	-0.169	-0.166	-0.0266
20	0.118	0.177	0.0496	-0.137	-0.167	-0.0256	0.0983	0.141
21	-0.0989	0.0890	0.192	0.0958	-0.0987	-0.198	-0.0715	0.114
22	-0.0530	-0.0615	0.0216	0.109	0.0561	-0.0927	-0.0859	-0.00234
23	-0.0384	0.0160	0.0340	-0.0479	-0.0342	0.0452	0.0394	-0.00909
24	-0.203	0.317	0.0957	-0.240	-0.0900	0.137	0.0315	0.0127
25	0.270	0.125	-0.191	0.0182	0.0485	-0.134	-0.0365	0.239
26	0.233	0.00252	-0.240	0.0603	0.167	-0.0379	-0.0756	-0.00320
27	-0.00701	0.142	-0.118	-0.0890	0.189	0.0798	-0.283	-0.0159
28	0.0589	0.106	-0.0837	-0.148	0.101	0.158	-0.107	-0.142
29	0.0348	-0.178	0.112	0.129	-0.149	-0.129	0.108	0.102
30	0.0788	0.0707	-0.140	0.0357	0.213	-0.171	-0.200	0.199
31	-0.0401	0.0693	0.0623	0.0297	-0.153	0.0337	0.130	-0.118
32	-0.108	0.0124	0.184	-0.150	-0.0817	0.235	-0.0754	-0.278
33	-0.155	0.0808	0.0123	-0.0643	0.187	-0.0911	-0.182	0.172
34	0.00870	0.129	0.0000726	-0.285	0.0952	0.241	-0.147	-0.0944
35	-0.0111	0.180	0.119	-0.0583	-0.191	0.0408	0.108	-0.00667
36	0.206	0.175	-0.236	-0.0850	0.125	0.0141	0.00714	0.00509
37	-0.260	0.214	0.0256	-0.114	0.0394	0.0279	-0.0805	0.151
38	-0.215	0.231	-0.249	0.183	0.0222	-0.141	0.0515	0.0678
39	-0.0661	0.0342	0.00706	-0.0454	-0.0225	0.118	-0.0438	-0.122
40	-0.252	0.211	-0.222	0.250	-0.269	0.301	-0.305	0.252
41	-0.0415	-0.0132	0.00253	0.0642	-0.0504	-0.0427	0.0866	-0.120
42	-0.133	0.00597	0.1000	-0.187	0.265	-0.155	-0.0178	-0.0177
43	-0.0280	0.0169	-0.0285	-0.0614	0.0890	-0.0231	0.100	-0.227
44	0.0133	0.125	-0.0475	0.00216	-0.108	-0.00208	0.195	-0.0952
45	0.0118	0.144	-0.169	0.0112	0.0538	-0.0967	0.217	-0.166
46	0.234	0.0675	-0.242	-0.127	0.103	0.258	-0.00939	-0.217
47	0.0458	0.165	0.191	-0.266	-0.128	0.00192	0.258	0.104
48	0.118	-0.0459	0.0371	-0.0474	0.0661	-0.0738	0.0235	0.0692
49	0.0711	-0.170	0.101	-0.105	0.175	-0.126	0.0553	-0.0643
50	0.170	-0.174	0.0482	0.0999	-0.202	0.225	-0.118	-0.0718
51	-0.0129	-0.103	0.225	-0.269	0.106	0.124	-0.228	0.256
52	0.0122	-0.110	0.117	-0.108	0.137	-0.0843	-0.0194	0.0438
53	0.202	-0.174	0.0343	0.0934	-0.133	0.152	-0.138	0.0479
54	0.146	-0.206	0.221	-0.165	0.0344	0.0945	-0.177	0.223
55	-0.176	0.0887	0.0329	-0.161	0.228	-0.205	0.136	-0.0375

Table B.2: **Mtx** columns 33 to 40

	33	34	35	36	37	38	39	40
1	-0.173	-0.170	-0.166	-0.162	-0.157	-0.151	-0.144	-0.138
2	-0.149	-0.164	-0.175	-0.182	-0.184	-0.181	-0.174	-0.162
3	0.0819	0.0698	0.0557	0.0392	0.0203	-0.000752	-0.0235	-0.0473
4	0.120	0.146	0.165	0.177	0.179	0.171	0.154	0.129
5	-0.140	-0.101	-0.0528	0.000415	0.0548	0.106	0.149	0.181
6	-0.140	-0.129	-0.0980	-0.0499	0.0101	0.0746	0.135	0.184
7	0.0648	0.120	0.165	0.192	0.197	0.179	0.138	0.0803
8	-0.118	-0.0656	-0.00429	0.0547	0.100	0.125	0.122	0.0947
9	-0.166	-0.189	-0.175	-0.125	-0.0513	0.0307	0.102	0.147
10	0.0689	-0.0372	-0.135	-0.197	-0.206	-0.161	-0.0755	0.0271
11	-0.184	-0.180	-0.119	-0.0188	0.0856	0.162	0.185	0.147
12	-0.00667	0.102	0.168	0.167	0.0996	-0.00787	-0.112	-0.171
13	-0.178	-0.0984	0.0227	0.132	0.177	0.140	0.0399	-0.0750
14	0.122	0.182	0.153	0.0441	-0.0863	-0.171	-0.167	-0.0789
15	-0.0609	0.0591	0.148	0.147	0.0606	-0.0583	-0.145	-0.152
16	-0.184	-0.115	0.0277	0.149	0.173	0.0857	-0.0555	-0.161
17	0.0352	0.158	0.168	0.0534	-0.0993	-0.185	-0.135	0.0131
18	0.120	-0.00228	-0.126	-0.140	-0.0507	0.0810	0.151	0.100
19	0.144	0.195	0.0557	-0.121	-0.187	-0.0927	0.0722	0.184
20	0.0521	-0.0874	-0.129	-0.0618	0.0605	0.135	0.0863	-0.0650
21	0.167	0.0600	-0.0995	-0.163	-0.0703	0.110	0.173	0.0457
22	0.0762	0.0616	-0.00539	-0.0585	-0.0604	0.00480	0.0525	0.0759
23	-0.0430	-0.0179	0.0169	0.0272	-0.000865	0.0199	-0.0273	-0.0399
24	0.00511	-0.0452	-0.0841	0.0245	0.111	0.0256	-0.0655	-0.0556
25	0.0377	-0.175	-0.0897	0.0494	0.0923	0.0413	0.0130	-0.0828
26	-0.0195	0.0575	0.0477	-0.0757	0.000772	0.0290	-0.0516	0.000230
27	0.302	-0.0543	-0.278	0.155	0.214	-0.272	-0.101	0.340
28	0.113	0.129	-0.140	-0.132	0.191	0.164	-0.303	-0.115
29	0.0158	-0.0672	-0.121	0.00685	0.166	0.0594	-0.200	0.00739
30	0.154	-0.153	-0.0539	0.0267	-0.0134	0.0686	0.0814	-0.189
31	-0.108	0.258	0.0411	-0.335	0.0305	0.281	-0.0428	-0.158
32	0.241	0.203	-0.278	-0.0839	0.172	0.0188	-0.0455	0.0261
33	0.0661	-0.166	0.0979	0.0499	-0.181	0.114	0.0828	-0.151
34	0.145	-0.0918	-0.00287	0.0916	-0.108	0.0327	0.165	-0.242
35	-0.0480	0.0430	-0.0242	0.00714	-0.0822	0.00507	0.209	-0.0228
36	-0.124	0.121	0.0685	-0.222	0.0474	0.259	-0.176	-0.0936
37	-0.126	-0.0827	0.236	-0.0866	-0.111	0.0662	0.00573	-0.00177
38	-0.121	0.131	-0.0171	-0.178	0.217	-0.0715	-0.0411	0.0472
39	0.128	-0.0516	0.0537	0.0233	-0.164	0.0565	0.162	-0.111
40	-0.171	0.104	-0.0964	0.118	-0.0777	0.00406	0.0292	-0.0588
41	0.192	-0.177	0.132	-0.229	0.312	-0.239	0.219	-0.289
42	0.114	-0.137	0.224	-0.231	0.00763	0.140	-0.0913	0.0847
43	0.182	-0.151	0.205	-0.0980	-0.0445	-0.0418	0.114	-0.00844
44	0.0192	-0.160	0.120	-0.00874	0.189	-0.296	0.121	-0.0765
45	-0.0228	0.0285	0.0404	0.0219	-0.0226	-0.0519	-0.0679	0.265
46	-0.199	0.221	0.204	-0.0105	-0.238	-0.171	0.245	0.149
47	-0.201	-0.214	0.0569	0.331	-0.0571	-0.0861	-0.258	0.0973
48	-0.151	0.188	-0.135	-0.00793	0.112	-0.118	0.113	-0.101
49	-0.0163	0.184	-0.212	0.142	-0.140	0.0928	0.0488	-0.0753
50	0.197	-0.206	0.130	0.0257	-0.196	0.254	-0.189	0.0788
51	-0.214	0.00336	0.227	-0.262	0.182	-0.0828	-0.0805	0.190
52	-0.0619	0.129	-0.118	0.0594	-0.0966	0.127	-0.0414	-0.0197
53	0.0161	0.00309	-0.0123	-0.00907	0.0141	-0.0573	0.160	-0.223
54	-0.202	0.101	0.0124	-0.107	0.193	-0.227	0.165	-0.0444
55	-0.0982	0.203	-0.223	0.185	-0.0979	-0.0354	0.152	-0.210

Table B.2: **Mtx** columns 41 to 47

	41	42	43	44	45	46	47
1	-0.131	-0.125	-0.119	-0.114	-0.110	-0.106	-0.103
2	-0.147	-0.130	-0.112	-0.0952	-0.0798	-0.0669	-0.0570
3	-0.0711	-0.0940	-0.115	-0.134	-0.149	-0.162	-0.171
4	0.0975	0.0624	0.0263	-0.00853	-0.0398	-0.0659	-0.0861
5	0.199	0.203	0.194	0.174	0.148	0.118	0.0881
6	0.215	0.223	0.209	0.174	0.122	0.0599	-0.00734
7	0.0124	-0.0576	-0.122	-0.174	-0.208	-0.224	-0.221
8	0.0466	-0.0124	-0.0714	-0.120	-0.150	-0.156	-0.139
9	0.154	0.124	0.0646	-0.0114	-0.0872	-0.147	-0.179
10	0.118	0.174	0.182	0.142	0.0656	-0.0279	-0.116
11	0.0636	-0.0373	-0.124	-0.171	-0.166	-0.112	-0.0250
12	-0.164	-0.0945	0.00884	0.106	0.164	0.164	0.106
13	-0.156	-0.166	-0.106	-0.00183	0.0987	0.157	0.152
14	0.0491	0.149	0.175	0.118	0.00785	-0.106	-0.168
15	-0.0665	0.0531	0.142	0.156	0.0897	-0.0270	-0.129
16	-0.163	-0.0660	0.0742	0.167	0.162	0.0598	-0.0742
17	0.151	0.184	0.0954	-0.0650	-0.189	-0.179	-0.0476
18	-0.0312	-0.135	-0.142	-0.0312	0.0966	0.153	0.101
19	0.151	-0.0268	-0.190	-0.185	-0.0273	0.154	0.213
20	-0.135	-0.0911	0.0389	0.136	0.115	-0.0166	-0.135
21	-0.0925	-0.165	-0.0922	0.106	0.220	0.0642	-0.139
22	-0.00913	-0.0713	-0.0766	0.0198	0.0923	0.0535	-0.0203
23	0.00310	0.0540	0.00793	-0.0211	-0.0154	-0.00147	-0.0109
24	-0.0267	0.0476	0.0800	0.0170	-0.0709	-0.0635	-0.0221
25	-0.116	0.0142	0.186	0.0563	-0.134	-0.0876	0.0200
26	0.113	-0.0447	-0.0790	0.0332	0.0131	-0.0457	0.0942
27	-0.0355	-0.297	0.115	0.200	-0.171	-0.0633	0.173
28	0.359	0.0315	-0.362	0.0832	0.293	-0.181	-0.160
29	0.139	-0.129	-0.0723	0.280	-0.00443	-0.299	-0.0182
30	0.00388	0.157	-0.0602	-0.164	0.225	0.0832	-0.292
31	0.0337	0.000431	-0.00171	0.115	-0.0841	-0.0603	0.137
32	-0.0911	0.0408	0.0748	-0.0900	-0.0000279	0.160	-0.120
33	0.0758	0.0370	-0.139	0.0990	0.0961	-0.189	0.0809
34	-0.0691	0.293	-0.00174	-0.203	-0.00668	0.0133	0.137
35	-0.258	-0.0139	0.201	0.0964	-0.0207	-0.269	-0.102
36	0.0316	0.0425	0.136	-0.0264	-0.308	0.153	0.199
37	0.147	-0.247	0.00345	0.205	-0.0458	-0.139	0.133
38	-0.0281	-0.0189	0.115	-0.154	0.0485	0.0986	-0.135
39	-0.0255	-0.0166	-0.00431	0.135	-0.0455	-0.151	0.112
40	0.0634	0.00960	-0.0367	-0.0207	0.0125	0.0322	-0.0117
41	0.254	-0.205	0.278	-0.288	0.193	-0.199	0.230
42	-0.0596	-0.0867	0.0964	0.0785	-0.170	0.151	-0.129
43	-0.0139	-0.0121	-0.136	0.228	-0.110	0.0713	-0.143
44	0.0934	0.128	-0.236	0.0820	-0.0669	0.156	-0.136
45	-0.271	0.199	-0.149	0.000935	0.133	-0.0711	-0.0279
46	0.0369	-0.340	0.0280	0.0640	0.247	-0.0958	-0.169
47	0.316	-0.112	-0.0712	-0.172	0.0974	0.149	0.0431
48	0.0449	-0.0415	0.103	-0.104	0.0764	-0.0808	0.00545
49	-0.00721	0.00434	0.0263	-0.00481	0.0657	-0.189	0.196
50	0.0362	-0.133	0.167	-0.120	0.0268	0.0510	-0.0775
51	-0.108	-0.0259	0.0923	-0.142	0.125	0.0202	-0.168
52	0.0339	-0.137	0.237	-0.181	0.0760	-0.00101	-0.133
53	0.213	-0.153	0.0123	0.167	-0.278	0.304	-0.243
54	-0.0890	0.206	-0.251	0.195	-0.0808	-0.0403	0.153
55	0.216	-0.159	0.0384	0.0921	-0.184	0.211	-0.162

Table B.2: **Mtx** columns 48 to 55

	48	49	50	51	52	53	54	55
1	-0.101	-0.0996	-0.0983	-0.0973	-0.0965	-0.0958	-0.0950	-0.0942
2	-0.0501	-0.0462	-0.0450	-0.0460	-0.0487	-0.0525	-0.0569	-0.0614
3	-0.177	-0.181	-0.182	-0.182	-0.181	-0.178	-0.176	-0.173
4	-0.100	-0.108	-0.112	-0.111	-0.109	-0.105	-0.101	-0.0970
5	0.0618	0.0408	0.0264	0.0186	0.0169	0.0200	0.0265	0.0348
6	-0.0738	-0.135	-0.186	-0.227	-0.256	-0.273	-0.280	-0.278
7	-0.201	-0.168	-0.126	-0.0788	-0.0307	0.0157	0.0584	0.0960
8	-0.101	-0.0477	0.0145	0.0786	0.139	0.192	0.236	0.270
9	-0.180	-0.149	-0.0935	-0.0216	0.0568	0.133	0.199	0.251
10	-0.180	-0.206	-0.190	-0.132	-0.0425	0.0668	0.183	0.294
11	0.0694	0.146	0.185	0.175	0.114	0.00859	-0.127	-0.276
12	0.0126	-0.0857	-0.159	-0.183	-0.146	-0.0497	0.0949	0.271
13	0.0852	-0.0149	-0.110	-0.163	-0.155	-0.0788	0.0561	0.228
14	-0.155	-0.0735	0.0425	0.142	0.183	0.134	-0.0128	-0.239
15	-0.162	-0.117	-0.0128	0.102	0.173	0.151	0.0171	-0.222
16	-0.165	-0.162	-0.0718	0.0585	0.166	0.177	0.0494	-0.218
17	0.106	0.192	0.161	0.0237	-0.147	-0.223	-0.104	0.238
18	-0.0253	-0.132	-0.147	-0.0580	0.0787	0.175	0.103	-0.172
19	0.0969	-0.0963	-0.215	-0.164	0.0379	0.229	0.195	-0.230
20	-0.122	-0.0229	0.125	0.143	0.0285	-0.132	-0.139	0.127
21	-0.175	-0.0776	0.0962	0.209	0.0981	-0.169	-0.225	0.182
22	-0.0818	-0.0692	0.0311	0.0951	0.0514	-0.0631	-0.0898	0.0655
23	0.0153	0.0209	0.00743	-0.0206	-0.0322	0.0174	0.0305	-0.0187
24	0.0689	0.0970	0.00121	-0.109	-0.0739	0.0632	0.104	-0.0705
25	0.0291	0.0610	0.114	-0.0823	-0.209	0.0256	0.267	-0.142
26	0.0392	-0.141	-0.0240	0.100	0.0240	-0.0473	-0.0146	0.0158
27	-0.0184	-0.160	0.0543	0.0925	-0.0277	-0.0248	-0.0137	0.0153
28	0.187	0.0780	-0.186	0.0119	0.105	-0.00827	-0.0699	0.0323
29	0.242	0.0233	-0.0692	-0.0539	-0.0334	0.0138	0.104	-0.0610
30	-0.0886	0.314	0.116	-0.274	-0.0798	0.153	0.0215	-0.0380
31	-0.0918	-0.174	0.279	0.124	-0.331	-0.0439	0.270	-0.111
32	-0.187	0.173	0.186	-0.155	-0.125	0.0604	0.0985	-0.0565
33	0.0751	-0.179	0.0881	0.194	-0.223	-0.0904	0.223	-0.0851
34	0.104	-0.235	-0.133	0.241	0.0724	-0.154	0.0118	0.0218
35	0.373	0.122	-0.330	-0.0718	0.208	-0.0451	0.000463	-0.0104
36	-0.104	-0.0284	-0.0691	-0.0655	0.200	0.0773	-0.260	0.109
37	-0.150	0.148	0.0696	-0.220	0.00210	0.267	-0.234	0.0667
38	0.0616	0.0349	-0.108	0.0701	0.122	-0.267	0.196	-0.0527
39	-0.000631	0.0165	0.0122	-0.0582	-0.0753	0.218	-0.162	0.0421
40	0.0237	-0.0816	0.0700	-0.0445	0.0720	-0.0661	0.0172	0.00262
41	-0.130	0.0702	-0.121	0.110	-0.0481	0.0388	-0.0377	0.0129
42	0.0432	0.0740	-0.0741	-0.0292	0.143	-0.208	0.156	-0.0469
43	0.0957	-0.0387	0.102	-0.129	0.0982	-0.108	0.0934	-0.0309
44	0.205	-0.357	0.346	-0.228	0.0960	0.0512	-0.0998	0.0388
45	-0.000909	0.0617	-0.133	0.272	-0.369	0.307	-0.151	0.0339
46	-0.0505	0.130	0.0948	-0.0518	-0.0425	-0.126	0.194	-0.0688
47	-0.206	0.0284	0.00389	0.0983	0.00640	-0.136	0.0928	-0.0181
48	0.143	-0.212	0.202	-0.161	0.0435	0.0853	-0.0948	0.0300
49	-0.101	-0.00265	0.116	-0.203	0.200	-0.126	0.0515	-0.0108
50	0.0646	-0.0488	0.0460	-0.0385	0.0317	-0.0397	0.0340	-0.0110
51	0.199	-0.138	0.0362	0.0698	-0.137	0.129	-0.0657	0.0141
52	0.262	-0.231	0.106	-0.0109	-0.0781	0.136	-0.0962	0.0255
53	0.0791	0.0994	-0.196	0.223	-0.195	0.111	-0.0329	0.00313
54	-0.210	0.173	-0.0899	0.0120	0.0666	-0.112	0.0800	-0.0220
55	0.0626	0.0401	-0.116	0.144	-0.113	0.0572	-0.0175	0.00270

C

Integrated Database

The information contained in the Integrated database (DB) was collected from seven different studies of central pressure conducted in different sites in Australia, as explained in Chapter 2. The data was read from the SCor.mdb files of the *SphygmoCor*® units used in the different studies. The SCor.mdb file is created in the *SphygmoCor*® installation and is not available directly from the *SphygmoCor*® commands. However, it is a standard Microsoft® database file and can be read with other software. The tables 'Patients' and 'M_PWA' where exported to *MySQL*®*4.1*. The fields available reflected the *SphygmoCor*® DB structure. Only the field 'AGE', calculated from other fields, was added to the table 'M_PWA' for convenience. The tables 'selMedian' was added to allow for the selection of one record per subject. Specifically, the record containing median HR. The available fields in the tables 'Patients' and 'M_PWA' and SQL commands to create the table 'selMedian' (and 'orderedMeas' required for 'selMedian') are presented next.

Database Fields

The fields for the tables 'Patients' and 'M_PWA' are presented with field name, type of information stored, validity of Null values, definition for DB Key and Default values.

Fields available for table 'Patients' in the Integrated DB

Field	Type	Null	Key	Default
SYSTEM_ID	varchar(5)		PRI	
STUDY_ID	varchar(16)		PRI	DATA
PATIENT_NO	int(11)		PRI	0
FAM_NAME	varchar(25)		MUL	
FIRST_NAME	varchar(25)	YES		NULL
OTHER_NAME	varchar(25)	YES		NULL
SEX	varchar(6)	YES		NULL
DOB	varchar(19)		MUL	
PATIENT_ID	varchar(10)	YES	MUL	NULL
CODE	varchar(15)	YES	MUL	NULL
STREET	varchar(30)	YES		NULL
TOWN	varchar(30)	YES		NULL
STATE	varchar(16)	YES		NULL
COUNTRY	varchar(20)	YES	MUL	NULL
ZIPCODE	varchar(6)	YES		NULL
EMAILADD	varchar(20)	YES		NULL
PHONE	varchar(20)	YES		NULL
NOTES	longtext	YES		NULL
CHARSPARE1	varchar(10)	YES		NULL
CHARSPARE2	varchar(20)	YES		NULL
OLESPARE1	longblob	YES		NULL
OLESPARE2	longblob	YES		NULL
MEMOSPARE1	longtext	YES		NULL
LNUMSPARE1	int(11)	YES		NULL
FNUMSPARE1	float	YES		NULL
NUMSPARE1	int(11)	YES		NULL
FNUMSPARE2	float	YES		NULL

Fields available for table 'M_PWA' in Integrated DB

Field	Type	Null	Key	Default
SYSTEM_ID	varchar(5)		PRI	
STUDY_ID	varchar(16)		PRI	DATA
PATIENT_NO	int(11)		PRI	0
DATETIME	varchar(19)		PRI	
AGE	smallint(6)	YES		NULL
DATA_REV	smallint(6)		MUL	0
SUB_TYPE	varchar(15)		MUL	
SAMPLE_RATE	smallint(6)			0
SIGNAL_UPSAMPLE_RATE	smallint(6)			0
EXPPULSE_UPSAMPLE_RATE	smallint(6)			0
FLOW	float	YES		NULL
BODY_MASS_INDEX	float	YES		NULL
HEIGHT	float	YES		NULL
WEIGHT	float	YES		NULL
MEDICATION	longtext	YES		NULL
NOTES	longtext	YES		NULL
OPERATOR	varchar(25)	YES		NULL
MESSAGE	longtext	YES		NULL
MEMSPARE1	longtext	YES		NULL
MEMSPARE2	longtext	YES		NULL
INTSPARE1	smallint(6)	YES		NULL
INTSPARE2	smallint(6)	YES		NULL
FLOATSPARE1	float	YES		NULL
UNITS	varchar(5)	YES		NULL
CAL_SP	float	YES		NULL
CAL_DP	float	YES		NULL
CAL_MP	float	YES		NULL
SP	float			0
DP	float			0
MP	float			0
HR	float			0
ED	float			0
CalcED	float			0
QUALITY_ED	smallint(6)	YES		0
EDMin	float	YES		NULL
EDTan	float	YES		NULL
EDOther	float	YES		NULL
P_PULSES	longblob			
P_AV	longblob			
P_TRIGS	longblob			
P_UNCAL_AV	longblob			
P_OLE_SPARE	longblob	YES		NULL
P_MATH_PARAMS	longblob	YES		NULL
P_SP	float			0
P_DP	float			0
P_MEANP	float			0
P_T1	float			0
P_T2	float			0
P_T1I	float	YES		NULL
P_T1R	float	YES		NULL
P_T1M	float	YES		NULL
P_T1Other	float	YES		NULL
P_T2I	float	YES		NULL

Continued on next page

Field	Type	Null	Key	Default
P_T2R	float	YES		NULL
P_T2M	float	YES		NULL
P_T2Other	float	YES		NULL
P_QUALITY_T1	smallint(6)	YES		0
P_QUALITY_T2	smallint(6)	YES		0
P_P1	float	YES		0
P_P2	float	YES		0
P_T1ED	float	YES		0
P_T2ED	float	YES		0
P_AI	float	YES		NULL
P_ESP	float	YES		0
P_MAX_DPDT	float	YES		NULL
P_MEMSPARE1	longtext	YES		NULL
P_MEMSPARE2	longtext	YES		NULL
P_INTSPARE1	smallint(6)	YES		NULL
P_INTSPARE2	smallint(6)	YES		NULL
P_FLOATSPARE1	float	YES		NULL
P_FLOATSPARE2	float	YES		NULL
P_NOISE_FACTOR	smallint(6)	YES		0
P_QC_PH	float	YES		NULL
P_QC_PHV	float	YES		NULL
P_QC_PLV	float	YES		NULL
P_QC_DV	float	YES		NULL
P_QC_OTHER1	float	YES		NULL
P_QC_OTHER2	float	YES		NULL
P_QC_OTHER3	float	YES		NULL
P_QC_OTHER4	float	YES		NULL
C_PULSES	longblob			
C_AV	longblob			
C_TRIGS	longblob			
C_UNCAL_AV	longblob			
C_OLE_SPARE	longblob	YES		NULL
C_MATH_PARAMS	longblob	YES		NULL
C_SP	float			0
C_DP	float			0
C_MEANP	float			0
C_T1	float	YES		NULL
C_T2	float	YES		NULL
C_T1I	float	YES		NULL
C_T1R	float	YES		NULL
C_T1M	float	YES		NULL
C_T1Other	float	YES		NULL
C_T2I	float	YES		NULL
C_T2R	float	YES		NULL
C_T2M	float	YES		NULL
C_T2Other	float	YES		NULL
C_QUALITY_T1	smallint(6)	YES		0
C_QUALITY_T2	smallint(6)	YES		0
C_P1	float	YES		0
C_P2	float	YES		0
C_T1ED	float	YES		0
C_T2ED	float	YES		0
C_AI	float	YES		NULL
C_ESP	float	YES		NULL
C_AP	float	YES		NULL

Continued on next page

Field	Type	Null	Key	Default
C_MPS	float	YES		NULL
C_MPD	float	YES		NULL
C_TTI	float	YES		NULL
C_DTI	float	YES		NULL
C_SVI	float	YES		NULL
C_PERIOD	float			0
C_DD	float	YES		0
C_ED_PERIOD	float	YES		0
C_DD_PERIOD	float	YES		0
C_PH	float	YES		0
C_P1_HEIGHT	float	YES		0
C_AGPH	float	YES		0
C_QC_OTHER1	float	YES		NULL
C_QC_OTHER2	float	YES		NULL
C_QC_OTHER3	float	YES		NULL
C_QC_OTHER4	float	YES		NULL
C_MEMSPARE1	longtext	YES		NULL
C_MEMSPARE2	longtext	YES		NULL
C_INTSPARE1	smallint(6)	YES		NULL
C_INTSPARE2	smallint(6)	YES		NULL
C_FLOATSPARE1	float	YES		NULL
C_FLOATSPARE2	float	YES		NULL
QIntlDBNum	smallint(6)	YES		NULL
QIntlDBTex	varchar(32)	YES		NULL

SQL Commands

The two SQL commands presented next are used for the selection of the record with the median HR value for each subject in the database. The 'orderedMeas' command should be run before 'selMedian'. The third SQL command is an example of a typical access to the DB.

Command 'orderedMeas' is a SQL command used to sort the selected records. This step is required for the selection of the median HR record per subject:

```
CREATE TABLE orderedMeas (myIdx INT NOT NULL AUTO_INCREMENT, PRIMARY KEY
(myIdx)) TYPE=MyISAM SELECT M_PWA.SYSTEM_ID, M_PWA.STUDY_ID, M_PWA.PATIENT_NO,
M_PWA.DATETIME, M_PWA.HR FROM PATIENT INNER JOIN M_PWA ON (PATIENT.PATIENT_NO =
M_PWA.PATIENT_NO) AND (PATIENT.STUDY_ID = M_PWA.STUDY_ID) AND (PATIENT.SYSTEM_ID
= M_PWA.SYSTEM_ID) WHERE ((m_pwa.SUB_TYPE)="RADIAL") ORDER BY M_PWA.SYSTEM_ID,
M_PWA.STUDY_ID, M_PWA.PATIENT_NO, M_PWA.HR;
```

Command 'selMedian' is an SQL command to select the subjects with median HR:

```
CREATE TABLE selMedian (PRIMARY KEY (SYSTEM_ID, STUDY_ID, PATIENT_NO,
DATETIME)) TYPE=MyISAM SELECT orderedMeas.SYSTEM_ID, orderedMeas.STUDY_ID,
orderedMeas.PATIENT_NO, orderedMeas.DATETIME FROM orderedMeas INNER
JOIN (SELECT counting.SYSTEM_ID, counting.STUDY_ID, counting.PATIENT_NO,
Floor((counting.myCount-1)/2)+counting.theMin AS thePos FROM (SELECT
orderedMeas.SYSTEM_ID, orderedMeas.STUDY_ID, orderedMeas.PATIENT_NO,
Min(orderedMeas.myIdx) AS theMin, Max(orderedMeas.myIdx) AS theMax,
Count(orderedMeas.DATETIME) AS myCount FROM orderedMeas GROUP BY
orderedMeas.SYSTEM_ID, orderedMeas.STUDY_ID, orderedMeas.PATIENT_NO) As counting )
As selM ON (orderedMeas.PATIENT_NO = selM.PATIENT_NO) AND (orderedMeas.STUDY_ID =
selM.STUDY_ID) AND (orderedMeas.SYSTEM_ID = selM.SYSTEM_ID) AND (orderedMeas.myIdx
= selM.thePos);
```

Select fields is a typical SQL command to select a subset of the data:

```
SELECT patient.SEX, m_pwa.AGE, m_pwa.HEIGHT, m_pwa.WEIGHT, m_pwa.P_SP,
m_pwa.P_DP, m_pwa.P_MEANP, m_pwa.ED, m_pwa.HR, m_pwa.C_SP, m_pwa.C_DP,
m_pwa.C_T1, m_pwa.C_P1, m_pwa.C_T2, m_pwa.C_P2, m_pwa.P_T1, m_pwa.P_P1,
m_pwa.P_T2, m_pwa.P_P2, m_pwa.C_AI, m_pwa.P_AI, m_pwa.P_AV, m_pwa.C_AV FROM
(m_pwa INNER JOIN selmedian ON (m_pwa.DATETIME = selmedian.DATETIME)
AND (m_pwa.PATIENT_NO = selmedian.PATIENT_NO) AND (m_pwa.STUDY_ID =
selmedian.STUDY_ID) AND (m_pwa.SYSTEM_ID = selmedian.SYSTEM_ID)) INNER JOIN
patient ON (selmedian.PATIENT_NO = patient.PATIENT_NO) AND (selmedian.STUDY_ID =
patient.STUDY_ID) AND (selmedian.SYSTEM_ID = patient.SYSTEM_ID) WHERE (m_pwa.C_T2
< 5000 AND m_pwa.C_P2 < 5000 AND m_pwa.C_AI < 5000 AND m_pwa.P_T2 < 5000 AND
m_pwa.P_P2 < 5000 AND m_pwa.P_AI < 5000 AND m_pwa.AGE > 22 AND m_pwa.AGE < 55 AND
(patient.SEX = "MALE" OR patient.SEX = "FEMALE")) ;
```

D

Detailed Results Chapter 5: 'Analysis of Estimated Central Arterial BP Parameters — Invasive Measurements'

This appendix presents the detailed results of the analysis of central arterial BP parameters presented in Chapter 5. The results are presented by $\mathcal{P}$. For each $\mathcal{P}$ the best fit models and coefficients' statistics are presented. The distributions of mean, SD and RMS are also presented for each of the EO used. The distributions of the ratios of variance between pairs of EOs are also included.

D.1 Aortic Systolic Pressure

Models and Coefficients

Average:

$$\widehat{{}_aSP}_{\texttt{Avg}} = 107.$$

	Estimate	SE	TStat	PValue
μ_{aSP}	107.	1.79	59.6	< 0.001

Linear:

$$\widehat{{}_aSP}_{\texttt{LR}} = -4.20 + 0.904_rSP$$

	Estimate	SE	TStat	PValue
C_0	-4.20	11.1	-0.378	0.707
C_{rSP}	0.904	0.0903	10.0	< 0.001

Linear Mean:

$$\widehat{{}_aSP}_{\texttt{LRM}} = -33.9 + 0.161Age + 1.77MP \\ -1.16_rDP + 0.511_rSP$$

	Estimate	SE	TStat	PValue
C_0	-33.9	8.29	-4.09	< 0.001
C_{rSP}	0.511	0.0842	6.07	< 0.001
C_{MP}	1.77	0.201	8.79	< 0.001
C_{rDP}	-1.16	0.172	-6.74	< 0.001
C_{Age}	0.161	0.0669	2.41	0.0196

Principal Components:

$$\widehat{{}_aSP}_{\texttt{PC}} = 118. + 0.406HR + 2.89PC_1 + 0.932PC_2 \\ +0.972PC_3 - 0.635_rDP$$

	Estimate	SE	TStat	PValue
C_0	118.	6.59	17.9	< 0.001
C_{PC_1}	2.89	0.190	15.2	< 0.001
C_{PC_3}	0.972	0.238	4.09	< 0.001
C_{PC_2}	0.932	0.241	3.88	< 0.001
C_{HR}	0.406	0.0584	6.95	< 0.001
C_{rDP}	-0.635	0.126	-5.06	< 0.001

Generalized Transfer Function:

The estimated model, $\mathcal{T}_G$, was 'trained' with the invasive data, as explained in section 4.2.3.

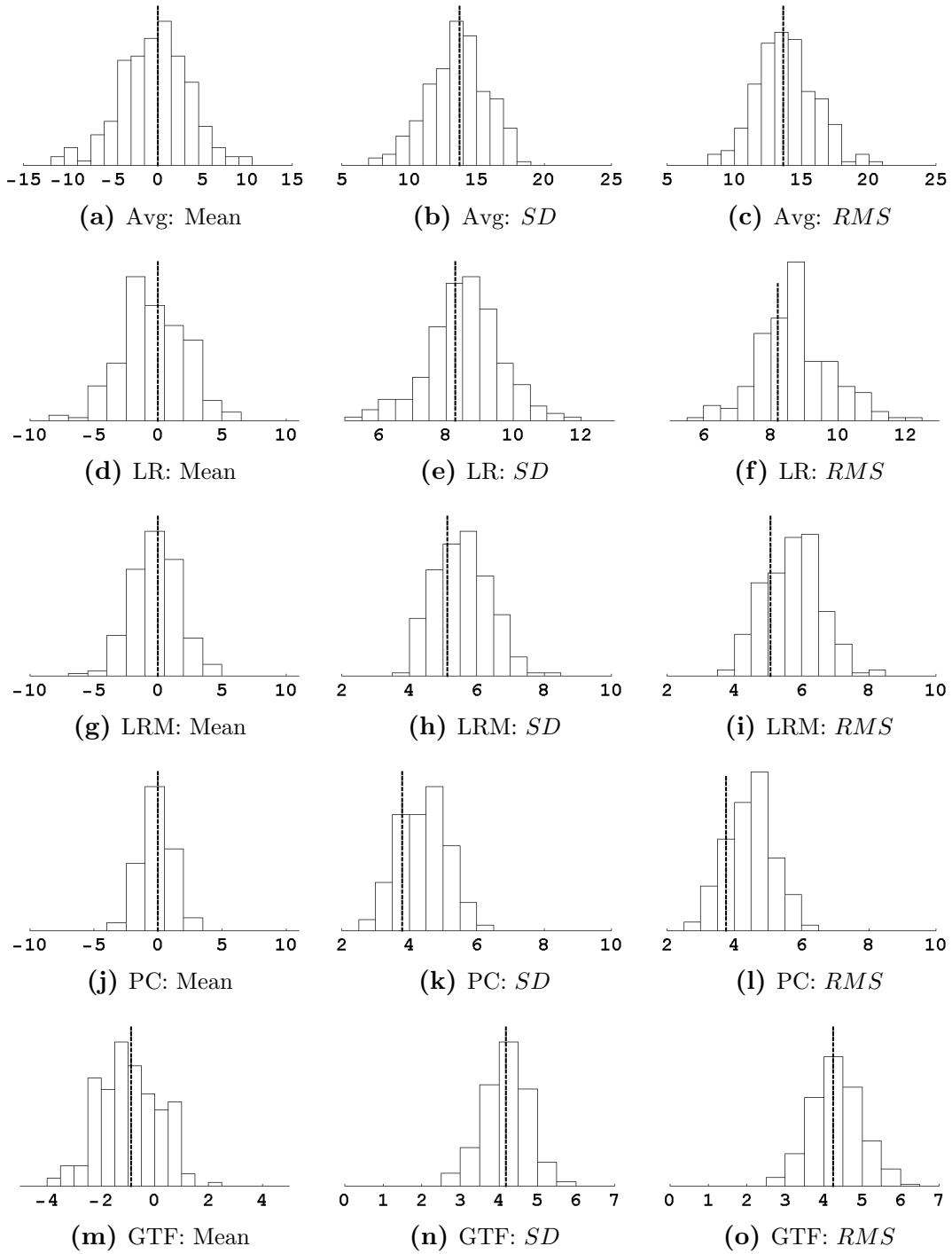

(a) Avg: Mean **(b)** Avg: SD **(c)** Avg: RMS

(d) LR: Mean **(e)** LR: SD **(f)** LR: RMS

(g) LRM: Mean **(h)** LRM: SD **(i)** LRM: RMS

(j) PC: Mean **(k)** PC: SD **(l)** PC: RMS

(m) GTF: Mean **(n)** GTF: SD **(o)** GTF: RMS

Figure D.1: Distribution of Mean, SD and RMS of the residuals ($_aSP$ - $_a\widehat{SP}$) for the different EO. All values in mmHg. Vertical bars indicate values estimated from all observations. Distributions were calculated using bootstrap method.

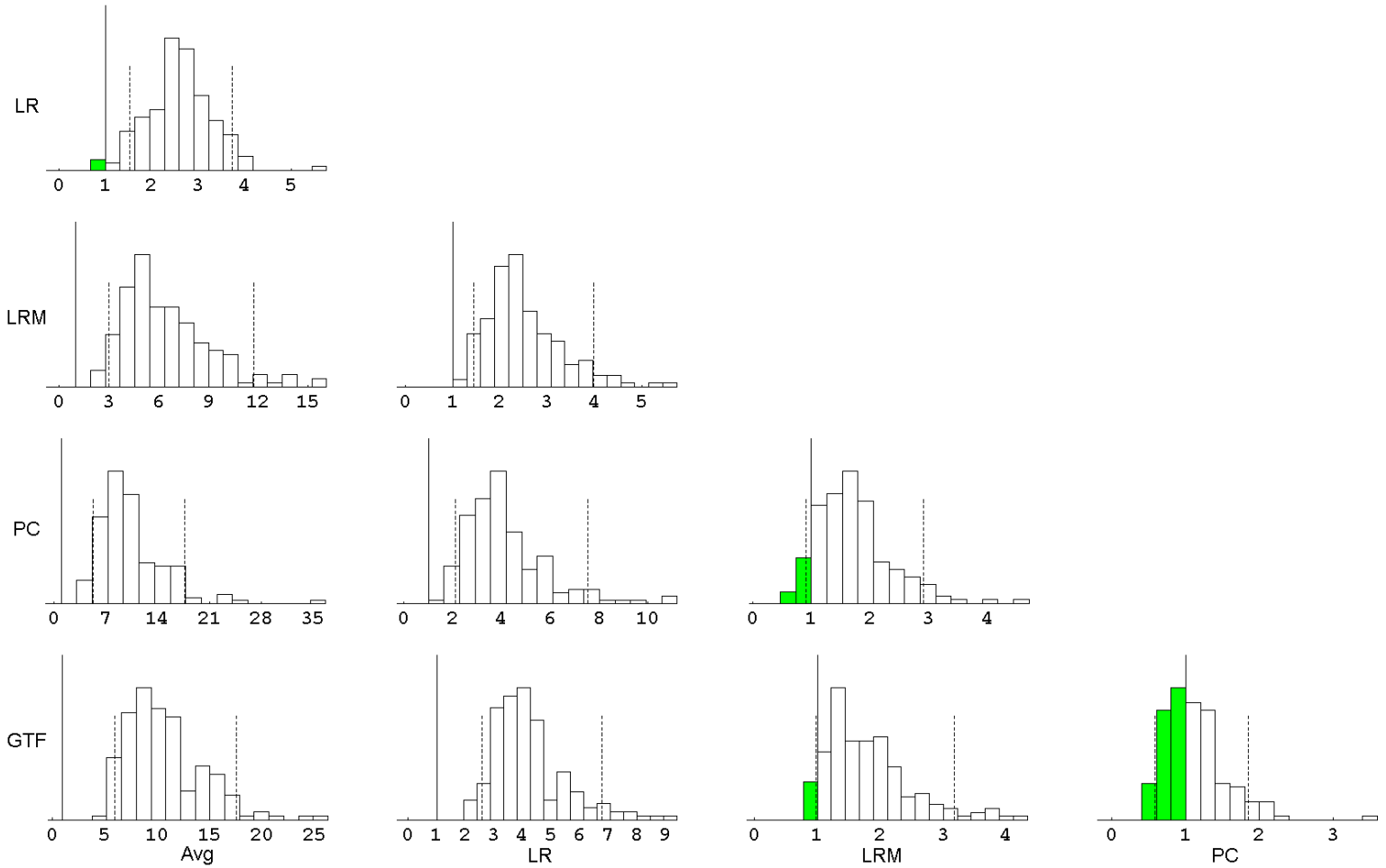

Figure D.2: Comparative histograms of ratios of variances of residuals ($_aSP - _a\widehat{SP}$): $\frac{Var[row]}{Var[column]}$ (see text, Chapter 5 section 5.1.2). Dotted lines indicate 95% of total observations. If unity is not included within dotted lines, the two EO (row and column) are significatly (at 95% confidence) different. If both dotted lines are to the right of unity, row EO is significantly better then column EO.

D.2 Aortic Diastolic Pressure

Models and Coefficients

Average:

$$\widehat{{}_aDP}_{\texttt{Avg}} = 62.0$$

	Estimate	SE	TStat	PValue
μ_{aDP}	62.0	1.42	43.6	< 0.001

Linear:

$$\widehat{{}_aDP}_{\texttt{LR}} = -9.65 - 0.0757Age + 0.0894H + 0.0890HR + 0.843_rDP$$

	Estimate	SE	TStat	PValue
C_0	-9.65	8.08	-1.19	0.237
C_{rDP}	0.843	0.0359	23.5	< 0.001
C_{HR}	0.0890	0.0246	3.62	< 0.001
C_{Age}	-0.0757	0.0339	-2.23	0.0298
C_H	0.0894	0.0418	2.14	0.0371

Linear Mean:

$$\widehat{{}_aDP}_{\texttt{LRM}} = 1.51 - 0.0710Age + 0.0973HR + 0.402MP + 0.568_rDP - 0.102_rSP + 1.53S$$

	Estimate	SE	TStat	PValue
C_0	1.51	4.66	0.325	0.747
C_{rDP}	0.568	0.0847	6.71	< 0.001
C_{HR}	0.0973	0.0237	4.10	< 0.001
C_{MP}	0.402	0.0896	4.48	< 0.001
C_{rSP}	-0.102	0.0401	-2.53	0.0145
C_{Age}	-0.0710	0.0297	-2.39	0.0203
C_S	1.53	0.704	2.17	0.0349

Principal Components:

$$\widehat{{}_aDP}_{\texttt{PC}} = 8.29 + 0.682MP - 0.764PC_2 - 0.731PC_4 + 0.302_rDP - 0.170_rSP$$

	Estimate	SE	TStat	PValue
C_0	8.29	3.12	2.65	0.0105
C_{MP}	0.682	0.114	5.96	< 0.001
C_{PC_2}	-0.764	0.128	-5.97	< 0.001
C_{rDP}	0.302	0.119	2.54	0.0141
C_{rSP}	-0.170	0.0348	-4.88	< 0.001
C_{PC_4}	-0.731	0.267	-2.73	0.00847

Generalized Transfer Function: explained in section 4.2.3.

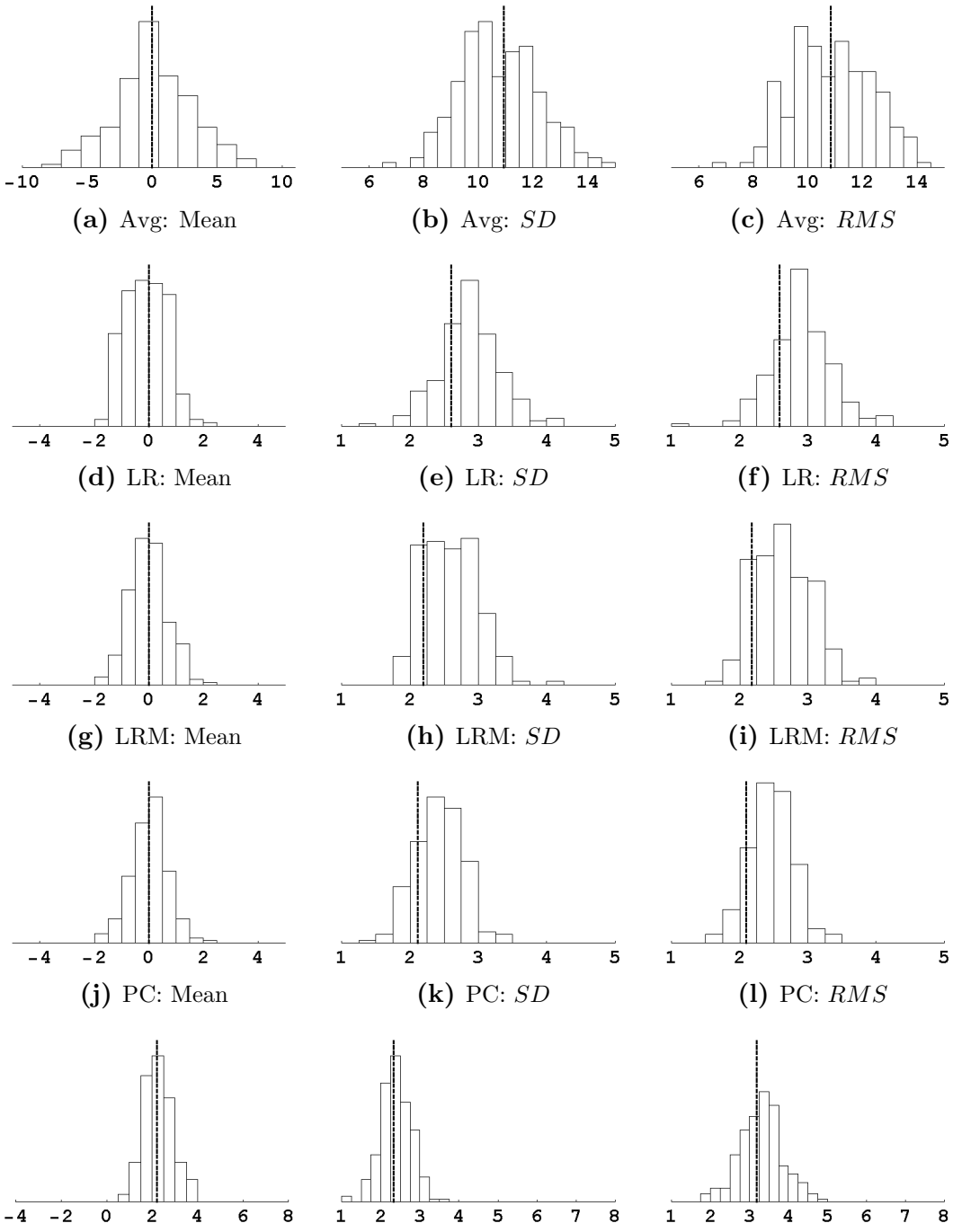

(a) Avg: Mean **(b)** Avg: SD **(c)** Avg: RMS

(d) LR: Mean **(e)** LR: SD **(f)** LR: RMS

(g) LRM: Mean **(h)** LRM: SD **(i)** LRM: RMS

(j) PC: Mean **(k)** PC: SD **(l)** PC: RMS

(m) GTF: Mean **(n)** GTF: SD **(o)** GTF: RMS

Figure D.3: Distribution of Mean, SD and RMS of the residuals ($_aDP$ - $_a\widehat{DP}$) for the different EO. All values in mmHg. Vertical bars indicate values estimated from all observations. Distributions were calculated using bootstrap method.

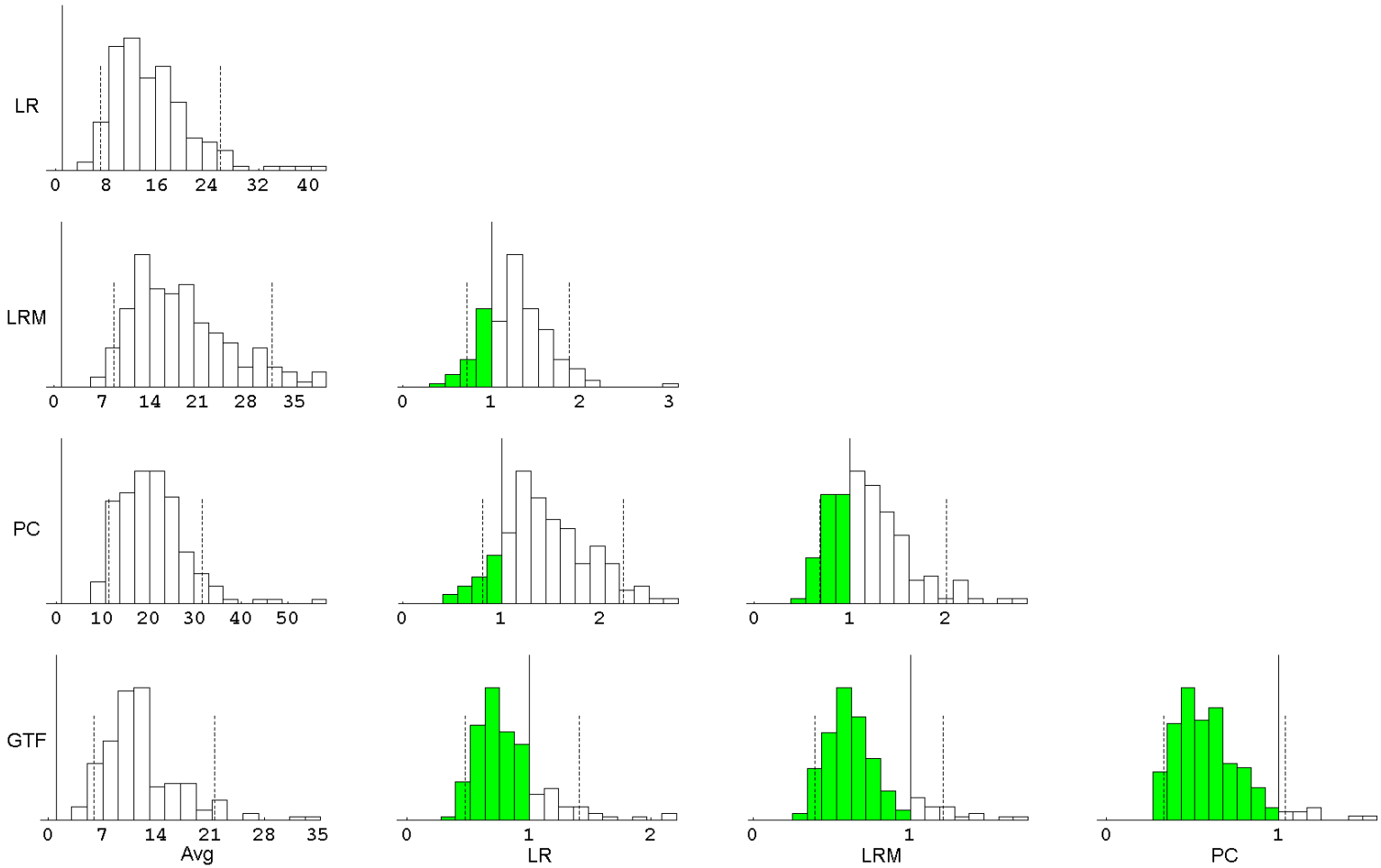

Figure D.4: Comparative histograms of ratios of variances of residuals ($_aDP - {}_a\widehat{DP}$): $\frac{Var[row]}{Var[column]}$ (see text, Chapter 5 section 5.1.2). Dotted lines indicate 95% of total observations. If unity is not included within dotted lines, the two EO (row and column) are significatly (at 95% confidence) different. If both dotted lines are to the right of unity, row EO is significantly better then column EO.

D.3 Aortic Pulse Pressure

Models and Coefficients

Average:

$$\widehat{{}_aPP}_{\texttt{Avg}} = 44.5$$

	Estimate	SE	TStat	PValue
$\mu_{{}_aPP}$	44.5	1.71	26.0	< 0.001

Linear:

$$\widehat{{}_aPP}_{\texttt{LR}} = -11.4 + 0.238Age - 0.227HR \\ -0.597_rDP + 0.787_rSP$$

	Estimate	SE	TStat	PValue
C_0	-11.4	13.2	-0.865	0.391
C_{HR}	-0.227	0.0735	-3.08	0.00324
$C_{{}_rSP}$	0.787	0.117	6.76	< 0.001
$C_{{}_rDP}$	-0.597	0.143	-4.17	< 0.001
C_{Age}	0.238	0.0947	2.52	0.0149

Linear Mean:

$$\widehat{{}_aPP}_{\texttt{LRM}} = -31.3 + 0.218Age - 0.164HR + 1.33MP \\ -1.64_rDP + 0.597_rSP$$

	Estimate	SE	TStat	PValue
C_0	-31.3	10.9	-2.87	0.00582
C_{HR}	-0.164	0.0585	-2.80	0.00702
$C_{{}_rSP}$	0.597	0.0966	6.18	< 0.001
$C_{{}_rDP}$	-1.64	0.208	-7.87	< 0.001
C_{MP}	1.33	0.224	5.94	< 0.001
C_{Age}	0.218	0.0741	2.94	0.00482

Principal Components:

$$\widehat{{}_aPP}_{\texttt{PC}} = -36.9 + 0.137Age + 2.05PC_2 + 3.40PC_4 \\ -0.206_rDP + 0.705_rSP$$

	Estimate	SE	TStat	PValue
C_0	-36.9	6.92	-5.34	< 0.001
C_{PC_2}	2.05	0.229	8.94	< 0.001
$C_{{}_rSP}$	0.705	0.0682	10.3	< 0.001
C_{PC_4}	3.40	0.431	7.89	< 0.001
C_{Age}	0.137	0.0602	2.28	0.0264
$C_{{}_rDP}$	-0.206	0.0932	-2.21	0.0313

Generalized Transfer Function: explained in section 4.2.3.

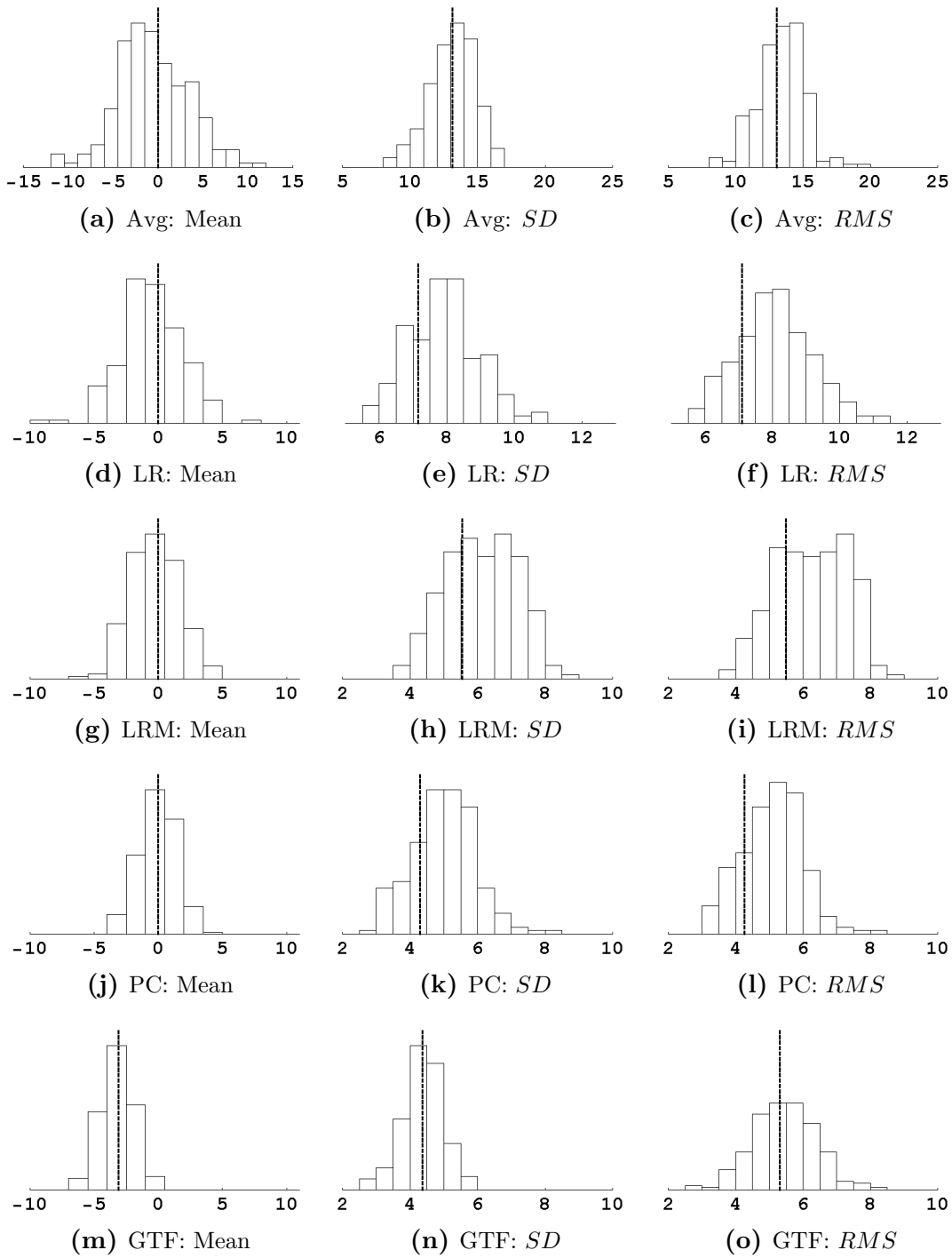

(a) Avg: Mean **(b)** Avg: SD **(c)** Avg: RMS

(d) LR: Mean **(e)** LR: SD **(f)** LR: RMS

(g) LRM: Mean **(h)** LRM: SD **(i)** LRM: RMS

(j) PC: Mean **(k)** PC: SD **(l)** PC: RMS

(m) GTF: Mean **(n)** GTF: SD **(o)** GTF: RMS

Figure D.5: Distribution of Mean, SD and RMS of the residuals ($_aPP$ - $_a\widehat{PP}$) for the different EO. All values in mmHg. Vertical bars indicate values estimated from all observations. Distributions were calculated using bootstrap method.

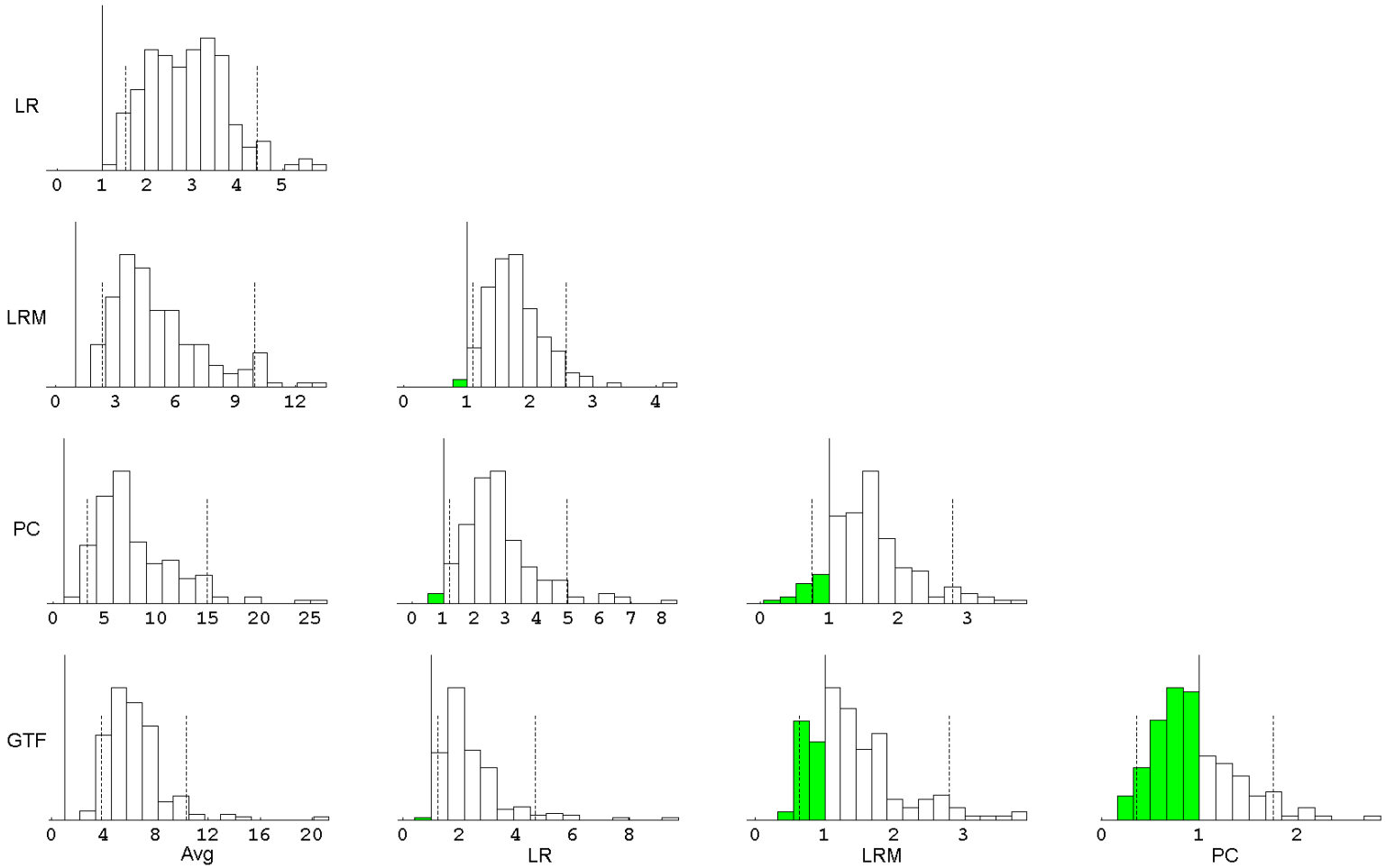

Figure D.6: Comparative histograms of ratios of variances of residuals ($_aPP - _a\widehat{PP}$): $\frac{Var[row]}{Var[column]}$ (see text, Chapter 5 section 5.1.2). Dotted lines indicate 95% of total observations. If unity is not included within dotted lines, the two EO (row and column) are significatly (at 95% confidence) different. If both dotted lines are to the right of unity, row EO is significantly better then column EO.

D.4 Aortic Augmentation Index

Models and Coefficients

Average:

$$\widehat{{}_aAIx}_{\texttt{Avg}} = 127.$$

	Estimate	SE	TStat	PValue
$\mu_{{}_aAIx}$	127.	5.02	25.2	< 0.001

Linear:

$$\widehat{{}_aAIx}_{\texttt{LR}} = 231. - 1.44HR$$

	Estimate	SE	TStat	PValue
C_0	231.	17.6	13.2	< 0.001
C_{HR}	-1.44	0.235	-6.11	< 0.001

Linear Mean:

$$\widehat{{}_aAIx}_{\texttt{LRM}} = 229. - 1.81HR + 1.92MP - 1.02_rSP$$

	Estimate	SE	TStat	PValue
C_0	229.	41.0	5.59	< 0.001
C_{HR}	-1.81	0.245	-7.40	< 0.001
C_{MP}	1.92	0.572	3.36	0.00142
C_{rSP}	-1.02	0.460	-2.23	0.0301

Principal Components:

$$\widehat{{}_aAIx}_{\texttt{PC}} = 157. - 1.54HR + 12.0PC_4 + 15.1PC_6 + 23.7PC_8 + 1.26_rDP$$

	Estimate	SE	TStat	PValue
C_0	157.	18.0	8.73	< 0.001
C_{HR}	-1.54	0.185	-8.30	< 0.001
C_{PC_4}	12.0	1.90	6.33	< 0.001
C_{rDP}	1.26	0.286	4.41	< 0.001
C_{PC_6}	15.1	3.94	3.84	< 0.001
C_{PC_8}	23.7	7.81	3.03	0.00377

Generalized Transfer Function: explained in section 4.2.3.

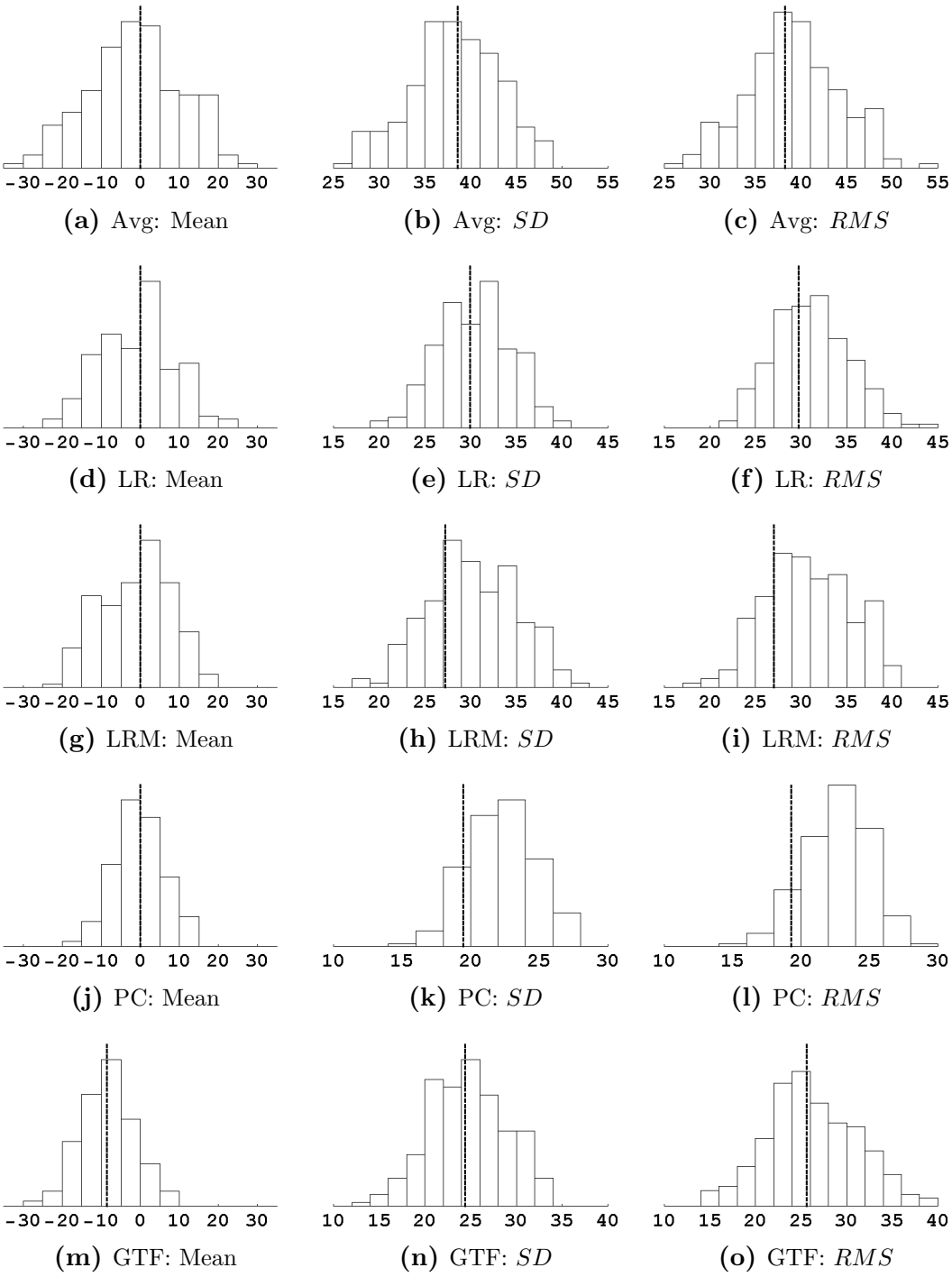

(a) Avg: Mean **(b)** Avg: SD **(c)** Avg: RMS

(d) LR: Mean **(e)** LR: SD **(f)** LR: RMS

(g) LRM: Mean **(h)** LRM: SD **(i)** LRM: RMS

(j) PC: Mean **(k)** PC: SD **(l)** PC: RMS

(m) GTF: Mean **(n)** GTF: SD **(o)** GTF: RMS

Figure D.7: Distribution of Mean, SD and RMS of the residuals ($_aAIx$ - $_a\widehat{AIx}$) for the different EO. All values in %. Vertical bars indicate values estimated from all observations. Distributions were calculated using bootstrap method.

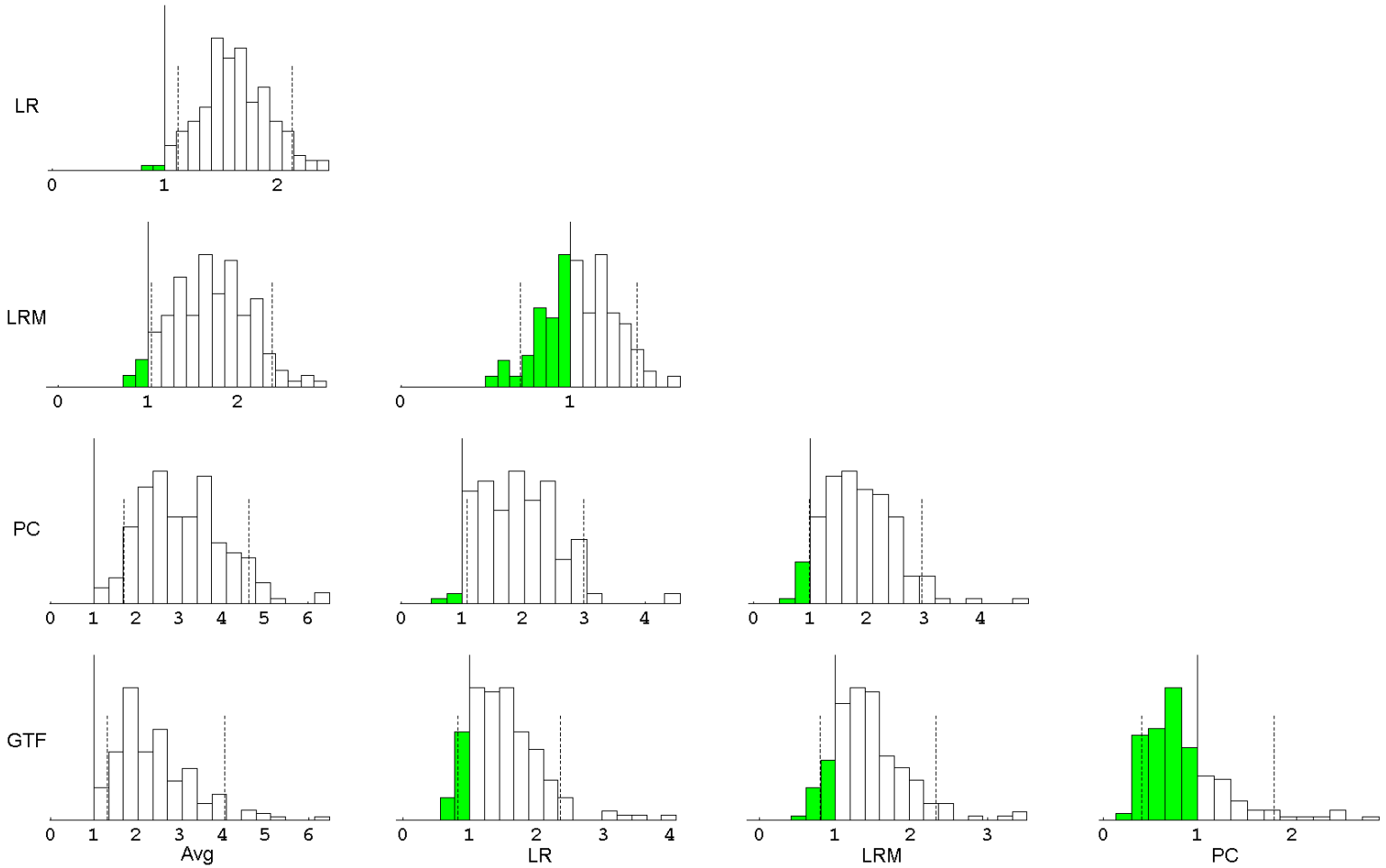

Figure D.8: Comparative histograms of ratios of variances of residuals $({}_aAIx - {}_a\widehat{AIx})$: $\frac{Var[row]}{Var[column]}$ (see text, Chapter 5 section 5.1.2). Dotted lines indicate 95% of total observations. If unity is not included within dotted lines, the two EO (row and column) are significatly (at 95% confidence) different. If both dotted lines are to the right of unity, row EO is significantly better then column EO.

D.5 Ejection Duration

Models and Coefficients

Average:

$$\hat{ED}_{\texttt{Avg}} = 314.$$

	Estimate	SE	TStat	PValue
μ_{ED}	314.	6.12	51.3	< 0.001

Linear:

$$\hat{ED}_{\texttt{LR}} = 659. - 1.03H - 2.30HR$$

	Estimate	SE	TStat	PValue
C_0	659.	70.2	9.38	< 0.001
C_{HR}	-2.30	0.200	-11.5	< 0.001
C_H	-1.03	0.398	-2.60	0.0119

Linear Mean:

$$\hat{ED}_{\texttt{LRM}} = 659. - 1.03H - 2.30HR$$

	Estimate	SE	TStat	PValue
C_0	659.	70.2	9.38	< 0.001
C_{HR}	-2.30	0.200	-11.5	< 0.001
C_H	-1.03	0.398	-2.60	0.0119

Principal Components:

$$\hat{ED}_{\texttt{PC}} = 556. - 0.663H - 1.76HR + 3.24PC_2 \\ +8.50PC_4 - 17.0PC_7$$

	Estimate	SE	TStat	PValue
C_0	556.	54.1	10.3	< 0.001
C_{HR}	-1.76	0.246	-7.15	< 0.001
C_{PC_7}	-17.0	4.87	-3.49	< 0.001
C_{PC_4}	8.50	1.68	5.07	< 0.001
C_{PC_2}	3.24	1.11	2.92	0.00515
C_H	-0.663	0.291	-2.28	0.0269

Generalized Transfer Function: explained in section 4.2.3.

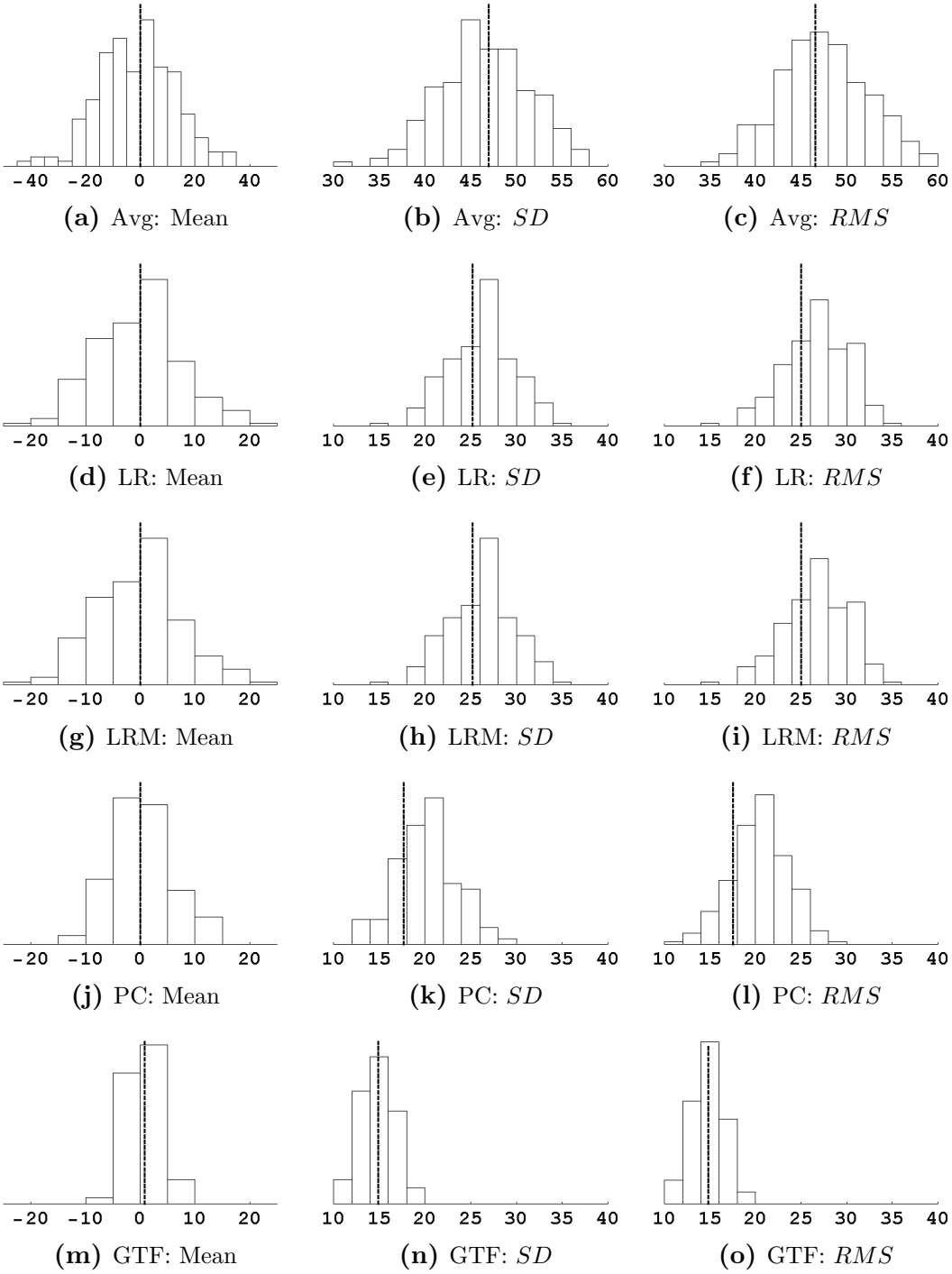

(a) Avg: Mean **(b)** Avg: SD **(c)** Avg: RMS

(d) LR: Mean **(e)** LR: SD **(f)** LR: RMS

(g) LRM: Mean **(h)** LRM: SD **(i)** LRM: RMS

(j) PC: Mean **(k)** PC: SD **(l)** PC: RMS

(m) GTF: Mean **(n)** GTF: SD **(o)** GTF: RMS

Figure D.9: Distribution of Mean, SD and RMS of the residuals (ED - $\hat{ED}$) for the different EO. All values in ms. Vertical bars indicate values estimated from all observations. Distributions were calculated using bootstrap method.

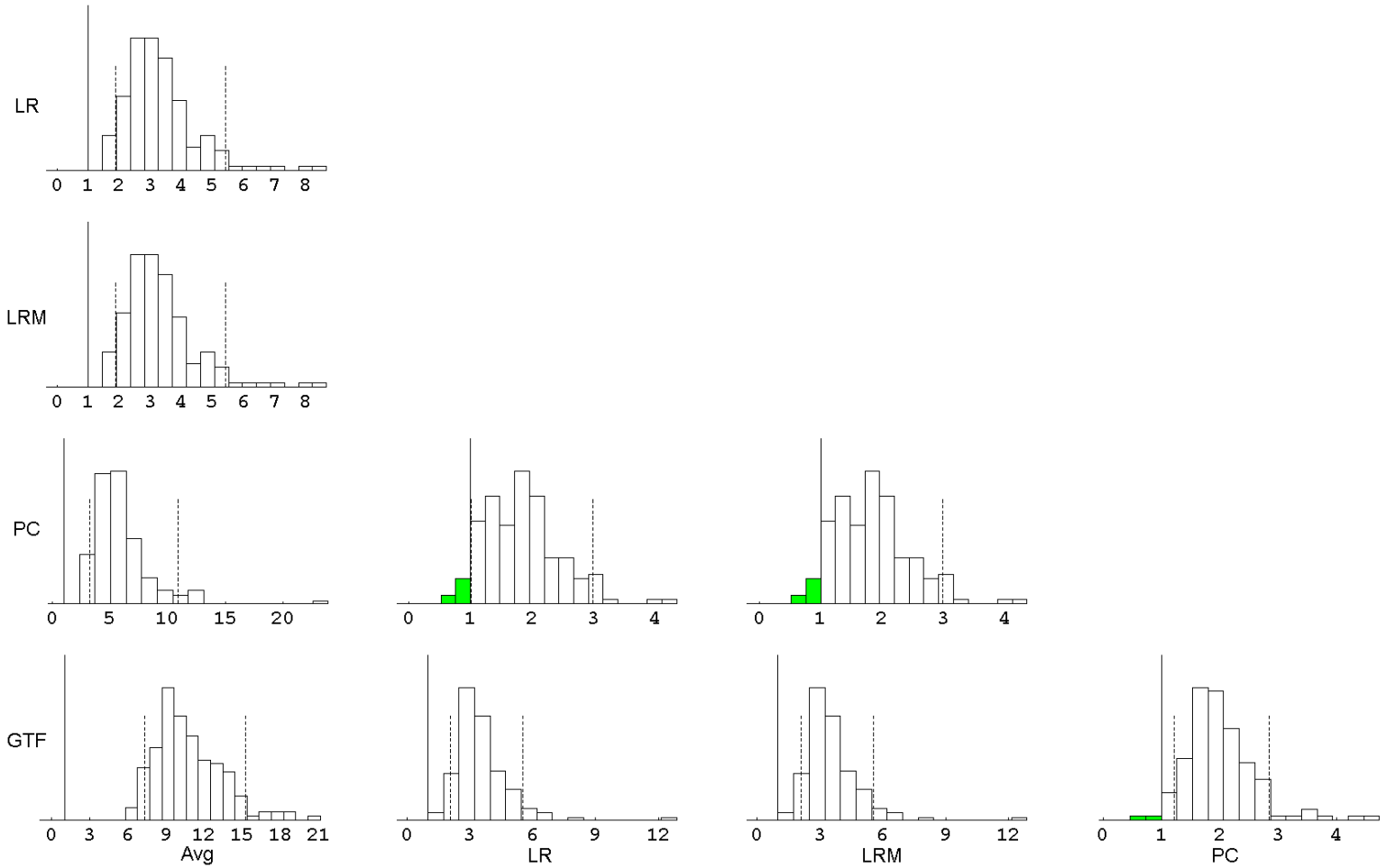

Figure D.10: Comparative histograms of ratios of variances of residuals ($ED - \hat{ED}$): $\frac{Var[row]}{Var[column]}$ (see text, Chapter 5 section 5.1.2). Dotted lines indicate 95% of total observations. If unity is not included within dotted lines, the two EO (row and column) are significatly (at 95% confidence) different. If both dotted lines are to the right of unity, row EO is significantly better then column EO.

D.6 Inverse Pulse Pressure Amplification

Models and Coefficients

Average:

$$\widehat{\mathtt{PPA}^{-1}}_{\mathtt{Avg}} = 76.2$$

	Estimate	SE	TStat	PValue
$\mu_{\mathtt{PPA}^{-1}}$	76.2	1.95	39.1	< 0.001

Linear:

$$\widehat{\mathtt{PPA}^{-1}}_{\mathtt{LR}} = 81.4 + 0.330Age - 0.348HR$$

	Estimate	SE	TStat	PValue
C_0	81.4	14.6	5.57	< 0.001
C_{HR}	-0.348	0.107	-3.25	0.00198
C_{Age}	0.330	0.159	2.07	0.0428

Linear Mean:

$$\widehat{\mathtt{PPA}^{-1}}_{\mathtt{LRM}} = 37.6 + 0.348Age - 0.335HR + 2.27MP \\ -1.44_rDP - 0.394_rSP$$

	Estimate	SE	TStat	PValue
C_0	37.6	18.8	2.00	0.0501
C_{HR}	-0.335	0.101	-3.32	0.00164
C_{MP}	2.27	0.386	5.88	< 0.001
C_{rDP}	-1.44	0.359	-4.01	< 0.001
C_{Age}	0.348	0.128	2.72	0.00886
C_{rSP}	-0.394	0.167	-2.36	0.0218

Principal Components:

$$\widehat{\mathtt{PPA}^{-1}}_{\mathtt{PC}} = 154. + 0.215Age + 0.271HR + 2.53PC_1 \\ +2.78PC_2 + 1.58PC_3 + 2.88PC_4 - 0.900_rSP$$

	Estimate	SE	TStat	PValue
C_0	154.	30.3	5.08	< 0.001
C_{PC_2}	2.78	0.441	6.32	< 0.001
C_{PC_1}	2.53	0.421	6.01	< 0.001
C_{PC_4}	2.88	0.692	4.16	< 0.001
C_{rSP}	-0.900	0.251	-3.59	< 0.001
C_{HR}	0.271	0.0910	2.98	0.00443
C_{Age}	0.215	0.0962	2.24	0.0295
C_{PC_3}	1.58	0.780	2.03	0.0477

Generalized Transfer Function: explained in section 4.2.3.

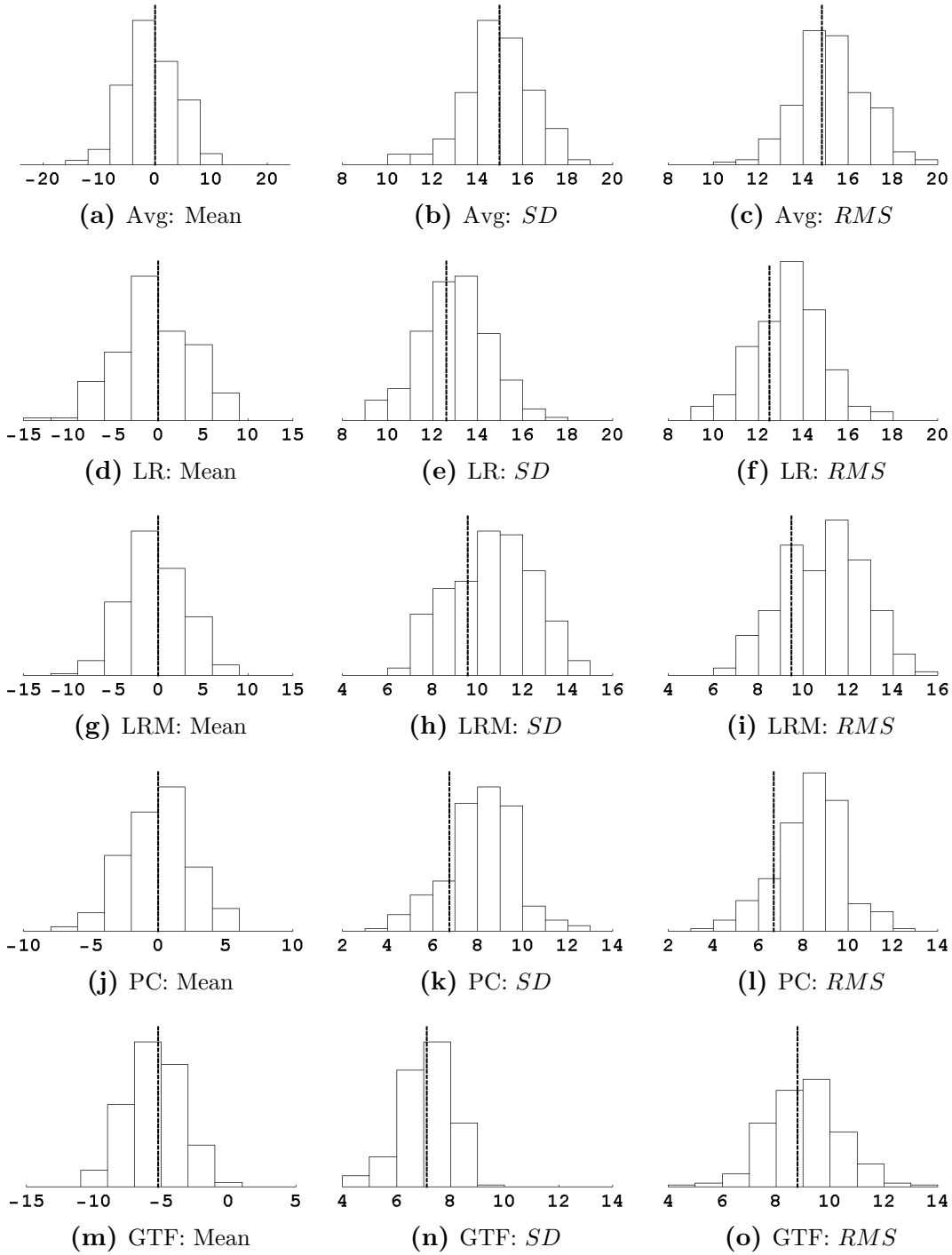

(a) Avg: Mean **(b)** Avg: SD **(c)** Avg: RMS

(d) LR: Mean **(e)** LR: SD **(f)** LR: RMS

(g) LRM: Mean **(h)** LRM: SD **(i)** LRM: RMS

(j) PC: Mean **(k)** PC: SD **(l)** PC: RMS

(m) GTF: Mean **(n)** GTF: SD **(o)** GTF: RMS

Figure D.11: Distribution of Mean, SD and RMS of the residuals (PPA^{-1} - $\widehat{\mathrm{PPA}^{-1}}$) for the different EO. All values in %. Vertical bars indicate values estimated from all observations. Distributions were calculated using bootstrap method.

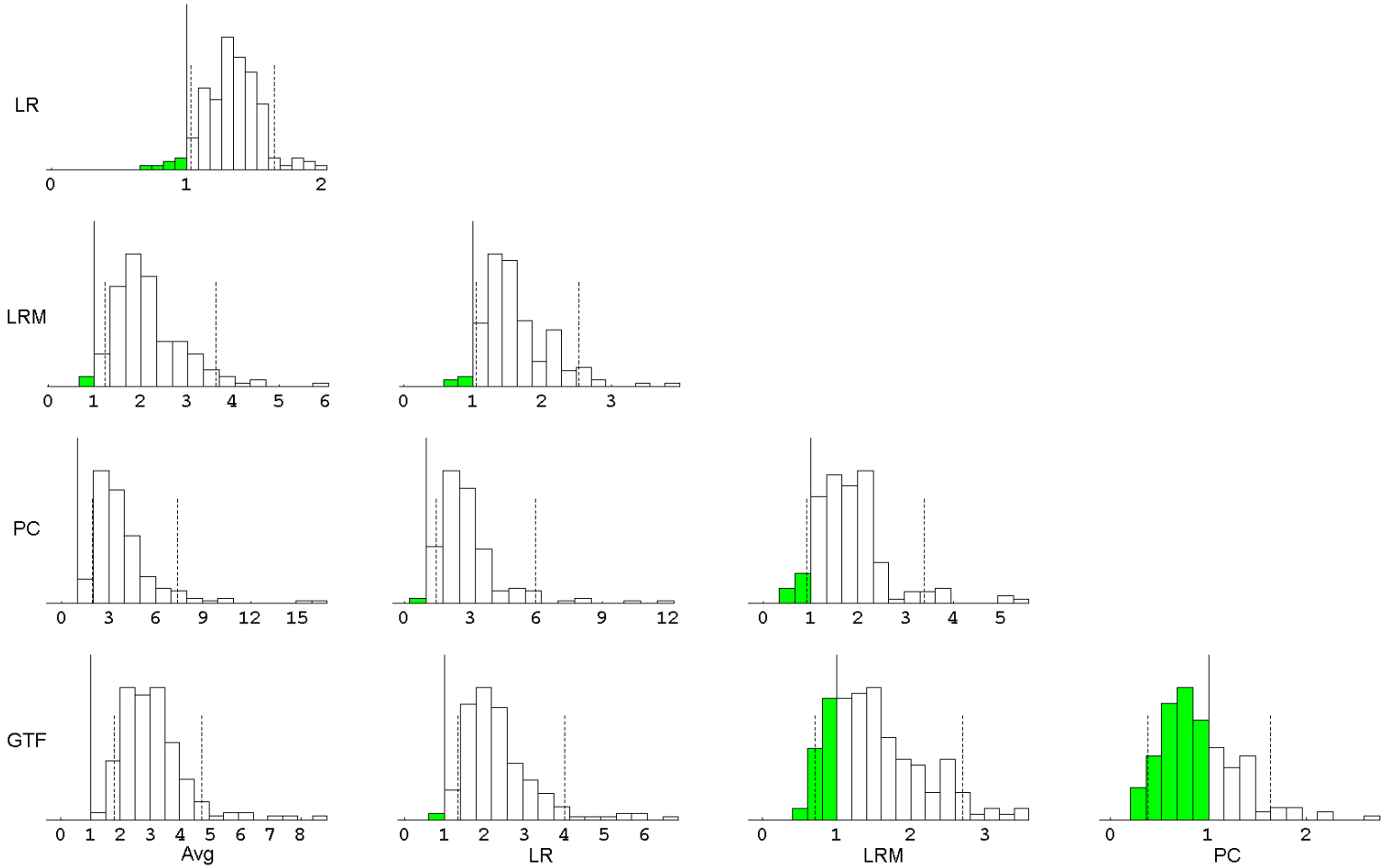

Figure D.12: Comparative histograms of ratios of variances of residuals ($\mathrm{PPA}^{-1} - \widehat{\mathrm{PPA}^{-1}}$): $\frac{Var[row]}{Var[column]}$ (see text, Chapter 5 section 5.1.2). Dotted lines indicate 95% of total observations. If unity is not included within dotted lines, the two EO (row and column) are significatly (at 95% confidence) different. If both dotted lines are to the right of unity, row EO is significantly better then column EO.

E

Detailed Results Chapter 6: 'Analysis of Estimated Central Arterial BP Parameters from Subject's Basic Information — Invasive and Non-Invasive Measurements'

This appendix presents the detailed results of the analysis of central arterial BP parameters presented in Chapter 6. The results are presented by $\mathcal{P}$. For each $\mathcal{P}$ the best fit models and coefficients' statistics are presented. The distributions of mean, SD and RMS are also presented for each of the EO used. The distributions of the ratios of variance between pairs of EOs are also included.

E.1 Aortic Systolic Pressure

Models and Coefficients

LR-PC:

$$\widehat{{}_aSP}_{\texttt{LR-PC}} = -23.2 + 0.226Age - 0.213HR + 0.356{}_rDP + 0.903{}_rSP$$

	Estimate	SE	TStat	PValue
C_0	-23.2	9.10	-2.55	0.0137
C_{rSP}	0.903	0.0755	12.0	< 0.001
C_{HR}	-0.213	0.0496	-4.30	< 0.001
C_{rDP}	0.356	0.0987	3.60	< 0.001
C_{Age}	0.226	0.0672	3.36	0.00146

LR-GTF:

$$\widehat{{}_aSP}_{\texttt{LR-GTF}} = -21.8 + 0.234Age - 0.151HR + 0.186{}_rDP + 0.955{}_rSP - 5.37S$$

	Estimate	SE	TStat	PValue
C_0	-21.8	7.17	-3.03	0.00377
C_{rSP}	0.955	0.0598	16.0	< 0.001
C_{Age}	0.234	0.0497	4.70	< 0.001
C_S	-5.37	1.21	-4.45	< 0.001
C_{HR}	-0.151	0.0377	-4.02	< 0.001
C_{rDP}	0.186	0.0762	2.44	0.0181

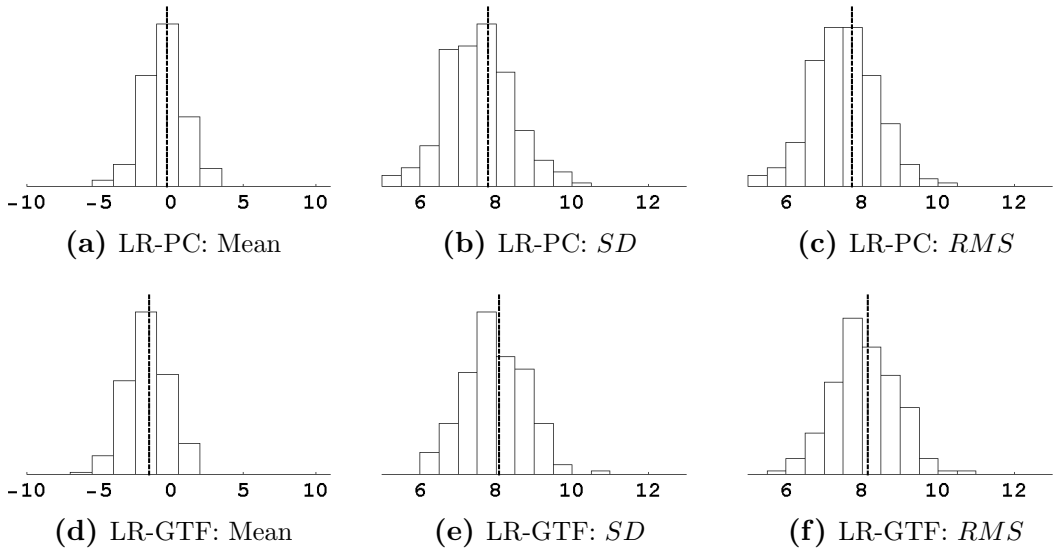

(a) LR-PC: Mean **(b)** LR-PC: SD **(c)** LR-PC: RMS

(d) LR-GTF: Mean **(e)** LR-GTF: SD **(f)** LR-GTF: RMS

Figure E.1: Distribution of Mean, SD and RMS of the residuals (${}_aSP$ - $\widehat{{}_aSP}$) for the different EO. All values in mmHg. Vertical bars indicate values estimated from all observations. Distributions were calculated using bootstrap method.

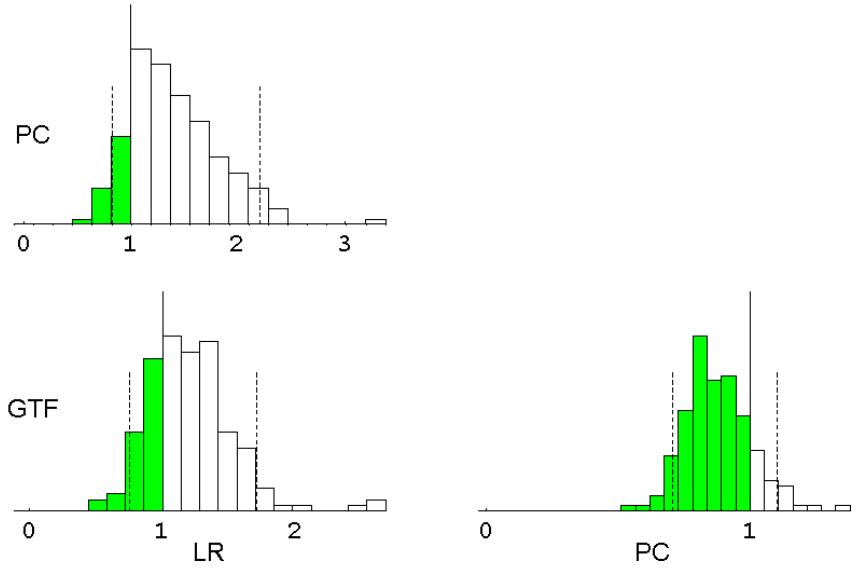

Figure E.2: Comparative histograms of ratios of variances of residuals $({}_aSP - {}_a\widehat{SP})$: $\frac{Var[row]}{Var[column]}$ (see text, Chapter 5 section 5.1.2). Dotted lines indicate 95% of total observations. If unity is not included within dotted lines, the two EO (row and column) are significatly (at 95% confidence) different. If both dotted lines are to the right of unity, row EO is significantly better then column EO.

E.2 Aortic Diastolic Pressure

Models and Coefficients

LR-PC:

$$ {}_a\widehat{DP}_{\texttt{LR-PC}} = 3.85 - 0.0516Age + 0.0317HR + 0.965_rDP $$

	Estimate	SE	TStat	PValue
C_0	3.85	2.36	1.63	0.110
C_{rDP}	0.965	0.0227	42.4	< 0.001
C_{HR}	0.0317	0.0158	2.01	0.0494
C_{Age}	-0.0516	0.0202	-2.55	0.0138

LR-GTF:

$$ {}_a\widehat{DP}_{\texttt{LR-GTF}} = -1.97 + 0.0709HR + 0.956_rDP $$

	Estimate	SE	TStat	PValue
C_0	-1.97	1.32	-1.49	0.142
C_{rDP}	0.956	0.0239	40.0	< 0.001
C_{HR}	0.0709	0.0151	4.70	< 0.001

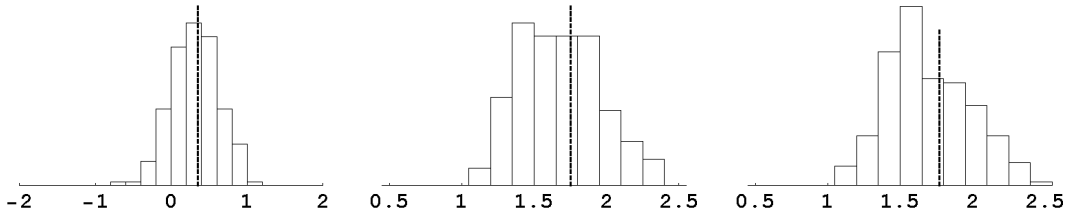

(a) LR-PC: Mean **(b)** LR-PC: SD **(c)** LR-PC: RMS

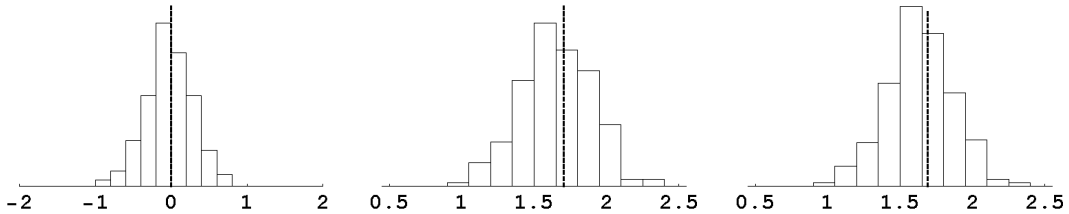

(d) LR-GTF: Mean **(e)** LR-GTF: SD **(f)** LR-GTF: RMS

Figure E.3: Distribution of Mean, SD and RMS of the residuals ($_aDP$ - $_a\widehat{DP}$) for the different EO. All values in mmHg. Vertical bars indicate values estimated from all observations. Distributions were calculated using bootstrap method.

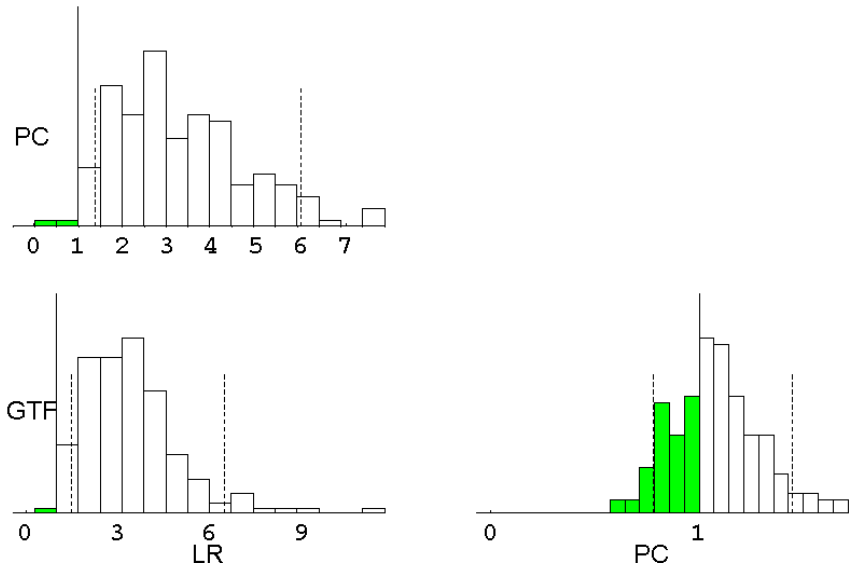

Figure E.4: Comparative histograms of ratios of variances of residuals ($_aDP - _a\widehat{DP}$): $\frac{Var[row]}{Var[column]}$ (see text, Chapter 5 section 5.1.2). Dotted lines indicate 95% of total observations. If unity is not included within dotted lines, the two EO (row and column) are significatly (at 95% confidence) different. If both dotted lines are to the right of unity, row EO is significantly better then column EO.

E.3 Aortic Pulse Pressure

Models and Coefficients

LR-PC:

$$\widehat{{}_aPP}_{\texttt{LR-PC}} = -28.5 + 0.322Age - 0.238HR \\ -0.548{}_rDP + 0.846{}_rSP$$

	Estimate	SE	TStat	PValue
C_0	-28.5	9.24	-3.09	0.00327
C_{HR}	-0.238	0.0501	-4.75	< 0.001
C_{rSP}	0.846	0.0734	11.5	< 0.001
C_{rDP}	-0.548	0.0963	-5.69	< 0.001
C_{Age}	0.322	0.0689	4.67	< 0.001

LR-GTF:

$$\widehat{{}_aPP}_{\texttt{LR-GTF}} = -13.8 + 0.262Age - 0.221HR - 0.772{}_rDP \\ +0.940{}_rSP - 3.66S - 0.0870W$$

	Estimate	SE	TStat	PValue
C_0	-13.8	7.14	-1.93	0.0589
C_{HR}	-0.221	0.0351	-6.29	< 0.001
C_{rSP}	0.940	0.0533	17.7	< 0.001
C_{rDP}	-0.772	0.0681	-11.3	< 0.001
C_{Age}	0.262	0.0448	5.85	< 0.001
C_S	-3.66	1.19	-3.06	0.00349
C_W	-0.0870	0.0344	-2.53	0.0146

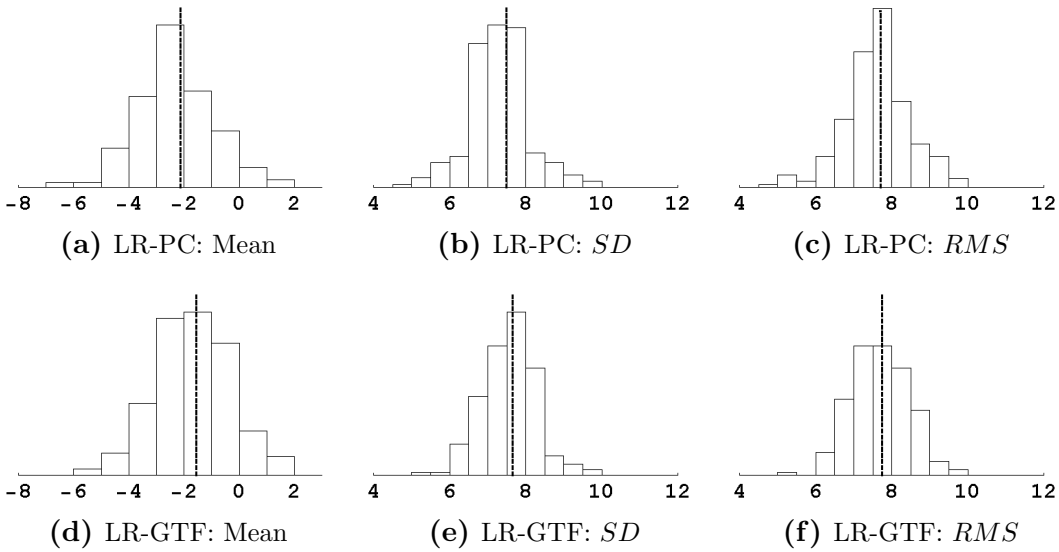

(a) LR-PC: Mean **(b)** LR-PC: *SD* **(c)** LR-PC: *RMS*

(d) LR-GTF: Mean **(e)** LR-GTF: *SD* **(f)** LR-GTF: *RMS*

Figure E.5: Distribution of Mean, SD and RMS of the residuals ($_aPP$ - $\widehat{{}_aPP}$) for the different EO. All values in mmHg. Vertical bars indicate values estimated from all observations. Distributions were calculated using bootstrap method.

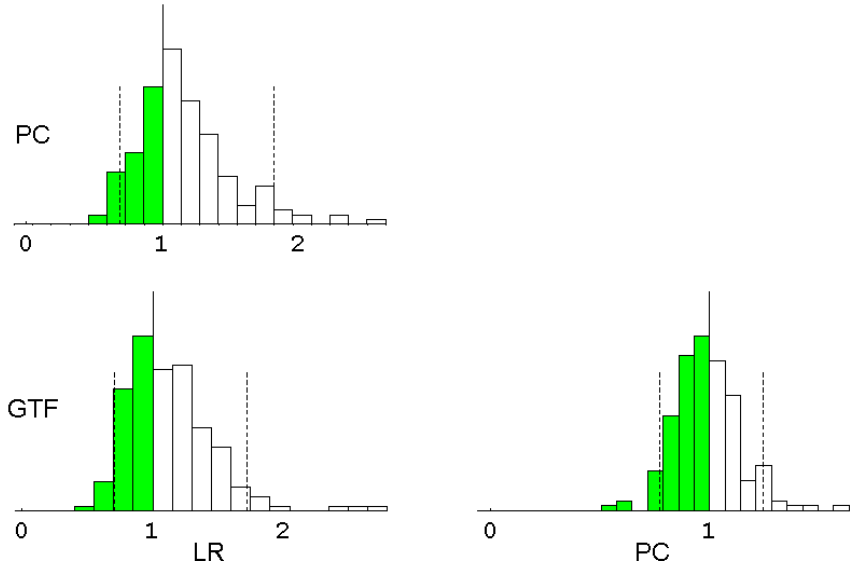

Figure E.6: Comparative histograms of ratios of variances of residuals $({}_aPP - {}_a\widehat{PP})$: $\frac{Var[row]}{Var[column]}$ (see text, Chapter 5 section 5.1.2). Dotted lines indicate 95% of total observations. If unity is not included within dotted lines, the two EO (row and column) are significatly (at 95% confidence) different. If both dotted lines are to the right of unity, row EO is significantly better then column EO.

E.4 Aortic Augmentation Index

Models and Coefficients

LR-PC:

$${}_a\widehat{AIx}_{\texttt{LR-PC}} = 208. - 1.48HR + 0.757_rDP_rDP$$

	Estimate	SE	TStat	PValue
C_0	208.	20.6	10.1	< 0.001
C_{HR}	-1.48	0.240	-6.18	< 0.001
C_{rDP}	0.757	0.371	2.04	0.0463

LR-GTF:

$${}_a\widehat{AIx}_{\texttt{LR-GTF}} = 200. - 1.49HR + 0.804_rDP_rDP$$

	Estimate	SE	TStat	PValue
C_0	200.	21.1	9.52	< 0.001
C_{HR}	-1.49	0.246	-6.08	< 0.001
C_{rDP}	0.804	0.380	2.11	0.0391

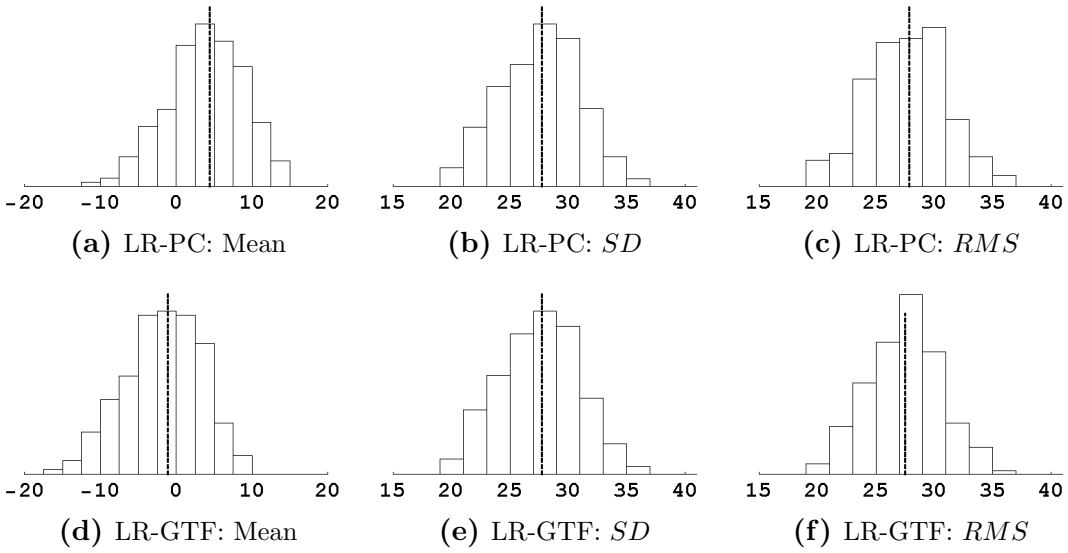

(a) LR-PC: Mean **(b)** LR-PC: SD **(c)** LR-PC: RMS

(d) LR-GTF: Mean **(e)** LR-GTF: SD **(f)** LR-GTF: RMS

Figure E.7: Distribution of Mean, SD and RMS of the residuals (${}_aAIx$ - ${}_a\widehat{AIx}$) for the different EO. All values in %. Vertical bars indicate values estimated from all observations. Distributions were calculated using bootstrap method.

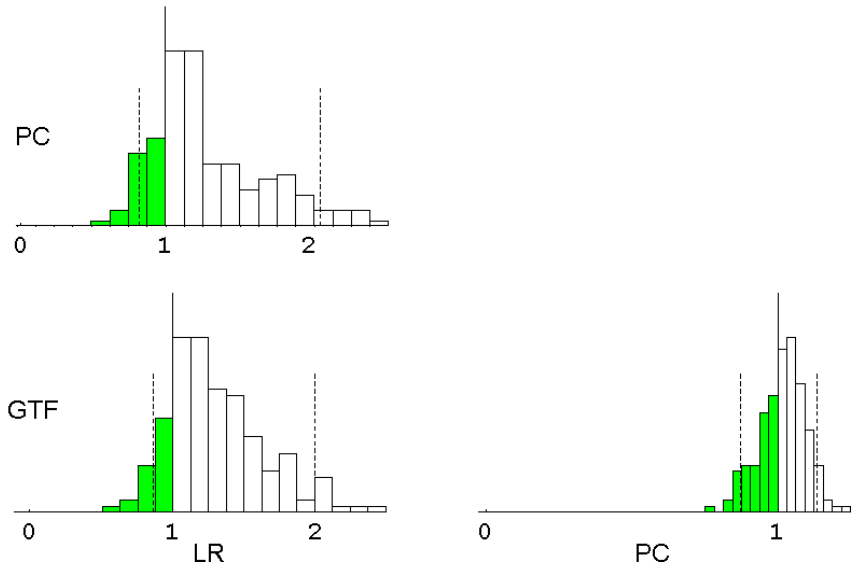

Figure E.8: Comparative histograms of ratios of variances of residuals (${}_aAIx - {}_a\widehat{AIx}$): $\frac{Var[row]}{Var[column]}$ (see text, Chapter 5 section 5.1.2). Dotted lines indicate 95% of total observations. If unity is not included within dotted lines, the two EO (row and column) are significatly (at 95% confidence) different. If both dotted lines are to the right of unity, row EO is significantly better then column EO.

E.5 Ejection Duration

Models and Coefficients

LR-PC:

$$\hat{ED}_{\texttt{LR-PC}} = 683. - 1.10H - 2.45HR$$

	Estimate	SE	TStat	PValue
C_0	683.	65.7	10.4	< 0.001
C_{HR}	-2.45	0.188	-13.0	< 0.001
C_H	-1.10	0.370	-2.97	0.00435

LR-GTF:

$$\hat{ED}_{\texttt{LR-GTF}} = 438. - 1.91HR - 0.912_r DP + 0.568_r SP - 12.5S$$

	Estimate	SE	TStat	PValue
C_0	438.	13.5	32.4	< 0.001
C_{HR}	-1.91	0.0831	-23.0	< 0.001
C_S	-12.5	2.62	-4.77	< 0.001
C_{rDP}	-0.912	0.161	-5.66	< 0.001
C_{rSP}	0.568	0.124	4.60	< 0.001

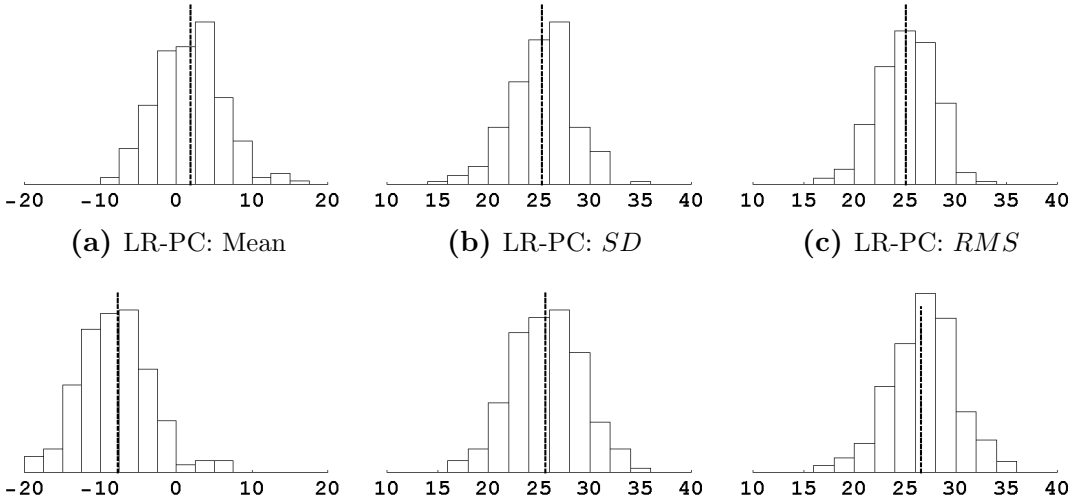

(a) LR-PC: Mean **(b)** LR-PC: SD **(c)** LR-PC: RMS

(d) LR-GTF: Mean **(e)** LR-GTF: SD **(f)** LR-GTF: RMS

Figure E.9: Distribution of Mean, SD and RMS of the residuals (ED - $\hat{ED}$) for the different EO. All values in ms. Vertical bars indicate values estimated from all observations. Distributions were calculated using bootstrap method.

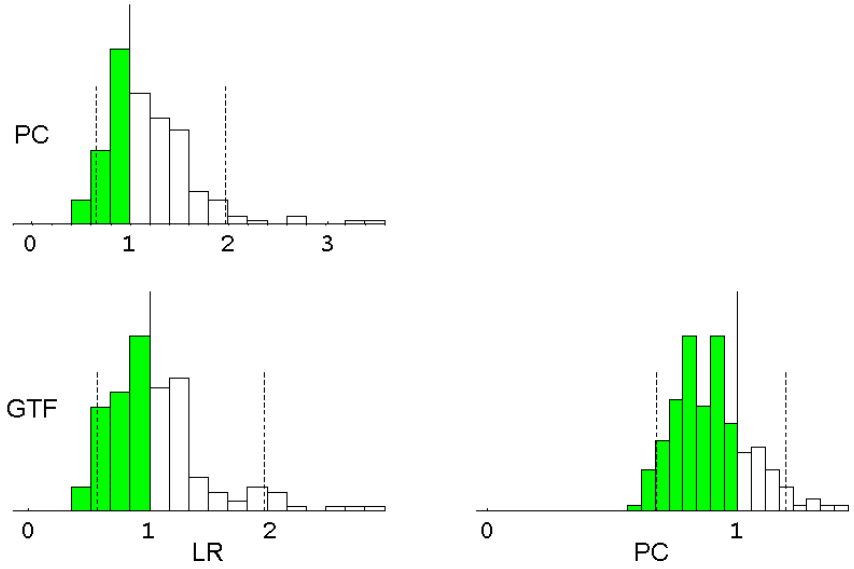

Figure E.10: Comparative histograms of ratios of variances of residuals ($ED - \hat{ED}$): $\frac{Var[row]}{Var[column]}$ (see text, Chapter 5 section 5.1.2). Dotted lines indicate 95% of total observations. If unity is not included within dotted lines, the two EO (row and column) are significatly (at 95% confidence) different. If both dotted lines are to the right of unity, row EO is significantly better then column EO.

E.6 Inverse Pulse Pressure Amplification

Models and Coefficients

LR-PC:

$$\widehat{\texttt{PPA}^{-1}}_{\texttt{LR-PC}} = 51. + 0.353Age - 0.410HR + 0.256_{r}SP$$

	Estimate	SE	TStat	PValue
C_0	50.7	15.9	3.19	0.00238
C_{HR}	-0.410	0.0735	-5.57	< 0.001
$C_{_rSP}$	0.256	0.103	2.48	0.0163
C_{Age}	0.353	0.114	3.09	0.00315

LR-GTF:

$$\widehat{\texttt{PPA}^{-1}}_{\texttt{LR-GTF}} = 57. + 0.461Age - 0.359HR + 0.219_{r}SP$$
$$-6.51S - 0.121W$$

	Estimate	SE	TStat	PValue
C_0	56.6	11.4	4.96	< 0.001
C_{HR}	-0.359	0.0484	-7.42	< 0.001
C_{Age}	0.461	0.0710	6.49	< 0.001
C_S	-6.51	1.92	-3.39	0.00133
$C_{_rSP}$	0.219	0.0607	3.61	< 0.001
C_W	-0.121	0.0557	-2.17	0.0350

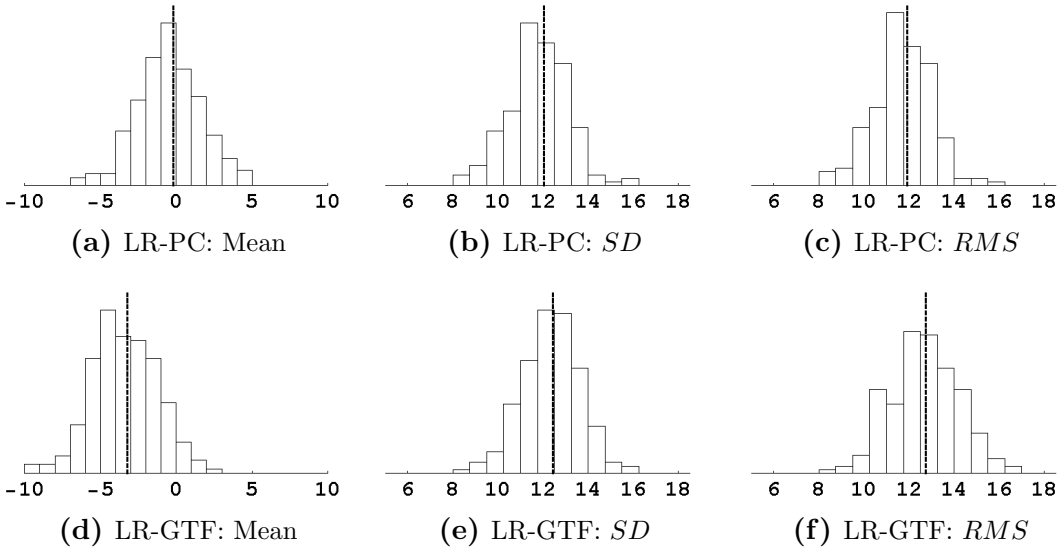

(a) LR-PC: Mean **(b)** LR-PC: *SD* **(c)** LR-PC: *RMS*

(d) LR-GTF: Mean **(e)** LR-GTF: *SD* **(f)** LR-GTF: *RMS*

Figure E.11: Distribution of Mean, SD and RMS of the residuals (PPA^{-1} - $\widehat{PPA^{-1}}$) for the different EO. All values in %. Vertical bars indicate values estimated from all observations. Distributions were calculated using bootstrap method.

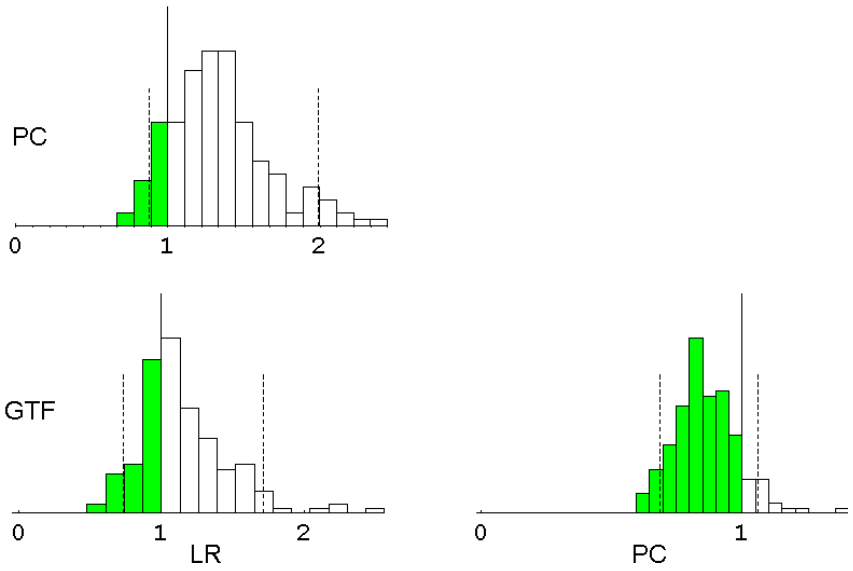

Figure E.12: Comparative histograms of ratios of variances of residuals (PPA^{-1} – $\widehat{PPA^{-1}}$): $\frac{Var[row]}{Var[column]}$ (see text, Chapter 5 section 5.1.2). Dotted lines indicate 95% of total observations. If unity is not included within dotted lines, the two EO (row and column) are significatly (at 95% confidence) different. If both dotted lines are to the right of unity, row EO is significantly better then column EO.

References

Working meeting on blood pressure measurement: suggestions for measuring blood pressure to use in populations surveys. *Rev Panam Salud Publica*, 14(5):300–2, 303–5, 2003.

Aaslid R. and Brubakk A. O. Accuracy of an ultrasound Doppler servo method for noninvasive determination of instantaneous and mean arterial blood pressure. *Circulation*, 64(4):753–9, 1981.

Amber R. B. and Babey-Brooke A. M. *The pulse in Occident and Orient: its philosophy and practice in India, China, Iran, and the West.* Santa Barbara Press, New York,, 1966.

Avolio A. A Multibranched Model of the Human Arterial System. *Medical and Biological Engineering and Computing*, 18:709–18, 1980.

Avolio A., Qasem A., and Park Y. J. Noninvasive estimation of baroreflex sensitivity using pressure pulse amplification. *IEEE Engineering in Medicine & Biology Magazine*, 20(2):53–8, 2001.

Batista-Foguet J. M., Coenders G., and Ferragud M. A. Using structural equation models to evaluate the magnitude of measurement error in blood pressure. *Stat Med*, 20(15):2351–68, 2001.

Beevers G., Lip G. Y., and O'Brien E. ABC of hypertension. Blood pressure mea-

surement. Part I-sphygmomanometry: factors common to all techniques. *Bmj*, 322(7292):981–5, 2001a.

Beevers G., Lip G. Y., and O'Brien E. ABC of hypertension: Blood pressure measurement. Part II-conventional sphygmomanometry: technique of auscultatory blood pressure measurement. *Bmj*, 322(7293):1043–7, 2001b.

Belani K. G., Buckley J. J., and Poliac M. O. Accuracy of radial artery blood pressure determination with the Vasotrac. *Can J Anaesth*, 46(5 Pt 1):488–96, 1999.

Bennett S. Blood pressure measurement error: its effect on cross-sectional and trend analyses. *J Clin Epidemiol*, 47(3):293–301, 1994.

Birch A. A. and Morris S. L. Do the Finapres and Colin radial artery tonometer measure the same blood pressure changes following deflation of thigh cuffs? *Physiol Meas*, 24(3):653–60, 2003.

Birkenhager W. H. and Reid John L. *Handbook of hypertension*. Elsevier, 1985.

Breit S. N. and O'Rourke M. F. Comparison of direct and indirect arterial pressure measurements in hospitalized patients. *Aust N Z J Med*, 4(5):485–91, 1974.

Burattini K.B., R. Campbell. Modified asymmetric T-tube model to infer arterial wave reflectionat the aortic root. *IEEE Transactions on Biomedical Engineering*, 36(8):805–814, 1989.

Camacho F., Avolio A., and Lovell N. H. Estimation of pressure pulse amplification between aorta and brachial artery using stepwise multiple regression models. *Physiol Meas*, 25(4):879–89, 2004.

Chan S. Power spectral analysis of arterial pressure signals: physiologic principles and clinical applications. *Acta Anaesthesiol Scand Suppl*, 110:119–20, 1997.

Chen C. H., Nevo E., Fetics B., Pak P. H., Yin F. C., Maughan W. L., and Kass D. A. Estimation of central aortic pressure waveform by mathematical transformation of radial tonometry pressure. Validation of generalized transfer function.[comment]. *Circulation*, 95(7):1827–36, 1997.

Cloud G. C., Rajkumar C., Kooner J., Cooke J., and Bulpitt C. J. Estimation of central aortic pressure by SphygmoCor requires intra-arterial peripheral pressures. *Clin Sci (Lond)*, 105(2):219–25, 2003a.

Cloud G. C., Rajkumar C., Kooner J., Cooke J., and Bulpitt C. J. Estimation of central aortic pressure by SphygmoCor requires intra-arterial peripheral pressures - Authors reply. *Clin Sci (Lond)*, 2003b.

Conroy R. M., O'Brien E., O'Malley K., and Atkins N. Measurement error in the Hawksley random zero sphygmomanometer: what damage has been done and what can we learn? *Bmj*, 306(6888):1319–22, 1993.

Cua C. L., Thomas K., Zurakowski D., and Laussen P. C. A comparison of the Vasotrac with invasive arterial blood pressure monitoring in children after pediatric cardiac surgery. *Anesth Analg*, 100(5):1289–94, table of contents, 2005.

Dahlof B., Devereux R., deFaire U., Fyhrquist F., Hedner T., Ibsen H., Julius S., Kjeldsen S., Kristianson K., Lederballe-Pedersen O., Lindholm L. H., Nieminen M. S., Omvik P., Oparil S., and Wedel H. The Losartan Intervention For Endpoint reduction (LIFE) in Hypertension study: rationale, design, and methods. The LIFE Study Group. *Am J Hypertens*, 10(7 Pt 1):705–13, 1997.

Dahlof B., Devereux R. B., Julius S., Kjeldsen S. E., Beevers G., deFaire U., Fyhrquist F., Hedner T., Ibsen H., Kristianson K., Lederballe-Pedersen O., Lindholm L. H., Nieminen M. S., Omvik P., Oparil S., and Wedel H. Characteristics of 9194 patients with left ventricular hypertrophy: the LIFE study. Losartan Intervention For Endpoint Reduction in Hypertension. *Hypertension*, 32(6):989–97, 1998.

Dahlof B., Devereux R. B., Kjeldsen S. E., Julius S., Beevers G., deFaire U., Fyhrquist F., Ibsen H., Kristiansson K., Lederballe-Pedersen O., Lindholm L. H., Nieminen M. S., Omvik P., Oparil S., and Wedel H. Cardiovascular morbidity and mortality in the Losartan Intervention For Endpoint reduction in hypertension study (LIFE): a randomised trial against atenolol. *Lancet*, 359(9311):995–1003, 2002.

Davies J. I., Band M. M., Pringle S., Ogston S., and Struthers A. D. Peripheral blood pressure measurement is as good as applanation tonometry at predicting ascending aortic blood pressure. *J Hypertens*, 21(3):571–6, 2003.

Dawber Thomas Royle. *The Framingham study : the epidemiology of atherosclerotic disease*. Harvard University Press, Cambridge, Mass., 1980.

Driscoll M. D., Arnold J. M., and Sherebrin M. H. Applied recording force and noninvasive arterial pulses. *Clin Invest Med*, 18(5):370–9, 1995.

Drzewiecki G. M., Melbin J., and Noordergraaf A. Arterial tonometry: review and analysis. *J Biomech*, 16(2):141–52, 1983.

Efron Bradley and Tibshirani Robert. *An introduction to the bootstrap*. Monographs on statistics and applied probability ; 57. Chapman & Hall, New York, 1993.

Freund M. and Wranne B. Ultrasound assessment of ductal closure, pulmonary blood flow velocity, and systolic pulmonary arterial pressure in healthy neonates. *Pediatr Cardiol*, 6(5):233–7, 1986.

Gardner R. M. Direct blood pressure measurement–dynamic response requirements. *Anesthesiology*, 54(3):227–36, 1981.

Garrow J. S. Zero-Muddler for Unprejudiced Sphygmomanometry. *Lancet*, 41:1205, 1963.

Hastie Trevor, Tibshirani Robert, and Friedman J. H. *The elements of statistical learning : data mining, inference, and prediction : with 200 full-color illustrations.* Springer series in statistics. Springer, New York, 2001.

Higham S. Sphygmomanometer cuff calibrated for corrected blood-pressure readings. *Br Med J*, 15(5126):906, 1959.

Hoeks A. P., Meinders J. M., and Dammers R. Applicability and benefit of arterial transfer functions. *J Hypertens*, 21(7):1241–3, 2003.

Hope S. A., Meredith I. T., and Cameron J. D. Is there any advantage to using an arterial transfer function? *Hypertension*, 42(3):e6–7; author reply e6–7, 2003a.

Hope S. A., Meredith I. T., and Cameron J. D. Effect of non-invasive calibration of radial waveforms on error in transfer-function-derived central aortic waveform characteristics. *Clin Sci (Lond)*, 107(2):205–11, 2004.

Hope S. A., Tay D. B., Meredith I. T., and Cameron J. D. Use of arterial transfer functions for the derivation of aortic waveform characteristics. *J Hypertens*, 21 (7):1299–305, 2003b.

Joffres M. R., Hamet P., MacLean D. R., L'Italien G J., and Fodor G. Distribution of blood pressure and hypertension in Canada and the United States. *Am J Hypertens*, 14(11 Pt 1):1099–105, 2001.

Kannel William B., Gordon Tavia, and (U.S.) National Heart Institute. *The Framingham study; an epidemiological investigation of cardiovascular disease.* U.S. Dept. of Health, Education, and Welfare, National Institutes of Health; for sale by the Supt. of Docs., U.S. Govt. Print. Off., Washington, [Bethesda, Md.,, 1968.

Karamanoglu M., O'Rourke M. F., Avolio A. P., and Kelly R. P. An analysis of the relationship between central aortic and peripheral upper limb pressure waves in man. *European Heart Journal*, 14(2):160–7, 1993.

Kelly R., Hayward C., Avolio A., and O'Rourke M. Noninvasive determination of age-related changes in the human arterial pulse. *Circulation*, 80(6):1652–9, 1989a.

Kelly R., Hayward C., Ganis J., Daley J., Avolio A., and O'Rourke M. Noninvasive registration of the arterial pressure pulse waveform using high-fidelity applanation tonometry. *Journal of Vascular Medicine and Biology*, 1:148–149, 1989b.

Kesteloot H. and Joossens J. V. *Epidemiology of arterial blood pressure*. Developments in cardiovascular medicine ; v. 8. M. Nijhoff ; distributor for the U.S. and Canada Kluwer Boston, The Hague ; Boston Hingham, MA, 1980.

Kleinbaum David G. *Survival analysis : a self-learning text*. Springer, New York, 1996.

Langewouters GJ., Wesseling K. H., and Goedhard W. J. The static elastic properties of 45 human thoracic and 20 abdominal aortas in vitro and the parameters of a new model. *Journal of Biomechanics*, 17:425–35, 1984.

Lemogoum D., Flores G., Van denAbeele W., Ciarka A., Leeman M., Degaute J. P., van deBorne P., and Van Bortel L. Validity of pulse pressure and augmentation index as surrogate measures of arterial stiffness during beta-adrenergic stimulation. *J Hypertens*, 22(3):511–7, 2004.

Manning T. S., Shykoff B. E., and Izzo Jr., J. L. Validity and reliability of diastolic pulse contour analysis (windkessel model) in humans. *Hypertension*, 39(5):963–8, 2002.

Matthys K. and Verdonck P. Development and modelling of arterial applanation tonometry: a review. *Technol Health Care*, 10(1):65–76, 2002.

Messerli F. H., Ventura H. O., and Amodeo C. Osler's maneuver and pseudohypertension. *N Engl J Med*, 312(24):1548–51, 1985.

Millasseau S. C., Patel S. J., Redwood S. R., Ritter J. M., and Chowienczyk P. J. Pressure wave reflection assessed from the peripheral pulse: is a transfer function necessary? *Hypertension*, 41(5):1016–20, 2003a.

Millasseau S. C., Ritter J. M., and Chowienczyk P. J. Response: Augmentation Index and the Radial-to-Aortic Transfer Function. *Hypertension*, 2003b.

Naqvi N. H. and Blaufox M. Donald. *Blood pressure measurement : an illustrated history*. Parthenon Pub. Group, New York, 1998.

Nelles Oliver. *Nonlinear system identification : from classical approaches to neural networks and fuzzy models*. Springer, Berlin ; New York, 2001.

Nichols Wilmer W., O'Rourke Michael F., Hartley Craig, and McDonald Donald A. *McDonald's blood flow in arteries : theoretic, experimental, and clinical principles*. Arnold ; Oxford University Press, London, New York, 4th edition, 1998.

Nocedal Jorge and Wright Stephen J. *Numerical optimization*. Springer series in operations research. Springer, New York, 1999.

O'Brien E. Automated blood pressure measurement: state of the market in 1998 and the need for an international validation protocol for blood pressure measuring devices. *Blood Press Monit*, 3(3):205–211, 1998.

O'Brien E. and Atkins N. A comparison of the British Hypertension Society and Association for the Advancement of Medical Instrumentation protocols for validating blood pressure measuring devices: can the two be reconciled? *J Hypertens*, 12(9):1089–94, 1994.

O'Brien E., Pickering T., Asmar R., Myers M., Parati G., Staessen J., Mengden T., Imai Y., Waeber B., Palatini P., and Gerin W. Working Group on Blood Pressure Monitoring of the European Society of Hypertension International Protocol for validation of blood pressure measuring devices in adults. *Blood Press Monit*, 7 (1):3–17, 2002.

O'Brien E. T. and O'Malley K. The sphygmomanometer. *Br Med J*, 2(6194):851–3, 1979.

Ochiai H., Miyazaki N., Miyata T., Mitake A., Tochikubo O., and Ishii M. Assessment of the accuracy of indirect blood pressure measurements. *Jpn Heart J*, 38 (3):393–407, 1997.

O'Rourke M. F. Pressure and flow waves in systemic arteries and the anatomical design of the arterial system. *J Appl Physiol*, 23(2):139–49, 1967.

O'Rourke M. F. Ascending aortic pressure wave indices and cardiovascular disease. *Am J Hypertens*, 17(8):721–3, 2004.

O'Rourke M. F. and Pauca A. L. Augmentation of the aortic and central arterial pressure waveform. *Blood Press Monit*, 9(4):179–85, 2004.

O'Rourke M. F. and Safar M. E. Letter Regarding Article by Devereux et al, "Regression of Hypertensive Left Ventricular Hypertrophy by Losartan Compared With Atenolol: The Losartan Intervention for Endpoint Reduction in Hypertension (LIFE) Trial". *Circulation*, 111:e377, 2005.

O'Rourke Michael F., Kelly Raymond P., and Avolio A. P. *The arterial pulse*. Lea & Febiger, Philadelphia, 1992.

Pauca A. L., O'Rourke M. F., and Kon N. D. Prospective evaluation of a method for estimating ascending aortic pressure from the radial artery pressure waveform. *Hypertension*, 38(4):932–7, 2001.

Pauca A. L., Wallenhaupt S. L., Kon N. D., and Tucker W. Y. Does radial artery pressure accurately reflect aortic pressure? *Chest*, 102(4):1193–8, 1992.

Penaz J. Photoelectric measurement of blood pressure, volume and flow in the finger. In *Digest of the 10th international conference on medical and biological engineering - Dresden. 1973; p104*, 1973.

Pythoud F., Stergiopulos N., Bertramt C. D., and Meister J. J. Effects Of Friction And Nonlinearities On The Separation Of Arterial Waves Into Their Forward And Backward Components. *Journal of Biomechmics*, 29:1419–1423, 1996.

Raftery E. B. Direct versus indirect measurement of blood pressure. *J Hypertens Suppl*, 9(8):S10–2, 1991.

Raftery E. B. and Ward A. P. The indirect method of recording blood pressure. *Cardiovasc Res*, 2(2):210–8, 1968.

Ranganathan Ananth. The Levenberg-Marquardt Algorithm, June 2004. URL `http://www.cc.gatech.edu/people/home/ananth/lmtut.pdf`. 17 Oct 2005.

Roman Mary J, Kizer Jorge R., Ali Tauqeer, Lee Elisa T., Galloway James M., Fabsitz Richard R., and Henderson Jeffrey A. Central Blood Pressure Better Predicts Cardiovascular Events Than Does Peripheral Blood Pressure: The Strong Heart Study. In *Scientific Sessions, American Heart Association, Dallas, TX, 2005*, November 2005. Session title: "Epidemiology: Traditional CVD Risk Factors".

Ruskin Arthur. *Classics in arterial hypertension.* C.C. Thomas, Springfield, Ill., 1956.

Sagiv M., Ben-Sira D., and Goldhammer E. Direct vs. indirect blood pressure measurement at peak anaerobic exercise. *Int J Sports Med*, 20(5):275–8, 1999.

Sato T., Nishinaga M., Kawamoto A., Ozawa T., and Takatsuji H. Accuracy of a continuous blood pressure monitor based on arterial tonometry. *Hypertension*, 21 (6 Pt 1):866–74, 1993.

Seber G. A. F. *Linear regression analysis.* Wiley, New York, 1977.

Shoukri M. M. and Pause C. A. *Statistical Methods for Health Sciences.* CRC Press, 2 edition, 1999.

Smith Lindsay I. A tutorial on Principal Component Analysis, 2002a. URL http://kybele.psych.cornell.edu/∼edelman/Psych-465-Spring-2003/PCA-tutorial.pdf. 21 Oct 2005.

Smith S. P. Internet visits: a new approach to chronic disease management. *J Med Pract Manage*, 17(6):330–2, 2002b.

Smulyan H, Siddiqui D. S., Carlson R. J., London G. M., and Safar M. E. Clinical Utility of Aortic Pulses and Pressures Calculated From Applanated Radial-Artery Pulses. *Hypertension*, 42:150–155, 2003.

Soderstrom S., Nyberg G., O'Rourke M. F., Sellgren J., and Ponten J. Can a clinically useful aortic pressure wave be derived from a radial pressure wave? *Br J Anaesth*, 88(4):481–8, 2002.

Staessen J. A., Wang J. G., Thijs L., and Fagard R. Overview of the outcome trials in older patients with isolated systolic hypertension. *J Hum Hypertens*, 13(12): 859–63, 1999.

Takazawa K., O'Rourke M. F., Fujita M., Tanaka N., Takeda K., Kurosu F., and Ibukiyama C. Estimation of ascending aortic pressure from radial arterial pressure using a generalised transfer function. *Zeitschrift fur Kardiologie*, 85 Suppl 3:137–9, 1996.

Tochikubo O., Watanabe J., Hanada K., Miyajima E., and Kimura K. A new double cuff sphygmotonometer for accurate blood pressure measurement. *Hypertens Res*, 24(4):353–7, 2001.

Verbeke F., Segers P., Heireman S., Vanholder R., Verdonck P., and Van Bortel L. M. Noninvasive Assessment of Local Pulse Pressure. Importance of Brachial-to-Radial Pressure Amplification. *Hypertension*, 46:244–248, 2005.

Wada T., Fujishiro K., Fukumoto T., and Yamazaki S. Relationship between ul-

trasound assessment of arterial wall properties and blood pressure. *Angiology*, 48 (10):893–900, 1997.

Wesseling K. H., Settels J.J., van derHoeven G.M., Nijboer J.A., Butijn M.W., and Dorlas J.C. Effects of peripheral vasoconstriction on the measurement of blood pressure in a finger. *Cardiovasc Research*, 19(3):139–45, 1985.

Wilkinson I. B., Franklin S. S., Hall I. R., Tyrrell S., and Cockcroft J. R. Pressure amplification explains why pulse pressure is unrelated to risk in young subjects. *Hypertension*, 38(6):1461–6, 2001.

Williams B. Pulse wave analysis and hypertension: evangelism versus scepticism. *J Hypertens*, 22(3):447–9, 2004.

Yasmin and Brown M. J. Similarities and differences between augmentation index and pulse wave velocity in the assessment of arterial stiffness. *Qjm*, 92(10):595–600, 1999.